

INFLUENCE OF DISTINCT MICRORNAs
ON WHITE AND BROWN ADIPOGENESIS IN HUMAN

DOCTORAL THESIS

Presented to the Faculty of Electrical Engineering
of Graz University of Technology
in Partial Fulfillment of the Requirements for the Degree of
Doctor of Engineering Sciences (Dr.techn.)

by

MICHAEL KARBIENER



Graz University of Technology
Institute for Genomics and Bioinformatics
Petergasse 14, 8010 Graz, AUSTRIA

Graz, May 2011

Abstract

While pharmacological treatments to fight obesity by reducing energy intake have repeatedly failed, increasing energy expenditure via thermogenesis in brown adipose tissue (BAT) constitutes a promising weight loss strategy. However, fat cell (adipocyte) development and physiology are still poorly characterized at the molecular level. This is most evident for non-protein-coding RNAs (ncRNAs), many of which have been discovered only a few years ago. MicroRNAs (miRNAs) are one such group of ncRNAs that direct post-transcriptional gene silencing via binding to complementary messenger RNAs (mRNAs), thereby dampening protein output.

Using human and mouse *in vitro* model systems, the global miRNA expression profile during adipogenesis was analyzed. Subsequently, three candidate miRNAs were selected for functional characterization. First, miR-27b was found to decrease during adipogenesis, was identified as the first miRNA in human to negatively regulate adipocyte differentiation, and was shown to directly target the adipogenic key transcription factor PPAR γ . Second, miR-30c, which increased during human adipogenesis, was found to promote adipocyte differentiation and directly target the adipokine PAI-1 and the receptor ALK2. Interestingly, combined silencing of PAI-1 and ALK2 recapitulated the pro-adipogenic effect of miR-30c. Thereby, for the first time in the study of adipogenesis, a miRNA was revealed as a possible coordinator of two previously unconnected pathways. Third, miR-26a was found to increase during human adipocyte differentiation. Interestingly, overexpression of miR-26a promoted a brown gene expression program, most importantly a pronounced upregulation of UCP1, which ultimately resulted in enhanced metabolic activity. In line with this, miR-26a was induced in white adipose tissue (WAT) of cold-exposed mice, suggesting this miRNA to be a physiological mediator of cold acclimation. Mechanistically, the transcription factors RB1 and RIP140, as well as the kinase S6K1, all known suppressors of the brown adipocyte phenotype, were validated as direct miR-26a targets.

In sum, three miRNAs have been identified as novel players in human adipogenesis. Especially the discovery of miR-26a as first miRNA to promote a brown phenotype might be of therapeutic impact to increase energy expenditure in fat for the purpose of weight loss.

Kurzdarstellung

Während sich die Pharmakotherapie zur Bekämpfung von Fettleibigkeit durch reduzierte Nahrungsaufnahme wiederholt als erfolglos herausgestellt hat, ist die Steigerung des Energieverbrauchs mittels Thermogenese im braunen Fett (BAT) eine vielversprechende Strategie zur Gewichtsreduktion. Fettzellentwicklung und -physiologie sind auf molekularer Ebene jedoch nach wie vor unzureichend charakterisiert. Dies trifft vor allem für nicht-Proteincodierende RNAs (ncRNAs) zu, von denen viele erst vor wenigen Jahren entdeckt wurden. MicroRNAs (miRNAs) sind eine bestimmte Gruppe solcher ncRNAs, die durch Bindung an komplementäre messenger RNAs (mRNAs) die Proteinsynthese hemmen.

Unter Verwendung humaner und muriner *in vitro* Modellsysteme wurden das miRNA-Expressionsprofil während der Fettzellendifferenzierung (Adipogenese) untersucht und drei miRNAs – miR-27b, miR-30c, miR-26a – für eine funktionelle Charakterisierung ausgewählt. miR-27b, deren Expression während der humanen Adipogenese zurückgeht, wurde als erste miRNA mit einem negativen Einfluss auf diesen Prozess identifiziert. Des Weiteren wurde ein direkter inhibitorischer Einfluss von miR-27b auf PPAR γ , einen der wichtigsten adipogenen Transkriptionsfaktoren, festgestellt. Für miR-30c konnten ein Anstieg der Expression während der Adipogenese, ein pro-adipogener Effekt sowie eine direkte Interaktion mit dem Adipokin PAI-1 und dem Rezeptor ALK2 nachgewiesen werden. Interessanterweise erzeugte die simultane Dämpfung von PAI-1 und ALK2 einen vergleichbaren pro-adipogenen Effekt. Dadurch konnte zum ersten Mal in der Adipogeneseforschung eine miRNA als möglicher Koordinator von zwei bisher nicht zusammenhängenden Signalwegen identifiziert werden. Zuletzt wurde ein Anstieg von miR-26a während der Adipogenese beobachtet. Interessanterweise induzierte die Überexpression von miR-26a ein braunes Gen-Expressionsprogramm, vor allem eine starke UCP1-Expression, was letztlich eine gesteigerte metabolische Aktivität der Fettzellen bewirkte. Weiters wurde im weißen Fettgewebe (WAT) von Mäusen, die einer kalten Umgebung ausgesetzt wurden, ein Anstieg von miR-26a beobachtet, was eine physiologische Rolle für diese miRNA bei der Adaption an Kälte vermuten lässt. Auf mechanistischer Seite konnte eine direkte Interaktion von miR-26a mit den Transkriptionsfaktoren RB1 und RIP140, sowie mit der Kinase S6K1, validiert werden.

Zusammenfassend wurden in dieser Arbeit drei miRNAs als neue Regulatoren in der humanen Adipogenese identifiziert. Vor allem die Entdeckung von miR-26a – als erste miRNA, die einen braunen Phänotyp induziert – könnte von therapeutischer Bedeutung sein, um einen gesteigerten Energieverbrauch im Fett zum Zwecke der Gewichtsreduktion zu erzielen.

Acknowledgements

Money talks– and therefore I want to start with thanking the funding agencies. This work was supported by GEN-AU, the national genomic research programme launched by the Austrian Ministry for Science and Research (BMWF), via the grants "Cross-species identification of adipo-specific microRNAs" (no. GZ 200.176/01-II/1a/2007) and "non-coding RNAs" (no. 820982). Furthermore, our collaboration with the Institute of Developmental Biology and Cancer (IDBC), Université Nice – Sophia Antipolis, was supported by the Austrian Agency for International Cooperation in Education & Research (OeAD), via the programme for Scientific and Technological Cooperation (WTZ "Amadée", grants no. FR11/2008 and no. FR14/2010).

I want to express my special gratitude to professor Rudolf Stollberger who immediately agreed on being my official doctoral supervisor. Furthermore, I feel honored to have as my second supervisor professor emeritus Gérard Ailhaud. This gives me not only the opportunity to learn a lot from his expert comments and scientific suggestions, but will also strengthen the fruitful collaboration between the IDBC and our institute.

This work would have never been possible without the help of many colleagues and collaborators. I want to thank Gerwin Bernhardt from Graz Medical University, and Alexandros Vegiopoulos and Stephan Herzig from the German Cancer Research Center, who contributed important tissue samples, as well as Mansour Djedaini and Didier Pisani from the IDBC for their skilled scientific work. I'd like to give my thanks to Hubert Hackl and Peter Opriessnig for bioinformatic support, to Juliane Strauss for an introduction to dissection of mice, and to Andreas Prokesch for a lot of practical and scientific input. I also had the pleasure to work with several talented students: Susanne Nowitsch and Christoph Fischer contributed important data to our research on miR-27b, while Hans Riegler, Cornelia Mutz, and Karin Mössenböck performed critical experiments on miR-26a. Thank you very much for that– and also for your questions from which I learned a lot. Furthermore, I experienced the best possible technical support from Claudia Neuhold– thank you. I also want to thank all other current and former members of the Institute for Genomics and Bioinformatics for creating such a positive and convenient working atmosphere.

It was an outstanding pleasure to get to know and be supported by Ez-Zoubir Amri from the IDBC– *merci beaucoup* for your manifold scientific input and the friendly reception in your lab.

I am deeply grateful to my mentor and supervisor throughout the last years, Marcel Scheideler– *thank you so much* for your optimism, your sincerity, your expertise, and your friendship!

I am indebted to my parents for their unfailing support and understanding.

Last, I want to thank Laura– for your encouragement and your love that is always with me to relieve from failure and beautify success.

Contents

1	Introduction	6
1.1	Obesity	6
1.1.1	Definition, Pathogenesis and Etiology	6
1.1.2	Consequences of obesity	8
1.1.3	Therapeutic strategies	10
1.2	The Adipose Organ	12
1.2.1	Developmental Origins	12
1.2.2	Opposing Functions of White and Brown Adipose Tissue	16
1.2.3	Molecular Regulation of Adipogenesis	19
1.2.4	Endocrine Functions of Adipose Tissue	29
1.3	microRNAs	32
1.3.1	RNA interference and microRNA discovery	33
1.3.2	microRNA biogenesis and function	35
1.3.3	Prediction and validation of microRNA–mRNA interactions	37
1.3.4	microRNAs in human disease	39
1.4	MicroRNAs and adipose tissue – state of knowledge	41
2	Aims	45
3	Materials and Methods	46
3.1	Materials	46
3.1.1	Standard laboratory equipment	46
3.1.2	Instruments	47
3.1.3	Microarrays	48
3.1.4	Analysis of triglyceride accumulation	48
3.1.5	RNA isolation	48
3.1.6	Cell culture	49
3.1.7	Reverse transcription, RT-PCR, and quantitative real-time RT-PCR	50
3.1.8	Western blot analysis	51
3.1.9	Cloning and luciferase assays	52
3.1.10	Oxygen consumption	53
3.2	Methods	53
3.2.1	Cell culture	53
3.2.1.1	Cultivation and passaging of cells	53
3.2.1.2	Thawing of cells	54

3.2.1.3	Determination of cell concentration and viability	54
3.2.1.4	Freezing of cells	54
3.2.1.5	Adipocyte differentiation of hMADS cells	54
3.2.1.6	Transfection of hMADS cells	55
3.2.1.7	Transfection of HEK293 cells	55
3.2.1.8	Human primary adipose derived stromal cells	56
3.2.2	Molecular biology and biochemistry	56
3.2.2.1	RNA isolation	56
3.2.2.2	MicroRNA expression profiling	57
3.2.2.3	Quantitative real-time RT-PCR	59
3.2.2.4	RT-PCR	61
3.2.2.5	Oil Red O staining	62
3.2.2.6	Quantification of triglyceride accumulation	62
3.2.2.7	Generation of luciferase reporter vectors	63
3.2.2.8	Luciferase reporter assays	68
3.2.2.9	Western blot analysis	68
3.2.2.10	Oxygen consumption measurements	69
4	Results	72
4.1	Differentially expressed microRNAs in human and mouse adipocyte differentiation	72
4.2	miR-27b impairs human adipocyte differentiation and targets PPAR γ	75
4.3	miR-30c promotes human adipocyte differentiation and targets PAI-1 and ALK2	79
4.4	miR-26a induces brown adipocyte characteristics and targets RB1, RIP140, and S6K1	86
5	Discussion	97
5.1	Discussion of methods	97
5.1.1	Microarrays	97
5.1.2	Quantitative real-time RT PCR	98
5.1.3	Luciferase reporter assays	100
5.1.4	Oxygen consumption measurements	101
5.1.5	<i>In vitro</i> approaches to identify genes with physiological relevance	103
5.2	Discussion of results	103
5.2.1	miR-27b in adipogenesis, lipid metabolism and beyond	103
5.2.2	miR-30c, a pro-adipogenic coordinator of distinct regulatory networks	107
5.2.3	miR-26a, a potential mediator of cold acclimation	111
	Abbreviations	118
	Bibliography	125

Chapter 1

Introduction

1.1 Obesity

1.1.1 Definition, Pathogenesis and Etiology

Obesity is defined as a condition in which adipose (fat) tissue mass exceeds 30 % and 20 % of body mass for women and men, respectively (Herold, 2006). For practical reasons, as an estimate for body fat percentage the World Health Organization (WHO) introduced the body mass index (BMI), the quotient of body weight (in kg) and the body height squared (in m²), along with intervals for categorization as summarized in table 1.1. Although the main medical and societal focus is on the plethora of follow-up complications (discussed in 1.1.2), obesity is classified as a disease itself (code E66. of the International Statistical Classification of Diseases and Related Health Problems 10th revision (ICD-10)), with exertional dyspnea, pains in joints and spinal column and decreased self-esteem as the main clinical symptoms (Herold, 2006).

A multitude of statistics on BMI distribution and BMI development in the populations of different nations has been published in the last decades, and essentially all of them highlight the alarming increase in the prevalence of obesity. In 2001, 21 % of U.S. adults (Mokdad et al., 2003), and only 6 years later, almost a third of U.S. adults were classified as obese (Agurs-Collins and Bouchard, 2008), with another third of the population being overweight. Moreover, childhood obesity shows a drastic increase from 6 to 17 % in the USA during the past 30 years for the group of 2 to 19-year-old individuals (Ogden et al., 2006). The situation is, however, not restricted to North America, as in 2008, more than 50 % of adults in Europe were obese or overweight, three times more people than

Table 1.1. BMI classification

classification	BMI range
underweight	< 18.50
normal range	18.50 – 24.99
overweight	25.00 – 29.99
obese class I	30.00 – 34.99
obese class II	35.00 – 39.99
obese class III	≥ 40.00

20 years before (Hyde, 2008). Furthermore, compared to the 1970s, ten times more children are obese nowadays in the WHO European Region (Hyde, 2008). As a (relatively late) reaction, the 48 member states of the WHO European Region have adopted a European charta for counteracting obesity in 2006, with the goal to reverse obesity prevalence trends before 2015 (Brug, 2007). Another sign of action at the supranational level was the initiation of the European Obesity Day (European Obesity Day (EOD)) on , launched to raise awareness and strengthen a collective consciousness of the obesity problem (Frühbeck, 2010). Yet obesity is not restricted to advanced economies, but an increasing health issue also in the developing world (Hossain et al., 2007). In fact, there is only one region worldwide – sub-Saharan Africa – in which obesity is not common (Haslam and James, 2005) and thus, it is fair to say that, since the end of the 20th century, obesity constitutes a global epidemic.

The pathogenesis of obesity is straightforward as a prolonged positive energy balance is the *conditio sine qua non*. In other words, obesity can only develop if energy uptake via ingestion continuously exceeds energy expenditure by maintenance work (necessary biochemical work to maintain syn-tropy), mechanical work (movements), and thermogenesis.

The etiology of obesity is, however, a complicated and highly individual issue: Environmental, behavioural, genetic and epigenetic factors can contribute to a constantly positive energy balance, making obesity a complex, multifactorial disease (Agurs-Collins and Bouchard, 2008). With regard to environmental and behavioural factors, it is obvious that the economical, technological and socio-cultural developments during the last 60 years substantially fuelled the increase of obesity: Never ever before, people had experienced such a surplus and diversity of affordable foods, and never ever before, the professional and private lives of entire populations had been so akinetic. Developments like sophisticated consumer goods marketing and unprecedented prosperity at the populational level are additional features of the so-called Western life style, a highly "obesogenic" environment.

Despite the environment's predominant role in the development of the obesity epidemic during the last decades, it must be recognized that not every individual shows the same response (both qualitatively and quantitatively) to these extrinsic stimuli. For example, an overfeeding study performed on identical twins showed a significantly lower variance in weight gain within pairs than between distinct pairs of twins (Bouchard et al., 1990). Likewise, another study showed a strong correlation between the BMI of adoptees and their biological, but not their adoptive parents (Stunkard et al., 1986). In line with such genetic influence, the 2005 update of the Human Obesity Gene Map listed 11 genes which, if mutated, evoke monogenic obesity (i.e. without additional mutations in any other gene) (Rankinen et al., 2006). Notably, most of these genes are expressed in (e.g. Proopiomelanocortin (POMC) (Krude et al., 1998), Melanocortin receptor 4 (MC4R) (Yeo et al., 1998)) or act on (e.g. Leptin (LEP) (Clément et al., 1998)) the hypothalamus, the central regulator of energy metabolism. Furthermore, distinct aspects of energy metabolism – which are strongly influenced by the individual genotype – have been identified as predictive for the risk of developing obesity: for example, resting metabolic rate (RMR) negatively correlates with weight gain (Ravussin et al., 1988), as does preferred oxidation of fat over carbohydrates, estimated by the respiratory quotient (RQ), ($\text{CO}_{2\text{generated}} / \text{O}_{2\text{consumed}}$) (Zurlo et al., 1990).

Thus, genetic background is an additional important parameter and adds to the environmental cues that determine the risk of becoming obese. Although the relative contributions of environment and genetics vary between studies, it has been estimated that roughly 30–40% of the BMI variance is attributable to genetics and that the remaining 60–70% are of environmental origin (Pi-Sunyer, 2002).

However, from a basic research perspective, exact quantification of the impacts of individual environmental and genetic factors appear not as interesting as the complex interactions between environment and genes that are just about to be discovered in the young field of epigenetics. As examples, three recent findings revealing an involvement of epigenetic mechanisms in the development of obesity will be mentioned here. First, overfeeding of rats not only induced the expected weight gain and associated co-morbidities, but also changes in the DNA methylation pattern of genes involved in body weight regulation (Plagemann et al., 2009). Second, a study showed that offspring of rats fed a high-fat diet exhibited higher body fat accumulation than offspring of the control group (fed a low-fat diet), even though the fertilized eggs of both groups were transplanted into surrogate mothers, thus providing a similar maternal environment (Wu and Suzuki, 2006). Third, mouse experiments have recently addressed the influence of changes in the dietary fatty acids (FA) composition to which Western populations had been exposed during the last decade. Interestingly, despite no changes in food intake, mice fed a diet rich in linoleic acid (LA) showed, over four generations, a gradual increase in body weight and fat mass compared to mice fed an isocaloric, isolipidic diet with lower LA amount (Massiera et al., 2010). Thus, during a time span too short for the genetic principles of mutation and selection to occur, diet composition seems to influence subsequent generations via epigenetic mechanisms, thereby highlighting the susceptibility of the genetic background for environmental cues and presumably adding a further layer onto the complex etiology of the obesity epidemic.

1.1.2 Consequences of obesity

In sharp contrast to previous ages, the majority of today's world population is living in a country where it is more probable to die from being overweight than underweight (WHO, 2010). This fact seems plausible considering the manifold maladies that constitute the consequences of a chronically positive energy balance. A short overview of the most prominent so-called obesity-associated diseases will be given in this section.

Most (if not all) follow-up diseases are considered to emerge due to direct or secondary effects of the exhausted capacity of adipose tissue for triglycerides (TG) storage. On the one hand, if the top end of this capacity is reached, an increase in blood TG levels and ectopic deposition of free FA in liver, skeletal muscle (SM) and pancreas occur, a phenomenon coined *lipotoxicity*, as lipids and their derivatives interfere with the normal physiological organ function. On the other hand, "stressed" adipose tissue responds by changing its pattern of secretory products (adipokines), which again has detrimental effects on peripheral tissues and organs (discussed in more detail in 1.2.4) and, importantly, is considered to provoke a state of chronic, low-grade inflammation, a hallmark of obesity.

Among the most prominent outcomes of ectopic free FA deposition and altered adipokine secretion are insulin resistance and its most serious form, type 2 diabetes. Indeed, a negative correlation between BMI and insulin sensitivity has been described (Kahn et al., 1993). A long-term study found women with $\text{BMI} \geq 25 \text{ kg m}^{-2}$ at substantially higher risk of developing diabetes than normal weight subjects (Colditz et al., 1995), and the vast majority of type 2 diabetes diagnoses coincides with increased body weight (Stevens et al., 2001). Interestingly, this association of obesity and deteriorated glucose metabolism – reflected by the term "diabesity", introduced already in the 1970s (Sims et al., 1973) – is strongly influenced by body fat distribution: abdominal/central

obesity, i.e. expansion of visceral fat, poses a higher risk for development of type 2 diabetes than peripheral obesity, i.e. expansion of subcutaneous adipose depots (Ohlson et al., 1985; Kaye et al., 1991; Kissebah and Krakower, 1994). As a consequence, the waist-to-hip ratio (WHR), quantifying abdominal obesity, is an important estimator of the type 2 diabetes risk, in addition to the BMI. Hypertension is another frequent comorbidity of the obese state. Being obese is tantamount to a five times higher risk of hypertension compared to normal weight (Wolf et al., 1997), and obesity itself might account for as much as 65 % and 78 % of overall hypertension in men and women, respectively (Kannel et al., 1993). Impaired kidney function, leading to increased Na and H₂O retention, increased activity of the sympathetic nervous system (SNS), and pathological changes of vascular walls are all features observed in obese individuals and known contributors to an elevated blood pressure. However, the distinct molecular mechanisms are just beginning to be discovered. Notably, adipokines again seem to be involved in the pathology. For example, adipose tissue is an important source of angiotensinogen (ATG), a component of the renin-angiotensin-aldosterone system (RAAS) which regulates renal fluid reabsorption. It is known that ATG levels not only correlate with blood pressure (Caulfield et al., 1996), but also with weight gain (Van Harmelen et al., 2000).

Two other consequences of obesity are cardiovascular and cerebrovascular diseases. Independently of other risk factors, a study calculated the risk of heart failure to increase by 7 % and 5 % per each BMI increment of 1 kg m⁻² for women and men, respectively (Kenchiah et al., 2002). Similarly, BMI is positively correlated with the incidence of strokes (Kurth et al., 2002). Hypertension is a well known risk factor for both diseases. In addition, dyslipidemia contributes to atherogenesis (i.e., remodeling of vascular walls by the accumulation of fatty substances), which again favours ischaemic and haemorrhagic vascular injuries. Moreover, expansion of adipose tissue leads to a decreased blood perfusion rate, such that the heart has to increase its stroke volume to meet the metabolic demand of the tissue. This in turn causes detrimental histological changes of the myocardium (Mathew et al., 2008), another reason for the association of obesity and heart failure.

It must be emphasized that many of the aforementioned epiphenomenons of the obese state influence each other and frequently occur in concert. This has led to the term "Metabolic Syndrome (MetS)" or "Syndrome X" as a group of clinical risk factors for developing type 2 diabetes or cardiovascular diseases. Exact definitions of MetS vary, but always include abdominal obesity and signs of disturbed glucose and fat metabolism like insulin resistance, raised blood glucose levels, raised blood TG levels, and reduced high density lipoprotein (HDL) cholesterol levels (Gupta and Gupta, 2010). As for obesity itself, the etiology of MetS is highly complex. Hence, a detailed description of influencing factors and of the pathophysiological mechanisms uncovered to date is beyond the scope of this thesis.

Besides metabolic complications, excess body weight is known to predispose for certain types of cancer. From a global perspective, a long-term survey revealed that severely obese women and men (BMI \geq 40 kg m⁻²) had an overall risk to die from cancer that was 62 % and 52 % higher than the risk of normal weight individuals, respectively (Calle et al., 2003). Specifically, the death rates for colorectal, liver, pancreatic and kidney cancer showed a significant association with BMI for both sexes (Calle et al., 2003). In addition, gender-specific, obesity-associated risks have been described in many studies for breast and endometrial cancer in women, as well as for prostate cancer in men. Although it is intuitively clear that a situation of excess nutrients is in favour of unrestricted cellular growth, the precise molecular events linking obesity and distinct forms of cancer are only partially discovered at present. As a general principle, oxidative stress that is generated as a by-product

of substrate oxidation in the form of reactive oxygen species (ROS) might contribute to cellular damage and subsequent accumulation of DNA mutations. As for colorectal cancer, elevated insulin levels might stimulate proliferation of colon cells (Berster and Göke, 2008). A relatively tight functional link has already been established between postmenopausal breast cancer and increased estrogen synthesis by adipose tissue in the obese state (Cleland et al., 1985), and recently, also adipokines and distinct intracellular signaling pathways have been added to this mechanism of carcinogenesis (Brown et al., 2009).

To conclude, two facts concerning the downstream disturbances caused by obesity shall be pointed out: First, adipose tissue is supposed to play a pivotal role in the development and progression of MetS (or single MetS components), and maybe also cancer, via its plethora of adipokines– paracrine signals to other tissues that partially act as mediators and amplifiers of the chronic, low-grade inflammatory state of obesity. Second, several parameters directly or indirectly related to metabolism have been identified as biomarkers that inversely correlate with longevity– e.g. insulin, glucose and body temperature (Chen et al., 2010). Together with the finding that modest calorie restriction prolongs lifespan in rodents and non-human primates (Colman et al., 2009; Mair and Dillin, 2008), it seems obvious that, although adipose tissue appears an elegant evolutionary solution to react on a sustained surplus intake of food, our bodies might be more vulnerable to a chronically positive energy balance than previously assumed.

1.1.3 Therapeutic strategies

Diminishing body fat can be approached via both sides of the energy balance equation, i.e. by decreasing energy intake and/or increasing energy expenditure. From a methodological viewpoint, three basic therapeutic strategies – lifestyle intervention, surgical procedures and pharmacotherapy – exist and will be described in this section.

Lifestyle intervention comprises reduced caloric intake and increased physical activity. On the one hand, eating less and doing some exercise certainly is the most straightforward, "natural" and cheapest way to lose weight, on the other hand, it is usually also the hardest as a substantial change in an individual's habits over a long-term period is demanded. Several diets have been developed for obese patients, e.g. low-calorie diets (LCDs) ($\leq 1200 \text{ kcal d}^{-1}$), very low calorie diets (VLCDs) ($\leq 800 \text{ kcal d}^{-1}$), low carbohydrate and low fat diets. While short-term weight loss is greater for patients on a VLCD compared to LCD, weight maintenance on a long-term perspective – generally the most difficult task in obesity therapy – is equal and rather disillusioning (Atkinson et al., 1993). The popular Atkins diet, a low-carbohydrate, high-fat and high-protein diet, was shown to lead to greater improvement of blood parameters for cardiovascular risk than a LCD, but was equally (un-)effective with respect to one-year weight loss (Foster et al., 2003). As for low-fat diets, the efficiency compared to other types of diet is not clear (Kaila and Raman, 2008). However, a recent survey comparing four LCDs differing in carbohydrate, protein and fat percentages found out that weight loss after two years was similar for all groups, implying that macronutrient composition might be less important than caloric intake (Sacks et al., 2009). Moreover, the same study found a strong association of weight loss with attendance to group sessions, a general finding of many surveys on weight loss (Dansinger et al., 2005; Turner-McGrievy et al., 2007) which highlights the strong influence of social components, i.e. a stimulating, encouraging, and supervisory environment,

on patient compliance and ultimately the outcome of dietary intervention.

Surgical procedures conducted on the gastrointestinal tract all aim at reducing energy intake by decreasing the efficiency of nutrient absorption and increasing satiety. One common intervention is gastric banding where a band positioned around the upper part of the stomach limits food intake (Lunca et al., 2005). Another type of surgery is the roux-en-Y gastric bypass, where the stomach and small intestine are arranged in a Y configuration, the upper part of the stomach being connected to the jejunum and the upper part of the small intestine (with the lower part of the stomach) being connected with the distal end of the small intestine. This gastrointestinal rearrangement both reduces food intake (via increased satiety) and absorption (Bult et al., 2008). In general, surgical interventions are only recommended for obesity classes II and III if lifestyle intervention or pharmacotherapy have failed. As a consequence of the dramatically increasing prevalence of obesity, though, bariatric surgery has also strongly increased in the last decades (Robinson, 2009). On the one hand, the medical risks of surgery are clearly existent, especially in persons with decreased overall fitness like severely obese. On the other hand, it is remarkable that bariatric surgery not only is effective in long-term weight loss, but also significantly ameliorates comorbidities like type 2 diabetes, hypertension and hyperlipidemia (Buchwald et al., 2004; Buchwald et al., 2009).

Only two pharmacological compounds are currently approved for long-term (> 12 weeks) treatment of obesity in the USA. Orlistat is an inhibitor of gastric and pancreatic lipase and thus lowers intestinal fat absorption (Drew et al., 2007). Sibutramine acts on the central nervous system (CNS) to decrease appetite by inhibiting the reuptake of the neurotransmitters norepinephrine (NE) and serotonin (Luque and Rey, 1999). The effect of both drugs appears limited: A meta-analysis that evaluated combination therapies of lifestyle intervention with pharmacological treatment found 2.9% and 4.6% greater weight loss compared to placebo with orlistat and sibutramine, respectively (Padwal et al., 2003). For short-term (≤ 12 weeks) treatment of obesity, further sympathomimetic compounds, e.g. phentermine or diethylpropion, are approved by the American Food and Drug Administration (FDA) (Glandt and Raz, 2011). These agents are derivatives of amphetamines and suppress appetite by enhancing the release of NE and dopamine. Liraglutide is a drug recently approved by the FDA and by the European Medicines Agency for the treatment of type 2 diabetes. It is a glucagon-like peptide-1 (GLP-1) receptor agonist inhibiting glucagon secretion, thereby lowering blood glucose levels. In addition, it also delays gastric emptying, leading to early satiety and thus reduced food intake (Barnett, 2009). Collectively, it is fair to say that the current pharmacological treatment of obesity is not satisfactory due to only minor effects on weight loss. In addition, adverse side effects are frequent, e.g. fecal urgency and chronic intestinal malabsorption of fat-soluble vitamins for orlistat and hypertension, insomnia and heart arrhythmias for sympathomimetic compounds like sibutramine (Powell and Khera, 2010). Of note, current discoveries in adipose tissue research might pave the way for the development of further pharmacological treatments, aimed at increasing energy expenditure via non-shivering thermogenesis in brown fat (discussed in detail in 1.2.2). The feasibility of such an approach has, in principle, already been shown in the 1930s, as administration of the compound 2,4-dinitrophenol, uncoupling substrate oxidation from adenosine triphosphate (ATP) synthesis and thereby boosting metabolic rate, caused weight losses of approximately 1.5 kg per week (Tainter et al., 1934). Although side effects due to the systemic uncoupling effect prevented a standardized use, the principle of drug-directed transformation of excess fat stores into heat is still a valid and interesting option for obesity treatment.

1.2 The Adipose Organ

A prolonged positive energy balance is associated with changes in several tissues, but undoubtedly the most dramatic alterations occur in adipose tissue. Moreover, as outlined in the previous section, adipose tissue is of fundamental relevance for the onset and progression of obesity-associated diseases, and is also in the focus of drug development to counteract the obesity epidemic.

During the last decades, considerable knowledge about adipose tissue has accumulated, depicting it no longer as a merely passive "energy tank", but as a highly dynamic energy storage with active participation in metabolism. Furthermore, while mainly regarded as a *tissue* in the past, the concept of an adipose *organ* is now widely apprehended in basic research (but not yet in the clinic). An organ is defined as a series of tissues organized within a structural unit and performing a certain interconnected function, and indeed, two different adipose tissues – white adipose tissue (WAT) and brown adipose tissue (BAT) – have been identified in mammals (Cinti, 2005). Both are working together in the balance of lipid metabolism, performing either thermogenesis or other metabolic functions (Cinti, 2001). An overview of the currently known molecular mechanisms implicated in the development and function of WAT and BAT will be presented in this section.

1.2.1 Developmental Origins

Deciphering the developmental routes leading to formation of the human adipose organ is a challenge for several reasons. First, various depots of WAT and BAT exist at distinct locations in the body. At least for WAT, differences between depots have already been described, e.g. the close association of increased visceral but not subcutaneous fat with insulin resistance (Karelis et al., 2004), have also been supported on a molecular level (Vohl et al., 2004), and hence might be explained by different developmental origins. Second, considerable differences exist between mammalian model organisms and human. For instance, WAT is macroscopically undetectable at birth in mice and rats while appearing already in the second third of gestation in the human fetus (Ailhaud et al., 1992). Furthermore, a frequently investigated fat pad in rodents, the epididymal WAT, has no clear counterpart in human (Harris and Leibel, 2008). Third, although the beginnings of a multicellular organism, i.e. the totipotent embryonic stem cells (ESC), and the mature adipocytes are fairly well defined on a molecular level, precise marker genes for discrimination of the many intermediate cell types lying between these two ends of development are still lacking.

One of the earliest steps of cellular differentiation is the formation of the three germ layers – ectoderm, mesoderm and endoderm – from ESC. Generally, most adipose depots are considered to have a mesodermal origin. As the mesoderm progresses during embryonic development, it gives rise to further specialized cell populations, e.g. the paraxial mesoderm, parts of which later form the axial skeleton and the muscles of the trunk, or the lateral mesoderm, forming e.g. the bones and muscles of limbs or the peritoneum. Presumably, different adipose depots are also generated by the different mesodermal cells contributing to the respective body part (Gesta et al., 2007). However, it has recently been shown that at least some cephalic WAT depots in mouse originate from cells expressing Sex determining region Y-box 10 (Sox10), a marker of the neural crest (Billon et al., 2007), which itself derives from the ectoderm (Fig. 1). Thus, at least two germ layers seem to contribute to adipose tissue development in mammals.

During development of the human fetus, the aggregation of mesenchymal cells has been described, with a remarkable spatio-temporal association to capillaries (Poulos et al., 2010), which is followed

by the occurrence of fat cell clusters (Ailhaud et al., 1992). Subsequently, these primitive organs develop into fat lobules (Laharrague and Casteilla, 2010), and at birth, adipose depots appear essentially at all locations where they can be found in later life. Recent studies support a continuous increase in adipocyte number during subsequent childhood and adolescence, and a rather constant number throughout later life, with approximately 10% of adipocyte turnover per year (Spalding et al., 2008). Hence, adipogenesis is not a process restricted to early life, but a lifelong event, which has long been known for rodents and was also anticipated from early human *in vitro* studies (Hauner et al., 1989). Still, it is remarkable that already at the age of two years, obese children have a nearly twofold higher adipocyte number than lean ones (Knittle et al., 1979), which supports the notion that the very early life is a period highly susceptible for adipose tissue expansion, provided the appropriate cues (e.g. favourable diet composition or genetic background) (Ailhaud and Guesnet, 2004).

Similar to the fetal stage (see above), it is generally accepted that also during childhood and later life, adipocytes are generated by differentiation of certain precursor cells rather than by cell division of the adipocyte itself. The differentiation process is further considered as unidirectional or irreversible, i.e. precluding de-differentiation of lipid-filled adipocytes to precursor cells. These dogmas have been challenged, though, by *in vitro* studies on unilocular adipocytes isolated from newborn rats and adolescent humans, showing that lipid-filled cells can divide, and also de-differentiate into fibroblast-like cells which then proliferate (Sugihara et al., 1987). However, whether it is solely a cell culture artifact, or whether this mechanism is of physiological relevance has not been shown to date. As for the classical, mesoderm-derived adipose tissues, the current model starts from multipotent mesenchymal stem cells (MSC), which can give rise to progenitor cells of several mesodermal cell types like muscle, bone and fat (Gregoire et al., 1998). Upon extrinsic stimuli, asymmetric cell divisions lead to the formation of an (unipotential) adipose progenitor cell, the adipoblast, which is subsequently committed to the preadipocyte stage where early adipogenic markers are already expressed (Ailhaud et al., 1992) (Fig. 1). Interestingly, it has recently been shown that a subset of adipocytes seems to be derived from circulating, bone marrow (BM)-derived cells of the haematopoietic lineage (Majka et al., 2010; Crossno et al., 2006; Sera et al., 2009). However, the general viewpoint is still that the vast majority of all types of adipocyte progenitor cells are adipose tissue-resident, namely as part of the stromal vascular fraction (SVF). This fraction makes up at least one third of adipose tissue and also contains many other cell types like endothelial cells, blood cells and fibroblasts. Independent studies have confirmed the high proliferative capacity of cells in the SVF (Pilgrim, 1971; Cook and Kozak, 1982), which supports the model that cell division occurs before differentiation. However, controversy exists regarding the question which cell type(s) actually proliferate(s) when exogenous stimuli relay the need for adipose tissue expansion. MSC, or mesenchymal stromal cells, are one candidate cell population. Originally identified in BM (Friedenstein et al., 1968; Friedenstein et al., 1966), Pittenger et al. first demonstrated that MSC proliferate extensively and can differentiate into adipocytes, chondrocytes and osteocytes (Pittenger et al., 1999). Cell populations with similar characteristics have subsequently been identified in many adult tissues (Salem and Thiemermann, 2010), including adipose (Zuk et al., 2001). Obviously, the opportunity to obtain such cells from various tissues for *in vitro* expansion and differentiation holds exciting potential for autologous (Salem and Thiemermann, 2010), but also allogenic (Wolbank et al., 2009) therapeutic transplantation. However, several basic biological questions about MSC are unsolved at present. First, the physiological relevance of the multilineage potential is often debated, e.g. whether an adipose tissue-derived MSC ever differentiates into an osteocyte in the *in*

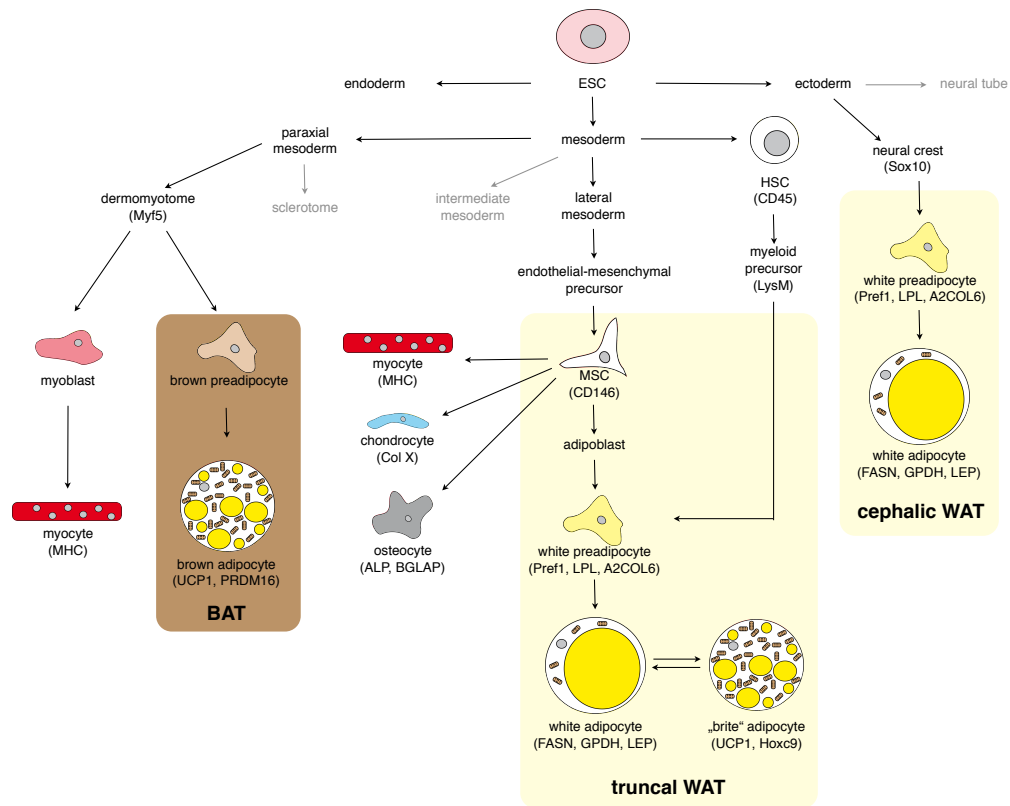


Figure 1. Developmental origins of white and brown adipose tissues. Distinct developmental lineages leading to the formation of white and brown adipocytes are depicted, with selected characteristic molecular markers added in parentheses. One of the earliest steps in life is the formation of the three germ layers – endoderm, mesoderm, and ectoderm – from ESC. The parenchymal cells of most adipose tissues are of mesodermal origin, although cephalic white adipocytes derive from the ectoderm via Sox10⁺ neural crest precursors (Billon et al., 2007). Whereas classical brown adipocytes and SM myocytes have been found to originate from a common, Myf5⁺ progenitor (Seale et al., 2008), white adipocytes originate from MSCs, which are stromal cells of many mesodermal tissues, including adipose tissue. MSCs might themselves be derived from an epithelial-mesenchymal precursor, the "mesenchymoangioblast" (Vodyanik et al., 2010). Molecular definitions of MSCs vary, although the expression of the pericyte marker CD146 (Crisan et al., 2008b) and the absence of endothelial (CD31) and hematopoietic (CD45) markers (Salem and Thiemermann, 2010) have been frequently proposed, in addition to multipotent differentiation characteristics towards not only adipogenic, but also osteogenic, chondrogenic, and myogenic lineages (Zuk et al., 2002). In addition, the existence of adipocytes and preadipocytes that originate from the myeloid lineage of HSC differentiation has been described (Majka et al., 2010). Upon appropriate stimuli, MSCs develop into unipotential adipoblasts and subsequently into preadipocytes, expressing already early adipocyte markers (Ailhaud et al., 1992). *In vivo*, terminally differentiated white adipocytes possess a single lipid droplet that accounts for most of the cell volume. Upon prolonged β -adrenergic stimulation, these cells have been shown to acquire molecular and morphological key features of brown adipocytes, e.g. UCP1 expression, high mitochondrial density, and multiple small lipid droplets (Cinti, 2005), but to lack a myogenic gene expression signature (Petrovic et al., 2010). Hence, these thermogenic adipocytes have been termed "brite" (brown-in-white) (Petrovic et al., 2010) or "beige" (Seale et al., 2011) adipocytes.

in vivo situation. Second, at least for adipose tissue, the actual contribution of MSC to regeneration of adult tissue is unknown (i.e. to which extent adipose tissue-derived MSC differentiate into mature adipocytes in the *in vivo* situation). Third, the similarity of MSC from different tissues with respect to their phenotype is also unclear. The latter question was recently addressed by a study isolating, on the basis of multiple cell surface markers, a population of perivascular cells (pericytes) from several human organs (skeletal muscle, pancreas, placenta, adipose tissue, BM) which could differentiate along myogenic, osteogenic, chondrogenic, and adipogenic lineages (Crisan et al., 2008b). Interestingly, another study also identified a population of pericyte-resembling cells in mouse WAT that gave rise to differentiated adipocytes *in vitro* and *in vivo* (Tang et al., 2008). However, the results of this mouse study differed from the human in two aspects: (i) the cells appeared as already committed adipocyte precursors (i.e. not as stem cells) based on the expression of an adipogenic key transcription factor; (ii) similar pericyte-like cells in other organs did not exhibit an adipogenic potential *in vitro*. Hence, although the exact developmental stage (multipotent or committed) remains elusive, both studies depict the mural cells surrounding the endothelial cells as a potential reservoir for generation of adipocytes. However, another recent study used human WAT samples to isolate a subpopulation of stromal vascular cells that was adipogenic and osteogenic *in vitro*, but negative for pericyte markers and also more frequently associated with adipocytes than with the vasculature (Maumus et al., 2011). Interestingly, this particular stromal vascular cell population was reduced in class II/III obesity subjects compared to class I, implying its potential involvement in adipocyte hyperplasia that is observed in severe obesity.

Compared to WAT, BAT development shows a rather different temporal pattern. It is already present at birth in most mammalian species (Ailhaud et al., 1992), supporting its essential role in coping with cold stress during the first days of extrauterine life (Enerback, 2010). However, while several BAT depots – e.g. interscapular, axillary, and cervical – can be found throughout life in mouse, BAT is rapidly replaced by WAT during growth of larger mammals like men (Lean and James, 1986). Although the previous phenomenon and cold exposure experiments (Cinti, 2001) suggest a considerable degree of plasticity between WAT and BAT (discussed in more detail in 1.2.2), several findings argue against a common white/brown precursor cell and imply a larger developmental gap between the two tissues. For instance, while SVF-derived precursor cells isolated from WAT differentiate into white adipocytes *in vitro*, precursor cells from BAT differentiate into brown adipocytes under the identical experimental conditions (Klaus et al., 1995). Furthermore, gene expression profiling demonstrated a myogenic signature of brown, but not white preadipocytes (Timmons et al., 2007). This close association of BAT with muscle was also supported by genetic fate mapping in mouse, as cells that during their development expressed the transcription factor *Engrailed 1 (En1)* developed into dermis, muscle and BAT, but not WAT (Atit et al., 2006). Finally, another mouse study used the myogenic regulatory factor *Myogenic factor 5 (Myf5)* to demonstrate that skeletal muscle (SM) and several BAT but no WAT depots originate from myogenic precursor cells (Seale et al., 2008) (Fig. 1).

In summary, it can be said that cumulative research findings have drawn a rather branched map of adipose tissue development (summarized in Fig. 1): Several distinct cell populations seem to be able to give rise to adipocytes, and the process of adipogenesis might be gradually different according to the developmental stage and the respective body part.

1.2.2 Opposing Functions of White and Brown Adipose Tissue

WAT and BAT, the two components of the adipose organ, are acting at the opposite borders of lipid metabolism: While the main function of WAT is to store energy and to provide it for other organs in fasting periods, BAT is specialized on *in situ* energy expenditure for the purpose of heating.

Regarding energy storage, the fact that essentially all higher animals rely on fat may be an evolutionary trend caused by the high energy density of lipids (9.1 kcal g^{-1}), which is approximately twice as high as the corresponding values of proteins or carbohydrates and thus makes fat the most efficient supply. While the liver's glycogen stores are depleted within hours of fasting (and thus serve as the "short-term-buffer"), the lipid stores of WAT are sufficient to provide triglycerides for several days. This remarkable storage capacity is also reflected at the morphological level: More than 90 % of a white adipocyte's volume are made up of a single lipid droplet. In order to accumulate such amounts of triglycerides, the white adipocyte is equipped with the enzymatic machinery to import food-derived FAs from the bloodstream (via membrane-bound lipoprotein lipase (LPL) and transmembrane FA transporters, e.g. CD36), to transport these FAs within the cytoplasm (via FA binding proteins), and to subsequently re-esterify the FAs to triglycerides. In addition, also glucose can be imported (via glucose transporters), transformed to acetyl-CoA (via glycolysis and pyruvate dehydrogenase) and subsequently used for *de novo* FA synthesis (via fatty acid synthase (FASN)) (Nussey and Whitehead, 2001). Conversely, the white adipocyte is also equipped with the protein cascade performing *lipolysis*, which is needed to mobilize fat stores during periods of fasting: protein kinase A (PKA, activated e.g. via NE/ β -adrenergic receptors or glucagon/glucagon receptor) phosphorylates perilipin A and hormone sensitive lipase (HSL), leading to translocation of HSL from the cytosol to the lipid droplets (Zechner et al., 2005), and also a redistribution of adipose triglyceride lipase (ATGL) from the cytosol and large lipid droplets to smaller lipid droplets (Bezire et al., 2009). Subsequently, ATGL is of major importance for hydrolysis of TGs to diglycerides, the latter being the major substrate for HSL which converts them into monoacylglycerides, which are finally hydrolyzed by monoglyceride lipase (Zimmermann et al., 2009). All three steps of TG hydrolysis yield FA, which enter the circulation for transport to other organs (coupled to serum albumin). Overall, FA import/ TG synthesis and lipolysis in WAT are reciprocally regulated by hormones that relay the nutritional status, most importantly insulin and glucagon (Berg et al., 2002).

In contrast to the widespread appearance of WAT across distinct phyla, BAT is a distinguishing feature of mammals. The usefulness of an inducible heating system which, in contrast to shivering, does not interfere with motor function, is evident in particular for small animals which are specifically susceptible for heat loss due to the high surface/volume ratio. Thus, the emergence of BAT might have been an evolutionary advantage to survive in situations of acute cold stress (Cannon and Nedergaard, 2004). Yet also bigger animals living in cold habitats and hibernating animals rely on BAT, and in contrast to earlier contention, also humans do not seem to fully lose their BAT depots at an early age, but possess active BAT throughout life (see below). Morphologically, the brown color of BAT can be explained by the facts that i) brown adipocytes have substantially lower intracellular TG stores than white adipocytes and thus are multilocular instead of unilocular adipocytes, and that ii) brown adipocytes have an exceptionally high density of mitochondria (Cinti, 2005). Further remarkable BAT traits are the high vascularization and the strong innervation by mainly sympathetic nerves (both higher than in WAT). In essence, these anatomical features reflect the prime function of BAT: Mainly activated by a neural stimulus, the tissue is designed for remark-

ably high metabolic activity and efficient distribution of the generated heat via the bloodstream. The mechanism of non-shivering thermogenesis in BAT has been delineated to a brown adipocyte-specific protein residing in the inner mitochondrial membrane, *Uncoupling protein 1 (UCP1)* (Nedergaard et al., 2001). The inner mitochondrial membrane is a major site of ATP production: electrons, derived from substrate oxidation in the tricarboxylic acid cycle and by FA β -oxidation, are transferred from coenzymes Nicotinamide adenine dinucleotide (NADH) and Flavine adenine dinucleotide (FADH₂) onto the electron transport chain (ETC), a series of four transmembrane protein complexes and two electron shuttles. As the electrons flow through the ETC, the free energy (ΔG) is used to pump protons from the mitochondrial matrix into the intermembrane space before the electrons are finally transferred onto O₂, generating H₂O. The energetically favourable back-flow of protons into the matrix is used by ATP Synthase, another transmembrane protein complex, to generate ATP (Alberts et al., 2002a). As a whole, the process is commonly known as *oxidative phosphorylation*, because oxidation of substrates is coupled to phosphorylation of adenosine diphosphate (ADP). UCP1 can uncouple substrate oxidation from ATP synthesis by generating an alternative route for protons to re-enter the mitochondrial matrix. If this route is open, all prior reactions are enabled to occur at a faster pace, ultimately resulting in an increased metabolic rate. As every series of biochemical reactions inevitably produces heat (the second law of thermodynamics), an increased metabolic rate is connected to increased heat production— which is the desired effect in the case of the brown adipocyte.

UCP1 is a confidable marker of brown adipocytes and as such always present— but not always active. Although the exact mechanisms remain to be elucidated, it is nowadays widely accepted that UCP1 is initially inactive due to direct binding of purine nucleotides (mainly millimolar concentrations of ATP under physiological conditions (Nicholls, 1976)), and that FAs (or derivatives thereof) can override this purine inhibition (Nicholls, 2006), leading to activation of UCP1-mediated uncoupled respiration. FAs are derived from lipolysis, which in brown adipocytes is triggered by NE (Nedergaard and Lindberg, 1979), released by sympathetic neurons and acting via β -adrenergic receptors. As for white adipocytes, the intracellular protein cascade involves activation of G_s proteins, followed by induction of adenylyl cyclase, an increase in cyclic adenosine monophosphate (cAMP) levels, subsequent activation of protein kinase A (PKA), and phosphorylation of PKA targets HSL and perilipin (Cannon and Nedergaard, 2004). FAs released from the lipid droplets can then enter the mitochondria to activate UCP1, and simultaneously serve as the primary substrate to be oxidized in the mitochondrial matrix (β -oxidation), thereby enabling an immediate elevation of the metabolic rate. However, prolonged UCP1 activation also leads to the import of substrates from the circulation, namely FAs and glucose. NE seems to be involved also in these processes, as it induces the release of LPL (acting on chylomicrons and very low density lipoproteins), and, in addition to insulin, also stimulates glucose uptake of brown adipocytes (Nedergaard and Cannon, 2010). Thus, BAT can indeed act as a sink for nutrients, and regarding the magnitude of this effect, it has been calculated that 50 g of active BAT could account for as much as 20% of daily energy expenditure (Rothwell and Stock, 1983).

The physiological importance of thermogenesis in BAT as a mechanism against cold stress has been established by numerous studies on rodents. For instance, prolonged cold exposure (i.e. chronic β -adrenergic stimulation) of mice over several weeks leads to BAT recruitment, i.e. a gradual increase in BAT mass, and a concomitant decrease in shivering (i.e. SM-derived thermogenesis). Again, NE appears as crucial mediator, as it (i) induces proliferation of brown preadipocytes (Bronnikov et al., 1992), and (ii) stimulates brown preadipocyte differentiation (Cannon and Nedergaard, 2004).

Importantly, also the accumulation of UCP1 protein is mediated by NE, as PKA phosphorylates the transcription factor cAMP response element binding protein (CREB), which then can bind to two cAMP response elements located upstream of the UCP1 transcription start site (TSS), thereby promoting UCP1 transcription. Indeed, the high inducibility of UCP1 by prolonged cold stress was the cause for its initial discovery (Ricquier and Kader, 1976), and also suggested a crucial involvement of this gene in non-shivering thermogenesis. This was subsequently proven by studies on UCP1^{-/-} mice, showing (i) that these animals do not survive an immediate transfer of from ambient temperature (20 °C) to acute cold stress (4 °C), and (ii) that, even though these animals can survive at 4 °C if the environmental temperature is decreased gradually, they never stop shivering in this situation (Golozoubova et al., 2001). Hence, no other mechanism of non-shivering thermogenesis can compensate for UCP1 loss.

The possibility of a second physiological role for BAT thermogenesis came from experiments with rats fed a high-energy "cafeteria" diet, showing that the enhanced caloric intake was paralleled by an increased metabolic rate, which was sensitive to antagonism of β -adrenergic signaling (Rothwell and Stock, 1979). It was subsequently demonstrated that this diet increased BAT mass (Himms-Hagen et al., 1981), as well as NE-stimulated metabolic activity of BAT (which is generally measured by O₂ consumption) (Rothwell and Stock, 1981). Hence, the theory of a diet-adaptation-recruited, NE-induced thermogenesis in BAT (often simply referred to as "diet-induced thermogenesis") emerged, implying BAT activation in response to caloric excess as a mechanism to prevent or ameliorate obesity (Cannon and Nedergaard, 2010). This concept has been criticized until today (Kozak, 2010). Among other factors, this discordance might be due to unequivocal results from studies with UCP1^{-/-} mice: While the initial survey introducing the UCP1^{-/-} mouse model clearly showed a sensitivity to cold stress (and hence the indispensability of UCP1 for β -adrenergically induced thermogenesis), the mice did not become obese, neither on a standard, nor on a high fat diet (HFD) (Enerbäck et al., 1997). According to second study, UCP1 deficiency might even protect against HFD-induced weight gain; however, the same study also described a considerable dependence of experimental outcome on the ambient temperature at which the animals are housed (Liu et al., 2003). Indeed, this appears to be a critical point, as "classical" housing temperatures of 18–22 °C impose a substantial, permanent cold stress on mice: In this situation, metabolic rates are 50–60 % higher than in the thermoneutral zone – which, for mice, is at \sim 30 °C (Golozoubova et al., 2004) –, and thus, a possible "obesogenic" effect of UCP1 deficiency might be masked because the entire heat production from metabolism is needed to compensate for heat loss (Cannon and Nedergaard, 2010). The results obtained in the aforementioned study by Enerbäck et al. (Enerbäck et al., 1997) presumably can be ascribed to this effect. Indeed, when Feldmann et al. conducted experiments at thermoneutrality, UCP1^{-/-} mice gained more weight on a standard diet and on a HFD compared to UCP1^{+/+} mice (Feldmann et al., 2009). This finding is of high interest for two reasons: First, it shows that there is a remarkably negative (i.e. dampening) effect of UCP1-mediated BAT thermogenesis on weight gain, at least at thermoneutrality. Second, the experimental setting might be a particularly suitable model for the current situation for humans, as today, at least in Western countries, people are situated almost permanently in a thermoneutral environment. It might thus be reasonable to propose that individual variations in the amount of UCP1 and hence of inducible BAT might either protect from or predispose to obesity. Recent studies in humans describing a negative correlation between BAT activity and BMI (van Marken Lichtenbelt et al., 2009a) are supportive of such a hypothesis.

For decades, the perception in human BAT research was that BAT is certainly present and needed

for the newborn, but that it disappears gradually during early life and is not present in adults. This tenet has been disproved during the last years, initially because of the reexamination of positron-emission tomography and computer tomography (PET/CT) data. PET/CT scans using the radioactive tracer ^{18}F -fluorodeoxyglucose were used in nuclear medicine since the 1990s to visualize tumor tissue due to its high glucose uptake rate. A recurring phenomenon in these scans was the appearance of symmetrical structures with high glucose uptake, e.g. at supraclavicular and paravertebral regions, which were shown to be cold-inducible (Nedergaard et al., 2007; Saito et al., 2009; Virtanen et al., 2009; van Marken Lichtenbelt et al., 2009b), and also to contain the histological features of BAT, including the presence of UCP1 (Zingaretti et al., 2009; Virtanen et al., 2009). Thus, although the prevalence varied considerably in the different surveys, it is fair to say that at least a fraction of adult humans possesses active BAT.

So far, the opposing functions of WAT and BAT have been described, and in 1.2.1, the possibility of a closer developmental relationship of BAT to muscle than to WAT has been presented. Still, there are also apparent indications for a considerable plasticity between WAT and BAT. First, several WAT depots in rat have been shown to express UCP1 mRNA and protein, and to contain not only unilocular, but also some multilocular adipocytes that possess mitochondria with brown adipocyte-like morphology (Cousin et al., 1992). Second, prolonged cold exposure of mice induces BAT marker proteins (e.g. UCP1) in WAT depots (Xue et al., 2009). Third, treatment of rats with the β_3 -adrenergic receptor agonist CL-316243 (CL) also led to the appearance of UCP1⁺, multilocular adipocytes in WAT (Himms-Hagen et al., 2000). Fourth, chronic exposure to agonists of the transcription factor peroxisome proliferator-activated receptor γ (PPAR γ), an adipogenic master gene discussed in 1.2.3, also induced the expression of UCP1 in WAT of rodents (Laplante et al., 2003; Carmona et al., 2007; Wilson-Fritch et al., 2004). Probably the most obvious analyses supporting the plasticity of WAT and BAT have been performed by Cinti: Compared to mice kept at ambient temperature, mice exposed to 4 °C exhibited a "global browning" of essentially all WAT depots (Cinti, 1999). Thus, although it is still debated whether brown adipocytes in WAT arise via a direct conversion of white adipocytes (Barbatelli et al., 2010) or via *de novo* differentiation of precursor cells (Petrovic et al., 2010), it is clear that environmental temperature can act as a stimulus influencing the balance between WAT and BAT, evoking an adaptation of the adipose organ to meet the necessary changes in metabolism.

1.2.3 Molecular Regulation of Adipogenesis

Even though the physiological stimuli leading to the development of adipose tissues *in vivo* are still speculative, research during the last decades has revealed a considerable number of genes that regulate adipogenesis. This can certainly be ascribed to the emergence of genetic engineering, most prominently targeted gene deletion/insertion and RNA interference (RNAi) techniques. In addition, several rodent and human adipocyte precursor cell lines have been established as convenient tools for the study of adipogenesis *in vitro*. These cells have been used extensively to screen and analyze not only genes, but also compounds, and in many cases have also been shown to be valid models for the *in vivo* situation. Some frequently used *in vitro* adipogenesis models will be presented below. Furthermore, a selection of hormones and synthetic compounds, as well as the most important transcription factors that regulate adipogenesis will be described. Although not always fully clarified, this section also attempts to describe the most plausible relations between distinct

hormones/compounds (= the "commanders") and the respective transcriptional regulators (= the "executors").

Initial investigations of (white) adipogenic differentiation *in vitro* date back to the 1970s, where a few cell lines were introduced which are still used today. The 3T3-L1 and 3T3-F442A preadipocyte cell lines were established from the parental mouse line 3T3 (which in turn was derived from mouse embryonic fibroblasts (Todaro and Green, 1963)) by selection for cells with high degree of spontaneous adipocyte differentiation (Green and Kehinde, 1974; Green and Kehinde, 1976). In contrast, the Ob17 preadipocyte cells were established from epididymal WAT of C57BL/6J *ob/ob* mice (Négrel et al., 1978). Another early established model is the multipotent C3H10T1/2 cell line, derived from mouse embryos, and, upon treatment with 5-azacytidine, able to differentiate along adipogenic, myogenic and chondrogenic lineages (Taylor and Jones, 1979). The immortality of the aforementioned cell lines is convenient, but also has its cause in genetic aberrations (aneuploidies) which usually are not the case *in vivo*. Hence, primary preadipocytes from the SVF of adipose tissue biopsies constitute a valuable alternative and as such have been isolated from several mammalian species, including human (Van et al., 1976; Hauner et al., 1987). The identification of multipotent MSC in various anatomical locations, e.g. BM and adipose tissue (cf. 1.2.1), provided another source of non-transformed models for adipogenic differentiation. However, both primary preadipocytes and MSC have only a limited lifespan *in vitro*. This disadvantage has been addressed by immortalization strategies, e.g. lentiviral transduction to overexpress the catalytic subunit of telomerase (TERT) (Wolbank et al., 2009), which was not only shown to increase the proliferative capacity, but also to preserve most characteristics of primary MSC. Another stem cell population had recently been isolated from WAT of infants or children and was termed human multipotent adipose-derived stem cells (hMADS cells). Remarkably, hMADS cells are non-transformed, have a normal karyotype, but still have been shown to perform more than 200 population doublings (PDs) *in vitro* without losing their differentiation potential towards adipogenic, osteogenic, and myogenic lineages (Rodriguez et al., 2005). Indeed, hMADS cells represent a faithful model system capable of adipokine secretion (Rodriguez et al., 2004a), and also differentiation *in vivo* (Elabd et al., 2007; Rodriguez et al., 2005).

A general model for adipocyte differentiation from a multipotent stem cell involves the following stages: (1) determination/commitment to an unipotential adipoblast/preadipocyte (Laharrague and Casteilla, 2010); (2) early phase of adipocyte differentiation (no lipid accumulation, but expression of early markers); (3) late phase of adipocyte differentiation (lipid accumulation and expression of late markers) (Ailhaud et al., 1992). To date, much more knowledge exists about the later two stages than about the first stage (Rosen and MacDougald, 2006), due to at least two reasons: First, most studies have used preadipocyte cell lines, in which the investigation of commitment is excluded *a priori*. Second, molecular markers that can distinguish between the multipotent stem cell and the committed adipoblast are still lacking.

Regardless of the model system, for adipogenesis the cells are usually permitted to reach confluence before a medium containing a cocktail of adipogenic substances (see below) is applied. Interestingly, in murine preadipocytes, the early markers LPL and collagen, type VI, $\alpha 2$ (COL6A2) appear already before treatment with adipogenic hormones and thus seem to be inducible just by confluence (Amri et al., 1986). Furthermore, the critical factor at confluence is not cell-cell contact but growth arrest, as actively growing (subconfluent) cells treated with thymidine (inducing a cell cycle block at G1/S stage) also respond with the induction of early markers (Ailhaud et al., 1989). For several murine

preadipocyte cell lines, a subsequent growth resumption has been described (Pairault and Green, 1979; Djian et al., 1982; Bernlohr et al., 1985), often referred to as "mitotic clonal expansion", which was also proposed as necessary to evoke changes in chromatin structure that subsequently enable access of transcription factors to regulatory elements of late marker genes (Otto and Lane, 2005). However, it appears not as an indispensable event for murine adipogenesis, as treatment of 3T3-L1 cells with a compound blocking Mitogen-activated protein kinase (MAPK) signaling inhibited mitotic clonal expansion, but not adipogenic differentiation (Qiu et al., 2001). Furthermore, efficient differentiation without indications for post-confluent mitoses was observed for adipogenesis of human preadipocytes (Newell et al., 2006) and adipose-tissue MSC (Ross et al., 2008). The morphological changes, though, seem rather uniform for all *in vitro* models: A few days after confluence and exposure to the adipogenic cocktail, the fibroblastoid appearance of cells changes to a more spherical shape (Armani et al., 2010), and the cells grow in size. Subsequently, late adipogenic markers are induced, most importantly proteins necessary for FA and TG processing like fatty acid binding protein 4 (FABP4) (also designated aP2) and glycerol-3-phosphate dehydrogenase (GPDH), as well as proteins for *de novo* FA synthesis like FASN, together with accumulation of intracellular lipid droplets (Rosen and Spiegelman, 2000). At least some adipokines, e.g. leptin and adiponectin (discussed in detail in 1.2.4) are among the genes expressed at significant levels in mature (i.e. terminally differentiated) adipocytes only.

In search for adipogenic substances, some endocrine regulators of adipogenesis could be inferred from diseases, either directly via clinical symptoms or indirectly via treatment side effects. For instance, prolonged injection of insulin leads to the emergence of ectopic fat pads at the injection site in type 1 diabetic patients (Nussey and Whitehead, 2001). Additionally, studies in rats support a role for insulin in lipid filling of pre-existing adipocytes, but also in adipocyte differentiation itself (Géloën et al., 1989). In line with this, insulin is used as an adipogenic factor in the medium of most *in vitro* model systems (Gregoire et al., 1998). As a second example, patients with Cushing's syndrome, characterized by high systemic levels of glucocorticoids (caused either by tumors of the pituitary or adrenal gland, or as side effect of glucocorticoid treatment), show expansion of visceral adipose depots (Ailhaud et al., 1992; Rebuffé-Scrive et al., 1988). This is consistent with reports describing a pro-adipogenic effect of cortisol in adipogenesis of murine preadipocytes (Schiwiek and Löffler, 1987) and human primary adipocyte precursor cells (Hauner et al., 1989). As a third example, deficiency in growth hormone (GH) (also known as somatotropin, produced by the pituitary gland) leads to adipocyte hypoplasia and hypotrophy in subcutaneous WAT (Bonnet and Rocour-Brumioul, 1981). Conversely, GH promotes adipocyte differentiation in murine systems (Morikawa et al., 1982), and has furthermore been shown to induce insulin-like growth factor 1 (IGF-1) expression in mouse preadipocytes (Doglio et al., 1987) (Fig. 2). IGF-1, in turn, has been identified as a central adipogenic compound of fetal calf serum (FCS), a frequent cell culture additive) (Smith et al., 1988), and thus might act as a paracrine mediator downstream of GH.

The notion that FAs themselves constitute a pro-adipogenic signal, inducing cellular processes that deal with their metabolism and storage, is essentially intuitive. Indeed, treatment of murine preadipocytes with palmitate (C16:0) during the first days of differentiation led to an increase in post-confluent mitoses and subsequently enhanced the number of differentiated adipocytes, as well as expression of late markers compared to cells in a standard medium (with triiodothyronine (T3), insulin and fetal bovine serum (FBS) as adipogenic factors) (Amri et al., 1994). The effects were independent from FA metabolization, as 2-bromopalmitate elicited even higher effects. Another FA with a stimulatory effect on adipogenesis is AA (C20:4(ω -6)): Supplementation of a chemically

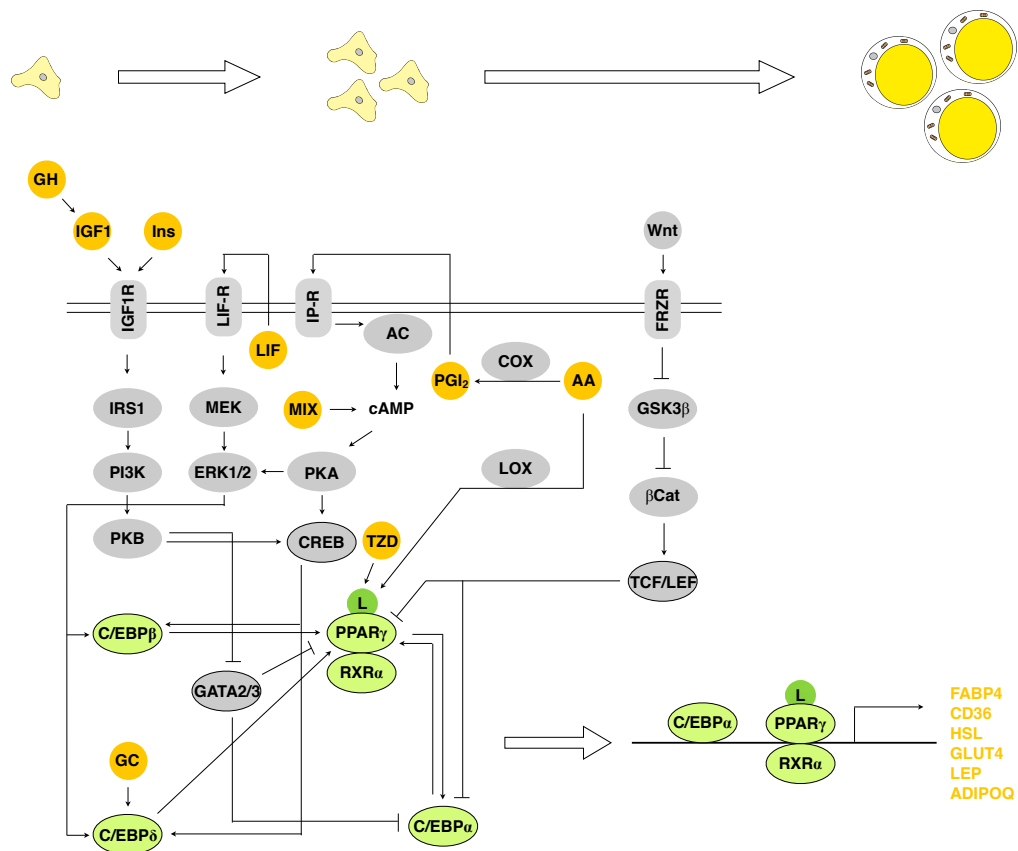


Figure 2. Regulation of white adipocyte differentiation. Selected pathways that stimulate or inhibit white adipogenesis are depicted. Substances that are frequently used as adipogenic media compounds are labeled in orange. Signaling proteins are labeled in grey; transcriptional regulators are depicted encircled and either grey or green to highlight adipogenic key transcription factors. Initially, growth hormone (GH), Insulin-like growth factor 1 (IGF1), or supraphysiological insulin (Ins) concentrations transmit a mitogenic signal via IGF1 receptor (IGF1R), insulin receptor substrate 1 (IRS1), phosphatidylinositol 3-kinase (PI3K), and protein kinase B (PKB, Akt), leading to induction of C/EBP β in preadipocytes (Farmer, 2006; Rosen and MacDougald, 2006). Both C/EBP β and C/EBP δ are upregulated by cAMP-elevating agents like PGI $_2$, metabolized from AA via COX (Massiera et al., 2003) and signaling via the prostacyclin receptor (IP-R), or synthetic compounds like MIX (IBMX) (Otto and Lane, 2005). This pathway involves PKA (activated by cAMP) and cAMP response element binding protein (CREB), which binds to CREs in the C/EBP β and C/EBP δ promoter regions (Belmonte et al., 2001). Similar to PGI $_2$, leukemia inhibitory factor (LIF) is secreted by preadipocytes, but signals via LIF receptor (LIF-R) (Aubert et al., 1999), MAPK kinase (MEK), and ERK to induce C/EBP β and C/EBP δ (Belmonte et al., 2001). C/EBP δ expression is furthermore promoted by glucocorticoids (GC) like Dex (Cao et al., 1991). Subsequently, C/EBP β and C/EBP δ induce expression of PPAR γ , which forms dimers with RXR α . Activity of PPAR γ also depends on ligands, which can be derived from AA via lipoxygenases (LOX) (Madsen et al., 2003). Alternatively, synthetic TZDs can serve as PPAR γ ligands. PPAR γ induces expression of C/EBP α and together, both transcription factors drive the expression of the mature adipocyte gene expression program (Lefterova et al., 2008). Among other negative regulators of adipogenesis, proteins of the Wnt family have been described (Prestwich and MacDougald, 2007). Wnts signal via frizzled receptors (FRZR) to inactivate glycogen synthase kinase 3 β (GSK3 β), leading to β -catenin (β Cat) accumulation and induction of the T cell factor/ lymphoid-enhancing factor (TCF/LEF) transcription factors, which blocks PPAR γ and C/EBP α expression. Furthermore, the GATA family of transcription factors has been described as anti-adipogenic (Tong et al., 2000) and is therefore downregulated by insulin signaling during early adipogenesis (Rosen and MacDougald, 2006).

defined differentiation medium (containing insulin, GH, T3, transferrin and fetuin) with AA promoted adipogenesis of murine Ob1771 cells, which otherwise required an adipogenic fraction of FBS for efficient differentiation (Gaillard et al., 1989). Thus, AA was identified as another adipogenic factor in bovine sera, in addition to GH (Nixon and Green, 1984) and IGF-1 (Smith et al., 1988). Interestingly, AA was also shown to induce a rapid increase in cAMP levels (Fig. 2), a previously known pro-adipogenic signal associated with mitotic clonal expansion of preadipocytes (Schmidt et al., 1990). Subsequently, the effects of AA on cAMP levels, as well as on adipogenesis, could be delineated to COX activity, an enzyme converting AA into PGH₂ (Massiera et al., 2003). PGH₂ in turn can be converted to PGI₂, which is secreted by preadipocytes and acts via the prostacyclin receptor (IP-R) (present on preadipocytes) to increase cAMP (Fig. 2). In summary, AA can act, via an autocrine/endocrine mechanism, to increase the pool of adipocyte precursors which can then differentiate and accumulate lipid. Studies with IP-R^{-/-} mice confirmed the *in vivo* relevance of this feedback loop (Massiera et al., 2003). It should be stated that other studies found an inhibitory effect of AA on adipogenesis *in vitro* (Casimir et al., 1996; Kamon et al., 2001; Petersen et al., 2003). This can be ascribed to differences in composition of the adipogenic cocktail, and/or supraphysiological AA concentrations. Furthermore, AA can be metabolized to other eicosanoids besides PGI₂, e.g. PGF_{2α}, for which both positive (Négrel et al., 1989) and negative (Serrero et al., 1992; Miller et al., 1996) effects on adipogenesis have been described. Thus, the biological stimuli induced by AA are very likely multi-faceted, and a further dissection of mechanisms induced by the individual AA derivatives, as well as the *in vivo* evaluation of findings derived from *in vitro* experiments, will help to harmonize conflicting findings.

As a rather simple hypothesis, a transcription factor with the potential of crucial relevance for adipogenesis should meet two criteria: (1) It should be highly expressed in adipocytes as compared to preadipocytes; (2) it should bind to the regulatory DNA regions (promoter or enhancer) of adipocyte marker genes. Since the late 1980s, studies designed to search for genes fulfilling these criteria have been performed, and several of these have successfully identified adipogenic "key regulatory genes". C/EBPα was identified as highly expressed in adipose tissue (Birkenmeier et al., 1989), as upregulated during 3T3-L1 adipocyte differentiation, and as a transcription factor binding to the murine Fabp4/aP2 promoter region (Christy et al., 1989). Inhibition of C/EBPα in 3T3-L1 cells impaired adipocyte differentiation (Lin and Lane, 1992), while overexpression of C/EBPα in non-adipogenic NIH-3T3 fibroblasts was sufficient to promote differentiation in a medium without adipogenic factors (Freytag et al., 1994). A global knockout of C/EBPα *in vivo* resulted in perinatal lethality in mice, but liver-specific re-expression could improve survival, and the resulting mice were largely devoid of WAT (but not BAT) (Linhart et al., 2001). Among other findings, these indicated the fundamental importance of C/EBPα for white adipogenesis. However, C/EBPα was found to be expressed in several other organs/tissues besides fat, e.g. liver, lung and intestine (Birkenmeier et al., 1989). Thus, it was unlikely that this factor alone can drive an adipocyte-specific gene program.

PPARγ is another transcription factor meeting the above defined criteria. PPARs are a family of nuclear hormone receptors, meaning that their function depends on activation by a small molecule ligand, and dimerization with other proteins (Wang, 2010). As such, PPARγ was identified as a component of the adipocyte regulatory factor 6 (ARF6) complex, which was found to be associated to promoter regions of the aP2 gene in adipocytes, but not in preadipocytes (Graves et al., 1992). The second protein in ARF6 was another nuclear hormone receptor, RXRα (Tontonoz et al., 1994a).

Alternative promoter usage and splicing of the PPAR γ gene was found to generate two isoforms, PPAR γ 1 and PPAR γ 2 (Tontonoz et al., 1994b; Fajas et al., 1997). PPAR γ 1 is expressed in several tissues including fat, but interestingly, the PPAR γ 2 isoform (differing from PPAR γ 1 due to additional amino acids at the N-terminus) was found to be rather adipose-specific (Tontonoz et al., 1994b). Subsequently, PPAR γ 2 was shown to induce adipogenic differentiation of NIH-3T3 fibroblasts cultured with adipogenic factors (Dex, Insulin, FBS) and a PPAR-activating ligand (Tontonoz et al., 1994c). It has later been shown, though, that also PPAR γ 1 possesses pro-adipogenic activity (Mueller et al., 2002). Most importantly, gene disruption studies in mouse confirmed the importance of PPAR γ : Due to the early embryonic lethality of a global PPAR γ knockout, one study analyzed chimaeric mice, but the fact that their adipose tissue consisted solely of wild type (wt) cells (and no PPAR γ ^{-/-} cells) confirmed the indispensability of PPAR γ (Rosen et al., 1999). A further study selectively ablated PPAR γ 2 expression in mice, which prevented embryonic lethality and led to a reduction of WAT and BAT depots (Zhang et al., 2004). Moreover, ESCs and MEFs derived from PPAR γ ^{-/-} embryos were incapable of adipocyte differentiation *in vitro* (Rosen et al., 1999; Kubota et al., 1999). In summary, it is fair to entitle PPAR γ the "master regulator" of adipogenesis, as no other factor has been discovered until now that can promote adipocyte differentiation in the absence of PPAR γ (Rosen and MacDougald, 2006).

On a genome-wide scale, recent investigations have revealed the binding of C/EBP α and PPAR γ to thousands of regulatory DNA elements in 3T3-L1 adipocytes, very often in concert (Lefterova et al., 2008). Thus, both transcription factors seem to cooperatively act in establishing the gene expression program of the mature adipocyte (Fig. 2). However, the induction of C/EBP α and PPAR γ themselves is not an immediately early event in adipogenesis *in vitro*, but seems to be due to the action of other, preceding transcription factors. Indeed, in a screen to identify C/EBP α -related proteins expressed during 3T3-L1 adipocyte differentiation, two further transcription factors, C/EBP β and C/EBP δ , were found as being induced already 24 h after exposure to adipogenic factors, but declining as differentiation proceeded (Cao et al., 1991). The same study furthermore showed that ectopic expression of C/EBP β enabled adipocyte differentiation of NIH-3T3 fibroblasts (in the presence of adipogenic factors). Interestingly, investigation of the promoters of both C/EBP α and PPAR γ revealed the presence of C/EBP regulatory elements (Christy et al., 1991; Clarke et al., 1997). Subsequently, the proposed cascade of adipogenic transcription factors was confirmed: It was shown that C/EBP β and C/EBP δ induce expression of PPAR γ (Wu et al., 1996) and that the latter is a major factor for inducing C/EBP α expression (Rosen and Spiegelman, 2000) (Fig. 2). Although C/EBP β ^{-/-} mice had no obvious defects in adipose tissue development (Tanaka et al., 1995), mice lacking both C/EBP β and C/EBP δ had reduced epididymal WAT and BAT depots, revealing a potential synergism of the two transcription factors (Tanaka et al., 1997). Interestingly, these double knockout mice had normal levels of C/EBP α and PPAR γ , implying an effect of C/EBP β and C/EBP δ on adipogenesis that is not related to their action as transcriptional inducers of PPAR γ .

For many *in vitro* adipogenesis models, differentiation is induced by an adipogenic cocktail containing cAMP elevating agents and glucocorticoids. For example, the standard cocktail for induction of 3T3-L1 cells consists of IBMX, (also designated MIX, a phosphodiesterase inhibitor), Dex (a synthetic glucocorticoid) and supraphysiological concentrations of insulin, acting predominantly via the IGF-1 receptor (Rosen and Spiegelman, 2000). At least partly, the cAMP effects might be mediated via C/EBP β upregulation, while Dex has been shown to promote C/EBP δ expression (Cao et al., 1991) (Fig. 2). Together with the mitogenic stimulus of IGF-1 receptor signaling (Zezulak and

Green, 1986), post-confluent mitoses are promoted before substantial levels of C/EBP α and PPAR γ accumulate in order to execute the terminal steps of adipocyte formation. PPAR γ , though, has to be ligand-activated, and hence a ligand or its precursor has to be provided by the differentiation medium. The true endogenous ligands of PPAR γ are still debated, but are widely supposed to be FAs or FA-derivatives and therefore might be derived e.g. from AA via the action of lipoxygenases (LOX, Fig. 2), enzymes that synthesize leukotrienes (Madsen et al., 2003). Standard differentiation of 3T3-L1 cells is conducted in the presence of FBS (or FCS), which is a rich source of different FAs, and thus provides a source for the PPAR γ ligand. In line with this, sufficient differentiation of Ob1771 preadipocytes in a chemically defined medium is only possible in the presence of AA (Gaillard et al., 1989). Another strategy for adipocyte differentiation under defined conditions involves synthetic PPAR γ ligands like rosiglitazone, a thiazolidinedione (TZD), which is necessary for differentiation of hMADS cells (Rodriguez et al., 2004a). Interestingly, primary preadipocytes can be efficiently differentiated without the addition of serum, FAs or TZDs (Deslex et al., 1987), but their differentiation capacity is reduced after proliferation *in vitro* (Hauner et al., 1989). Thus, it is assumed that primary preadipocytes still possess sufficient amounts of the endogenous PPAR γ ligand (or the capacity to synthesize the ligand), but that the ligand (or the capacity) is progressively lost in the *in vitro* environment.

In addition to the aforementioned pro-adipogenic genes, several negative regulators of adipogenesis have been identified. Among others, the transcription factors GATA2 and GATA3 have been described as decreasing early during adipogenic differentiation of 3T3-F442A preadipocytes, and to impair adipogenesis if constitutively expressed (Tong et al., 2000) (Fig. 2). Furthermore, Wnt signaling has been identified as an anti-adipogenic pathway (Fig. 2): Its inhibition permitted spontaneous differentiation of 3T3-L1 preadipocytes without adipogenic factors (Ross et al., 2000), and transgenic mice overexpressing Wnt10b under the control of the aP2 promoter have a reduced WAT mass, as well as non-functional BAT (Longo et al., 2004). Another extracellular protein with inhibitory action on adipogenesis is Preadipocyte factor 1 (Pref-1, Dlk1). Expressed and secreted by preadipocytes but absent in adipocytes, Pref-1 has been shown to prevent adipocyte differentiation of 3T3-L1 cells (Smas and Sul, 1993; Sul, 2009). Furthermore, Pref-1^{-/-} mice display increased (Moon et al., 2002), while mice overexpressing Pref-1 display decreased WAT and BAT mass (Lee et al., 2003).

In contrast to the plenty *in vitro* systems available for studying white adipocyte differentiation, models for brown adipogenesis are relatively sparse. To date, a lot of studies have relied on primary cultures of preadipocytes derived from the BAT SVF of various mammals (Rehnmark et al., 1989; Champigny et al., 1992; Klaus et al., 1991; Casteilla et al., 1991). In order to yield more convenient models, some transformed cell lines, e.g. the HIB 1B (Klaus et al., 1994) or the HB2 cell lines (Irie et al., 1999), have been established from rodent BAT. However, beside the oncogenic transformation (which might limit the suitability of these models with respect to certain physiological aspects), they also express rather low levels of UCP1 (and other markers of the brown phenotype) in comparison to BAT (Rohlfs et al., 1995; Hansen and Kristiansen, 2006). Interestingly, continuous rosiglitazone treatment has recently been shown to induce adipogenesis with expression of UCP1 mRNA and protein, as well as other BAT markers, in a subpopulation of cells isolated from human SM; however, the ability for brown adipogenesis seemed to decline by subsequent passaging (Crisan et al., 2008a). Likewise, addition of rosiglitazone during differentiation of mouse primary preadipocytes derived from epididymal WAT promoted UCP1 expression and NE-induced thermogenesis (Petrovic et al., 2010). A similar effect has recently been demonstrated in hMADS cells, where chronic

rosiglitazone treatment resulted in the expression of UCP1 and other BAT markers, and also enhanced uncoupled respiration (Elabd et al., 2009). Although a thorough comparison between these *in vitro*-differentiated brown adipocytes and brown adipocytes from either mouse or human BAT (e.g. analysis of quantitative differences in UCP1 protein levels and thermogenic activity) has not been published yet, it is fair to say that hMADS cells constitute a highly valuable tool to study brown adipogenesis, as they are at present the only such model for human that can be extensively propagated *in vitro* without a loss of differentiation capacity.

The remarkable effect of rosiglitazone on promotion of a brown phenotype in various cells already highlights a role of ligand-activated PPAR γ for brown adipogenesis. Indeed, the importance of PPAR γ for BAT development could also be inferred from *in vivo* studies (Barak et al., 1999; Rosen et al., 1999). Mechanistically, the induction of UCP1 is (at least partly) mediated via a PPAR response element (PPRE) in a UCP1 enhancer region that is conserved between rodents and human (Barbera et al., 2001; Sears et al., 1996) (Fig. 3). As for other transcription factors with pivotal role in white adipogenesis, the dispensability of C/EBP α (Linhart et al., 2001), but the involvement of C/EBP β and C/EBP δ (Tanaka et al., 1997) in BAT development have already been mentioned above.

However, neither of the aforementioned transcriptional regulators is selectively expressed in BAT versus WAT, and hence other decisive genes must be implied in the establishment of a brown versus a white phenotype (regardless of the type of progenitor cell). In a screen for proteins that directly interact with PPAR γ in brown adipocytes, PGC-1 α was initially identified as being expressed in mouse BAT, but not in WAT (Puigserver et al., 1998) (but was subsequently also detected there (Tsukiyama-Kohara et al., 2001)). PGC-1 α was shown to be induced in BAT and SM upon cold exposure, to enhance PPAR γ -mediated UCP1 transcription, and, if overexpressed, to induce brown adipocyte-like traits in 3T3-F442 cells (Puigserver et al., 1998). In addition, PGC-1 α was shown to promote mitochondriogenesis and to increase oxygen consumption in myoblast cells (Wu et al., 1999a). Subsequently established PGC-1 α ^{-/-} mice exhibited an abnormal BAT morphology with larger lipid droplets and sensitivity to cold; however, the same study also highlighted the importance of this gene in other tissues like liver and brain (Lin et al., 2004). Thus, it is not clear whether the effects of PGC-1 α are autonomous to BAT or at least partly originate from secondary effects in other tissues, e.g. the CNS via defective SNS signaling (Uldry et al., 2006).

In another screen performed by Spiegelman and co-workers, the zinc finger protein PRDM16 was identified as being highly expressed in brown adipocytes compared to white adipocytes *in vitro* (Seale et al., 2007). PRDM16 mRNA was also found to be expressed at high levels in mouse BAT, but essentially absent in WAT *in vivo*, and some low levels were expressed in brain, heart and lung. Expression of PPAR γ 2 and Prdm16 or a control vector in non-adipogenic fibroblasts enabled adipocyte differentiation of these cells in the presence of adipogenic factors, and although lipid accumulation and expression of general adipocyte markers was similar between PPAR γ 2/Prdm16 and PPAR γ 2/control cells, PRDM16 promoted expression of brown adipocyte markers *in vitro*. Furthermore, mice expressing PRDM16 under the control of the aP2 promoter showed a more pronounced expression of BAT markers and a more BAT-like morphology of WAT depots after treatment with a β 3-adrenergic receptor agonist. Reduced expression of BAT markers upon knockdown of PRDM16 during differentiation of primary BAT-derived preadipocytes confirmed the necessity of PRDM16 for brown adipogenesis, and biochemical studies indicated that PRDM16 stimulates PGC-1 α activity via direct interaction (Seale et al., 2007) (Fig. 3). A subsequent study established PRDM16 as a decisive factor between myoblasts and brown adipocytes: While PRDM16 knockdown in primary

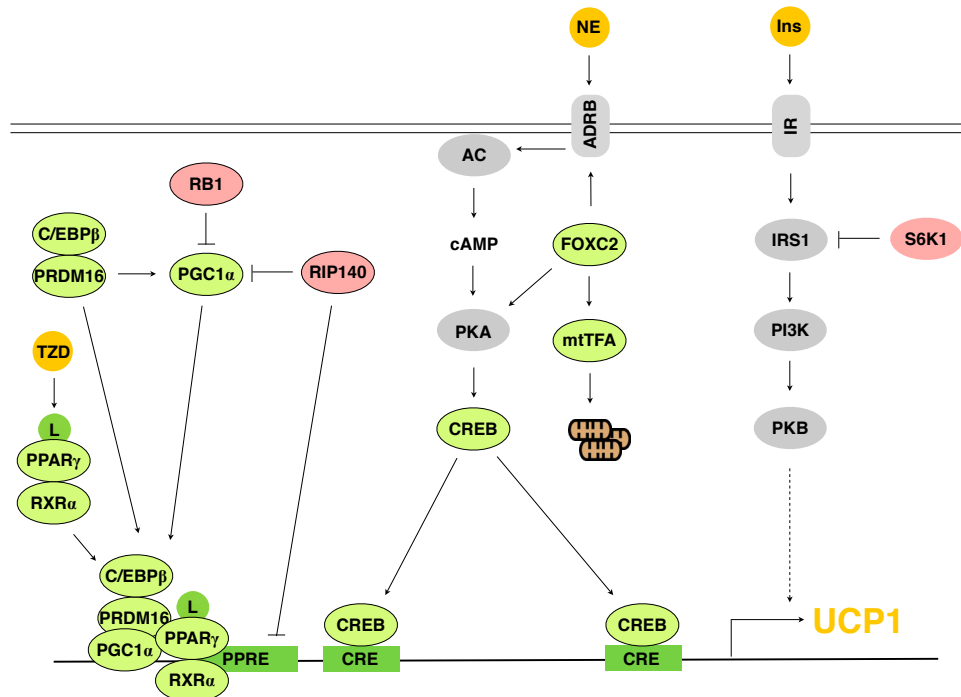


Figure 3. Regulation of UCP1 expression during brown adipocyte differentiation.

Selected pathways that stimulate or inhibit expression of UCP1, the classical brown adipocyte marker and indispensable protein for BAT thermogenesis, are schematized. Positive transcriptional regulators of UCP1 are depicted in green and encircled; inhibitors of UCP1 are depicted in red; signaling proteins are labeled in grey. Norepinephrine (NE) is the initial physiological stimulus, released by neurons of the sympathetic nervous system (SNS) and binding to β -adrenergic receptors (ADRB) on the brown adipocyte cell surface. The signal is transmitted via activation of adenylyl cyclase (AC), leading to enhanced cyclic adenosine monophosphate (cAMP) levels, activation of protein kinase A (PKA) and phosphorylation of cAMP response element binding protein (CREB) (Cannon and Nedergaard, 2004). Subsequently, activated CREB enters the nucleus to bind to two conserved cAMP response elements (CRE) in the UCP1 enhancer and promoter regions, thereby inducing UCP1 transcription. The transcription factor forkhead box C2 has been described to enhance β -adrenergic signaling (Cederberg et al., 2001), and also to stimulate mitochondriogenesis via induction of the mitochondrial transcription factor A (mtTFA) (Lidell et al., 2011). A central regulator of UCP1 expression is PPAR γ coactivator 1 α (PGC-1 α), which potentiates the action of PPAR γ at the PPAR response element (PPRE) located in the UCP1 enhancer region (Puigserver et al., 1998). Furthermore, PGC-1 α is induced by a complex of C/EBP β and PR domain containing 16 (PRDM16) (Kajimura et al., 2009), and PRDM16 has also been shown to directly interact with and stimulate the transcriptional activity of PPAR γ (Seale et al., 2008). In addition to these PPAR γ -interacting proteins, activation of PPAR γ by thiazolidinediones (TZDs) has also been shown to promote UCP1 expression (Laplante et al., 2003; Elabd et al., 2009). Nuclear receptor interacting protein 1 (RIP140) was found to directly interact with PGC-1 α and inhibit its function (Hallberg et al., 2008), and to have a repressive action at the UCP1 enhancer (Christian et al., 2005). Furthermore, retinoblastoma (RB1) protein was shown to block PGC-1 α transcription (Scimè et al., 2005). Insulin signaling, mediated via insulin receptor (IR), insulin receptor substrate 1 (IRS1), phosphatidylinositol 3-kinase (PI3K), and protein kinase B (PKB), was also demonstrated as important for brown adipogenesis and UCP1 expression (Fasshauer et al., 2001). The suppressive role of ribosomal protein S6 kinase (S6K1) on UCP1 and other BAT characteristics (Um et al., 2004) might be due to its interference with insulin signaling by inhibitory phosphorylation of IRS1 (Um et al., 2006).

brown preadipocytes resulted in differentiation towards skeletal myocytes, PRDM16 overexpression in myoblasts promoted brown adipogenesis (Seale et al., 2008) (Fig. 1). Additionally, the study showed a stimulation of PPAR γ transcriptional activity by PRDM16, presumably via direct interaction (Fig. 3). In a further study, the effect of PRDM16 was shown to depend on direct interaction with C/EBP β (Fig. 3), and transplantation of MEFs overexpressing both genes into nude mice led to the formation of brown fat pads that exhibit pronounced glucose uptake *in vivo* (Kajimura et al., 2008). Interestingly, although the introductory publication described PRDM16 as "virtually absent in WAT" (Seale et al., 2007), a recent study by Spiegelman and co-workers put their own statement into perspective by detection of PRDM16 protein in subcutaneous WAT of mice (Seale et al., 2011). Furthermore, the study again investigated aP2-PRDM16 mice, showing that PRDM16 overexpression selectively induces a brown gene expression program and thermogenesis in subcutaneous WAT, thereby ameliorating HFD-induced weight gain and improving insulin sensitivity (Seale et al., 2011). Another promoter of the brown adipocyte phenotype is the transcription factor Forkhead box C2 (FOXC2). FOXC2 was identified as being expressed exclusively in adult human WAT, and in mouse WAT and BAT (Cederberg et al., 2001). Genetic ablation of FOXC2 results in embryonic or perinatal lethality; however, fat-specific overexpression of FOXC2 in mice could be investigated. The transgenic mice showed a marked expansion of interscapular BAT, but a reduction of intraabdominal WAT, the latter exhibiting a brown color (Cederberg et al., 2001). Moreover, transgenic mice had lower body fat percentage, were more insulin sensitive and gained less weight on a HFD compared to wt littermates. The effects could be explained by elevated levels of β -adrenergic receptors and a FOXC2-mediated transcriptional induction of RI α , the regulatory subunit of PKA (Cederberg et al., 2001). Hence adipocytes overexpressing FOXC2 exhibited an increased sensitivity for β -adrenergic stimulation (Fig. 3). Subsequent studies have further elicited the transcriptional activities of FOXC2 in adipocytes, showing that it can stimulate mitochondrial biogenesis by induction of the mitochondrial transcription factor A (mtTFA, Tfam) (Lidell et al., 2011) (Fig. 3), and modulate the adipose tissue vasculature by promoting transcription of the vascular remodeling factor Ang-2 (Xue et al., 2008).

Aside from transcriptional regulators, COX activity has recently been implied in the "browning" of WAT in response to cold: Exposure to 4°C induced COX-2 mRNA in intra-abdominal WAT of mice, and the emergence of multilocular, UCP1⁺ adipocytes in WAT by β -adrenergic stimulation was shown to be dependent on COX-2 activity (Vegiopoulos et al., 2010). Furthermore, the presence of a PGI₂ analogue during adipocyte differentiation of human mesenchymal stem cells induced BAT markers (Vegiopoulos et al., 2010), while administration of a PGE₂ analogue produced similar effects in WAT of mice (Madsen et al., 2010). As for PGI₂, a relation of these recent findings to earlier studies in which PGI₂ promoted (white?) adipogenic differentiation of Ob1771 preadipocytes (Massiera et al., 2003; Vassaux et al., 1992) would be interesting, but the expression of BAT markers was not assessed in the early studies.

Gene silencing or overexpression studies have also revealed negative regulators of the brown phenotype. RIP140 is a corepressor of many nuclear receptors. RIP140^{-/-} mice have a pronounced reduction of total body fat compared to wt mice, and are less prone to weight gain and metabolic disturbances on a HFD due to the emergence of brown (UCP1⁺) adipocytes in WAT (Leonardsson et al., 2004). Subsequent *in vitro* studies with MEFs and primary preadipocytes confirmed the increased metabolic activity of RIP140^{-/-} adipocytes and also showed a recruitment of RIP140 to the UCP1 enhancer region (Christian et al., 2005) (Fig. 3). In addition, RIP140 protein was found to directly interact with and thereby inhibit PGC-1 α in brown adipocytes (Hallberg et al., 2008) (Fig.

3). The RB1 gene is a famous tumor suppressor protein (also designated pRB), but was later discovered to regulate adipogenesis as fibroblasts from pRB^{-/-} mice failed to differentiate into adipocytes, and was also shown to directly interact with and activate C/EBPs (Chen et al., 1996b). Interestingly, a study comparing adipogenesis of MEFs from pRB^{-/-} and wt mice showed that absence of pRB did not prevent differentiation, but resulted in expression of BAT markers and increased mitochondrial density (Hansen et al., 2004). Mechanistically, a repression of PGC-1 α transcription by pRB was shown in 3T3-L1 cells via binding of pRB to the PGC-1 α promoter (Scimè et al., 2005) (Fig. 3). The *in vivo* relevance was further confirmed in mice with adipose-tissue specific pRB deficiency, which were protected against HFD-induced weight gain due to increased energy expenditure, most likely caused by increased thermogenesis in WAT and BAT depots (Dali-Youcef et al., 2007). Further genes with an inhibitory effect on the brown phenotype *in vitro* and *in vivo* include the transcription factor TWIST1, inhibiting PGC-1 α via direct interaction (Pan et al., 2009) and S6K1, the knockout of which induced PGC-1 α and UCP1 expression in WAT (Um et al., 2004).

To conclude, while general regulators of adipogenesis have been identified in the last years, there are also molecular regulators which are either important for development of a brown or a white phenotype. Importantly, at least some BAT depots seem to be more closely related to SM than to WAT, and it has been argued that these depots contain the "genuine" brown adipocytes. However, it is also a fact that, under certain physiological and pharmacological conditions, adipocytes very closely resembling genuine brown adipocytes emerge within classical WAT depots (Fig. 1). These brown-like adipocytes are different from genuine brown adipocytes in that they lack the expression of some SM-related markers and thus have been designated "brite" (Petrovic et al., 2010) (brown-in-white) or "beige" (Seale et al., 2011) adipocytes. Still, these brite adipocytes express UCP1, are capable of thermogenesis and thus of potential significance for whole-body energy homeostasis. Indeed, it has been shown that the ability to induce brite adipocytes in WAT correlates with the degree of weight loss in response to treatment with β_3 -adrenergic receptor agonists (Guerra et al., 1998). From a basic research perspective, it will be of interest to find out whether brown adipocytes in BAT of adult humans more resemble the genuine brown or the brite adipocytes (Seale et al., 2011). From a therapeutic perspective, it might be of even higher interest to evaluate whether a transformation of existing WAT into BAT is possible without side effects, and at a scale that is large enough to significantly enhance the metabolic rate.

1.2.4 Endocrine Functions of Adipose Tissue

The discovery of signaling proteins which are released by adipose tissue into the bloodstream has resulted in a paradigm shift, as adipose tissue today is no longer considered a merely passive energy tank. Most follow-up complications of the obese state have not only been linked to the exhausted lipid-storage capacity of adipose tissue, but also to altered serum levels of adipose tissue-secreted factors (Ahima and Flier, 2000). Thus, elucidating the physiology and pathophysiology of adipose tissue cytokines (adipokines) might provide crucial starting points for drug development to fight the sequels of obesity. Some of these adipokines will be discussed in this section.

The starting point for adipokine research was the discovery that a single gene mutation was responsible for a severely obese phenotype in the *ob/ob* mouse (Zhang et al., 1994). The corresponding *ob* gene was shown to code for a protein which is produced almost exclusively by adipose tissue

and subsequently released into the bloodstream. As invalidation of this secretory factor caused obesity, it was deduced to act negatively on energy balance and was therefore named *leptin* (from the greek term for "thin") (Halaas et al., 1995). Within adipose tissue, leptin is synthesized mainly by adipocytes (Fain et al., 2004b). Plasma levels of leptin are positively correlated to BMI and decrease after weight loss (Maffei et al., 1995). Thus, leptin constitutes a hormonal signal by which adipocytes (the body's long-term energy storage) relay nutritional status. Recipient cells of the leptin signal were shown to be neurons located in the hypothalamus, in which high expression of the leptin receptor ObRb was found (Lee et al., 1996). Interestingly, the phenotype of another mouse obesity model (*db/db* mice) was shown to be caused by mutations in the ObRb gene (Chen et al., 1996a), and thus, the leptin effect was proposed to be predominantly mediated via central, hypothalamic signals. Subsequent studies revealed that Leptin, via its receptor, simultaneously inhibits neurons expressing orexigenic peptides (neuropeptide Y (NPY), Agouti-related peptide(AgRP)), and stimulates neurons expressing POMC to generate and release melanocortins out of POMC (Oswal and Yeo, 2010). Melanocortins, in turn, elicit neuronal signals which decrease food intake and increase energy expenditure (Coll et al., 2008). Although leptin administration to leptin deficient mice could induce pronounced weight loss (Halaas et al., 1995), its use for treatment of obese humans has turned out as only modestly effective (Heymsfield et al., 1999). As mentioned above, leptin levels correspond to body/fat mass and therefore are highest in the obese state, and hence, a resistance to leptin has been proposed, caused by decreased transport of the hormone across the blood-brain barrier and/or by diminished leptin receptor function (Oswal and Yeo, 2010). It is therefore accepted that the physiological importance of leptin is not its action as a satiety signal, but rather as a starvation signal which, if declining, triggers food intake as well as other mechanisms to re-achieve a positive energy balance (Friedman, 2000). Interestingly, leptin and UCP1 seem to be inversely correlated in adipose tissue as leptin is mainly produced by white adipocytes (Cinti, 2001), and leptin synthesis by brown adipocytes is increased in warm-acclimated animals in which UCP1 is decreased (Cancello et al., 1998). However, the effects of leptin clearly have a stimulatory component on non-shivering thermogenesis: Intravenous administration of leptin increased the sympathetic outflow to BAT in rats (Haynes et al., 1997), and a mouse model with enhanced signaling of leptin-sensitive neurons developed UCP1⁺ adipocytes within WAT depots, leading to enhanced metabolic activity and reduced weight (Plum et al., 2007).

An adipokine with main effects on other metabolic tissues is *adiponectin* (Acrp30, ADIPOQ), identified in 1995 in mouse as an adipose tissue-selective gene that is highly induced during adipocyte differentiation *in vitro* (Scherer et al., 1995). Subsequent analysis revealed a high and exclusive expression of adiponectin also in human adipose tissue (Maeda et al., 1996), and relatively high circulating levels in the range of $\mu\text{g/mL}$ (Chandran et al., 2003). In contrast to leptin and most other adipokines, adiponectin serum levels were found to be decreased in the obese state (Arita et al., 1999), and also to be low in individuals with type 2 diabetes or the risk of developing the disease (Hotta et al., 2000; Daimon et al., 2003). Adiponectin shares homology to collagens type VIII and X, and to a factor of the human complement system, C1q (Nakano et al., 1996; Scherer et al., 1995), and forms homomultimers in the bloodstream, which is possibly necessary for its function (Waki et al., 2003). The importance of adiponectin for insulin sensitivity was underscored by *in vivo* studies of adiponectin-deficient mice, which developed insulin resistance (Kubota et al., 2002; Maeda et al., 2002), while transgenic mice with higher circulating adiponectin levels displayed improved glucose tolerance (Combs et al., 2004). In line with this, the two identified receptors for adiponectin, adipoR1 and adipoR2, are primarily expressed in muscle and liver, respectively (Ker-

shaw and Flier, 2004). Adiponectin was shown to enhance FA β -oxidation in muscle (Yamauchi et al., 2001), to increase glucose uptake of myocytes, and to suppress gluconeogenesis in liver (Yamauchi et al., 2002; Chandran et al., 2003). Thus, adiponectin seems to improve the metabolic profile via pleiotropic mechanisms, and it is conceivable that TZDs, which are used as insulin-sensitizing drugs, exert their effect in part via PPAR γ -mediated upregulation of adiponectin in overweight and obese subjects (Maeda et al., 2001). In addition to the beneficial effects on glucose metabolism, adiponectin has also anti-atherogenic activity, evidenced by epidemiological studies which showed lower levels in patients with coronary heart disease (compared to age- and BMI-matched controls) (Ouchi et al., 1999), by studies with mouse models of atherosclerosis (Okamoto et al., 2002), and by *in vitro* experiments showing a protective effect against inflammatory stimuli in endothelial cells (Ouchi et al., 2000).

TNF α is an inflammatory cytokine produced mainly by immune cells, but was discovered to be also expressed at significant levels in adipose tissue of obese and diabetic mice (Hotamisligil et al., 1993) and humans (Hotamisligil et al., 1995). While initial findings proposed adipocytes to be the main source of adipose tissue TNF α (Hotamisligil et al., 1993), later studies showed a predominant contribution of non-adipocyte cells (Fain et al., 2004a; Xu et al., 2003). Indeed, the infiltration of WAT by macrophages is well described in obesity (Xu et al., 2003), very likely contributing to the state of chronic low-grade inflammation (Gregor and Hotamisligil, 2011), and might also be causative of the elevated TNF α production (Weisberg et al., 2003). Although TNF α treatment induces insulin resistance (Lang et al., 1992) and inhibition of TNF α improves insulin sensitivity in rodents (Hotamisligil et al., 1994), only some studies identified a correlation between BMI and circulating TNF α levels (Dandona et al., 1998; Zahorska-Markiewicz et al., 2000) while others were not able (Hauner et al., 1998). Hence, it is still unclear whether TNF α is an adipokine with relevant endocrine mechanisms. What is widely accepted, though, is the local contribution of TNF α to detrimental changes in adipose tissue. For instance, the anti-adipogenic action of TNF α is well-established (Xu et al., 1999) and has been delineated to inhibition of PPAR γ and C/EBP α transcription (Cawthorn and Sethi, 2008; Ron et al., 1992). TNF α also acts to increase lipolysis in adipocytes (Patton et al., 1986), thereby contributing to elevated levels of serum FAs. Furthermore, the local effects of TNF α include the regulation of other adipokines: adiponectin, the aforementioned beneficial adipokine, is decreased by TNF α (Fasshauer et al., 2002), while the secretion of other adipokines with adverse effects on metabolism, e.g. interleukin-6 (IL-6), is induced (Ahn et al., 2007). Altogether, these effects might explain at least in part the described association of TNF α with insulin resistance (Cawthorn and Sethi, 2008).

Another important adipokine which is induced by TNF α is *Plasminogen activator inhibitor-1* (PAI-1) (also designated SERPINE1) (Sawdey and Loskutoff, 1991; Hou et al., 2004). PAI-1 is a serine protease central to the fibrinolytic system, preventing the degradation of fibrin clots via inhibition of plasminogen activators, and as such was initially discovered to be synthesized by endothelial cells (van Mourik et al., 1984). However, Juhan-Vague and co-workers showed that PAI-1 is also secreted by adipose tissue (Morange et al., 1999), and that its expression in adipose tissue is positively correlated with BMI (Alessi et al., 2000). Plasma PAI-1 levels are also elevated in subjects with impaired glucose tolerance (Pannacchiulli et al., 2002) or MetS (Alessi and Juhan-Vague, 2006), and interestingly, high baseline PAI-1 levels in healthy individuals have been identified as predictor for the development of type 2 diabetes (Festa et al., 2006). Due to its inhibitory role on fibrinolysis, PAI-1 appears as a cause for thrombotic disease states, and indeed, PAI-1 plasma levels are correlated with the risk for cardiovascular disease (Kohler and Grant, 2000). Similar to TNF α , it

has been revealed that adipocytes are not the only and maybe just a minor source of PAI-1: A study on human adipose tissue found higher PAI-1 protein levels in the SVF than in the AF for both subcutaneous and visceral samples (Bastelica et al., 2002), and also during adipocyte differentiation of hMADS cells, PAI-1 secretion could never be detected (Chiellini et al., 2008). However, another study with mice found comparable mRNA levels of PAI-1 between SVF and AF (Samad and Loskutoff, 1996). Despite these conflicting data, it is generally accepted that the amounts of PAI-1 produced by adipose tissue substantially contribute to plasma PAI-1 levels (Morange et al., 1999). Although epidemiological studies strongly suggest a connection between PAI-1 and insulin resistance, data on molecular mechanisms by which PAI-1 might impair insulin signaling is sparse. For instance, a study on murine fibroblasts showed that PAI-1 can impair the stimulating action of $\alpha v \beta 3$ integrin on insulin signaling via competitive binding to vitronectin (VN) (López-Alemayn et al., 2003).

Angiotensinogen ATG is the precursor of angiotensin II, a peptide that increases blood pressure, and is mainly synthesized by the liver. However, ATG is also produced by human WAT (Karlsson et al., 1998), which also expresses many other components of the RAAS (Schling et al., 1999). Beside the local effect of angiotensin II as a stimulator of adipocyte differentiation (Saint-Marc et al., 2001), it has recently been shown that ATG synthesis by WAT is relevant to ATG plasma levels: Fat-specific reexpression of ATG in ATG^{-/-} mice leads to the emergence of ATG in the bloodstream and restores blood pressure, and wt mice overexpressing ATG in adipose tissue were hypertensive (Massiéra et al., 2001). Thus, the positive correlation between body weight and expression of ATG in WAT (Van Harmelen et al., 2000) seems to explain (at least partly) the frequent association between hypertension and obesity (Wolf et al., 1997).

1.3 microRNAs

Although philosophical discussions and scientific studies about biology had been performed already in ancient Greece, the most groundbreaking insights into the molecular mechanisms of life have probably been revealed in the last century, with the discovery of DNA as the uniform genetic substance across all species of life on earth. As the principle of DNA appeared that fundamental approaches to relate it to the wide range of complexity among living beings were obvious. However, it was soon realized that the amount of cellular DNA does not correspond to the complexity of an organism, as for example the genome size of several amphibians is in the range of 10^{11} bp, while the human genome comprises only $3.2 * 10^9$ bp. A solution to this incoherence seemed to emerge from studies on genome structure, showing that at least in eukaryotes the vast majority of DNA is non-(protein-)coding and was therefore regarded as "junk" DNA that is dispensable for the function of an organism (Alberts et al., 2002b). However, when taking into consideration only the number of "genes" (at that time defined as a protein-coding DNA sequence (exons) plus introns and flanking untranslated regions), the paradox still remained: For example, the human genome harbors fewer than 20 000 (Goodstadt and Ponting, 2006), while the protozoan *Tetrahymena thermophila* (a single-cell eukaryote) has 27 000 (Eisen et al., 2006) such genes.

Today, it seems that focus on the non-coding part of the genome has solved the complexity problem, as it was found that the fraction of non-coding DNA (in % of total DNA) correlates well with the complexity of different organisms, from bacteria via protozoans, plants and arthropods

through to vertebrates (Taft et al., 2007). As an interesting complementary finding, a recent study on 1% of the human genome revealed that, unexpectedly, the majority of DNA is transcribed (ENCODE Project Consortium et al., 2007), meaning that there is substantial transcriptional activity beyond the borders of previously annotated, protein-coding ORFs (Johnson et al., 2005). Indeed, there are estimations that as much as 98% of transcriptional output in human are believed to be non-coding RNA (ncRNA) (Mattick, 2001). This implies that ncRNA is *precisely not* "junk", but probably the distinguishing factor enabling the development of a complex, multicellular mammal as opposed to a more simple unicellular eukaryote— despite the comparable number of protein-coding DNA sequences. Correspondingly, multi-faceted regulatory roles of various ncRNA species in a broad range of cellular processes have already been discovered (but might still be the tip of the iceberg). For instance, PIWI-interacting RNAs (piRNAs) appear necessary for transposon silencing in the germline (Khurana and Theurkauf, 2010), endogenous small interfering RNAs (endo-siRNAs) are implied in viral defence mechanisms (Ghildiyal and Zamore, 2009), promoter-associated RNAs (PARs) seem to work in transcriptional regulation (Taft et al., 2009), and long non-coding RNAs (lncRNAs) function as epigenetic regulators (Wilusz et al., 2009).

MicroRNAs (miRNAs) are probably the best characterized class of ncRNAs and have already been linked to diverse processes like cell growth, cell division, cell death, or cell differentiation. This section will summarize the discovery of miRNAs, their biogenesis and mechanisms of action, and will also discuss some involvements of miRNAs in diseased states uncovered to date.

1.3.1 RNA interference and microRNA discovery

In order to interfere with the function of protein-coding genes, RNA antisense strategies have been pursued in the 1990s, where e.g. a plasmid encoding an RNA transcript with perfect antisense complementarity to the gene of interest was introduced in cells of model organisms like the nematode *Caenorhabditis elegans* (*Cel*) (Fire et al., 1991). In this case, the large amounts of antisense transcript were thought to base-pair with the endogenous (sense) mRNA and thereby prevent translation. However, in a crucial study on *RNA interference* (*RNAi*) in *Cel* by Fire and co-workers, four important observations were made: First, double-stranded RNA (dsRNA), i.e. a complex of sense and antisense transcript with perfect complementarity) was far more efficient in silencing a gene of interest than either the (single-stranded) sense or antisense RNA. Second, dsRNA treatment efficiently and specifically decreased the mRNA levels of the gene of interest. Third, very low concentrations of dsRNA were effective, raising the possibility of a catalytical mechanism of action, and/or endogenous amplification of the silencing signal. Fourth, the dsRNA effect was transmitted both horizontally (i.e. spreading from injected cells to other cells) and vertically (i.e. passed on to the progeny) (Fire et al., 1998). A similar phenomenon of RNAi was subsequently reproduced in other animals, but also fungi and plants (Mello and Conte, 2004). Furthermore, extracts of dsRNA-transfected cells from the fruitfly *Drosophila melanogaster* (*Dme*) were shown to possess a nuclease activity that is specific against RNAs with complementary sequences (Hammond et al., 2000). As the same study also found an association of this enzyme with small RNAs that were derived from the (longer) transfected dsRNA, the term *RNA-induced silencing complex* (*RISC*) was introduced in order to designate a catalytic protein-RNA complex that is central to the mechanism of RNAi. Tuschl and co-workers subsequently demonstrated that duplexes of 21- and 22-nt RNAs, paired with short 3'-overhangs, serve as "guides" for sequence-specific mRNA degradation, and that the mRNA

is cleaved in the middle of the region complementary to the guide RNA (Elbashir et al., 2001b). The potency of these *small interfering RNAs (siRNAs)* for specific gene "knockdown" was further demonstrated in human cells (Elbashir et al., 2001a). Altogether, it is fair to say that research within three years was sufficient to introduce an unprecedented, powerful and convenient tool to study gene function, and only a decade later, RNAi techniques are used in essentially all molecular biology laboratories around the world.

The discovery that many eukaryotic cells are equipped with an enzymatic machinery for targeted RNA degradation simultaneously raised the question for its physiological purpose. First explanations suggested RNAi to be a cellular defense mechanism against invaders like viruses (Ratcliff et al., 1999), which frequently rely on dsRNA intermediates. This is certainly true for plants and lower vertebrates, however, the necessity of this mechanism in mammals is debated (Cullen, 2006). In addition, though, another purpose for RNAi is known today, a purpose connected to initial observations which had been made even before the groundbreaking studies on dsRNA: Already in 1993, Ambros and co-workers described that the (previously known) gene *lin-4*, necessary for normal postembryonic development of *Cel*, was transcribed but not translated and hence exerting its function as RNA (Lee et al., 1993). The same study also found a 22 nt region of *lin-4* with sequence complementarity to the 3' UTR of the protein-coding gene *lin-14* and therefore suggested an antisense RNA-RNA interaction as mechanism of action. However, it was not before 2000 that the second gene with similar properties was discovered: *let-7* was demonstrated by Ruvkun and co-workers to be another non-coding gene that regulated *Cel* development, and also to give rise to a 21 nt RNA with remarkable complementarity to sequences in the 3'-untranslated region (3'UTR)s of protein-coding genes (Reinhart et al., 2000). Strikingly, homologs of the 21 nt form of *let-7* could be identified in many other animal species including human (Pasquinelli et al., 2000). A more general biological mechanism of gene regulation could thus be anticipated. This notion was further supported by a set of three publications describing the identification of several further small RNAs in *Cel*, *Dme*, zebrafish, frog, mouse and human cells or tissues, and also introducing a the new term *microRNAs* (miRNAs) for these endogenously expressed transcripts (Lagos-Quintana et al., 2001; Lee and Ambros, 2001; Lau et al., 2001).

The similar size of microRNAs (miRNAs) compared to siRNAs immediately suggested a similar mechanism of action. On the other hand, several differences between miRNAs and siRNAs were also apparent from the beginning. For instance, while siRNA mechanisms always resulted in degradation of the target mRNA, the first discovered miRNAs had a negative effect on target protein levels without affecting mRNA stability. Furthermore, while siRNAs are processed from two molecules of larger dsRNA, miRNAs are generated via transcription of a single RNA molecule that folds into a characteristic hairpin loop. However, it was subsequently shown that the two pathways of miRNA- and siRNA-mediated RNAi converge at least at a certain point, as invalidation of the gene *dcr-1* in *Cel* abolished both the effect of siRNAs, as well as processing of the *lin-4* and *let-7* precursor RNAs (Grishok et al., 2001).

In summary, methodological studies focused on silencing the expression of protein-coding genes were of substantial importance beyond the technical field, as they paved the way to explain the mechanisms of RNA-directed gene regulation in a physiological context, a phenomenon which had already been observed before.

1.3.2 microRNA biogenesis and function

Since the discovery of the first mammalian miRNAs a decade ago, several hundreds of distinct miRNAs have been identified in mouse and human. Mapping of miRNA sequences to the genome revealed that approximately 50 % of human miRNAs are located in introns of protein-coding genes, while the remaining 50 % have been designated as "intergenic" (Rodriguez et al., 2004b) (Fig. 4). Although it was initially assumed that intronic miRNAs are generally co-transcribed with their "host genes" and thus are controlled by the same transcriptional regulators (Saini et al., 2007), recent investigations have also shown host gene-independent transcription (Ozsolak et al., 2008; Monteys et al., 2010). Approximately a third of human miRNAs is organized in clusters, meaning that two or more miRNAs originate from a single primary transcript (Lee and Dutta, 2009). Mostly, miRNAs are transcribed by RNA polymerase II (although an RNA polymerase III-dependent transcription has been described (Borchert et al., 2006)), and as for mRNAs, a 5' cap structure and a 3' poly(A) tail are added to the primary transcript (Cai et al., 2004) (Fig. 4). These primary miRNAs (pri-miRNAs), often several thousand nt in length, contain a characteristic intramolecular secondary structure, the hairpin, which serves as substrate for two sequential endonucleolytic processing steps catalyzed by two distinct protein complexes (Fig. 4). The first complex contains the protein *DiGeorge syndrome critical region gene 8* (*DGCR8*), which binds to the pri-miRNA and serves as a "molecular ruler" for another protein, the RNase III enzyme *Drosha* that cleaves both at the 5' and 3' end to release the precursor miRNA (pre-miRNA) (Han et al., 2006). The generated pre-miRNAs, approximately 70 nt in length, are subsequently exported from the nucleus via a mechanism involving the Ran-GTP dependent cargo transporter *Exportin 5* (Lund et al., 2004). Once in the cytoplasm, pre-miRNAs are subjected to the second processing step by assembly of a complex containing *TAR* (*HIV*) *RNA-binding protein 2* (*TRBP*) and another RNase III enzyme, *Dicer*, which cleaves off the hairpin loop and thereby generates a miRNA-miRNA* duplex of two 21-25 nt RNAs (Jinek and Doudna, 2009). *Dicer* is the mammalian homologue of the *Dme* gene *dcr-1*, which was found necessary for both miRNA and siRNA function (Grishok et al., 2001) (see also previous chapter), and hence, it is at this stage that miRNA and siRNA pathways converge. Subsequently, the miRNA* or passenger strand is released and degraded, while the "mature" miRNA becomes part of the miRNA-induced silencing complex (miRISC). Thermodynamic stability of the miRNA duplex ends, but also the identity of 5' nucleotides, are considered as parameters that influence which RNA strand becomes the mature miRNA or the miRNA* (Krol et al., 2010).

Once incorporated into the RISC, miRNAs (and siRNAs) serve to guide their associated effector proteins to target mRNAs via Watson-Crick pairing, resulting in posttranscriptional repression (Bartel, 2009). In contrast to siRNAs, the sequences of the miRNA and the respective *miRNA recognition element* (*MRE*) (on the target mRNA) usually have only imperfect complementarity in animals (Fig. 4). It is therefore difficult to predict which MREs are indeed effectively targeted by a specific miRISC, and in fact, precise rules have not been fully elucidated yet. However, the combination of bioinformatic and experimental approaches has revealed some criteria that seem to be of importance. First, perfect and contiguous base pairing of the miRNA nucleotides 2–8, the "miRNA seed", to the corresponding "seed match" in the mRNA are a key determinant. Second, the central region of the miRNA-MRE interaction often contains bulges, while the following 3'-part of the miRNA again shows a certain extent of base pairing to the MRE (though not as stringent as the homology between seed and seed match). Third, most verified miRNA-mRNA interactions have been found in the 3'UTR of mRNAs (Filipowicz et al., 2008). Exceptions to every of the

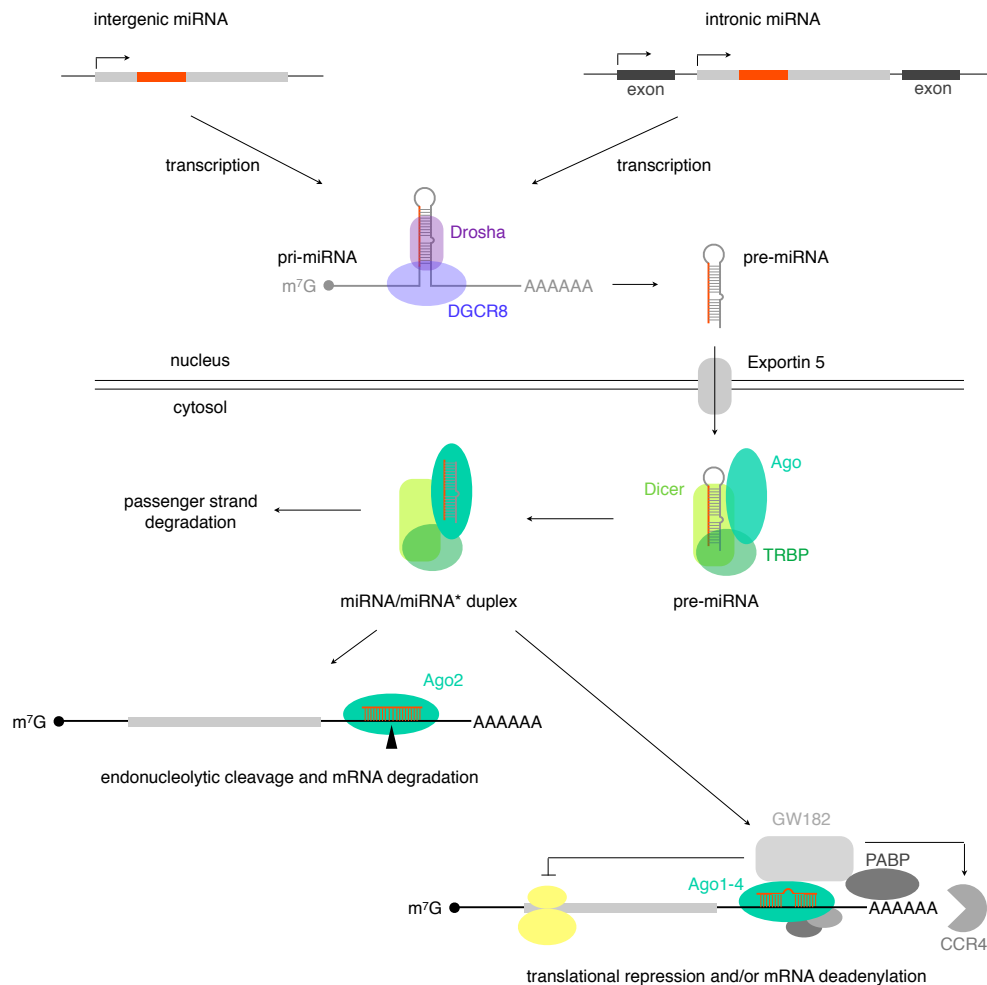


Figure 4. Biogenesis and regulatory mechanisms of microRNAs. An overview of the generation of miRNAs and their canonical ways of action is schematized following recent publications (Filipowicz et al., 2008; Krol et al., 2010). MiRNAs have been identified in intergenic regions, as well as in introns of protein-coding genes (Rodriguez et al., 2004b). These intronic miRNAs are frequently co-transcribed with their host genes, but can also be controlled by separate transcriptional regulators (Ozsolak et al., 2008; Monteys et al., 2010). The primary transcripts, designated pri-miRNAs, can be several thousand nucleotides (nt) in length, are 5'-capped and 3'-polyadenylated, and have a part that folds into a characteristic hairpin loop. This structure is recognized by a protein complex containing the dsRNA-binding protein Digeorge syndrome critical region gene 8 (DGCR8) and the RNase III enzyme Drosha, processing the pri-miRNA into the ~70 nt precursor miRNA (pre-miRNA), which is subsequently exported from the nucleus by the Exportin 5 cargo transporter (Lund et al., 2004). A second processing step, performed by a protein complex containing the dsRNA binding protein TRBP and the RNase III enzyme Dicer, generates the ~20-bp miRNA/miRNA* duplex. Usually, the passenger (miRNA*) strand is released from the protein complex, while the guide (miRNA) strand is incorporated into the miRNA-induced silencing complex (miRISC). Within the miRISC, the mature miRNA (labeled in red) is associated to proteins of the Argonaute (Ago) family and guides the protein complex to mRNAs with sufficient sequence complementarity. Endonucleolytic cleavage of target mRNAs is facilitated only by Ago2, provided that perfect complementarity between miRNA and the respective miRNA recognition element (MRE) exists. In contrast, all four human Ago proteins participate in repression of translation and mRNA deadenylation, mediated by the GW182 protein that interacts with the poly(A) binding protein (PABP), leading to recruitment of the CCR4-NOT deadenylase complex (Tritschler et al., 2010).

mentioned rules have been shown in several organisms (Vella et al., 2004; Tay et al., 2008; Lee et al., 2009).

Within the RISC, miRNAs (and siRNAs) are associated to *Argonaute* (*Ago*) proteins. Four different Ago proteins (Ago1-4) have been identified in mammals, of which only Ago2 has "slicer" activity and thus functions in siRNA-mediated mRNA cleavage, while all Ago proteins are implicated in miRNA-mediated mechanisms of post-transcriptional gene silencing (PTGS) (Filipowicz et al., 2008). These mechanisms comprise endonucleolytic cleavage of the target mRNA (if the miRNA is incorporated into Ago2), but also deadenylation of mRNAs (Wu et al., 2006) and translational repression (Fig. 4). The latter has been shown to depend on an intact 5' cap (Pillai et al., 2005) and can involve both mechanisms that prevent translation initiation (Kiriakidou et al., 2007) as well as polypeptide elongation (Maroney et al., 2006). It is not fully elucidated which factors determine whether a particular miRNA-MRE interaction leads to mRNA destabilization or translational inhibition. For mammalian cells, though, high-throughput studies (microarrays, proteomics) revealed that the majority of miRNA-mRNA interactions involves at least a mild decrease of target mRNA levels (Lim et al., 2005; Selbach et al., 2008; Baek et al., 2008). Moreover, a recent study on human and mouse cells compared the relative effect of miRNA-mediated mRNA destabilization and miRNA-mediated translational inhibition on decreased protein output, and identified reduced mRNA levels as the predominant factor (Guo et al., 2010).

Beside the canonical way of action described above, a few studies have demonstrated additional mechanisms by which miRNAs can regulate gene expression. For example, miR-373 and miR-205 have been shown to induce transcription of some (but not all) genes with complementary sequences in their promoters (Place et al., 2008; Majid et al., 2010). Moreover, another effect of miRNAs at the transcriptional level has been demonstrated in plants, as the ratio of miRNAs and their target mRNAs seems to influence the methylation status of genes encoding target mRNAs (Khraiweh et al., 2010). Finally, at least one study showed that miRNAs can also act as positive regulators of translation: Upon cell cycle arrest (but not during proliferation), miR-369-3 directs a protein complex to the mRNA of TNF α to induce TNF α protein synthesis; a similar mechanism was also apparent for let-7 and HMGA2 (Vasudevan et al., 2007).

1.3.3 Prediction and validation of microRNA–mRNA interactions

Identification of direct miRNA–mRNA interactions is of utmost importance to dissect the effect of a miRNA in any biological process, but is also an intricate task (see 1.3.2 and below). As the combinatorial possibilities for imperfect hybridizations between a miRNA of approximately 23 nt and a 3'UTR of hundreds to thousands of nt are essentially indefinite, the demand for bioinformatic tools was already apparent at the beginnings of miRNA research. A powerful prediction should therefore present a list of highly confident miRNA–MRE pairs, i.e. include as few false positives as possible, but simultaneously should not discard any true miRNA–MRE interaction (false-negatives). Several prediction tools have been established throughout the last decade and are usually available for biologists as convenient online interfaces, all using a different combination or weighting of rules that have been recognized by the study of verified miRNA–MRE interactions.

Clearly, the probability of a true interaction between a miRNA and a MRE is dependent on the degree of sequence homology. Thus, algorithms that somehow quantify this degree (e.g. by simple counting of base pairs, or via thermodynamic calculations) are implemented in essentially every tar-

get prediction tool. However, this rather basic rule could soon be refined as perfect base pairing of 7-mer sequences within the mRNA to the miRNA seed was a powerful additional rule to reduce the number of false-positive predictions (Lewis et al., 2003). The seed region was also confirmed experimentally as a crucial determinant for miRNA–mRNA interactions (Doench and Sharp, 2004), and correspondingly, several prediction tools, e.g. TargetScan (Friedman et al., 2009) or PicTar (Krek et al., 2005), have implemented the "seed criterion". A second important factor is preferential evolutionary conservation: If mRNA sequences are compared between different organisms, and a particular region is found to be more conserved than would be expected by chance, this region might have a biological function as a MRE. Indeed, this "conservation criterion" was shown as valid to predict true miRNA–mRNA interactions (Lewis et al., 2003). Further rules implement the number of potential binding sites for a particular miRNA–mRNA pair as a scoring factor, or consider the flanking regions of MREs, which can e.g. influence the accessibility for the RISC (Obernosterer et al., 2008).

Typically, a prediction tool generates a list of several hundreds of mRNAs that could be targeted by a particular miRNA. Experimental approaches are then in demand to validate these predictions. Up to now, the central experiments to verify or discard individual miRNA–MRE interactions are reporter gene essays where the 3'UTR (or MRE) of interest is cloned downstream of a reporter gene to evaluate the dependency of reporter protein levels on the action of the respective miRNA. The most frequently used reporter genes for this purpose are *luciferases*, enzymes that emit photons as a by-product of a chemical reaction (Cali et al., 2008). In typical *in vitro* experiments, luciferase reporter plasmids are transfected into cells together with synthetic oligonucleotides that either mimic the miRNA of interest, or have an antisense sequence and thereby should inhibit the endogenously expressed miRNA (Kuhn et al., 2008). Cell lysates are subsequently assayed for luciferase activity, which is quantified by a luminometer. Data is evaluated by comparing transfections in which the miRNA of interest has been modulated to control transfections (which usually include a small oligonucleotide with scrambled sequence). If a predicted miRNA–mRNA interaction could be verified, the action of the miRNA can be further delineated to individual, predicted MREs by luciferase assays with point-mutated reporters.

Using reporter gene assays to validate all predicted miRNA–mRNA interactions for a particular miRNA of interest is usually not possible and thus, biologists are faced with the challenge to select a few highly promising from the large list of predicted interactions. However, some issues can be worked out in advance to make a choice for candidate targets to be finally validated. First, the co-existence of miRNA and mRNA of interest in the same cell type are a prerequisite for a functional relation in any biological context (Kuhn et al., 2008). Second, the susceptibility to miRNA modulation is a necessary (but not sufficient) feature of direct targets and can be assessed both at mRNA or protein level, either for a few number of candidates (qRT-PCR, Western blots) or even on a large scale (microarrays (Nicolas et al., 2008), proteomics (Selbach et al., 2008; Baek et al., 2008)). Third, a thorough study of literature related to the respective field of research can certainly help to identify "meaningful" target genes, e.g. genes which have been shown to evoke a phenotype that is opposed to the phenotype of the respective miRNA.

Finally, it must be stated that not only the number of predicted miRNA–mRNA interactions is usually high, but that also the number of true interactions is estimated to be in the range of several hundreds for a single miRNA (Friedman et al., 2009). Thus, in addition to identify true miRNA–mRNA interactions, the questions arises which targets are the main mediators of the miRNA effect in the respective biological process. An interesting experimental approach that addresses this issue

has recently been described: By using small synthetic oligonucleotides ("target protectors") that selectively interfere with miRNA action at a particular MRE, Choi et al. could identify individual miRNA–mRNA pairs as major determinants of zebrafish development (Choi et al., 2007). A similar strategy has also been used in *Dme* (Gehrke et al., 2010). Meanwhile, such target protectors are commercially available, and therefore more detailed insights into the physiology of distinct miRNA–mRNA axes are to be expected soon.

1.3.4 microRNAs in human disease

As more and more miRNAs were discovered in mammals during the last decade, also the number of cellular functions in which miRNAs were shown to participate increased. After more than a decade of research, it is fair to say that miRNAs might be implicated in almost every cellular process, and consequently, the dysregulation of miRNA expression has been implicated in a broad range of human pathologies (Filipowicz et al., 2008). A selection of diseased states that are associated with, or even be caused by aberrant levels of miRNAs by will be presented below.

Already in 2002, deletion of a chromosomal region that harbours miR-15 and miR-16 was reported in the majority of individuals with B cell chronic lymphocytic leukemia (CLL) (Calin et al., 2002). Even though this deletion included protein-coding genes as well, it was later shown that miR-15 and miR-16 directly target the antiapoptotic protein Bcl-2, thereby confirming the relevance of miRNAs for this type of malignancy (Cimmino et al., 2005). Since these initial findings, a large number of other miRNAs has been associated with most, if not all types of cancer. Thus, an overview of all so far discovered relationships between individual miRNAs and malignancies is beyond the scope of this thesis and furthermore has been extensively reviewed in the recent past (Visone and Croce, 2009; Sassen et al., 2008; Shenouda and Alahari, 2009; Garzon et al., 2009). Instead, several key principles and interesting facts shall be pointed out.

First, miRNAs can be both oncogenic and tumor suppressive. For example, let-7 is an established tumor suppressor that prevents proliferation of breast tumor-initiating cells (Yu et al., 2007), while miR-21 has been identified as an "oncomiR" in a multitude of different cancers (Krichevsky and Gabriely, 2009), including breast cancer (Yan et al., 2011). Thus, distinct miRNAs can have detrimental or protective effects with respect to a certain type of cancer. Notably, a particular miRNA can be oncogenic and tumor suppressive, depending on the cell type: While miR-26a promoted tumor formation in a mouse glioma model (Huse et al., 2009), the same miRNA also impaired the progression of hepatocellular carcinoma (HCC) *in vivo* (Kota et al., 2009).

A second interesting finding came from miRNA expression profiling studies performed with multiple human tissues in order to compare cancerous to normal samples. It was found that the expression profiles of approximately 200 miRNAs were able to accurately classify tumors with respect to their origin and differentiation state, which was not possible by mRNA expression profiles (although these comprised approximately 16000 distinct transcripts) (Lu et al., 2005). In other words, the information content of a relatively small array of miRNAs with respect to malignant diseases is surprisingly high, revealing an interesting diagnostic potential that was confirmed by subsequent studies (Iorio et al., 2005; He et al., 2005). Apart from diagnosis, the prognostic potential of "miRNA signatures" or single miRNAs has also been shown, e.g. for CLL (Calin et al., 2005), lung (Yanaihara et al.,

2006) and colon adenocarcinoma (Schetter et al., 2008).

Third, a study demonstrated that proliferating cells tend to express mRNAs with shorter 3'UTRs than growth-arrested cells (Sandberg et al., 2008). It is therefore tempting to speculate that the mechanism of transformation includes an "escape" of messages from miRNA-mediated downregulation.

Fourth, research on prostate cancer unexpectedly revealed that miRNAs are present in the bloodstream of mice and humans, and that serum levels of miR-141 could discriminate between individuals with prostate cancer and healthy controls (Mitchell et al., 2008). Differential miRNA serum profiles were subsequently reported for other types of cancer (Chen et al., 2008; Ng et al., 2009) and further diseases (see below), firmly establishing the potential of circulating miRNAs as biomarkers.

Aside from cancer, there is also ample data on the involvement of miRNAs in normal cardiac function and miRNA dysregulation in cardiovascular diseases (Small et al., 2010). For example, the muscle specific miRNAs miR-1 and miR-133a have both been shown as necessary for normal heart development in mouse: Deficiency of the miR-1-2 gene (one of two loci encoding mature miR-1) resulted in late embryonic or postnatal death due to ventricular septal defects in approximately half of the transgenic mice (Zhao et al., 2007). A similar phenotype was observed for deletion of miR-133a (Liu et al., 2008). Both miRNAs were also downregulated in *post mortem* samples of myocardial infarction compared to healthy adult hearts (Bostjancic et al., 2010). Moreover, miR-133 levels were also found decreased in mouse and human models of cardiac hypertrophy, and the phenotype could be recapitulated *in vivo* by synthetic anti-miR-133 "antagomirs" (Carè et al., 2007).

With respect to metabolic diseases, different serum miRNA profiles between normal and type 2 diabetic individuals have been described (Chen et al., 2008). Interestingly, a second study identified a "diabetes miRNA signature" that was apparent even before the onset of the disease and hence could serve as a prospective risk factor (Zampetaki et al., 2010). Mechanistically, it was shown that miR-375, a pancreatic islet-specific miRNA, controls insulin secretion by β -cells (Poy et al., 2004). A subsequent *in vivo* study revealed a role for this miRNA in glucose homeostasis, as genetic ablation of miR-375 resulted in hyperglycaemia. However, this effect could not be ascribed to plasma insulin, the levels of which were comparable between miR-375^{-/-} and wt mice, but to increased α -cell mass and corresponding increased plasma glucagon levels (Poy et al., 2009).

A potential involvement of miRNAs in cholesterol metabolism, which is often disturbed as a consequence of obesity, has recently been shown by studies on miR-33. This miRNA is intronic to sterol-regulatory element-binding factor-2 (SREBF-2), a transcription factor that regulates cholesterol synthesis, and has been shown to target ATP-binding cassette transporter A1 (ABCB1), which mediates cholesterol efflux from cells into HDL (Rayner et al., 2010). Overexpression of miR-33 in mouse liver reduced plasma HDL (Rayner et al., 2010), while systemic antagonism in mice evoked the opposite (Najafi-Shoushtari et al., 2010). The findings were recently corroborated by a transgenic mouse model lacking miR-33 (Horie et al., 2010).

At the moment, the most advanced studies on miRNA-based therapies have focused on miR-122, a miRNA which is specifically expressed at high levels in liver. Functional investigation revealed that, surprisingly, miR-122 is a host factor that is necessary for Hepatitis C virus (HCV) replication by direct interaction of the miRNA with the 5'UTR of the viral genome (Jopling et al., 2005). Another study focused on miR-122 inhibition by systemic administration of anti-miR-122 "antagomirs" in

mice. This treatment resulted in downregulation of several genes involved in cholesterol biosynthesis, which was also manifested by significantly decreased plasma cholesterol levels (Krützfeldt et al., 2005). Subsequent mouse *in vivo* experiments showed that miR-122 inhibition also increased hepatic FA oxidation and could ameliorate hepatic steatosis in obese mice (Esau et al., 2006). Together, a dual therapeutic potential of miR-122 antagonism – for treatment of HCV infection and hypercholesteremia – was apparent and meanwhile has also been confirmed by two studies in non-human primates. In 2008, Elmén et al. published studies on african green monkeys in which they used a synthetic antisense oligonucleotide (LNA-antimiR) that consisted of a mixture of DNA and locked nucleic acids (LNAs) and therefore could bind to miR-122 with high efficiency. Three intravenous injections of this LNA-antimiR within 5 days were sufficient to lower plasma cholesterol for months without any observable side effects (Elmén et al., 2008). Another LNA-based anti-miR-122 oligonucleotide was applied on a weekly basis to chimpanzees with chronic HCV infection. A more than 300-fold reduction of viral titers could be observed that did not change for several weeks after treatment end, and notably, neither adverse side effects nor viral escape mutations (leading to treatment resistance) were reported (Lanford et al., 2010).

Collectively, miR-122 appears to be the foremost candidate for a miRNA-based drug that could have clinical impact. This is underscored by a patent of Regulus Therapeutics Inc., claiming the use of miR-122 for therapy of HCV infections, which has recently been granted by the European Patent Office and the United States Patent and Trademark Office (Regulus Therapeutics, 2010). Furthermore, the compound miravirsen (SPC3649, used in the preliminary chimpanzee studies (Lanford et al., 2010)), is proprietary of Santaris Pharma A/S and as such currently investigated in phase 2a clinical trials, with the goal to monitor safety and tolerability in treatment-naïve HCV patients (Santaris Pharma, 2010).

1.4 MicroRNAs and adipose tissue – state of knowledge

Based on the previous introductory chapters, this section will focus on the so far discovered involvements of miRNAs in adipocyte biology and obesity.

The general necessity of miRNA-mediated processes for adipogenesis was first demonstrated by *in vitro* studies showing that silencing of Drosha in 3T3-L1 preadipocytes (Wang et al., 2008), and similarly knockdown of Dicer in human BM-MSC (Oskowitz et al., 2008), strongly impaired adipocyte differentiation. Likewise, gene targeting resulting in expression of non-functional Dicer impaired adipocyte differentiation of MEFs and mouse primary preadipocytes (Mudhasani et al., 2010). The same group subsequently analyzed the phenotype of mice in which Dicer function was ablated in adipose tissue (via an aP2-Cre transgene). In line with the previous *in vitro* observations, adipose-specific lack of Dicer resulted in a severe depletion of WAT (Mudhasani et al., 2011). Interestingly, BAT mass and morphology seemed to be unaffected, but the expression of genes involved in the thermogenic function of BAT (*Ucp1*, *Pgc1 α* , *Cox8b*) was strongly reduced (Mudhasani et al., 2011). Collectively, these results suggest a strong involvement of miRNAs in white adipogenesis, as well as in the function of brown adipocytes.

Even prior to the aforementioned studies, screenings for miRNAs differentially expressed during adipogenesis, as well as functional investigation of particular miRNA candidates had been performed.

The first publication on a miRNA and fat metabolism had been performed in *Drosophila* and showed that flies deficient in dme-miR-14 had increased fat accumulation, while additional copy numbers of the miR-14 gene had the opposite effect (Xu et al., 2003). Furthermore, another *Drosophila* study identified dme-miR-8 as a negative regulator of Wnt signaling, a pathway with established anti-adipogenic function (see 1.2.3) (Kennell et al., 2008). Overexpression of two miRNA clusters containing the mouse homologues of dme-miR-8 (the miR-200c/141 and miR-200b,a/429 clusters) promoted adipocyte differentiation of murine ST2 cells (Kennell et al., 2008).

The first list of differentially expressed miRNAs during adipogenesis of a mouse system was presented by Kajimoto et al. who cloned and analyzed cDNA libraries at two stages of 3T3-L1 differentiation (Kajimoto et al., 2006). Since this initial screening, several *in vitro* studies have presented miRNAs with a role in mouse adipogenesis. Overexpression of the miR-17~92 cluster increased adipogenesis of 3T3-L1 preadipocytes, which was also observed when the direct target Rb2/p130 was silenced (Wang et al., 2008). Two miRNAs, miR-24 and miR-31, were found to be upregulated during adipogenesis of C3H10T1/2 mesenchymal stem cells; while miR-24 promoted differentiation, miR-31 had a negative effect, probably via direct targeting of C/EBP α (Sun et al., 2009a). A study on 3T3-L1 preadipocytes showed upregulation of let-7 during differentiation, and an anti-adipogenic effect of let-7 overexpression, likely due to inhibition of mitotic clonal expansion via direct targeting of HMGA2 (Sun et al., 2009b). Furthermore, miR-448 abundance was shown to increase during 3T3-L1 adipogenesis, and to directly target the transcription factor KLF5, thereby attenuating differentiation (Kinoshita et al., 2010). miR-27a and miR-27b were identified as down-regulated during adipogenesis, and overexpression of either inhibited differentiation of 3T3-L1 and OP9 cells (Lin et al., 2009). However, a further dissection of the anti-adipogenic action of miR-27, most importantly the search for direct target mRNAs, was not performed in this study. Similarly, miR-143 and miR-103 were described to accelerate adipogenesis of 3T3-L1 cells (Xie et al., 2009), while miR-378/378* increased lipogenic gene expression and TG accumulation in ST2 cells (Gerin et al., 2010), but in either instance without presenting direct target mRNAs that might mediate the effects. The role of miRNAs as gatekeepers of related differentiation programs was investigated in a study with murine mesenchymal stem cells: miR-204 and miR-211 were demonstrated to directly target Runx2, an osteogenic transcription factor with inhibitory effects on PPAR γ , and correspondingly, overexpression of miRNA-204 promoted adipogenesis while inhibiting osteoblast differentiation (Huang et al., 2010a). Finally, miR-375 has recently been described to be expressed and upregulated during 3T3-L1 adipocyte differentiation (although it was initially considered as specifically expressed in the pancreas (Poy et al., 2004)). Overexpression of miR-375 increased, while inhibition of miR-375 decreased adipogenesis, possibly via an influence of the miRNA on ERK1/2 phosphorylation (Ling et al., 2011).

Up to now, a function in adipogenesis of human systems has been published for five microRNAs. Already in 2004, Esau et al. characterized (via microarrays) the miRNA expression profile during adipogenesis of human preadipocytes, and were the first to assign a function to a miRNA in human by showing that inhibition of miR-143 impaired adipocyte differentiation (Esau et al., 2004). The authors also suggested a potential direct miR-143 target, ERK5, but did not validate the direct interaction via luciferase reporter assays (Esau et al., 2004). In addition, a study in 3T3-L1 preadipocytes documented moderate inhibition of adipogenesis upon ERK5 silencing (Sharma and Goalstone, 2005), which is contradictory to the pro-adipogenic effect of miR-143. Thus, the relevant miR-143 targets in the context of adipocyte differentiation remain to be discovered. Our group identified miR-27b as the first microRNA with an anti-adipogenic function in human (Karbiener

et al., 2009), which was in line with a previous study in mouse models (Lin et al., 2009). Moreover, we also presented PPAR γ as a direct miR-27b target, thereby suggesting a plausible mechanism of action for this miRNA in adipogenesis (Karbiener et al., 2009). The direct interaction of miR-27 with the PPAR γ 3'UTR was subsequently confirmed for mouse as well (Kim et al., 2009b). miR-21 was described as the third miRNA with a function in human adipocyte differentiation: its overexpression increased, while its silencing decreased adipocyte differentiation of adipose tissue-derived MSC (Kim et al., 2009b). Interestingly, TGFBR2, a transmembrane receptor which is known to mediate transforming growth factor β (TGF β)-elicited anti-adipogenic signals, was identified as a direct miR-21 target, and because the action of TGF β on differentiation was dampened by miR-21 overexpression, it was postulated that the main effect of this miRNA in the context of adipogenesis is via its modulation of TGF β signaling (Kim et al., 2009b). Subsequently, miR-130a and miR-130b were shown to be downregulated during adipogenesis of human preadipocytes, and silencing and overexpression experiments revealed an anti-adipogenic function for these miRNAs (Lee et al., 2010). Similar to miR-27, miR-130a and miR-130b were shown to target PPAR γ , but interestingly, an atypical MRE within in the PPAR γ CDS was identified (Lee et al., 2010). Finally, miR-335 has recently been described as decreasing during adipogenesis and osteogenesis of human BM-MSC, to impair MSC proliferation, and to negatively act on both differentiation lineages (Tomé et al., 2010). The study also identified RUNX2 as a direct miR-335 target, which seems plausible for an anti-osteogenic function, but does not explain the anti-adipogenic effects.

Apart from the implications of miRNAs in fat cell development, there are also indications for a miRNA component in metabolic disturbances. For example, Klötting et al. have recently profiled human subcutaneous and visceral WAT (Klötting et al., 2009). Interestingly, they found depot-specific differences in miRNA levels (e.g. higher levels of miR-27a in visceral than subcutaneous samples of obese diabetic patients), and also significant correlations between individual miRNAs and metabolic parameters like fasting plasma glucose (Klötting et al., 2009). Another study recorded global miRNA expression profiles during 3T3-L1 adipocyte differentiation and in adipocytes derived from epididymal WAT of obese and lean mice (Xie et al., 2009). Interestingly, an inverse relationship between the expression during adipogenesis and the expression in adipocytes from obese versus lean mice was observed for many miRNAs: for example, while miR-442b or miR-143 were upregulated during *in vitro* differentiation, the same miRNAs were expressed at lower levels in adipocytes from obese compared to lean mice (Xie et al., 2009). Notably, treatment of 3T3-L1 adipocytes with TNF α , a well-documented inflammatory cytokine (see 1.2.4), also led to downregulation of some miRNAs that were induced during adipogenesis. Thus, the detrimental changes caused by chronic inflammation in the obese state likely also involve changes in miRNA expression levels. In favor of this is also a recent study on miR-519d (Martinelli et al., 2010): This miRNA was highly upregulated in subcutaneous WAT of obese compared to nonobese individuals, and interestingly, it was also inversely correlated to protein levels of PPAR α , a transcription factor that can suppress obesity-associated inflammatory processes in WAT (Tsuchida et al., 2005). The predicted direct interaction of miR-519d and PPAR α mRNA was confirmed experimentally (Martinelli et al., 2010), providing a possible explanation for detrimental changes induced by miR-519d in obesity.

Few studies have so far addressed miRNA expression in brown adipocytes. In 2008, Cannon and co-workers analyzed a selection of miRNAs during adipocyte differentiation of murine white and brown primary preadipocytes (Walden et al., 2009). Because mRNA expression profiling (Tim-

mons et al., 2007) and other studies (see 1.2.1) have suggested a close relationship of BAT and SM, they assayed the expression of some miRNAs which had been identified as highly enriched in muscle (Lagos-Quintana et al., 2002; McCarthy, 2008), and miR-143 as a known regulator of adipocyte differentiation. While miR-143 was found to be present in both types of adipocytes (with higher expression in white compared to brown), the three muscle-enriched miRNAs miR-1, miR-206 and miR-133 were found to be highly expressed only in the brown lineage (Walden et al., 2009). Moreover, a subsequent study showed that miR-206 was not induced by chronic exposure of white preadipocytes to rosiglitazone, a treatment which substantially triggers expression of UCP1 and other brown markers (Petrovic et al., 2010). Thus, miR-206 was proposed to be a marker able to distinguish "genuine" brown adipocytes from "brite" adipocytes, at least in mouse. Finally, a recent study published miRNA expression profiles of murine brown and white primary preadipocytes undergoing adipocyte differentiation (Keller et al., 2011). Interestingly, the global miRNA profile was rather similar between differentiation of brown and white lineages.

To conclude, considerable amount of research data, accumulated during the last years, suggests a strong involvement of miRNAs in the biogenesis of WAT and likely also in the detrimental changes in WAT of obese individuals. Although preliminary studies likewise indicate a role for miRNAs in the function of BAT, a function of a distinct miRNA in the brown phenotype, or as regulator of the myogenic/brown and white/brite balances, has not been described to date.

Chapter 2

Aims

At the beginning of the 21st century, it is fair to say that excessive body weight is neither restricted to certain geographical regions, nor to certain population groups. Hence, obesity constitutes a global epidemic with substantial impact on public health systems, most importantly due to the wide range of followup diseases like type 2 diabetes, cardiovascular complications, and certain types of cancer. Although technological and socio-cultural developments of the last decades are major causes for the steady increase in prevalence, it is clear that genetics are an additional factor that determines the risk of becoming obese. However, the influences of distinct genes and gene networks on fat cell development and physiology are still poorly characterized. This is especially true for non-protein-coding RNAs ncRNAs, many of which have been discovered only a few years ago, but have already revolutionized our notion of regulatory mechanisms in biology. microRNAs (miRNAs) are one such group of ncRNAs and have already been implicated in various developmental processes and pathologies.

The overall aim of this thesis was the identification of miRNAs that influence human adipogenesis, using hMADS cells as human *in vitro* model system. Prior to the onset of this project, global miRNA expression profiling during adipocyte differentiation of hMADS cells had been performed and served as starting point for the subsequent aims:

- First, mouse embryonic fibroblasts (MEFs), a murine adipogenesis model, were analyzed for global miRNA expression during adipocyte differentiation. Thereby, a second data set, in addition to human adipogenesis, was generated.
- Second, both miRNA expression data sets were compared, combined with gene expression data (which had been acquired prior to the start of this thesis), and analyzed for predicted direct target mRNAs using multiple, publicly available algorithms.
- Third, based on the previous data evaluation, three miRNAs that were differentially expressed during adipocyte differentiation of hMADS cells were selected for functional validation. This included transfection of oligonucleotides in order to modulate intracellular miRNA levels, followed by adipocyte differentiation and genotypic as well as phenotypic analyses. If possible, these *in vitro* studies were complemented by the analysis of murine and human fat tissue samples, or cells derived thereof.

Chapter 3

Materials and Methods

3.1 Materials

3.1.1 Standard laboratory equipment

product name	company / product number
PIPETMAN Neo P2N	Gilson / F144561
PIPETMAN Neo P10N	Gilson / F144562
PIPETMAN Neo P20N	Gilson / F144563
PIPETMAN Neo P100N	Gilson / F144564
PIPETMAN Neo P200	Gilson / F123601
PIPETMAN Neo P1000	Gilson / F123602
Multipette [®] plus	Eppendorf / 4981 000.019
PIPETBOY acu	VWR / 612-0928
0.2 mL PCR Tubes	Biozym / 710980
1.5 mL Microcentrifuge Tubes	Sarstedt / 72.690.001
2 mL Microcentrifuge Tubes	Biozym / 710190
1.5 mL Safe-Lock Tubes	Eppendorf / 0030 123.328
15 mL PP Centrifuge Tubes	Corning / 430791
50 mL PP Centrifuge Tubes	Greiner Bio-One / 227261
10 µL Pipette Tips	Biozym / 720031
100 µL Pipette Tips	Greiner Bio-One / 685290
1000 µL Pipette Tips	Corning / 4868
10 µL Filter Tips	Biozym 693010 /
100 µL Filter Tips	Biopointscientific / 342-4050
1 mL SafeSeal-Tips	Biozym / 691000
CELL STAR [®] Serological Pipette, 5 mL	Greiner Bio-One / 606107
CELL STAR [®] Serological Pipette, 10 mL	Greiner Bio-One / 607180
CELL STAR [®] Serological Pipette, 25 mL	Greiner Bio-One / 760107
2 mL Pasteur Pipettes	Lactan / R4518.1

3.1.2 Instruments

product name	company
Microcentrifuge 5415R	Eppendorf
CR 4 22 Centrifuge	Jouan
6K16 High Volume Refrigerated Centrifuge	Sigma
MS1 Minishaker	IKA Works
MR2001K Magnetic Stirrer & Hotplate	Heidolph
Explorer Analytical Balance	OHAUS
DNA120 SpeedVac [®]	ThermoSavant
Thermomixer Compact	Eppendorf
Shaking Incubator 3033	GFL
Water Bath	GFL
Sonopuls UW2070	Bandelin
Ultra-TURRAX [®] T25	IKA
SPECTRAMax PLUS ³⁸⁴ Absorbance Microplate Reader	Molecular Devices
Microgrid II	Biorobotics
Heraeus Function Line Incubator Type T 6	Kendro Laboratory Products
CO ₂ -Incubator CB210	Binder
LaminAir Model 1.2	Holten
OT340 Hotplate	medite
CKX41 Inverted Light Microscope	Olympus
C-4040ZOOM Digital Camera	Olympus
NanoDrop [®] ND-1000	Thermo Scientific
PTC-225 PCR Cycler	MS Research
Gel Doc 2000 Gel Documentation System	BioRad
ABI PRISM [®] 7000 Sequence Detection System	Applied Biosystems
Mini Orbital Shaker SSM1	Stuart
Tecan HS 400 Hybridization Station	Tecan
GenePix 4000B Scanner	Axon Instruments
MP-300V Agarose Gel Electrophoresis Device	Cleaver Scientific
Gel Doc 2000 TM Gel Documentation System	BioRad
Mini Tran-Blot [®] Electrophoretic Transfer Cell	BioRad
ORION II Microplate Luminometer	Berthold
Microx TX 3 Micro Fiber Optic Oxygen Transmitter	PreSens
Arpege40 liquid N ₂ tank	Air Liquide

3.1.3 Microarrays

product name	company / product number
miRCURY™ LNA microRNA Array ready-to spot probe set	Exiqon / 208010-A
Nexterion HiSens E slides	Schott / 1125813
DEPC-treated H ₂ O	Roth / T143.3
miRCURY LNA™ microRNA Hy3/Hy5 Power Labeling Kit	Exiqon / 208032
Bovine Serum Albumin	PAA / K45-001
Sodium Citrate Tribasic Dihydrate	Sigma / C7254
NaCl	Roth / 3957.2
Sodium Dodecyl Sulfate	Sigma / 4360.2
miRCURY LNA™ Array, 2x Hybridisation Buffer	Exiqon / 208020

3.1.4 Analysis of triglyceride accumulation

product name	company / product number
Formaldehyde Solution 36.5 %	Sigma / F8775
Phosphate Buffered Saline (PBS)	Invitrogen / 10010015
Oil Red O	ICN Biomedicals / I155984
2-Propanol	Roth / 7343.1
Aqua Bidestillata Sterilis (ddH ₂ O)	Fresenius Kabi / 0698961/01A
Triglycerides Kit	Thermo Scientific / TR22203
Glycerol ≥98 %	Roth / 7530.1
BCA™ Protein Assay Kit	Thermo Scientific / 23227
96-well multiwell plate	Biozym / 710880

3.1.5 RNA isolation

product name	company / product number
TRIzol® Reagent	Invitrogen / 15596018
Chloroform ≥99 %	Sigma / C2432
2-propanol	Roth / 7343.1
Ethanol absolute	AustrAlco / UN1770
DEPC-treated H ₂ O	Roth / T143.3

3.1.6 Cell culture

product name	company / product number
Phosphate Buffered Saline (PBS)	Invitrogen / 10010015
Dulbecco's Modified Eagle Medium (DMEM) 1g/l Glucose	Lonza / BE12-707F
Ham's F12	Lonza / BE12-615F
Dulbecco's Modified Eagle Medium (DMEM) 4.5 g/l Glucose	Invitrogen / 41966029
Fetal Bovine Serum	Pan Biotech / P30-3300
L-Glutamine (200 mM)	Invitrogen / 25030024
HEPES Buffer Solution (1M)	Invitrogen / 15630-122
Trypsin, 0.5 % (10x) with EDTA	Invitrogen / 15400054
Collagenase Type I	Worthington / CLS 1
Bovine Serum Albumin (fatty acid free)	PAA / K31-002
250 µm Nylon Mesh	VWR / 510-9526
Cell Strainer 100 µm Nylon	BD Falcon / 952360
Cell Strainer 40 µm Nylon	BD Falcon / 352340
Red Blood Cell Lysing Buffer	Sigma / R7757
Normocin	Invivogen / ant-nr-2
Penicillin-Streptomycin	Invitrogen / 15140122
Trypan Blue Solution – 0.4 %	Sigma / T8154
Hemocytometer	Neubauer / T728.1
Cellstar 100 mm Cell Culture Dishes	Greiner Bio-One / 664160
Cellstar 145 mm Cell Culture Dishes	Greiner Bio-One / 639160
Cell culture 6-well Multiwell Plates	Greiner Bio-One / 657160
Cell culture 12-well Multiwell Plates	Greiner Bio-One / 665180
Cell culture 24-well Multiwell Plates	Corning / 3524
Cell culture 96-well Multiwell Plates	Corning / 3596
Dimethylsulfoxide (DMSO)	Sigma / 472301
2 mL Cryotubes	Lactan / E3091
Nuclease-free H ₂ O	Exiqon / 203400-02
Aqua Bidestillata Sterilis (ddH ₂ O)	Fresenius Kabi / 0698961/01A
HiPerFect Transfection Reagent	QIAGEN / 301707
DharmaFECT Duo Transfection Reagent	Dharmacon / T-2010
miRIDIAN Mimic hsa-miR-27b	Dharmacon / C-300589-05-0005
miRIDIAN Mimic hsa-miR-30c	Dharmacon / C-300541-03-0005
miRIDIAN Mimic hsa-miR-26a	Dharmacon / C-300499-05-0005
miRIDIAN Mimic Negative Control #1	Dharmacon / CN-001000-01-20
anti-hsa-miR-26a antisense oligonucleotide	Exiqon / 138463-00
non-targeting control antisense oligonucleotide	Exiqon / EQ 866923
ON-TARGETplus SMARTpool siRNA human SERPINE1	Dharmacon / L-019376-01-0005
ON-TARGETplus SMARTpool siRNA human ACVR1	Dharmacon / L-004924-00-0005
ON-TARGETplus SMARTpool siRNA human RB1	Dharmacon / L-003296-00-0005
ON-TARGETplus SMARTpool siRNA human NRIP1	Dharmacon / L-006686-00-0005
ON-TARGETplus SMARTpool siRNA human RPS6KB1	Dharmacon / L-003616-00-0005
siGENOME Non-Targeting siRNA pool #2	Dharmacon / D-001206-14-20
0.22 µm Syringe Filters	Biochrom / P99722
20 mL Sterile Syringes	Lactan / RC539.1

3.1.7 Reverse transcription, RT-PCR, and quantitative real-time RT-PCR

product name	company / product number
RQ RNase-Free DNase	Promega / M6101
100 mM dNTP Set	Invitrogen / 10297018
Random Hexamer Primers	Invitrogen / 48190011
Oligo dT ₍₁₂₋₁₈₎ Primers	Invitrogen / 18418012
RNase OUT TM Recombinant Ribonuclease Inhibitor	Invitrogen / 10777019
SuperScript II Reverse Transcriptase Kit	Invitrogen / 18064014
Aqua Bidestillata Sterilis (ddH ₂ O)	Fresenius Kabi / 0698961/01A
Platinum [®] SYBR [®] Green qPCR SuperMix-UDG w/ROX	Invitrogen / 11744500
<i>Taq</i> DNA Polymerase (recombinant)	Fermentas / EP0401
PeqGOLD Universal Agarose	PEQLAB / 35-1020
Ethidium Bromide Solution 1 %	Lactan / 2218.1
1 kb Plus DNA Ladder	Invitrogen / 10787-018
100 bp DNA Ladder	Invitrogen / 15628-019
6x DNA Loading Dye	Fermentas / R0611
PCR SingleCap 8-SoftStrips 0.2 ml	Biozym / 710980
TaqMan [®] miRNA Assay hsa-miR-27b	Applied Biosystems / 4427975
TaqMan [®] Assay RNU5B	Applied Biosystems / 001004
TaqMan [®] MicroRNA Reverse Transcription Kit	Applied Biosystems / 4366596
TaqMan [®] Gene Expression Master Mix (2x)	Applied Biosystems / 4370048
hsa-miR-30c, LNA TM PCR Primer Set	Exiqon / 204783
hsa-miR-26a, LNA TM PCR Primer Set	Exiqon / 204724
5S rRNA (hsa, mmu) PCR Primer Set, UniRT	Exiqon / 203906
RNU5G (mmu, hsa) PCR Primer Set, UniRT	Exiqon / 203908
Universal cDNA Synthesis Kit	Exiqon / 203300
SYBR Green Master Mix, Universal RT	Exiqon / 203400
ROX Reference Dye, 1 mM	Roche / 04673549001
MicroAmp [®] Optical 96-Well Reaction Plates	Applied Biosystems / N801-0560
MicroAmp [®] Optical Adhesive Film	Applied Biosystems / 4311971

3.1.8 Western blot analysis

product name	company / product number
TRIS	Roth / 5429.3
NaCl	Roth / 3957.2
HCl	Roth / K025.1
Nonidet P40 (NP40)	Roche / 13269300
Triton X-100	Roth / 3051.2
TWEEN [®] 20 Detergent, Molecular Biology Grade	Merck / 655204
Sodium Orthovanadate	Sigma / S6508
NaF	Merck / 27860.231
β -Glycerophosphate	Sigma / G9891
Protease Inhibitor Cocktail (PIC)	Roche / 11836170001
Methanol	Roth / 83885
Sodium dodecyl sulfate (SDS)	Merck / APPCA2263
Bovine serum albumin (BSA)	PAA / K45-001
EDTA	Roth / R80431
Glycine, reagentplus 99%	Sigma / G7126
Cell Scrapers	Becton Dickinson / 353087
BCA [™] Protein Assay Kit	Thermo Scientific / 23227
ATX Ponceau S red staining solution	Fluka / 09276
BioTrace [™] NT Nitrocellulose Transfer Membrane	Pall / 66485
Extra Thick Blot Paper	BioRad / 170-3966
NuPAGE [®] Antioxidant	Invitrogen / NP0005
NuPAGE [®] MOPS SDS Running Buffer (20X)	Invitrogen / NP0001
NuPAGE [®] Novex 10% Bis-Tris Gel 1.0 mm, 10 well	Invitrogen / NP0301
anti-Uncoupling Protein-1 (UCP-1) (145-159) Rabbit pAb	calbiochem / 662045
anti- β -tubulin Mouse mAb	Sigma / T5201
Polyclonal Swine Anti-rabbit antibody	DakoCytomation / P0399
Polyclonal Goat Anti-mouse antibody	DakoCytomation / P0447
Restore Plus Western Blot Stripping Buffer	ThermoScientific / 46430
SeeBlue [®] Plus2 Pre-Stained Standard	Invitrogen / LC5925
SimplyBlue [™] SafeStain	Invitrogen / LC6060
SuperSignal West Pico Chemiluminescent Substrate	Pierce / 34077
Amersham Hyperfilm ECL (18 x 24 cm)	GE Healthcare / 28-9068-36
Tetenal Developer Concentrate	Foto Ehmman / 30048
Tetenal Fixer Concentrate	Foto Ehmman / 30049

3.1.9 Cloning and luciferase assays

product name	company / product number
DNeasy Blood & Tissue Kit	QIAGEN / 69504
High Fidelity PCR Enzyme Mix	Fermentas / K0192
PeqGOLD Universal Agarose	PEQLAB / 35-1020
Ethidium Bromide Solution 1%	Lactan / 2218.1
GeneRuler™ 1 kb DNA Ladder, 250–10000 bp	Fermentas / SM0311
6x DNA Loading Dye	Fermentas / R0611
PureLink™ Quick Gel Extraction Kit	Invitrogen / K2100-12
XhoI Restriction Enzyme	Promega / R6165
NotI Restriction Enzyme	Promega / R6435
4-CORE® Buffer Pack	Promega / R9921
Bovine Serum Albumin, Acetylated	Promega / R3961
QIAquick PCR Purification Kit	QIAGEN / 28106
psiCHECK-2 Luciferase Vector	Promega / C8021
T4 DNA Ligase	Invitrogen / 15224017
DH5α™ Competent Cells	Invitrogen /
S.O.C. Medium	Invitrogen / 15544034
Select Agar	Sigma / A5054
Pepton	Roth / 8986.1
Yeast Extract	Sigma / Y1625
MgCl ₂	Sigma / M8266
MgSO ₄	Sigma / M2773
NaCl	Roth / 3957.2
α-D(+)-Glucose Monohydrate, ≥99.5 %	Roth / 6780.2
Ampicillin Sodium Salt	Sigma / A9518
<i>Taq</i> DNA polymerase (recombinant)	Fermentas / EP0402
QIAprep Spin Miniprep Kit	QIAGEN / 21706
Dual-Luciferase Reporter Assay System	Promega / E1980
Passive Lysis Buffer (PLB)	Promega / E1941
96-well Assay Plate Flat Bottom, Non-treated, White	Costar / 3912
Polystyrene	
QuickChange® Lightning Site-Directed Mutagenesis Kit	Stratagene / 210519

3.1.10 Oxygen consumption

product name	company / product number
1.8 mL HPLC Vials, with Septum Screw Cap	Knauer / A0637
Magnetic Stirrer Bar, Cylindric, 5 x 2 mm	VWR / 442-0361
Glucose Oxidase from <i>Aspergillus niger</i>	Sigma / G2133
α -D(+)-Glucose Monohydrate, $\geq 99.5\%$	Roth / 6780.2
Dulbecco's Modified Eagle Medium (D-MEM) (1x), Powder (Low Glucose)	Invitrogen / 31600-083
F-12 Nutrient Mixture (Ham), Powder	Invitrogen / 21700-026
NaHCO_3	Sigma / S5761
Oligomycin from <i>Streptomyces diastatochromogenes</i>	Sigma / O4876
Antimycin A from <i>Streptomyces sp.</i>	Sigma / A8674
10 μL Syringe 701N	Hamilton / 80300
Oxygen microsensor	Presens / NTH-Pst1

3.2 Methods

3.2.1 Cell culture

3.2.1.1 Cultivation and passaging of cells

For experiments, hMADS cells originally established from 2 different donors were used. hMADS-2 cells were isolated from the pubic fat pad of a 5 year old male donor; hMADS-3 cells were isolated from the prepubic fat pad of a 4 months old male donor (Rodriguez et al., 2005). Cells between passage (P) 17 and P31 were used.

Medium for proliferation of hMADS cells was termed "Medium I" and consisted of Dulbecco's Modified Eagle Medium (DMEM), 1 g L^{-1} Glucose, 2 mM L-Glutamine, 10 mM HEPES, $100 \mu\text{g mL}^{-1}$ Normocin, 10% Fetal Bovine Serum (FBS) and 2.5 ng mL^{-1} human Fibroblast Growth Factor 2 (hFGF2). In this medium, hMADS cells had population doubling times of 48-96 h (depending on the passage number, i.e. the replicative age of cells). At densities in the range of 50–80% of optical confluence, passaging of cells was performed at passaging ratios between 1:2 and 1:5, depending on the actual population doubling time.

Medium for proliferation of HEK293 cells was termed "HEK Medium" and consisted of DMEM, 4.5 g L^{-1} Glucose, 2 mM L-Glutamine, 25 mM HEPES, $100 \mu\text{g mL}^{-1}$ Normocin and 10% FBS. At densities of 60–80% confluence, passaging of HEK293 cells was performed at passaging ratios between 1:5 and 1:15.

For passaging, old medium was aspirated and cells were washed with Phosphate Buffered Saline (PBS) before incubation with 0.05% Trypsin with EDTA in PBS (1 mL per 100 mm cell culture dish) for 3–5 min at 37°C . Subsequently, Trypsin was inactivated by addition of the respective growth medium (prewarmed to 37°C), and the cell suspension was transferred to new culture dishes according to the desired passaging ratio. The usual volume of medium was 10 mL per 100 mm cell culture dish. Cells were incubated at 37°C in a humidified

atmosphere with 5% CO₂.

3.2.1.2 Thawing of cells

Cryotubes containing 1 mL aliquots of frozen hMADS cells or HEK293 cells were transferred from liquid N₂ to the water bath (37°C). After 3 min, thawed cell suspensions were diluted with 10 mL DMEM supplemented with 10% FBS and centrifuged for 7 min at 600 * *g*. Supernatant was decanted, the cell pellet was resuspended in 10 mL of growth medium (Medium I or HEK Medium, respectively) and cells were seeded into a 100 mm cell culture dish. Cells were incubated at 37°C in a humidified atmosphere with 5% CO₂. Medium was changed after 16–24 h.

3.2.1.3 Determination of cell concentration and viability

Concentration of cell suspensions was determined using a hemocytometer. Therefore, 50 µL cell suspension were mixed with 10 µL Trypan Blue solution and pipetted in the interspace of the hemocytometer and a coverslip, the height of which is 0.1 mm. Subsequently, living (i.e. non-stained) cells of 5-9 big squares of each counting chamber were counted and the cell concentration was calculated according to the equation

$$c = \frac{n_C}{n_{SQ}} * f * 12000 \quad (3.1)$$

where c is the cell concentration in cells/mL, n_C is the number of counted living cells, n_{SQ} is the number of big squares in which cells were counted, f is a dilution factor (only to be included if the original cell suspension had been diluted due to convenience for counting), and the factor 12000 includes both the scaling from the volume above one big square (0.1 mm) to the final unit (1 cm = 1 mL), as well as the dilution factor due to mixing of the cell suspension with the Trypan Blue solution (6/5).

Viability was calculated from the fraction of counted living cells divided by total counted cells and was usually above 95%.

3.2.1.4 Freezing of cells

Cell populations between 60 and 80% optical confluence were used for freezing. Therefore, suspensions of HEK293 and hMADS cells were generated by trypsinization as described in 3.2.1.1. After centrifugation for 7 min at 600 * *g*, the cell pellet was resuspended in the appropriate volume of freezing medium, consisting of 10% Dimethylsulfoxide (DMSO) in FBS. Aliquots of 1 mL were pipetted into cryotubes and immediately transferred to -80°C. After 24 h, cryotubes were transferred into liquid N₂ tanks for long-time storage.

3.2.1.5 Adipocyte differentiation of hMADS cells

Depending on the media composition, hMADS cells have been shown do differentiate into white adipocytes (Rodriguez et al., 2004a), but also into cells that exhibit key features of

brown adipocytes (Elabd et al., 2009). For both differentiation protocols, hMADS cells were seeded at a density of $7500 \text{ cells cm}^{-2}$ into 12-well or 6-well plates, and proliferated in Medium I (cf. 3.2.1.1). When optical confluence was reached (designated as day -2), cells were cultivated in Medium I without hFGF2 for two further days, i.e. until day 0. Subsequently, adipocyte differentiation was induced by "Medium II", consisting of DMEM(1 g L^{-1} Glucose)/ Ham's F12 (50:50), 2 mM L-Glutamine, 10 mM HEPES, $100 \mu\text{g mL}^{-1}$ Normocin, $860 \mu\text{M}$ ($= 5 \mu\text{g mL}^{-1}$) human insulin, $10 \mu\text{g mL}^{-1}$ apo-transferrin, 0.2 nM T3, 100 nM rosiglitazone, $100 \mu\text{M}$ IBMX and $1 \mu\text{M}$ Dex. At day 3, the medium was changed to Medium II without IBMX and Dex. For differentiation into brown adipocytes, cells were kept in this medium until day 14–17, whereas for white adipocyte differentiation, rosiglitazone was omitted from the medium from day 9 on. Generally, media were changed every two to three days and the media volumes were 1 mL and 2 mL per well of a 12-well and 6-well plate, respectively.

3.2.1.6 Transfection of hMADS cells

Transient transfection of hMADS cells (at day -2) with oligonucleotides (siRNAs, miRNA mimics or anti-miRNA ASOs) was performed using HiPerFect Transfection Reagent according to the manufacturer's instructions. Briefly, Medium I was changed 1 h before transfection. Standard transfections had a final oligonucleotide concentration of 5 nM. Therefore, stock solutions of oligonucleotides ($20 \mu\text{M}$ in PBS, stored at -80°C) were thawed on ice and diluted to $2 \mu\text{M}$ working solutions using sterile, nuclease-free H_2O . Subsequently, transfection mixtures were generated consisting of $3 \mu\text{L}$ oligonucleotide working solution, $97 \mu\text{L}$ DMEM (without any additives) and $6 \mu\text{L}$ HiPerFect Transfection reagent per well of a 12-well plate. The reactions were mixed and incubated at room temperature for 10 min and finally added dropwise onto the cells while gently swaying the plate. Medium was changed after two days to induce adipogenic differentiation (cf. 3.2.1.5). For transfections of cells in 6-well-plates and 10 cm dishes, volumes of the transfection reaction were scaled by a factor of 2 and 12, respectively. In experiments with an oligonucleotide concentration higher than 5 nM, dilution of the stock solutions was adjusted appropriately, and the volume of HiPerFect Transfection reagent was scaled as recommended by the manufacturer.

3.2.1.7 Transfection of HEK293 cells

HEK293 cells were seeded into 96-well plates at a density of 2×10^4 cells per well, with a volume of $100 \mu\text{L}$ HEK Medium per well. After 16 h, cotransfection of HEK293 cells with reporter vectors and miRNA mimics were performed using the DharmaFECT Duo Transfection Reagent. First, a nucleic acid solution was prepared consisting of 100 ng reporter vector and 10 pmol miRNA mimics in $20 \mu\text{L}$ DMEM (without any additives) per condition (assayed in technical duplicates). Second, a DharmaFECT Duo solution was prepared consisting of $0.6 \mu\text{L}$ DharmaFECT Duo Transfection Reagent in $20 \mu\text{L}$ DMEM (without any additives) per well. Nucleic acid solutions and DharmaFECT Duo solution were combined in sterile

0.2 mL polymerase chain reaction (PCR) tubes (yielding 40 μ L transfection solution per condition), mixed by pipetting and incubated at room temperature for 20 min. Meanwhile, old medium was removed and 80 μ L HEK Medium were added onto the cells to be transfected. Finally, 20 μ L transfection reaction were added per well, yielding a final miRNA mimic concentration of 50 nM, and the cells were incubated at 37 °C in a humidified atmosphere with 5 % CO₂ for 48 h, followed by analysis (see 3.2.2.8).

3.2.1.8 Human primary adipose derived stromal cells

Adipose tissue biopsies obtained from surgeries of varicose veins or inguinal herniae were used to isolate human primary adipose derived stromal cells (hPASCs) by a method adapted from Hauner et al. (Hauner et al., 1989). Biopsies were transported to the lab on ice in "Medium A", consisting of DMEM(1 g L⁻¹ Glucose)/ Ham's F12 (50:50), 15 mM HEPES, 50 μ g mL⁻¹ Penicillin/Streptomycin and 100 μ g mL⁻¹ Normocin. Tissues were repeatedly rinsed in PBS to decrease the number of attached red blood cells. Using sterile scissors and tweezers, adipose tissue was cut into small pieces. Pieces were then transferred to "Medium B" (3 mL per g tissue), consisting of 200 U mL⁻¹ Collagenase Type I and 20 mg mL⁻¹ FA-free Bovine Serum Albumin (BSA) in Medium A, and incubated for 45 min at 37 °C with mild agitation. Collagenase digested suspensions were diluted 1:5 with "Medium C", consisting of Medium A with 8 % FBS, and filtered through a 250 μ m mesh. The filtrate was centrifuged for 5 min at 600 * g. Subsequently, the supernatant was filtered through a 100 μ m and a 40 μ m mesh and centrifuged as above. The cell pellets obtained from both centrifugation steps were then resuspended in 10 mL Medium C, combined, filtered through a 100 μ m mesh and again centrifuged as above. The cell pellet was resuspended in 1 mL red blood cell lysis buffer and incubated for 1 min before addition of 20 mL "Medium D", consisting of Medium A with 2 mM L-Glutamine and 10 % FBS. After centrifugation as above, the cell pellet was resuspended in Medium D, cell concentration was determined and cells were seeded at 2×10^4 – 3×10^4 cells cm⁻² in 24-well plates. Medium was removed after 16 h and hPASCs were washed thrice with PBS to remove residual contaminating red blood cells. Subsequently, hPASCs were grown to confluence in Medium D, followed by transfection as described in 3.2.1.6 (transfection volumes were scaled by a factor of 0.5). Two days later, adipocyte differentiation was induced by changing the medium to DMEM(1 g L⁻¹ Glucose)/ Ham's F12 (50:50), 2 mM L-Glutamine, 10 mM HEPES, 100 μ g mL⁻¹ Normocin, 860 μ M (= 5 μ g mL⁻¹) human insulin, 10 μ g mL⁻¹ apo-transferrin, 0.2 nM T3, 100 nM rosiglitazone, 100 μ M IBMX and 1 μ M Dex. IBMX was omitted from day 3 on, and medium was changed every two to three days. Experiments were analyzed at day 9 and 16 of adipocyte differentiation.

3.2.2 Molecular biology and biochemistry

3.2.2.1 RNA isolation

Total RNA was isolated from TRIzol[®] samples by a method based on the manufacturer's instructions. For RNA harvest from cells, medium was aspirated, cells were washed once

with PBS and 400 μ L TRIzol[®] Reagent were added to each well of a 12-well-plate (3 ml per 100 mm cell culture dish). For RNA harvest from murine WAT samples, tissue was placed in 15 mL PP centrifuge tubes and immediately frozen in liquid N₂. Subsequently, 2 mL TRIzol[®] Reagent per g tissue were pipetted onto the frozen samples, followed by homogenization with the Ultra-TURRAX[®]. Samples were usually stored at -80°C between harvest and RNA isolation and therefore thawed at room temperature for 35 min. After addition of 0.2 mL chloroform per mL TRIzol[®] Reagent, samples were shaken vigorously for 2 min, incubated for 3 min at room temperature, and centrifuged for 17 min at 4°C and $1.2 \times 10^4 *g$. Subsequently, the upper (aqueous) phase was pipetted into new 1.5 mL Safe-Lock tubes, and 0.5 mL 2-propanol per mL TRIzol[®] Reagent were added. Samples were mixed and incubated for 10 min at room temperature before centrifugation for 20 min at 4°C and $1.2 \times 10^4 * g$. The supernatant was decanted and 1 mL 75 % Ethanol (diluted from Ethanol absolute with Diethylpyrocarbonate (DEPC)-treated H₂O) per mL TRIzol[®] Reagent were added to the RNA pellet. After centrifugation for 8 min at 4°C and 7600 * g , the supernatant was decanted and the tubes were incubated for 10 min with open caps to allow evaporation of residual Ethanol. Finally, RNA was dissolved in 10–25 μ L DEPC-treated H₂O (depending on pellet size) and incubated at 55°C for 10 min. RNA concentration and purity were determined by spectrophotometry using the NanoDrop[®] ND-1000. RNA was stored at -80°C .

3.2.2.2 MicroRNA expression profiling

Two independent differentiation experiments were performed with MEFs cells as previously described in (Prokesch et al., 2011) to yield samples for microRNA expression profiling. During each experiment, RNA samples of proliferating cells, cells at start of adipocyte differentiation, as well as 10 h, 20 h, 3 days and 8 days after induction were collected and isolated as described in 3.2.2.1.

Hybridizations were performed on a TECAN HS400 Hybridization Station, using Nexte-rion HiSens Sildes E spotted with the miRCURY LNATM Array ready-to-spot probe set no. 208010-A, which consists of 2,056 capture probes and covers all miRNAs of miRBase version 9.2 for detection of mature miRNAs. All hybridizations were repeated with reversed dye assignment (dye-swap).

Prior to the hybridization procedure, the TECAN HS400 Hybridization Station (including the miRNA microarray slides used for hybridization) had to be prepared and the RNA samples had to be labeled with the fluorescent Cy3 and Cy5 dyes. Although described separately in the following sections, both procedures were generally performed in parallel.

A 20x concentrated stock solution of saline sodium citrate (SSC) was prepared by dissolving 15 g NaCl and 175 g sodium citrate tribasic dihydrate in 1 L ddH₂O and adjusting the pH to 7.0 with 1 M HCl. A stock solution of 10 % sodium dodecyl sulfate (SDS) was prepared by dissolving 10 g SDS in 100 mL ddH₂O. Subsequently, five buffer solutions as listed in Table 3.1 were prepared. Prehybridization Buffer was warmed to 55°C and other buffers were degassed by incubation for 10 min in an ultrasonication water bath. During prepa-

Table 3.1. Buffers for microRNA expression profiling

name	composition
Prehybridization Buffer	5x SSC 0.1 % SDS 1 % BSA
Wash Buffer X	0.2 % SDS
Wash Buffer I	2x SSC 0.2 % SDS
Wash Buffer II	1x SSC
Wash Buffer III	0.2x SSC

Table 3.2. Hybridization protocol for microRNA expression profiling

step	action	reagent	parameter specification
1	Wash	Wash Buffer X	1 run, 23 °C, 1 min wash
2	Injection	Prehybridization buffer	39 °C
3	Hybridization	Prehybridization buffer	39 °C, 20 min , high agitation frequency
4	Wash	Wash Buffer I	1 run, 39 °C, 1 min wash
5	Injection	sample	64 °C
6	Hybridization	sample	64 °C, 16 h , medium agitation frequency
7	Wash	Wash Buffer I	2 runs, 64 °C, 1 min wash, 1 min soak
8	Wash	Wash Buffer II	2 runs, 23 °C, 1 min wash, 1 min soak
9	Wash	Wash Buffer III	2 runs, 23 °C, 1 min wash, 1 min soak
10	Wash	Wash Buffer III	1 run, 23 °C, 30 s wash
11	Slide drying	CO ₂	30 °C, 5 min

ration and hybridization, the TECAN HS400 Hybridization Station was controlled via the HS Control Manager software. First, the microfluidic system and hybridization chambers of the station were rinsed with ddH₂O. Second, the degassed buffers were connected to the respective liquid channels, followed by the "Prime" routine. Third, the miRNA microarray slides were placed into the hybridization chambers, the hybridization protocol (summarized in Table 3.2) was started and prehybridization of the slides was performed by injection of 90 μ L Prehybridization Buffer per hybridization chamber (step 2 of the hybridization protocol).

The miRCURY LNATM microRNA Power Labeling Kit was used for Cy3 and Cy5 labelling of RNA samples as described by the manufacturer. Briefly, 0.5 μ L CIP Buffer and 0.5 μ L CIP enzyme were added to 5 μ g of RNA sample (in a volume of 3 μ L nuclease-free H₂O) and the reactions were incubated at 37 °C for 30 min, and at 95 °C for 5 min (using the PTC-225 PCR cycler). Samples were placed on ice for 2 min, and 1.5 μ L of Cy3 or Cy5 fluorescent dye (dissolved in nuclease-free H₂O) were added. Subsequently, the labeling reactions were completed by addition of 3 μ L Labeling buffer, 2 μ L DMSO and 2 μ L Labeling enzyme. The PTC-225 PCR cycler was used for incubation at 16 °C for 60 min, followed by incubation at 65 °C for 15 min. Pairs of Cy3 and Cy5 labeled samples were then combined and diluted

with 50 μL 2x Hybridization Buffer. Finally, 25 μL nuclease-free H_2O were added to reach a final volume of 100 μL and the ready-to-hybridization samples were incubated at 90 $^\circ\text{C}$ for 3 min before injection into the hybridization chambers of the TECAN HS400 Hybridization Station (step 5 of the hybridization protocol, see Table 3.2).

After hybridization, miRNA microarray slides were scanned with a GenePix 4000B microarray scanner at 10 μm resolution and the resultant TIFF images were analyzed with GenePix Pro 4.1 software. Raw data was subsequently processed using ArrayNorm (Pieler et al., 2004) for normalization and Genesis software (Sturn et al., 2002) for analysis.

3.2.2.3 Quantitative real-time RT-PCR

For quantification of mRNA levels, RNA samples were first DNase digested using the RQ1 RNase-Free DNase according to the manufacturer's recommendations. Briefly, 0.5–1 μg of total RNA were brought to a volume of 6.2 μL with DEPC-treated H_2O , and 0.8 μL 10x reaction buffer and 1 μL (=1 U) of DNase enzyme were added before incubation at 37 $^\circ\text{C}$ for 30 min. The reaction was terminated by addition of 1 μL Stop Buffer and incubation at 65 $^\circ\text{C}$ for 10 min.

DNase digested RNA samples were then used for cDNA synthesis using the SuperScript II Reverse Transcriptase Kit. First, 1 μL dNTP mix (10 mM), 1 μL oligo(dT)₁₂₋₁₈ primers (500 ng μL^{-1}) and 1 μL random hexamer primers (250 ng μL^{-1}) were added to each sample, followed by incubation at 65 $^\circ\text{C}$ for 5 min. After cooling on ice for 2 min, 4 μL 5x First Strand Buffer, 2 μL Dithiothreitol (0.1 mM), and 1 μL RNaseOUTTM Recombinant Ribonuclease Inhibitor per sample were added. Reactions were mixed and incubated at 42 $^\circ\text{C}$ for 2 min. Finally, 1 μL (=200 U) SuperScript II Reverse Transcriptase was added to reach a final volume of 20 μL per reaction and three incubation steps (25 $^\circ\text{C}$ for 10 min, 42 $^\circ\text{C}$ for 50 min, 70 $^\circ\text{C}$ for 15 min) were performed to yield cDNA stock solutions that were stored at -20 $^\circ\text{C}$.

For quantitative real-time RT PCR (qRT-PCR), cDNA working solutions were established by diluting stock solutions with ddH₂O to a final RNA concentration of 1 ng μL^{-1} . qRT-PCR was performed in MicroAmp[®] Optical 96-well Reaction Plates. In general, each combination of cDNA sample and primer pair (=mRNA to be analyzed) was assayed in triplicate, with reactions consisting of 4.5 μL primer mix (800 nM of forward and reverse primer in ddH₂O), 4.5 μL cDNA working solution and 9 μL 2x Platinum[®] SYBR[®] Green qPCR SuperMix-UDG w/ROX. Sequences of used primer pairs are listed in Table 3.3. qRT-PCR runs were performed on an ABI PRISM[®] 7000 Sequence Detection System with the following program: 2 min at 50 $^\circ\text{C}$, 10 min at 95 $^\circ\text{C}$, 40 cycles of 2 min at 60 $^\circ\text{C}$ and 15 s at 95 $^\circ\text{C}$. A dissociation protocol (from 60 $^\circ\text{C}$ to 95 $^\circ\text{C}$) was performed at the end of each run to check for unspecific amplification products.

For quantification of miR-27b levels, the TaqMan[®] microRNA Assays for hsa-miR-27b and RNU5B were used in combination with the TaqMan[®] MicroRNA Reverse Transcription (RT) Kit. For each sample, two RT reactions were performed by combining 10 ng total RNA

Table 3.3. Primer pairs used for quantitative real-time RT-PCR.

gene / RefSeq ID	forward primer (5'→3')	reverse primer (5'→3')	amplicon (bp)
ALK2 / NM_001150	TCCCTAGTATGGAAGATGAGAA	CTGGTAGACGTGGAAGCCAT	150
C/EBP α / NM_004364	CTTGTGCCTTGGAAATGCAA	GCTGTAGCCTCGGGAAGGA	112
C/EBP β / NM_005194	AACCAACCGCACATGCAGAT	GGCAGAGGGAGAAGCAGAGAGT	103
C/EBP δ / NM_005195	GGTGCCCGCTGCAGTTTC	CACGTTTAGCTTCTCTCGCAGTTT	90
CHOP10 / NM_004083	CCTCCTGGAAATGAAGAGGA	TGGAATCTGGAGAGTGAGGG	136
CIDEA / NM_001279	GGCAGGTTACGTGTGGATA	GAAACACAGTGTGGCTCAAGA	64
CPT1 β / NM_152246	CCAGGATCTGGGCTATGTGT	GGGCGCACAGACTCTAGGTA	136
CTDSP2 / NM_005730	TGCATAGTCCCTTAAAGCCAATCAACA	TCAAAGAGTTCCCCATGCGTCT	136
CTDSPL / NM_001008392	GGCCAAGTATGCAGACCTGTGG	CTTTGCTCAGTCCCGCCCA	140
FABP4 / NM_001442	TGTGCAGAAATGGGATGGAAA	CAACGTCCCTTGGCTTATGCT	132
FASN / NM_004104	TGAACTCCTTGGCGGAAGAGA	GTAGGACCCCGTGGAAATGTCA	153
GLUT4 / NM_001042	CGTCGGGCTTCCAACAGATA	CACCGCAGAGAACACAGCAA	92
GPDH / NM_005276	TTGTGGTGCCCCATCAGTTC	CCCAATCACTCCGAGATGA	141
KLF4 / NM_004235	CCCACACAGGTGAGAAACCT	AATGCTCGGTGCGATTTT	139
LPL / NM_000237	TGGAGGTACTTTTCAGCCAGGAT	TCGTGGGAGCACTTCACTAGCT	102
PAI-1 / NM_000602	ACCTGGGAATGACCGACATGT	CTCTCGTTCACCTCGATCTTCACT	118
PGC1 α / NM_013261	ACAACACTTACAAGCCAAACCA	GCCTGCAGTTCAGAGAGT	136
PPAR γ / NM_138712	AGCCTCATGAAGAGCCTTCCA	TCCGGAAGAAACCCTTGCA	120
RB1 / NM_000321	TGGACTTCCAGAGGTTGAAAAT	CGTGGTGTCTCTGTGTTTCA	147
RIP140 / NM_003489	TTGGAGACAGACGAAACACTGA	TCTACGCAAGGAGGAGGAGA	143
RXR α / NM_002957	GCCCTCGAGCCAATGAGAA	GGAGTCGGGAGTCTGAAACCA	132
S6K1 / NM_003161	CCATATGAACCTGGCATGGA	TTTCCATAGCCCCCTTACC	131
SREBP1c / NM_004176	AGGCCATCGACTACATTCG	TCCTTCAGAGATTTGCTTTTGTG	104
TBP / NM_003194	ACGCCAGCTTCGGAGAGTTC	CAAACCGCTTGGGATTATATTCG	136
UCP1 / NM_021833	GTGTGCCCAACTGTGCAATG	CCAGGATCCAAGTCGCAAGA	95
mAlk2 / NM_007394	AACATCACGGCCAGCTGCC	ACTGCAAACACCACCGAGAGGATGA	101
mPai-1 / NM_008871	ACATGTTTAGTGCAACCTGGC	CTGAGATGACAAAGGTGTGGAG	144
mPths2 / NM_011198	CGCAAACGCTTCTCCCTGAAGCC	TTTTCCACCAGCAGGGCAGGGT	134
mRb1 / NM_009029	TGAGAGACCGACATTTGGACCAGA	AACACGTTTAAAGGTCTCCTGGGC	143
mRip140 / NM_173440	TCAGGCTGAGGCAGACGATAC	CCTCGCAACTTCCTTAGCACA	125
mS6K1 / NM_028259	TGGACCATGGGGAGTTGGACC	AGCCCCCTTTACCAAGTACCCGA	144
mUcp1 / NM_009463	TGAACCCGACAACCTCCGAA	GGCCTTACCTTGGATCTGAA	138
mUxt / NM_013840	CTCACAGAGCTCAGCGACAGC	AAATCTGCAGGCCTTGTAGTTCTC	104

(in a volume of 5 μ L ddH₂O) with 3 μ L 5x RT primer solution (hsa-miR-27b or RNU5B) and 7 μ L of an RT MasterMix which consisted of 0.15 μ L dNTP mix (100 mM), 1 μ L (=50 U) MultiScribeTM Reverse Transcriptase, 1.5 μ L 10x RT buffer, 0.19 μ L (=3.8 U) RNase Inhibitor and 4.16 μ L nuclease-free H₂O. RT reactions were placed into the PTC-225 PCR cyclor and incubated at 16 °C for 30 min, at 42 °C for 30 min and at 85 °C for 5 min. Subsequent qRT-PCR reactions were pipetted into MicroAmp[®] Optical 96-well Reaction Plates and consisted of 9 μ L 2x TaqMan[®] Gene Expression Master Mix, 6.9 μ L DEPC-treated H₂O, 0.9 μ L 20x TaqMan[®] Assay (hsa-miR-27b or RNU5B) and 1.2 μ L of the respective reverse transcribed sample. The setup of qRT-PCR runs was identical as for the conventional SYBR[®] Green method described above.

For quantification of miR-30c and miR-26a levels, the miRCURY LNATM Universal RT

Table 3.4. Primer pairs used for RT-PCR.

gene	RefSeq ID	forward primer (5'→3')	reverse primer (5'→3')	amplicon (bp)
RB1	NM_000321	ACTCGAACACGA- ATGCAAAGCAG	GGGTCCTCTATACC- TAAGATCTGGCA	931
RIP140	NM_003489	AGGGATGGAAAAA- CAGGGCCAC	GCCTATGCCTTCACT- TCTCCATGATGT	645
S6K1	NM_003161	GGCCTTTTGATGAA- TGTCTTCCACAGT	TCCTCCACCCC- TGCCCACAA	1734

microRNA PCR system (Exiqon) was used as described by the manufacturer. 20 ng total RNA of each sample were brought to a volume of 14 μ L with nuclease-free H₂O, and after addition of 4 μ L 5x reaction buffer and 2 μ L of Enzyme Mix, the reactions were incubated in the PTC-225 PCR cyler at 42 °C for 60 min, followed by heat inactivation at 95 °C for 5 min. These RT reactions were then diluted 1:80 with a solution containing 381 nM ROX reference dye in nuclease-free H₂O. Primer pairs for detection of miR-26a, miR-30c, 5S rRNA and RNU5G were dissolved in 220 μ L nuclease-free H₂O. Subsequently, qRT-PCR reactions were pipetted into MicroAmp[®] Optical 96-well Reaction Plates. These reactions consisted of 9 μ L SYBR Green Master Mix, Universal RT, 1.8 μ L PCR primer mix and 7.2 μ L diluted cDNA sample (with ROX). The setup of qRT-PCR runs was identical as for the conventional SYBR[®] Green method described above.

All qRT-PCR raw data was stored and analyzed using the QPCR application (Pabinger et al., 2009), with AnalyzerMiner (Zhao and Fernald, 2005) C_q and efficiency calculation algorithms.

3.2.2.4 RT-PCR

For amplification of predicted miR-26a-MREs within the 3'UTRs of RB1, RIP140, and S6K1, RNA was reverse transcribed as described in 3.2.2.3 except that no DNase digestion was performed. For every sample, an additional reaction without reverse transcriptase was performed in parallel to check potential amplification of genomic DNA at subsequent PCR. RT-PCR was performed in reactions of 20 μ L, consisting of 1 ng reverse transcribed RNA (or control, non-reverse transcribed RNA), 5 U *Taq* DNA Polymerase, 1x *Taq* Buffer (with KCl), 10 mM dNTP mix, 25 mM MgCl₂, and 800 nM of each primer. Sequences of used primer pairs are listed in table 3.4. For all reactions, the RT-PCR conditions were 3 min at 95 °C, 35 cycles of 30 s at 95 °C, 30 s at 64 °C, and 1 min at 72 °C, and 15 min at 72 °C for final elongation. Subsequently, RT-PCR reactions were mixed with 4 μ L of 6x loading dye and applied on 1 – 1.5% agarose gels containing Ethidium bromide for DNA visualization. Electrophoresis was performed at 80 V for 45 min. Amplification of desired products was checked under UV light by comparison of sample DNA bands with bands of 100 bp DNA ladder or 1 kb Plus DNA ladder and documented using the Gel Doc 2000 Gel Documentation System.

3.2.2.5 Oil Red O staining

For fixation, a working solution of 3.6% formaldehyde in PBS was prepared by dilution of 36.5% formaldehyde stock solution. Oil Red O stock solution was prepared by dissolving 10 g Oil Red O in 500 mL 2-propanol, and Oil Red O working solution was generated by mixing with ddH₂O in a ratio of 3:2. The working solution was incubated at room temperature for 10 min and then filtered to eliminate precipitates. Cells were washed with PBS and incubated at room temperature for 15 min with formaldehyde working solution. After 2 washing steps with PBS, fixed cells were incubated at room temperature with Oil Red O working solution for 30 min. Stained cells were washed 3 times with PBS before phase contrast photography. A solution of 50% Glycerol in PBS was used for long-term storage of stained cells.

3.2.2.6 Quantification of triglyceride accumulation

Intracellular triglyceride accumulation was quantified using the Infinity Triglycerides Kit. Therefore, 12-well plates containing the cells to be analyzed were put on ice and medium was aspirated. After the cells were washed with 1 mL PBS (4 °C), 300 μ L PBS (4 °C) were pipetted into every well and cells were detached from the bottom of the well by scraping with a 1000 μ L pipette tip. Subsequently, this suspension was transferred into 1.5 mL microcentrifuge tubes and homogenized by ultrasonication for 20 s using the Sonopuls UW2070. A dilution series of 4 mM glycerol standard in phosphate buffered saline (PBS) was established, and 15 μ L of each homogenized sample and each standard solution were then pipetted into the wells of a 96-well plate. In general, every sample and standard solution was analyzed in duplicates. Finally, 200 μ L of Infinity Triglycerides reagent were added to each well and the plate was incubated for 10 min at 37 °C before recording absorbance at 500 nm with a SPECTRAMax PLUS³⁸⁴ absorbance microplate reader.

To normalize triglyceride concentration values, the protein concentration of each sample was determined using the BCATM Assay Kit. Therefore, a dilution series of at 2 mg mL⁻¹ bovine serum albumin (BSA) standard was prepared in PBS, and 20 μ L of every sample and standard solution were pipetted into a 96-well plate. Again, every sample and standard solution was assayed in duplicates. A BCA Protein Assay reagent was prepared by diluting Reagent B 1:50 with Reagent A, and reactions were initiated by addition of 200 μ L BCA Protein Assay Reagent to each well containing sample or standard solution. Subsequently, the 96-well plate was incubated at 37 °C for 30 min before absorbance at 562 nm was recorded on a SPECTRAMax PLUS³⁸⁴ absorbance microplate reader.

For both triglyceride and protein raw data, the respective dilution series of standards was used to transform absorbance values of samples into concentrations, i.e. μ M triglyceride and mg total protein per mL. Finally, protein concentration of each sample was used for normalization of triglyceride amounts, yielding μ mol triglycerides per mg total protein. This normalized triglyceride concentration was used for comparison of different samples.

3.2.2.7 Generation of luciferase reporter vectors

Primers for PCR-based amplification of 3'UTRs were designed using the NCBI Primer-BLAST tool (www.ncbi.nlm.nih.gov/tools/primer-blast/). In order to facilitate cloning of the desired DNA fragments into the multiple cloning site (MCS) of the psiCHECK-2 vector, a 12-nt DNA sequence consisting of CATCAG plus the XhoI recognition sequence CTCGAG was added to the 5' end of all forward primers. Similarly, a 14-nt DNA sequence consisting of CGGATC plus the NotI recognition sequence GCGGCCGC was added to the 5' end of all reverse primers. Complete sequences of used primers are listed in table 3.5. PCR was performed using High Fidelity PCR Enzyme Mix according to the manufacturer's instructions. Each reaction consisted of 5 μ L High Fidelity PCR Buffer (5x), 1 μ L 10 mM dNTP mix, 2 μ L of a mix containing 12.5 μ M of the respective forward and reverse primer in DEPC-treated H₂O, either 200 ng of genomic DNA (isolated from hMADS cells) or 50 ng of RNA (from hMADS cells) that had been reverse transcribed as described in 3.2.2.3 as DNA template, and DEPC-treated H₂O to reach a final volume of 50 μ L. A summary of distinct PCR protocols used for 3'UTR amplification is depicted in table 3.6, while specifications of cycling parameters for individual genes can be found in table 3.7.

After PCR, reactions were mixed with 10 μ L 6x loading dye and agarose gel electrophoresis was performed on 1% agarose gels containing Ethidium bromide for DNA visualization. Usually, electrophoresis was performed at 105 V with a run time of 60 min. Amplification of desired 3'UTR regions was checked under UV light by comparison of sample DNA band with bands of a GeneRuler™ 1 kb DNA Ladder, documented using the Gel Doc 2000 Gel Documentation System, and DNA bands of interest were cut with a scalpel and transferred to 1.5 mL microcentrifuge tubes. PCR products were then isolated using the PureLink Quick Gel Extraction Kit. Briefly, 300 μ L per 100 mg of agarose gel were added and tubes were incubated at 50 °C for 15 min. Reactions were applied to a spin column (placed on a collection tube) and centrifuged at $1.3 \times 10^4 *g$ for 1 min. Flowthrough was discarded and 700 μ L wash buffer were added to each column. Reactions were incubated at room temperature for 5 min, then centrifuged as above and the flowthrough was discarded. After another centrifugation step as above, columns were placed onto a clean 1.5 mL microcentrifuge tube, 20 μ L ddH₂O were added, reactions were incubated at room temperature for 1 min and then centrifuged at $1.3 \times 10^4 *g$ for 2 min. The flowthrough was once again pipetted onto the column and incubation and centrifugation were performed as before to yield the purified DNA fragments.

Digestion of DNA fragments with XhoI and NotI restriction enzymes (Promega) was performed in reactions of 20 μ L, consisting of 150–500 ng purified DNA, 2 μ L 10x Buffer D (Promega), 0.2 μ L acetylated BSA (Promega), 0.5 μ L XhoI and 0.5 μ L NotI restriction enzymes (=5 U), and ddH₂O. Reactions were incubated at 37 °C for 1 h and subsequently purified using the QIAquick PCR Purification Kit (QIAGEN). Briefly, samples were mixed with 100 μ L Buffer PBI and pipetted onto a QIAquick spin column (placed in a collection tube) for centrifugation at $1.3 \times 10^4 *g$ for 1 min. The flowthrough was discarded, 750 μ L

Table 3.5. Primers designed for PCR-based 3'UTR amplification

gene	3'UTR length	foward primer (5'→3')	reverse primer (5'→3')
PPARG NM_015869	210 bp	CATCAGCTCGAGCAGAGAGT- CCTGAGCCACT	CGGATCGCGGCCCGCACTATCA- GCAATTTTCATAATATGGT
SERPINE1 NM_000602	1101 bp	CATCAGCTCGAGTCCGGCAC- AACCCACAGAA	CGGATCGCGGCCCGCAAGCACT- CAAGGGCAAGGATATGA
ACVR1 NM_001105	1081 bp	CATCAGCTCGAGTTTTTCATAG- TGTCAGAAGGAA	CGGATCGCGGCCCGCGCACGTA- ATGGATAAATCTGA
RB1 NM_000321	1819 bp	CATCAGCTCGAGATCTCAGGA- CCTTGGTGG	CGGATCGCGGCCCGCAGAACAC- AACATCAGACCATT
NRIP1 NM_003489	3481 bp	CATCAGCTCGAGCTGGGAAG- CGTGCTAACGATAAAGA	CGGATCGCGGCCCGCACAAAGT- GAATCTGTGGATGTATGCC
RPS6KB1 NM_003161	3605 bp	CATCAGCTCGAGCAGAGCAA- TGCTTTTAATGA	CGGATCGCGGCCCGCTTTACAT- TCATTC AATCCGAA

Buffer PE were added to each sample and columns were centrifuged as before. After discarding of flowthrough and another centrifugation at $1.3 \times 10^4 *g$ for 1 min, each column was placed onto a clean 1.5 mL microcentrifuge tube, 20 μ L ddH₂O were added and samples were incubated for 1 min before centrifugation as above. The flowthrough was once again pipetted onto the column and incubation and centrifugation were performed as before to yield the XhoI and NotI digested DNA fragments.

Digestions of psiCHECK-2 vector with XhoI and NotI restriction enzymes were performed similarly to digestions of PCR-amplified 3'UTR DNA fragments with 1 μ g of plasmid DNA as input. After digestion, the solutions were applied to a 1 % agarose gel, electrophoresis was carried out as described above and bands containing the double-digested DNA backbone were cut under UV light. Subsequently, plasmid DNA was purified with the PureLink Quick Gel Extraction Kit as described above.

Ligation of PCR-amplified 3'UTR DNA fragments (insert) with psiCHECK-2 vector backbone was performed using T4 DNA Ligase (Invitrogen). Therefore, the respective insert DNA was combined with backbone DNA at a molar ratio of 3:1 to yield ≈ 100 ng total DNA in a volume of 15 μ L ddH₂O. After addition of 4 μ L 5x reaction buffer and 1 μ L (=1 U) T4 DNA Ligase, reactions were incubated at 26 °C for 1 h, and at 16 °C for 72 h. Subsequently, transformation of DH5 α *E. coli* cells was carried out. Therefore, 10 μ L of ligation reaction were mixed with 50 μ L of DH5 α solution (thawed on ice), mixed carefully and incubated on ice for 30 min. Subsequently, reactions were transferred to 42 °C for 20 s and back to ice. 2 min later, 300 μ L S.O.C. Medium (prewarmed to 37 °C) were added and reactions were incubated at 37 °C with shaking at 225 rpm for 60 min. Finally, reactions were plated onto Luria-Bertani (LB)-Agar-plates (1 % pepton, 1 % NaCl, 0.5 % yeast extract and 1.5 % agar) containing 100 μ g mL⁻¹ Ampicillin and incubated at 37 °C for 14–18 h.

To analyze cloning of 3'UTR DNA fragments into the psiCHECK-2 vector, colony PCRs were performed using *Taq* polymerase (Fermentas) and a primer pair homologous to 2 regions up-

Table 3.6. PCR conditions for 3'UTR amplification

PCR designation	genes	PCR protocol		
		[°C]	t[min]	cycles
classic	PPARG, ACVR1, NRIP1	94	5:00	1
		94	0:30	
		T_A	0:30	n_C
		72	t_1	
		72	10:00	1
		4	—	1
touchdown	SERPINE1, RB1	94	5:00	1
		94	0:30	
		T_A	0:30	$10, T_{A(i+1)} = T_{A(i)} - 0.5^\circ\text{C}$
		T_B	t_1	
		94	0:30	
		T_C	0:30	n_C
		T_B	t_2	
		72	10:00	1
		4	—	1
		large fragments	RP6KB1	94
94	0:30			
T_A	0:30			n_C
T_B	t_1			
94	0:30			
T_A	0:30			$25, t_{2(i+1)} = t_{2(i)} + 10\text{ s}$
T_B	t_2			
T_B	10:00			1
4	—			1

Table 3.7. PCR specifications for 3'UTR amplification

gene	RefSeq	template	T_A [°C]	t_1 [min:s]	T_B [°C]	t_2 [min:s]	T_C [°C]	n_C	amplicon [bp]
PPARG	NM_015869	cDNA	60	0:30	—	—	—	40	236
SERPINE1	NM_000602	cDNA	61	0:50	72	0:50	56	25	868
ACVR1	NM_001105	cDNA	52	0:30	—	—	—	25	983
RB1	NM_000321	gDNA	58	1:50	72	1:50	53	20	1836
NRIP1	NM_003489	gDNA	55	2:40	—	—	—	35	3279
RPS6KB1	NM_003161	gDNA	52	4:00	68	4:10	—	10	3838

and downstream of the psiCHECK-2 MCS (sequences (5'→3'): F: TAAGAAGTTCCTAA-CACCG; R: CGAGGTCCGAAGACTCATTTAG). The reactions consisted of 2 μL 10x Taq Buffer, 1.2 μL 25 mM MgCl_2 , 0.4 μL 10 mM dNTP mix, 0.16 μL of a primer mix containing 12.5 μM forward and reverse sequencing primer, 0.2 μL (=1 U) *Taq* Polymerase and ddH₂O up to 20 μL . For inoculation, colonies on the LB-Agar-plates were touched with a sterile 200 μL pipette tip which was then dipped into the PCR reactions. Conditions for subsequent PCR were 94 °C for 2 min, followed by 30 cycles of 94 °C/30 s, 50 °C/30 s and 72 °C/1 min, followed by a final elongation step of 10 min at 72 °C. Reactions were then applied to a 1 % agarose gel and electrophoresis was performed as described above. Colonies corresponding

to reactions that yielded the expected DNA fragment were used for inoculation of 5 mL LB Medium containing $100 \mu\text{g mL}^{-1}$ Ampicillin, which was subsequently incubated at 37°C with shaking at 225 rpm for 14 h. Afterwards, plasmid purification was performed using the QIAprep Spin Miniprep Kit (QIAGEN) as described by the manufacturer. Briefly, suspensions were centrifuged at $4500 \times g$ and 4°C for 10 min, the supernatant was decanted and the bacterial pellet was resuspended in 250 μL Buffer P1 and transferred into a 1.5 mL microcentrifuge tube. 250 μL Buffer P2 were added, the reactions were mixed by inverting the tube several times, and 350 μL Buffer N3 were added. Samples were mixed again and centrifuged at $1.6 \times 10^4 \times g$ for 10 min. Subsequently, the supernatants were applied to QIAprep spin columns (placed onto collection tubes), centrifuged at $1.6 \times 10^4 \times g$ for 1 min and the flowthrough was discarded. 500 μL Buffer PB were applied on each column, reactions were again centrifuged at $1.6 \times 10^4 \times g$ for 1 min and flowthrough was again discarded. Next, 750 μL Buffer PE were pipetted on each column and reactions were centrifuged as in the last step, followed by discarding of the flowthrough. To dry the columns, reactions were once again centrifuged as before. Subsequently, columns were placed onto clean 1.5 mL microcentrifuge tubes, 40 μL ddH₂O were added, reactions were incubated at room temperature for 1 min and then centrifuged at $1.4 \times 10^4 \times g$ for 1 min. The flowthrough was once again pipetted onto the column and reactions were again incubated and centrifuged as in the last step to yield purified psiCHECK-2 vectors.

After purification, solutions of 14 μL were prepared containing 1 μg of the respective vector and 1.43 μM of either the forward or the reverse primer already used for colony PCR (see above). These solutions were sent to AGOWA for sequencing, and using BLAST, obtained sequences were compared to the theoretical sequences that emerged from the cloning design. Subsequently, psiCHECK-2 vectors containing, in correct orientation, the PCR-amplified 3'UTR sequences of interest were used for transfection of HEK293 cells (see 3.2.1.7). For convenience, psiCHECK-2 reporter vectors with inserted 3'UTRs of interest were named p2-PPARG, p2-PAI-1 (=SERPINE1), p2-ALK2 (=ACVR1), p2-RB1, p2-NRIP1 and p2-S6K1 (=RPS6KB1).

Site-directed mutagenesis of wildtype psiCHECK-2 reporters was performed using the QuikChange[®] Lightning Site-Directed Mutagenesis Kit. Primers were designed using a software provided by Integrated DNA Technologies (www.eu.idtdna.com), from which the primers were also ordered at Polyacrylamid Gel Electrophoresis (PAGE) purification grade. Primers sequences are listed in table 3.8. As the RB1 and RPS6KB1 3'UTRs each harbour two predicted miR-26a recognition elements, two sets of primers (for two independent mutagenesis reactions) were designed. Primer lyophilisates were dissolved in ddH₂O to reach stock concentrations of $1 \mu\text{g mL}^{-1}$. Working solutions of 100 ng mL^{-1} were established by dilution with ddH₂O. Mutagenesis reactions consisted of 50 ng of the respective wildtype psiCHECK-2 reporter in 39 μL ddH₂O, 5 μL 10x reaction buffer, 1.25 μL of the respective forward and reverse primer working solutions, 1 μL dNTP mix, 1.5 μL QuikSolution[™] reagent and 1 μL QuikChange[®] Lightning enzyme. PCR was carried out in the PTC-225 PCR cycler with

Table 3.8. Primer pairs designed for site-directed mutagenesis of psiCHECK-2 reporters.

wt reporter vector	primer	primer sequence (5'→3') (mutated bases in bold)	generated reporter
p2-PPARG	F	ATTCTGAGGGAAAAATCTGACACCTAA- GAAATTTAC CA CAAAAAAGCATTTTA- AAAAGAAAAGGTTTGTAGAATAT	p2-PPARG-m
p2-PPARG	R	ATATTCTAAAACCTTTTCTTTTAAA- ATGCTTTTT GTGT GTAAATTCTTAG- GTGTCAGATTTTCCCTCAGAAT	
p2-PAI-1	F	GGGTTATTTTGGAGTGTAGGTGACTT- GACAT CTCATTGAAGCAGATTTTTGC- TTCTT	p2-PAI-1-m
p2-PAI-1	R	AAGGAAGCAAAAATCTGCTTCAATGA- GATGT CAAGTCACCTACACTCCAAAA- TAACCC	
p2-ALK2	F	GCTGCATTTTACACATGTGCTGAT CTA - TTCAATGATGCCGAACATTAGGAATT	p2-ALK2-m
p2-ALK2	R	AATTCCTAATGTTCCGGCATCATT GAAT - AGATCAGCACATGTGTA-AAATGCAGC	
p2-RB1	F	GCAATTGTTTGGGTGATTCCCTAAGCC- AGTACA AAATGTTAGTCATTGTTATTT- ATACAAG	p2-RB1-m1
p2-RB1	R	CTTGTATAAATAACAATGACTAACAT- TT GTACT GGCTTAGGAATCACCCAA- ACAATTGC	
p2-RB1	F	ACTGAATTTATAAAGTACCCATCTAGT- ACA ACTAAAAGTAAAGTGTCTGCCA- GATCTTAGG	p2-RB1-m2
p2-RB1	R	CCTAAGATCTGGCAGAACA CTTACTT - TT AGTT GTACTAGATGGGTACTTTATA- AATTCAGT	
p2-NRIP1	F	AATTATCTATAATCACTACTAGTTAGG- ATATTGATTTAAAATTTGTTCTAG TACA A- GTGGTTTCTAAGATTTTATATTA	p2-NRIP1-m
p2-NRIP1	R	TAATATAAAAATCTTAGAAACCA CTTGT - ACTAGAACAATTTTAAATCAATATCCTA- ACTAGTAGTGATTATAGAATAATT	
p2-S6K1	F	GGTAAGTGATAAAAGAGATTAAGTGCT- TTTTTTTCATC GA ACATTATTTTCTTT- AAAATCAGCTATTACAGGATATTTTTTT	p2-S6K1-m1
p2-S6K1	R	AAAAAATATCCTGTAATAGCTGATTTTA- AAGAAAATAAT GTTCT GATGAAAAAAA- GCACTTAATCTCTTTTATACACTTACC	
p2-S6K1	F	GCTTTTCATCTTGATTTAGTTGACTGTA- CCATAT CATTTTCGGATTGAATGAATGTA- AAGCGGCC	p2-S6K1-m2
p2-S6K1	R	GGCCGCTTTACATTCATTCAATCCGAAAT- GATATGGT ACAGTCAACTAAATACAAGA- TGAAAAGC	

the following conditions for the p2-S6K1 and p2-NRIP1 reporters: 95 °C for 2 min, 18 cycles of 95 °C for 20 s, 60 °C for 10 s and 68 °C for 5 min, and a final elongation step of 68 °C for 5 min.

For other reporters, the cycling conditions were identical except for duration of the elongation step during cycling, which was 4.17 min for p2-PAI1, p2-ALK2 and p2-RB1 reporters, and 3.5 min for the p2-PPARG reporter. Next, 2 µL of DpnI enzyme solution were added to each reaction, samples were mixed by pipetting, incubated at 37 °C for 5 min and then kept on ice. For transformation, aliquots of XL10-Gold[®] ultracompetent cells were thawed on ice and 45 µL bacterial suspension were mixed with 2 µL β-mercaptoethanol and incubated

on ice for 2 min. Subsequently, 2 μL of DpnI-digested sample were added, reactions were carefully mixed and incubated for 30 min on ice, followed by exposure to 42 $^{\circ}\text{C}$ for 30 s and incubation on ice for 2 min. 500 μL of prewarmed (37 $^{\circ}\text{C}$) NZY⁺ broth (consisting of 0.5 % NaCl, 1 % pepton, 0.5 % yeast extract, 12.5 mM MgCl₂, 12.5 mM MgSO₄ and 0.4 % glucose in ddH₂O) were added to each sample and reactions were incubated at 37 $^{\circ}\text{C}$ with shaking at 225 rpm for 1 h. Finally, 100 μL of each reaction was plated on LB-Agar plates with 100 $\mu\text{g mL}^{-1}$ Ampicillin and plates were incubated at 37 $^{\circ}\text{C}$ for 18 h. Colonies yielded from the transformation were used for inoculation of 5 mL LB Medium containing 100 $\mu\text{g mL}^{-1}$ Ampicillin. After incubation at 37 $^{\circ}\text{C}$ with shaking at 225 rpm for 14 h, plasmid purification and preparation of plasmids for sequencing were performed as described above. BLAST was subsequently used to compare the obtained with the expected sequencing results, and reporter vectors bearing the desired point mutations were finally used for transfection of HEK293 cells (see 3.2.1.7). For convenience, psiCHECK-2 reporters with mutated 3'UTRs of interest were named p2-PPARG-m, p2-PAI-1-m, p2-ALK2-m, p2-RB1-m1, p2-RB1-m2, p2-NRIP1-m, p2-S6K1-m1 and p2-S6K1-m2.

3.2.2.8 Luciferase reporter assays

Medium was carefully removed from HEK293 cells transfected 48 h ago (see 3.2.1.7), and cells were washed with 30 μL PBS per well. Lysis was performed by addition of 30 μL Passive Lysis Buffer (PLB, diluted 1:5 with ddH₂O from 5x stock) and incubation at room temperature with shaking (100 rpm) for 25 min. Subsequently, lysates were frozen at -20 $^{\circ}\text{C}$ and thawed for luciferase assays. Prior to measurements, the two-channel liquid system of the ORION II microplate luminometer was cleaned with 70 % Ethanol and ddH₂O, followed by priming with LARII and Stop&Glo[®] reagents (diluted 1:50 with Stop&Glo[®] Buffer), respectively. 6 μL of samples were pipetted into wells of a 96-well flat bottom assay plate (each sample assayed in duplicate), and the measurement was started. First, firefly luciferase (FL) activity was measured by addition of 25 μL LARII reagent per well, with 2 s pre-measurement delay and a subsequent photon flux integration time of 10 s. Next, 25 μL Stop&Glo[®] reagent per well were added and *Renilla* luciferase RL activity was recorded with identical settings as before. For every well, RL activities were normalized to FL activities, followed by averaging of technical replicates and comparison between different samples.

3.2.2.9 Western blot analysis

For harvest of cells to be analyzed by Western blots, a protein extraction buffer (PEB) was prepared consisting of 25 mM Tris-Cl (pH 7.4), 100 mM NaCl, 1 mM EDTA, 0.5 % Triton X-100, 0.5 % Nonidet P40, 0.5 mM sodium orthovanadate, 10 mM NaF, 10 mM β -glycerophosphate and 1x protease inhibitor cocktail. 6-well plates with cells were put on ice, medium was aspirated and cells were washed with 2 mL PBS (4 $^{\circ}\text{C}$) per well. 150 μL PEB (4 $^{\circ}\text{C}$) were added per well, and cells were detached using a cell scraper. Usually, cells of two wells (treated identically during the experiment) were pooled at this step, followed

by mixing and three ultrasonication treatments (10 s each). Protein lysates were then centrifuged at $1.4 \times 10^4 \text{ *g}$ and 4°C for 10 min. Subsequently, 40 μL aliquots of protein lysate were prepared and stored at -80°C . Additionally, the protein concentration of each sample was determined (in duplicates) using the BCATM Protein Assay Kit. Therefore, a dilution series of 2 mg mL^{-1} BSA standard (in 0.9% NaCl) was prepared. 2 μL of each sample were combined with 10 μL of 0.9% NaCl, and 10 μL of BSA standard solutions were combined with 2 μL PEB in the wells of a 96-well multiwell plate. Subsequent steps were performed as described in 3.2.2.6.

For polyacrylamide gel electrophoresis, 50 μg of protein sample or 10 μL of Plus2 Pre-Stained Standard were prepared in 1x NuPAGE[®] LDS Sample Buffer and 0.5M DTE to reach a final volume of 40 μL . After incubation at 70°C for 10 min, samples were loaded on 10% Bis-Tris gels which were placed in 1x MOPS SDS Running Buffer supplemented with 833 μL of antioxidant solution per 1000 mL of buffer. Subsequently, electrophoresis was run for 1 h at 175 V. For transfer of proteins, nitrocellulose membranes were activated by incubation in ddH₂O for 5 min, followed by assembly of a transfer sandwich that was placed in transfer buffer consisting of Tris-Glycine-SDS buffer (25 mM Tris, 192 mM glycine, 0.1% SDS, pH 8.3) and 20% methanol. Transfer was performed at 4°C , 120 V and 0.5 A for 90 min using the Mini Trans-Blot Electrophoretic Transfer Cell. Efficiency of transfer was controlled by staining of membranes and the polyacrylamide gels with PonceauS and SimplyBlue SafeStain, respectively. After transfer, membranes were blocked in TBS-T buffer (10 mM Tris, 150 mM NaCl, 0.1% Tween-20, pH 7.5) supplemented with 5% BSA. Primary antibodies were diluted in TBS-T buffer with 1% BSA (1:750 and 1:2000 for anti-UCP1 and anti- β Tubulin antibody, respectively), and incubation of membranes with primary antibodies was carried out at 4°C over night. Subsequently, membranes were washed thrice with TBS-T buffer, and incubated with secondary antibody solution (swine anti-mouse for UCP1, goat anti-mouse for β -Tubulin, 1:2000 dilution in TBS-T with 1% BSA) for 2 h at room temperature. Finally, membranes were again washed three times in TBS-T and Pierce SuperSignal enhanced chemiluminescence (ECL) substrate was applied to detect the chemiluminescent signal on an ECL film. Stripping of blots was performed by incubation of membranes at room temperature for 15 min, followed by re-blocking as described above.

3.2.2.10 Oxygen consumption measurements

Oxygen consumption was recorded using a luminescent nanosensor-based detection system consisting of an oxygen microsensor and a transmitter device (connected to a computer). Calibration of sensors was carried out prior to measurements of cellular respiration using two aqueous solutions tempered to 37°C : (i) ddH₂O saturated with O₂ (corresponding to 100% O₂ oxygen saturation, or 207 μM O₂), and (ii) a glucose solution to which glucose oxidase was added immediately before measurement (leading to deprivation of O₂ from the aqueous solution, corresponding to 0% oxygen saturation). Adipocytes from a 100 mm cell culture plate were used for a single measurement. Medium was transferred to a 15 mL tube

and centrifuged for 7 min at $600 * g$. Meanwhile, adipocytes were washed once with PBS and incubated with 700 μL trypsin (1x) for 5 min at 37°C . Subsequently, 600 μL of a "2x measurement medium" (2x DMEM/Ham's F12, 20% FBS, 20 mM HEPES, 4 mM L-Gln, 2x Normocin) were added and the cell suspension was carefully mixed by pipetting. After centrifugation of medium, the supernatant was discarded and the pelleted cells were carefully resuspended in 100 μL 2x measurement medium before being added back to the cell suspension containing detached adipocytes. Subsequently, cell concentration and viability were determined to calculate the volume of cell suspension corresponding to $5 * 10^5$ living cells, which was carefully pipetted into a 1.8 mL chromatography vial containing a magnetic stirrer bar. The remaining volume of the vial was filled with 1x measurement medium (a 1:2 dilution of 2x measurement medium with ddH₂O), and a screw cap with septum was used to close the measurement chamber. Finally, a needle containing the oxygen microsensor was inserted through the septum into the cell suspension and the vial was placed in 37°C -tempered H₂O above a magnetic stirrer set to 500 rpm. Measurement was performed by recording the phase shift ϕ of the light pulse, which is dependent on O₂ concentration (see below), in intervals of 1 sec, with dynamic averaging of signals within an interval of 4 measurement points. Usually, a linear oxygen consumption could be observed after 5 min. After recording respiration of adipocytes in 1x measurement medium (without any additives), oligomycin (100 $\mu\text{g mL}^{-1}$ stock solution in ethanol) was added through the septum with a Hamilton syringe to reach a final concentration of 0.5 $\mu\text{g mL}^{-1}$. After several minutes, antimycin A (200 $\mu\text{g mL}^{-1}$ stock solution in ethanol) was added with a Hamilton syringe to reach a final concentration of 1 $\mu\text{g mL}^{-1}$, and antimycin A-insensitive respiration was recorded before the measurement was terminated. Usually, adipocytes from three cell culture dishes were measured serially as technical replicates.

For transformation of recorded phase shifts into O₂ concentration, luminescence decay time τ was calculated according to the equation

$$\tau = \frac{\tan \phi}{2 * \pi * f} \quad (3.2)$$

where ϕ is the phase shift and f is the frequency of modulation (i.e. 4520 Hz for the used device). Subsequently, the O₂ concentration was calculated according to the Stern-Volmer equation

$$[\text{O}_2] = \frac{\tau_0 - \tau}{K_{\text{SV}}} \quad (3.3)$$

where τ_0 is the luminescence decay time in a solution without O₂, τ is the actual luminescence decay time in the solution, and K_{SV} is the Stern-Volmer constant, which is calculated from luminescence decay times of the two calibration solutions and the known molar concentrations of O₂ in ddH₂O at 100% and 0% oxygen saturation (i.e. 207 μM and 0 μM at 37°C) according to the formula:

$$K_{\text{SV}} = \frac{\tau_{100} - \tau_0}{207 - 0} \quad (3.4)$$

Finally, O_2 consumption rates were calculated by fitting a linear regression function over time intervals of 30 sec to 2 min. Basal respiration was defined as antimycin A-sensitive respiration. Likewise, respiration rate after addition of oligomycin was corrected for antimycin A-insensitive oxygen consumption rate to quantify uncoupled respiration.

Chapter 4

Results

4.1 Differentially expressed microRNAs in human and mouse adipocyte differentiation

Recently, the mRNA expression profile of hMADS cells during adipocyte and osteoblast differentiation was investigated (Scheideler et al., 2008). Interestingly, bioinformatic analyses revealed that the majority of differentially expressed mRNAs harbored miRNA seed matches which were significantly over-represented (compared to a large control set of human mRNAs). Thus, a regulatory role for miRNAs in both differentiation lineages could be anticipated. In order to further characterize this potential regulatory role with respect to adipogenesis, we first decided to generate miRNA expression profiles during adipocyte differentiation of a human and a mouse *in vitro* system, hMADS cells and MEFs, respectively. For hMADS cells, these miRNA array data had already been generated prior to the start of this thesis, with cells harvested at confluence (day -2), at the start of differentiation (day 0), and at days 1, 2, 5, 10, and 15 of adipogenesis. MEFs, which differentiate at a faster pace, were analyzed at the start of differentiation, and 10 h, 20 h, 3 and 8 days afterwards. The miRNA expression profiles were obtained using in-house-generated two-color microarrays, whereby proliferating hMADS cells and MEFs served as reference samples for human and mouse experiments, respectively.

Microarrays revealed 38 differentially expressed miRNAs during adipocyte differentiation of hMADS cells (Fig. 5A). Similarly, a set of 33 miRNAs was identified to be dynamically regulated in MEF adipogenesis (Fig. 5B). Interestingly, the MEF miRNA set contained several human miRNAs for which corresponding mouse homologs have not been discovered so far. Conversely, mmu-miR-290 was detected in hMADS cells, but is without human counterpart at present. The overlap of both data sets consisted of four miRNAs with congruent expression profiles: miR-30c, miR-31, miR-222 and miR-378 (designated miR-442b in the human data set, as this was the former miRNA ID which has been replaced by miR-378 in 2007). While miR-30c and miR-378 were both strongly upregulated during adipogenesis, miR-31 and miR-222 expression decreased.

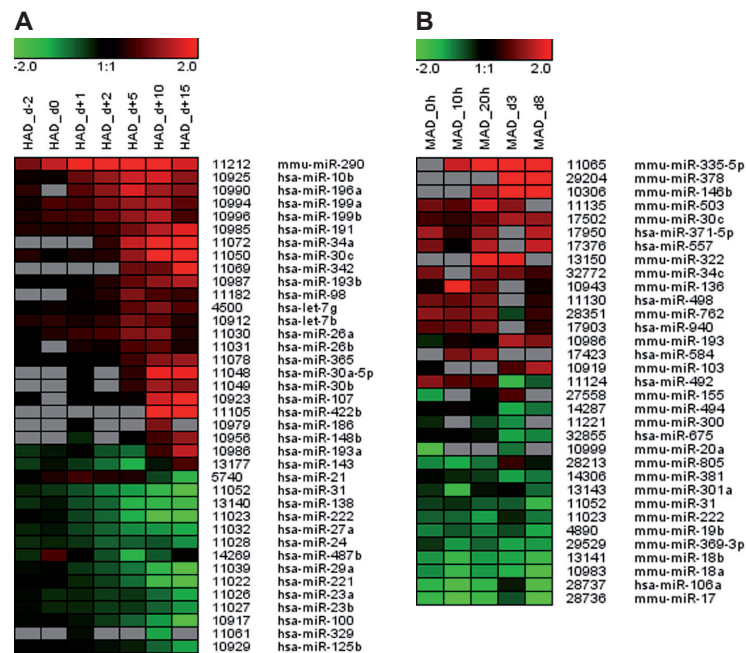


Figure 5. microRNAs with differential expression during adipocyte differentiation of hMADS cells and MEFs. hMADS-2 cells (A) and MEFs (B) were stimulated to undergo human (HAD) and mouse adipocyte differentiation (MAD) respectively. Total RNA was isolated at indicated timepoints to perform hybridizations on a miRNA microarray as described in Materials and Methods. For each cell model, RNA from proliferating cells was used as reference. Data is shown as heat map with miRNAs in rows and timepoints of differentiation in columns. Data has been filtered for miRNAs which could be measured at two or more timepoints, and which at one or more timepoints exhibit more than 2-fold differential expression levels compared to reference. Grey fields designate missing values due to restrictive quality control of raw data. For miRNAs with human (hsa) prefix in (B), either a mouse homolog has not been identified to date, or the mouse homolog was not detected. Likewise, miR-290 has a mouse (mmu) prefix in (A), as no human homolog for has been found so far.

Based on the initial cross-species survey described above, the main aim of this thesis was to characterize particular miRNAs with respect to human adipocyte differentiation. The prime criterion of differential expression at least during human adipogenesis was extended by different additional criteria to select the three "candidate" miRNAs as follows:

- **miR-27:** both family members, miR-27a and miR-27b, were downregulated during human adipogenesis (Fig. 5A and data not shown), and six out of ten algorithms predicted a direct interaction of miR-27b with PPAR γ . Furthermore, PPAR γ and miR-27b were identified to have anticorrelated expression during adipogenesis of hMADS cells. Thus, miR-27b was chosen as first candidate for functional studies.
- **miR-30:** Three members of the miR-30c family – miR-30a, miR-30b and miR-30c – were upregulated during human adipogenesis (Fig. 5A). In addition, miR-30c had a similar expression profile during adipocyte differentiation of MEFs (Fig. 5B), and had

also been shown to be upregulated in other human and mouse studies (Esau et al., 2004; Xie et al., 2009). Moreover, PAI-1 and activin A receptor, type I (ALK2) were predicted as miR-30c targets by several algorithms, and found to exhibit anticorrelated expression compared to miR-30c during adipogenesis of hMADS cells. As PAI-1 is an adipokine with implications in the sequels of obesity, and as ALK2 is a component of bone morphogenetic protein (BMP) signalling which is known to influence adipogenesis, both predicted direct targets were considered as interesting. Thus, miR-30c was chosen as second candidate for functional studies.

- **miR-26:** Two members of the miR-26 family – miR-26a and miR-26b – were upregulated during adipocyte differentiation of hMADS cells (Fig. 5A). A similar expression profile was also shown in a study with BM-MSK (Oskowitz et al., 2008). Furthermore, inhibition of miR-26a was found to increase osteogenic differentiation of adipose tissue-derived MSC (Luzi et al., 2008). Due to the close developmental relationship of adipogenesis and osteogenesis, we hypothesized a potential regulatory role of miR-26a also in adipocyte differentiation and therefore chose this miRNA as third candidate for functional studies.

Results obtained for each of the three candidate miRNAs will be summarized in the following three sections.

4.2 miR-27b impairs human adipocyte differentiation and targets $\text{PPAR}\gamma^1$

miRNA expression profiling revealed miR-27b to be downregulated during adipogenesis of hMADS cells. This was subsequently confirmed by qRT-PCR for miR-27b at selected time-points (Fig. 6A). Indeed, miR-27b levels decreased by 40% during adipogenesis as compared with proliferating hMADS cells. Assuming that this decrease of miR-27b is a prerequisite to allow adipogenesis in human, miR-27b overexpression should impair adipogenic differentiation.

Thus, we transiently transfected hMADS cells with 5 nM miR-27b mimics or non-targeting control (NTC) before adipogenic differentiation. miR-27b transfected hMADS cells exhibited a 3-fold increase of mature miR-27b expression measured by qRT-PCR two days post transfection (data not shown).

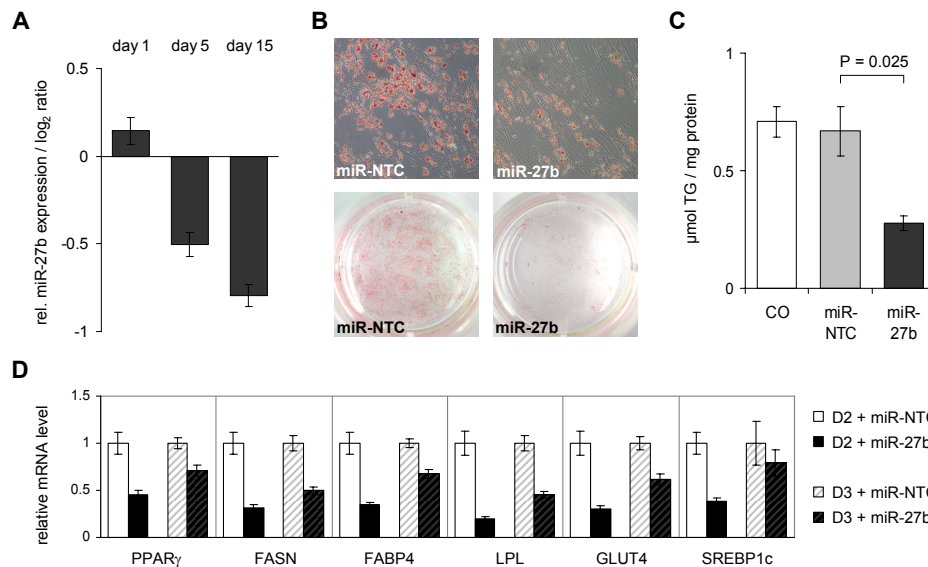


Figure 6. miR-27b expression and involvement in human adipocyte differentiation. hMADS cells were stimulated to undergo adipocyte differentiation two days post confluence. (A) Total RNA was prepared at the indicated time points, subjected to quantitative real-time RT-PCR for miR-27b, and miR-27b abundance is presented relative to day 0, with error bars denoting the SEM from qRT-PCR triplicates. (B-D) hMADS cells were transfected at confluence (day - 2) with 5 nM miR-27b mimic or miR-NTC, adipocyte differentiation was induced after 48 h (day 0), and was analyzed 9–12 days later. (B) hMADS cells were stained with Oil red O. One out of four independent but comparable experiments is shown. (C) Triglyceride accumulation was quantified and normalized to protein amount. The data shown are mean value \pm SEM ($n = 4$) and significance was determined by Student's t -test. (D) Total RNA was prepared from hMADS adipocytes and subjected to quantitative real-time RT-PCR analysis. Data is presented relative to control (miR-NTC) transfected cells, with error bars denoting the SEM from qRT-PCR triplicates. CO = cells only (untreated); NTC = non-targeting control; D2 = hMADS-2 cells; D3 = hMADS-3 cells; TG = triglycerides.

¹This section comprises data that has been published in 2009 (Karbiener et al., 2009).

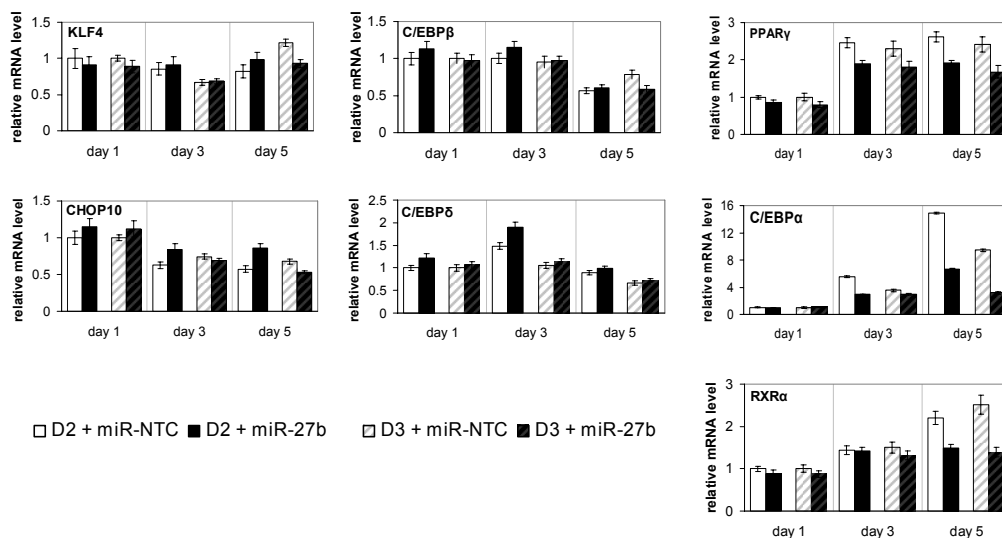


Figure 7. miR-27b-induced changes in expression of transcription factors involved in adipogenesis. hMADS cells of two donors were transfected at confluence (day-2) with 5 nM miR-27b mimic or non-targeting control and adipocyte differentiation was induced at day 0. The time points indicate the day of differentiation, at which total RNA was prepared and subjected to quantitative real-time RT-PCR analysis for KLF4, CHOP10, C/EBP β , C/EBP δ , C/EBP α , PPAR γ , and RXR α . Data is presented relative to control (miR-NTC) transfected cells, with error bars denoting the SEM from qRT-PCR triplicates. NTC = non-targeting control; D2 = hMADS-2 cells; D3 = hMADS-3 cells.

miR-27b overexpression resulted in decreased lipid droplet formation at terminal differentiation (day 9–12 of differentiation), as shown by Oil Red O staining (Fig. 6B). This was also confirmed by quantification of intracellular triglycerides, showing that increasing miR-27b abundance significantly reduced triglyceride accumulation (Fig. 6C). Expression

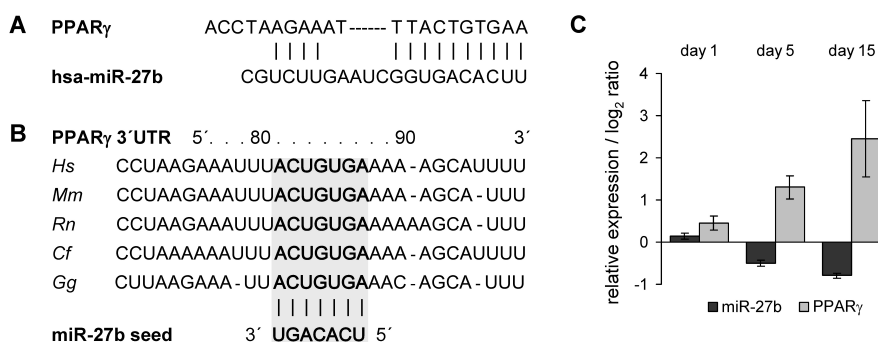


Figure 8. Indications for a miR-27b target site in the 3'UTR of PPAR γ . (A) The predicted, single binding site of miR-27b in the 3'UTR of human PPAR γ . (B) Conservation of the miR-27b binding region in the PPAR γ 3'UTR between vertebrates, with the miR-27b seed match highlighted in grey (TargetScan). (C) Reciprocal expression levels of miR-27b and PPAR γ mRNA during adipocyte differentiation of hMADS cells relative to day 0 as reference. Data is presented relative to day 0, with error bars denoting the SEM from qRT-PCR triplicates.

analysis of adipogenic marker genes revealed PPAR γ , FASN, FABP4, LPL, glucose transporter 4 (GLUT4), and sterol regulatory element binding transcription factor 1 (SREBP1c) as repressed at terminal differentiation stage in hMADS cells of two donors, respectively (Fig. 6D). To delineate the mechanism by which miR-27b inhibits human adipogenesis, we again transfected hMADS cells with miR-27b and investigated expression changes in the cascade of the adipogenic key transcription factors Kruppel-like factor 4 (KLF4), C/EBP-homologous protein 10 (CHOP10), C/EBP β , C/EBP δ , PPAR γ , and C/EBP α at early stages of adipocyte differentiation, including day 1, 3, and 5 after differentiation induction. KLF4, CHOP10, C/EBP β and C/EBP δ were not significantly affected by miR-27b on mRNA level (Fig. 7), whereas induction of PPAR γ and C/EBP α during early onset of adipogenesis was blunted by miR-27b (Fig. 7). In addition, the expression of a heterodimerization partner of PPAR γ , RXR α , was also affected at these time points (Fig. 7). Due to the pronounced negative effect of miR-27b on human adipogenesis, we hypothesized that one or more transcription factors known to promote adipocyte differentiation might be directly targeted by miR-27b. In order to test this hypothesis, we first obtained a general list of putative direct miR-27b target mRNAs by generating an intersection of those target genes that were jointly predicted by miRanda, (Betel et al., 2008) PicTar 4-/5-way (Lall et al., 2006), TargetScan 4.2/5.1 (Friedman et al., 2009), EIMMo (Gaidatzis et al., 2007), and rna22 (Miranda et al., 2006). Second, we matched these with the candidate transcription factors that we found to be repressed by miR-27b. The remaining putative direct target gene for miR-27b was PPAR γ with a single miR-27b binding site (Fig. 8A). This miR-27b response element is highly conserved among mammals (Fig. 8B), as is the miR-27b sequence itself. Furthermore, miR-27b and PPAR γ were found to be reciprocally expressed during adipocyte differentiation of hMADS cells (Fig. 8C). To examine whether miR-27b directly interacts with the predicted miR-27b response element in the 3'UTR of PPAR γ , the 3'UTR of human PPAR γ

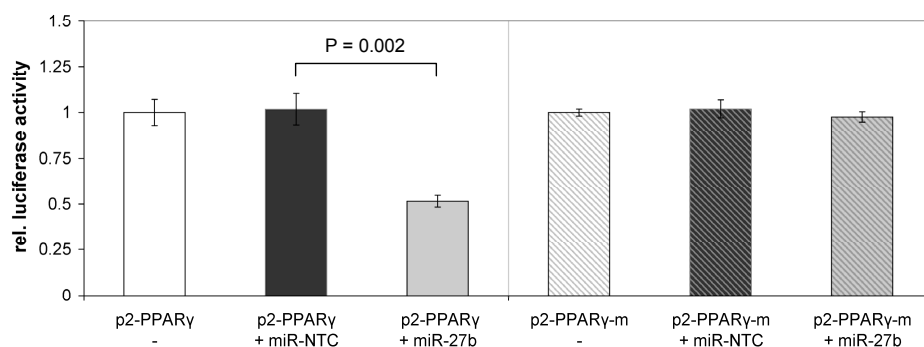


Figure 9. Specific miR-27b binding to the 3'UTR of PPAR γ . Two psiCHECK-2 vector constructs, containing either the PPAR γ 3'UTR (p2-PPAR γ), or the PPAR γ 3'UTR with a mutation in the miR-27b seed region (p2-PPAR γ -m), were transfected into HEK293 cells either alone or in combination with 50 nM miR-NTC or miR-27b mimic. Renilla luciferase activity was normalized to firefly luciferase. Data are presented as means \pm SEM from three independent experiments and relative to transfections of vectors only. Significance was determined using Student's *t*-test.

was cloned downstream the Renilla luciferase coding sequence and cotransfected with 50 nM miR-27b mimic into HEK293 cells. Indeed, Renilla luciferase activity decreased by 50% compared with non-targeting control transfected cells. In addition, site-directed mutagenesis within the predicted miR-27 seed match abolished the inhibitory effect of miR-27b on Renilla luciferase activity (Fig. 9). These results demonstrate that miR-27b indeed directly binds to the designated miR-27b response element in the 3'UTR of human PPAR γ to decrease PPAR γ protein levels and thus inhibit adipogenesis.

4.3 miR-30c promotes human adipocyte differentiation and targets PAI-1 and ALK2²

We identified changes in expression levels of miR-30c in microarray studies of hMADS cells and MEFs during adipocyte differentiation (Fig. 5). In order to validate the dynamics of miR-30c expression, we performed adipocyte differentiation of hMADS-2 and hMADS-3 cells, originally established from two different donors, and collected RNA samples at several timepoints for miRNA qRT-PCR. As mature miR-30c can be generated from two distinct pre-miRNAs, both residing in intronic regions of distinct host genes, we were also interested in the expression profiles of these host genes, namely nuclear transcription factor Y, γ (NFYC) and C6orf155. Indeed, miR-30c levels increased 2- to 4-fold during adipogenesis, with a large increase at early stage between day 1 and day 5 (Fig. 10). Furthermore, NFYC mRNA was modestly upregulated at late stages (day 9 and day 16), while C6orf155 expression showed a peak at day 5, followed by a decrease (Fig. 10). Assuming that the increase of miR-30c is associated with adipogenesis, we hypothesized that altering miR-30c levels should modulate adipocyte differentiation.

To assess our hypothesis, we transiently transfected hMADS-2 and hMADS-3 cells at confluence with miR-30c mimics or non-targeting control (miR-NTC), followed 48 h later by induction of adipocyte differentiation. miR-30c transfected hMADS cells exhibited a 50- to 300-fold increase of mature miR-30c abundance as measured by qRT-PCR 3 and 5 days post transfection (Fig. 11).

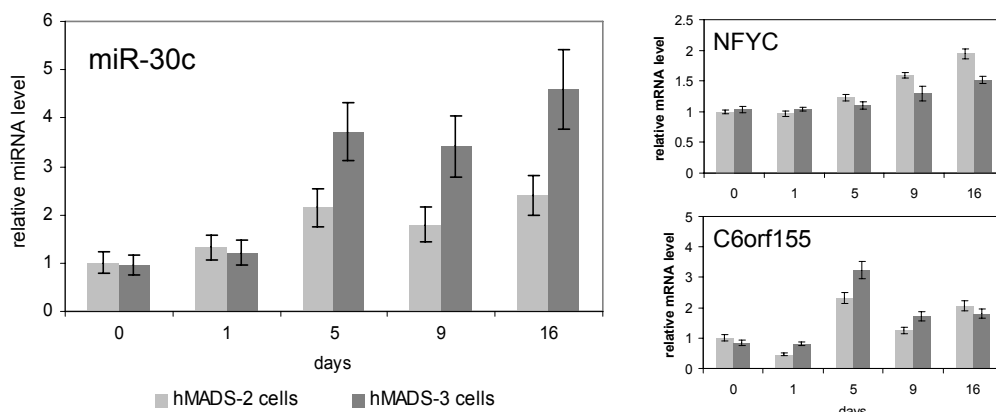


Figure 10. Changes in expression of miR-30c and its host genes during adipogenesis of hMADS cells. hMADS-2 and hMADS-3 cells were stimulated to undergo adipocyte differentiation two days post confluence (day 0). Total RNA was prepared at the indicated time points and subjected to quantitative real-time RT-PCR for miR-30c, NFYC and C6orf155. miR-30c abundance was normalized to 5S rRNA; NFYC and C6orf155 expression was normalized to TBP. Data is presented relative to day 0, with error bars denoting the SEM from qRT-PCR triplicates.

²This section comprises data that has been accepted for publication in 2011 (Karbiener et al., 2011).

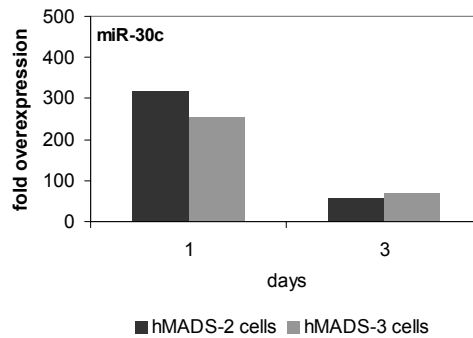


Figure 11. miR-30c levels after transfection of hMADS cells with miR-30c mimics. hMADS-2 and hMADS-3 cells were transfected at confluence (day -2) with 5 nM miR-30c mimic or non-targeting control mimic (miR-NTC). Adipocyte differentiation was induced 48 h later (day 0). RNA of cells at day 1 and day 3 of adipocyte differentiation was analyzed by quantitative real-time RT-PCR for mature miR-30c. 5S rRNA was used as internal reference. For each sample, miR-30c levels are presented as ratio of miR-30c transfected to miR-NTC transfected cells.

Notably, for both hMADS cell populations, increasing miR-30c abundance resulted in enhanced induction of adipocyte marker genes compared to miR-NTC transfection (Fig. 12A). PPAR γ and FABP4 expression already increased at day 1, and C/EBP α reached increased levels at day 3 of differentiation. While for hMADS-2 cells elevated marker gene expression was blunted at day 9 (Fig. 12B, upper panel), the miR-30c effect was still evident in hMADS-3 cells, as indicated by still increased expression levels of PPAR γ , C/EBP α , FABP4, FASN and GLUT4 (Fig. 12B, lower panel). To further investigate the impact of miR-30c on differentiation, lipid accumulation of miR-30c or miR-NTC transfected hMADS cells was analyzed at day 9 of differentiation by Oil Red O staining and quantification of intracellular triglycerides. In line with elevated mRNA levels of adipocyte marker genes, miR-30c significantly increased triglyceride accumulation of hMADS cells (Fig. 12C). Interestingly, although triglyceride levels of control transfected cells differed between hMADS-2 and hMADS-3 cells (Fig. 12C), miR-30c enhanced triglyceride levels to a similar value of approximately 1.5 μmol triglyceride / mg protein at day 9. Altogether, marker gene expression as well as triglyceride accumulation indicate that miR-30c promotes adipogenesis of hMADS cells.

To search for putative direct target mRNAs of miR-30c, we generated an intersection of those genes that were jointly predicted by miRanda (Betel et al., 2008), PicTar (Lall et al., 2006), TargetScan (Friedman et al., 2009) and ElMMo (Gaidatzis et al., 2007). We identified Plasminogen activator inhibitor-1 (PAI-1, also designated SERPINE1) and activin A receptor, type I (ALK2, also designated ACVR1, ACTRI) as putative direct miRNA targets, each with a single miR-30c binding site that is highly conserved among mammals (Fig. 13A). Interestingly, PAI-1 and ALK2 are downregulated during adipocyte differentiation of hMADS cells as indicated by gene expression analysis (Fig. 13B). To investigate whether PAI-1 and ALK2 are responsive to miR-30c, we transfected miR-30c and monitored the expression levels of PAI-1 and ALK2 afterwards. Indeed, PAI-1 and ALK2 mRNA levels were

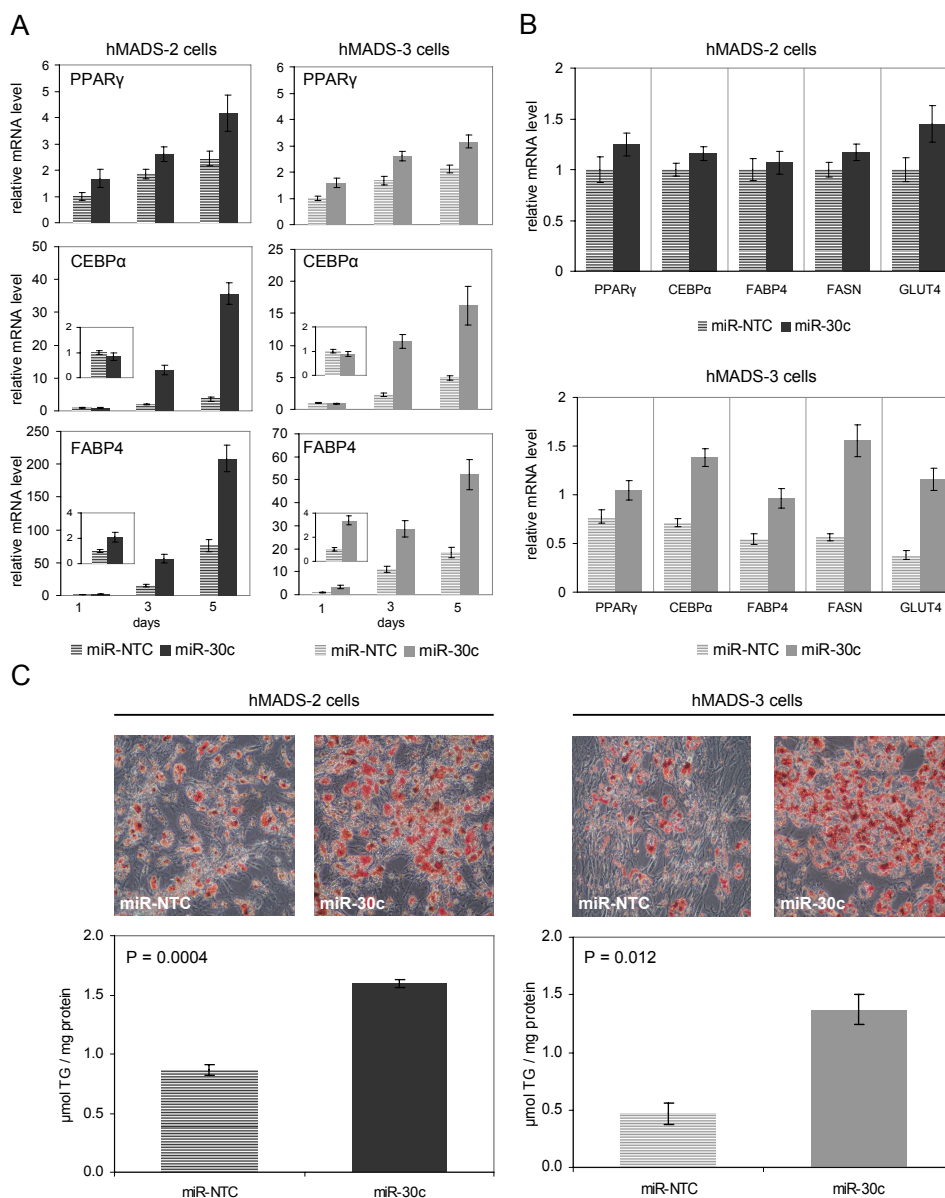


Figure 12. miR-30c promotes adipocyte differentiation of hMADS cells. hMADS-2 and hMADS-3 cells were transfected at confluence (day =2) with 5 nM miR-30c mimic or non-targeting control mimic (miR-NTC). Adipocyte differentiation was induced 48 h later (day 0). (A) RNA of cells at day 1, 3 and 5 after induction of adipocyte differentiation was analyzed by quantitative real-time RT-PCR for expression of PPAR γ , C/EBP α and FABP4. mRNA levels were normalized to TBP and are presented relative to miR-NTC transfected cells at day 1, with error bars denoting the SEM from qPCR triplicates. For C/EBP α and FABP4, framed inserts depict expression levels at day 1. (B) RNA of cells at day 9 of adipocyte differentiation was analyzed by quantitative real-time RT-PCR for expression levels of PPAR γ , C/EBP α , FABP4, FASN and GLUT4. mRNA levels were normalized to TBP and are presented relative to miR-NTC transfected hMADS-2 cells, with error bars denoting the SEM from qPCR triplicates. (C) Analysis of triglyceride accumulation at day 9 of adipocyte differentiation. Representative pictures of hMADS-2 and hMADS-3 cells stained with Oil Red O for visualization of intracellular triglycerides are shown in the upper panel. Quantification of triglyceride accumulation, normalized to total protein, is depicted in the lower panel. Data are presented as mean \pm SEM (n=3) and significance was determined by Student's *t*-test.

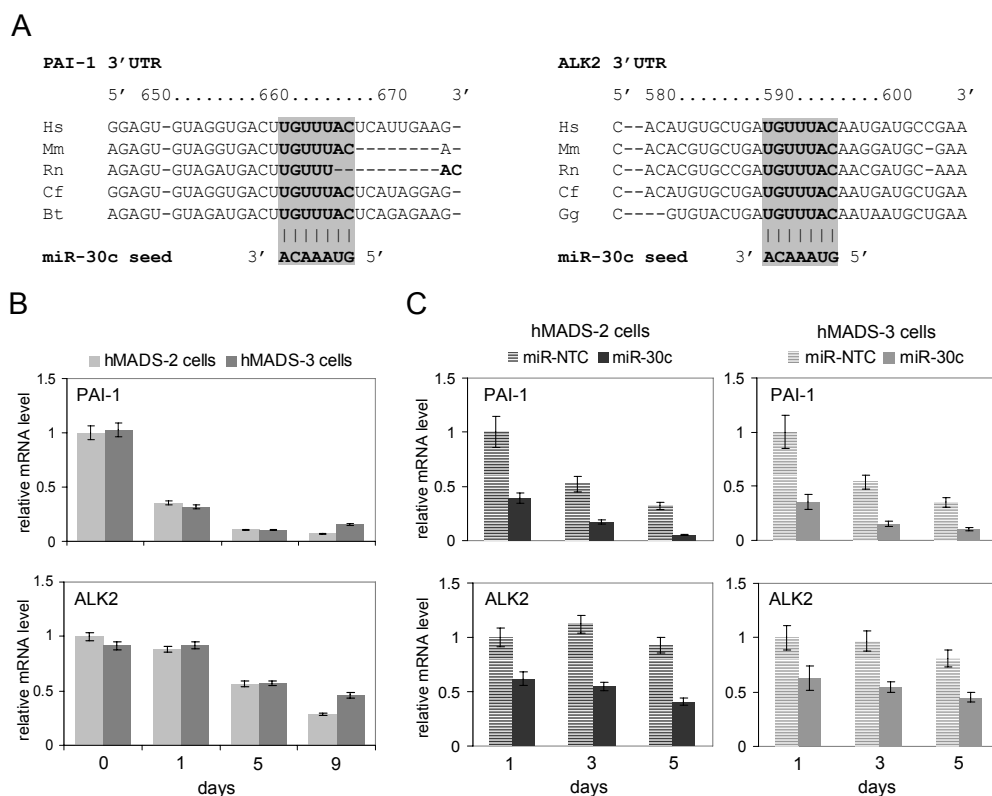


Figure 13. PAI-1 and ALK2 are predicted miR-30c targets with inverse expression to miR-30c. (A) Sequence conservation of the predicted miR-30c binding sites in the 3'UTRs of PAI-1 and ALK2, with the miR-30c seed and seed matches highlighted in grey. (B) hMADS-2 and hMADS-3 cells were analyzed by quantitative real-time RT-PCR for PAI-1 and ALK2 mRNA levels at day 0, 1, 5 and 9 of adipocyte differentiation. mRNA levels were normalized to TBP and are presented relative to day 0, with error bars denoting the SEM from qRT-PCR triplicates. (C) hMADS-2 and hMADS-3 cells were transfected at confluence (day -2) with 5 nM miR-30c mimic or non-targeting control mimic (miR-NTC). Adipocyte differentiation was induced 48 h later (day 0). PAI-1 and ALK2 mRNA levels were analyzed by quantitative real-time RT-PCR at day 1, 3 and 5. mRNA levels were normalized to TBP and are presented relative to miR-NTC transfected cells at day 1, with error bars denoting the SEM from qRT-PCR triplicates.

decreased in miR-30c transfected cells compared with miR-NTC transfected cells (Fig. 13C). Plasma PAI-1 levels have been shown to rise with increasing BMI, presumably contributing to the increased risk of obese subjects for type 2 diabetes and atherothrombotic events. In line with these findings, pro-inflammatory cytokines which are increased in the obese state, e.g. Tumor necrosis factor- α (TNF α), are known to induce PAI-1 expression; however, PAI-1 regulation is not yet completely understood. We thus aimed to investigate a potential role of miR-30c as mediator of the PAI-1 induction observed in the obese state. Therefore, we analyzed the levels of miR-30c and PAI-1 in WAT in mouse models of nutritionally or genetically induced obesity. Indeed, WAT of *ob/ob* mice not only showed the expected increases in PAI-1 mRNA levels compared to wild type mice, but also lower levels of miR-30c (Fig. 14A). A similar result was obtained for WAT samples of wild type mice fed a HFD com-

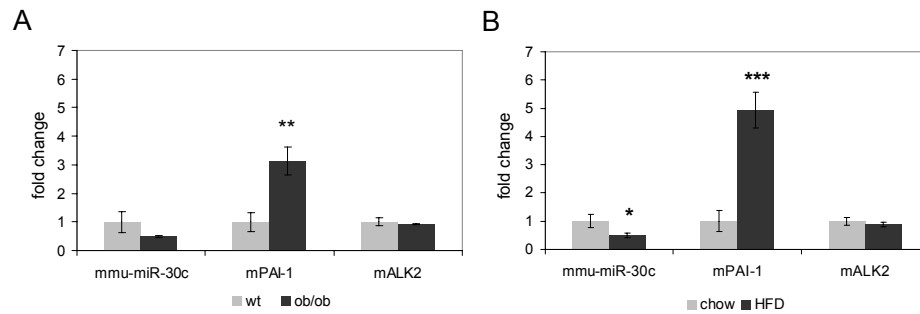


Figure 14. Analysis of miR-30c, ALK2 and PAI-1 expression in white adipose tissue of murine obesity models. (A) Ob/ob mice (n=3) and their wild type littermates (n=6) were fed a chow diet after weaning. RNA from WAT of 4 months old mice was analyzed by quantitative real-time RT-PCR for expression levels of miR-30c, mPAI-1 and mALK2. 5S rRNA was used as internal reference for miR-30c; mUxt mRNA was used as internal reference for mPAI-1 and mALK2. Data are presented as mean \pm SEM and relative to wild type mice. Student's *t*-test: ** $P < 0.01$ vs. mice on chow diet. (B) Wild type mice were fed a chow diet (n=3) or a high fat diet (HFD, n=5) after weaning. RNA from WAT of 4 months old mice was analyzed by quantitative real-time RT-PCR for expression levels of miR-30c, mPAI-1 and mALK2 as described above. Student's *t*-test: * $P < 0.05$; *** $P < 0.001$ vs. wild type mice on chow diet.

pared to littermates on a chow diet (Fig. 14B). Thus, the reciprocal expression of miR-30c and PAI-1, which was already observed during adipocyte differentiation *in vitro*, appears to be existent also *in vivo* in WAT. In contrast, ALK2 mRNA levels did not show any differential expression between obese and normal weight states (Fig. 14A&B). To validate the predicted interaction of miR-30c with the PAI-1 and ALK2 mRNAs, the 3'UTRs of human PAI-1 and ALK2 were cloned into the psiCHECK-2 vector downstream the Renilla luciferase coding sequence and co-transfected with miRNA mimics into human embryonic kidney 293

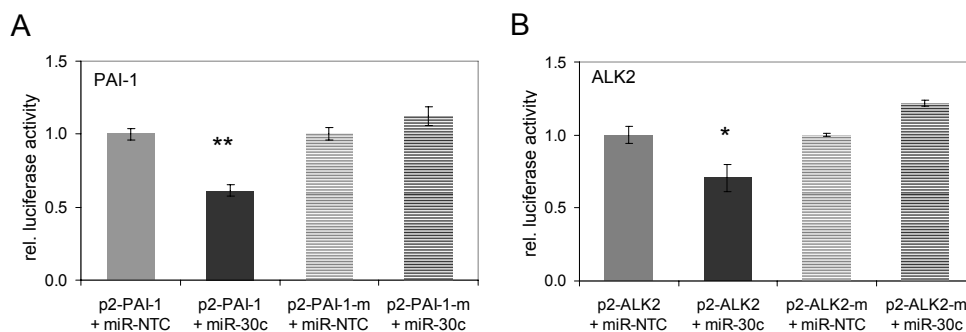


Figure 15. miR-30c directly targets human PAI-1 and ALK2. Luciferase reporter vectors, containing either (A) the wild type 3'UTR of PAI-1 (p2-PAI-1) or (B) ALK2 (p2-ALK2), or 3'UTRs with mutated miR-30c seed matches (p2-PAI-1-m and p2-ALK2-m, respectively), were co-transfected with 50 nM miR-30c mimic or non-targeting control mimic (miR-NTC) into HEK293 cells. 48 h later, cells were harvested and luciferase reporter assays were performed. For each sample, Renilla luciferase activity was normalized to firefly luciferase. Data are presented as means \pm SEM from three independent experiments and relative to miR-NTC transfections. Student's *t*-test: * $P < 0.05$; ** $P < 0.01$ vs. corresponding co-transfection with miR-NTC.

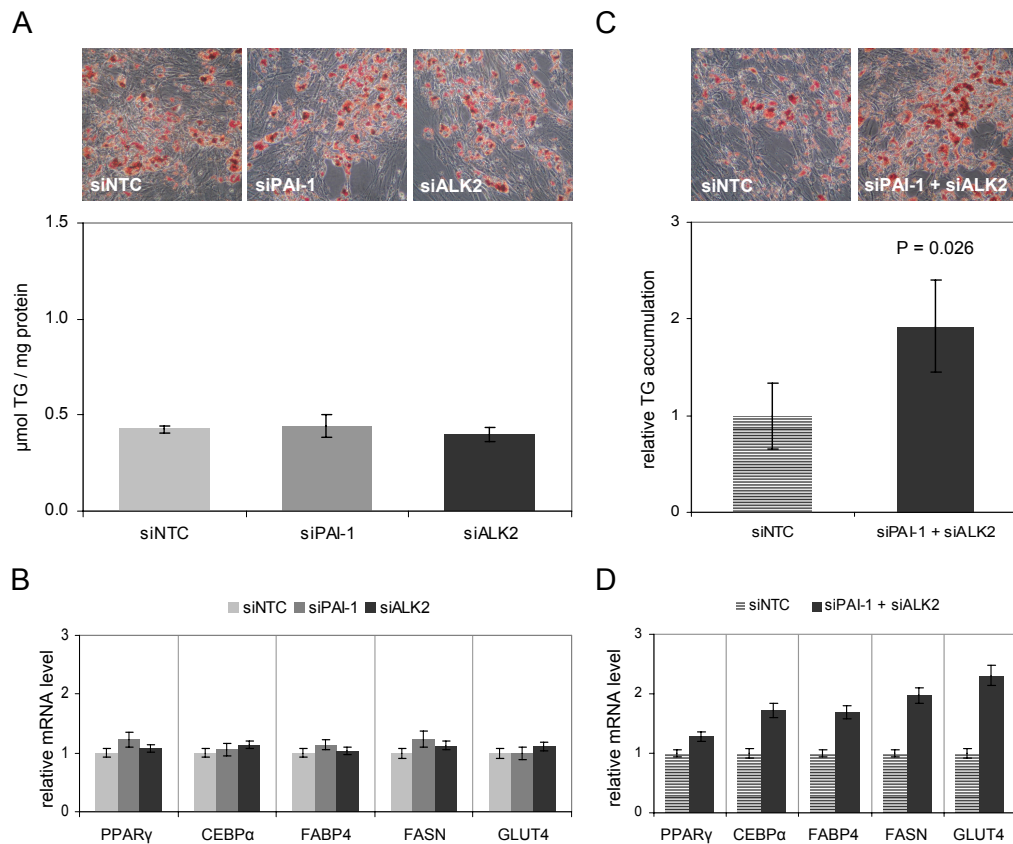


Figure 16. Effects of miR-30c target gene silencing on human adipocyte differentiation. hMADS-3 cells were transfected at confluence (day -2) with 5 nM siRNA against PAI-1 (siPAI-1) and ALK2 (siALK2), either separately (A&B) or in combination (C&D), or with equal concentrations of a non-targeting control siRNA (siNTC). Adipocyte differentiation was induced 48 h later (day 0). (A&C) Analysis of triglyceride accumulation at day 9 of adipocyte differentiation. Representative pictures of cells stained with Oil Red O for visualization of intracellular triglycerides are shown in the upper panel. Quantification of triglyceride accumulation, relative to total protein, is depicted in the lower panel. Data are presented as mean \pm SEM ($n=3$) and significance was determined by Student's *t*-test. (B&D) Analysis of PPAR γ , C/EBP α , FABP4, FASN and GLUT4 mRNA levels by quantitative real-time RT-PCR at day 9 after start of differentiation. mRNA levels were normalized to TBP and are presented relative to siNTC transfected cells, with error bars denoting the mean \pm SEM from qRT-PCR triplicates.

cells (HEK293 cells). Indeed, co-transfections of the PAI-1 and ALK2 reporters with miR-30c resulted in 40% and 30% lower relative luciferase activity compared to co-transfections with miR-NTC, respectively (Fig. 15A&B). Thus, miR-30c directly binds to the 3'UTRs of PAI-1 and ALK2. To investigate whether the predicted miR-30c binding sites mediate the repressive effect on PAI-1 and ALK2, site-directed mutagenesis of the putative seed matches was performed. Indeed, mutation of the predicted miR-30c seed match derepressed relative luciferase activity for both PAI-1 and ALK2 reporters, thus abolishing the inhibitory effect of miR-30c (Fig. 15A&B). These results demonstrated that PAI-1 and ALK2 are both regulated by miR-30c, each via a single conserved miR-30c binding site in its 3'UTR. As

PAI-1 and ALK2 are direct targets of miR-30c, we aimed at analyzing whether either of them mediates the pro-adipogenic miR-30c effect. PAI-1 is a protein secreted by adipose tissue which has been implicated in various complications of the obese state, though its role in adipogenesis appears controversial. ALK2 is a BMP type I receptor known to mediate BMP7 signalling (Macías-Silva et al., 1998) and has been shown to regulate BMP9-induced osteogenic differentiation (Luo et al., 2010) as well as chondrogenesis (Shen et al., 2009). Thus, a regulatory function of ALK2 might be hypothesized also for adipogenesis. To assess whether PAI-1 or ALK2 play a role in human adipogenesis, we transfected hMADS cells with siRNAs to silence each target (siPAI-1, siALK2), and subsequently induced adipocyte differentiation. Neither PAI-1 nor ALK2 silencing evoked any changes in triglyceride accumulation (Fig. 16A) or in the expression of adipocyte marker genes (Fig. 16B) at day 9 compared to control (siNTC) transfected cells. Thus, the pro-adipogenic miR-30c effect could not be reproduced by single silencing of the validated miR-30c targets PAI-1 or ALK2. In light of these results, we aimed to investigate whether both targets have a cooperative impact on adipogenesis. We transfected hMADS cells either with a pool of siRNAs against PAI-1 and ALK2, or with siNTC, and subsequently initiated adipocyte differentiation. Intriguingly, Oil Red O staining at day 9 revealed that co-silencing of PAI-1 and ALK2 resulted in elevated lipid accumulation compared to siNTC, and quantification of triglycerides revealed that this increase was significant (Fig. 16C). Furthermore, the adipocyte marker genes PPAR γ , C/EBP α , FABP4, FASN, and GLUT4 showed elevated mRNA levels upon co-silencing of PAI-1 and ALK2 (Fig. 16D). We thus propose that co-silencing of PAI-1 and ALK2 phenocopies, at least in part, the promoting effect of miR-30c on human adipogenesis.

4.4 miR-26a induces brown adipocyte characteristics and targets RB1, RIP140, and S6K1³

We initially identified miR-26a by microarray studies as differentially expressed during adipocyte differentiation of hMADS cells (Fig. 5A). Using miRNA qRT-PCR, we could confirm a modest upregulation of miR-26a during adipogenesis (Fig. 17). As hMADS cells can be differentiated into white adipocytes (by withdrawal of rosiglitazone from day 9 on), but also directed towards a brown phenotype (by permanent exposure to rosiglitazone) (Elabd et al., 2009), we examined potential differences in miR-26a levels between these two types of adipocytes. However, miR-26a abundance was not significantly different between white and brown/brite hMADS adipocytes at day 10, 13 and 16 of adipocyte differentiation (Fig. 17). Mature miR-26a can be generated from two pre-miRNAs, both residing in introns of closely related host genes of the CTD small phosphatase family: While pre-miR-26a-1 is located within the CTD (carboxy-terminal domain, RNA polymerase II, polypeptide A) small phosphatase-like (CTDSPL) (also designated RBSP3, HYA22) gene, pre-miR-26a-2 is intronic to CTD (carboxy-terminal domain, RNA polymerase II, polypeptide A) small phosphatase 2 (CTDSP2) (OS4, SCP2). In order to investigate the transcriptional activity at both loci during hMADS adipogenesis, we also analyzed expression of the miR-26a host genes. Both CTDSPL and CTDSP2 transcripts were present in differentiating hMADS cells, with CTDSPL mRNA exhibiting similar kinetics as miR-26a, while CTDSP2 mRNA was found highest at the start of differentiation but declining afterwards (Fig. 17).

A study on osteoblast differentiation of human adipose-derived MSC showed that expression of osteogenic markers increased upon inhibition of miR-26a, and that miR-26a directly targets SMAD family member 1 (SMAD1) (Luzi et al., 2008), a transcriptional mediator of BMP-elicited effects on adipogenesis (Jin et al., 2006) and osteogenesis (Miyazono, 2000). We thus hypothesized that miR-26a might also have a regulatory function during human adipocyte differentiation (via targeting of SMAD1 or other mRNAs). To test this hypothesis, we overexpressed miR-26a by transient transfection of hMADS-3 cells at confluence with miRNA mimics, followed by adipocyte differentiation. Interestingly, increasing miR-26a abundance resulted in accelerated adipogenesis. At day 9, a two-fold higher accumulation of intracellular triglycerides was observed for cells transfected with miR-26a compared to cells transfected with a non-targeting control mimic (miR-NTC, Fig. 18A). However, this difference was no longer existent at day 16, neither for cells differentiated without rosiglitazone during the last seven days, ("white protocol", d16-R9), nor for cells exposed to rosiglitazone throughout the entire differentiation ("brown protocol", d16-R16, Fig. 18A). We subsequently analyzed the expression of a set of genes related to adipogenesis (Fig. 18B and data not shown) for the aforementioned conditions. In line with triglyceride accumulation, two-fold higher FABP4 mRNA levels were observed for miR-26a-transfected hMADS-3 cells compared to controls at day 9, but no (or even a slightly opposite) effect was

³This section comprises data that resulted in a PCT patent application (application number PCT/EP2011/057361).

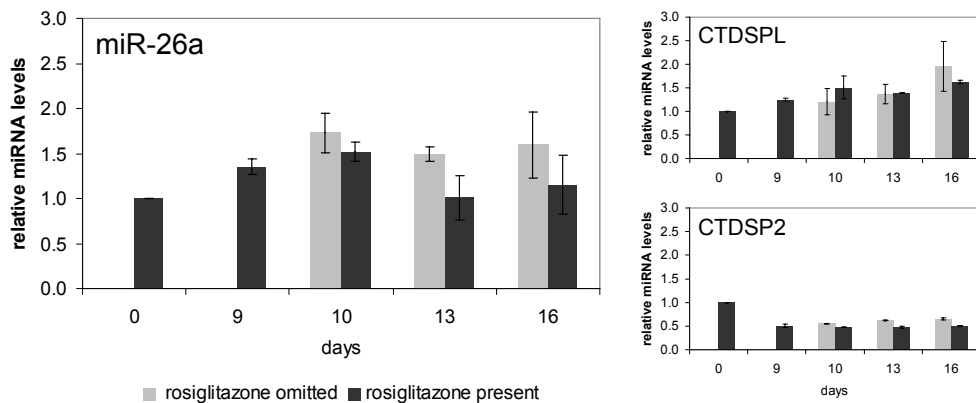


Figure 17. Expression of miR-26a and its host genes during adipogenesis of hMADS cells. hMADS-2 cells were stimulated to undergo adipocyte differentiation two days post confluence. At day 9, supplementation of the medium with rosiglitazone was either continued (=rosiglitazone permanent) or ceased (=rosiglitazone omitted) in order to promote a phenotype of brown/brite or white adipocytes, respectively. Total RNA was prepared at the indicated timepoints and subjected to quantitative real-time RT-PCR for miR-26a, CTDSPL and CTDSP2. miR-26a abundance was normalized to 5S rRNA; CTDSPL and CTDSP2 expression was normalized to TBP. Merged data from three independent experiments is presented relative to day 0; error bars denote standard error of the mean.

found for both conditions at day 16 (Fig. 18B). Moreover, the expression of GPDH, another late marker for adipogenesis, was largely unaffected by miR-26a. Of all genes tested, the one most differentially expressed at day 9 was UCP1, showing an almost 50-fold upregulation in hMADS cells transfected with miR-26a compared to miR-NTC (Fig. 18B). Importantly, miR-26a also elevated UCP1 mRNA in white adipocytes at day 16 (4-fold higher levels), and was furthermore able to augment the induction of UCP1 by continuous rosiglitazone treatment (Fig. 18B). We thus decided to characterize in more detail the possible involvement of miR-26a in the establishment of a brown/brite adipocyte phenotype. In a series of further experiments, we used hMADS-2 cells (established from another individual than hMADS-3 cells) to confirm that UCP1 mRNA levels are significantly elevated in adipocytes derived from miR-26a-transfected cells compared to control transfected cells (Fig. 19A, upper panel). In order to assess whether the pronounced transcriptional induction of UCP1 is also reflected at protein level, we performed Western blots for UCP1 protein. Indeed, while at day 9 the protein levels for miR-NTC-treated cells were below detection limit, UCP1 protein was present in miR-26a-treated cells (Fig. 19A, lower panel). Similarly, UCP1 protein was virtually absent at day 16 in miR-NTC-transfected white adipocytes (d16-R9), but present in miR-26a-transfected adipocytes (Fig. 19A, lower panel). Interestingly, while UCP1 mRNA dropped as miR-26a-transfected adipocytes progressed from day 9 to day 16 in the absence of rosiglitazone, a further increase for UCP1 protein levels was observed (Fig. 19A, lower panel). The presence of UCP1 protein in control transfected cells which had been differentiated according to the "brown protocol" (d16-R16) confirmed previous observations (Elabd et al., 2009). Importantly, though, miR-26a appeared as a potent stimulus in

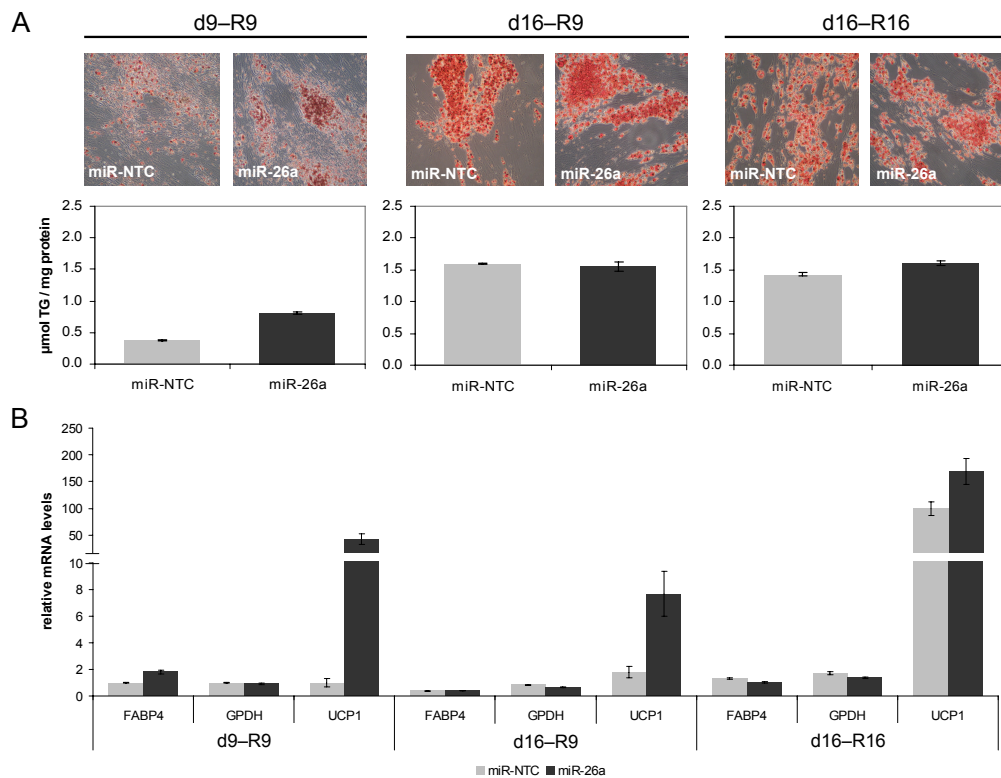


Figure 18. miR-26a accelerates adipocyte differentiation of hMADS cells. hMADS-3 cells were transfected at confluence (day -2) with 5 nM miR-26a mimic of non-targeting control mimic (miR-NTC). Adipocyte differentiation was induced 48 h later (day 0). Rosiglitazone was either withdrawn from the medium at day 9 (R9), or added throughout the entire differentiation (R16). Data from one of two independent and comparable experiments is shown. (A) Analysis of triglyceride accumulation at day 9 of adipocyte differentiation. Representative pictures of hMADS-3 cells stained with Oil Red O for visualization of intracellular triglycerides are shown in the upper panel. Quantification of triglyceride accumulation, relative to total protein, is depicted in the lower panel. Error bars denote standard error of the mean from three wells analyzed separately. (B) RNA of cells at day 9 and day 16 of adipocyte differentiation was analyzed by quantitative real-time RT-PCR for expression of FABP4, GPDH, and UCP1. mRNA levels were normalized to TBP and are presented relative to miR-NTC-transfected cells at day 9, with error bars denoting the standard error of the mean from quantitative real-time RT-PCR triplicates.

addition to rosiglitazone, as miR-26a-transfected hMADS adipocytes exhibited substantially higher UCP1 protein accumulation in the d16-R16 condition (Fig. 19A, lower panel).

Beside UCP1, we also assessed the expression of other brown adipocyte marker genes. PGC-1 α , an important coactivator of PPAR γ in BAT and responsible for normal BAT function (see 1.2.3), was found to be elevated by miR-26a at day 9 and day 16 (Fig. 19B). Similarly, carnitine palmitoyl transferase 1 β (CPT1 β), an enzyme involved in import of long-chain FAs into mitochondria which has been used as a "brown marker" in numerous studies (Petrovic et al., 2010; Leonardsson et al., 2004; Um et al., 2004), was increased by miR-26a at day 9 and at day 16 in brown/brite adipocytes, but not at day 16 for white adipocytes (Fig. 19B). Lastly, cell death-inducing DFFA-like effector a (CIDEA), which has been described

as highly expressed in mouse BAT compared to other tissues (Zhou et al., 2003), was also slightly induced by miR-26a at day 9 and at day 16 in white but not in brown adipocytes (Fig. 19B).

hMADS-2 and hMADS-3 cells had been originally established from pubic and pre-pubic adipose tissue of a 5 year and 4 months old donor, respectively (Rodriguez et al., 2005). To test whether the ability of miR-26a to elevate expression of brown marker genes is restricted to cells from young individuals, or whether this phenomenon might extend to adipocyte precursor cells from older subjects, we used WAT biopsies of adult humans for primary cell culture experiments. By enzymatic digestion and centrifugation of WAT samples, we isolated human primary adipose-derived stromal cells (hPASC), which were subsequently transfected with miR-26a or miR-NTC before adipocyte differentiation was induced. Indeed, we could confirm previous results obtained with hMADS cells, as four out of four hPASC cultures exhibited elevated levels of UCP1 after 16 days of differentiation, of which three also showed elevated PGC1 α levels (Fig. 19C). Collectively, our data indicate that increasing miR-26a abundance in adipocyte precursor cells promotes the expression of brown adipocyte marker genes, most importantly UCP1, the indispensable factor for thermogenesis in BAT.

Chronic exposure to PPAR γ ligands evoked brown adipocyte traits not only in hMADS adipocytes (Elabd et al., 2009), but also in primary adipocytes derived from mouse epididymal WAT (Petrovic et al., 2010), and *in vivo* in WAT depots of mice (Carmona et al., 2007) and rats (Laplante et al., 2003). We were interested whether this effect might be miR-26a dependent. Therefore, we inhibited endogenous miR-26a by transient transfection of hMADS-2 cells with antisense oligonucleotides (anti-miR-26a or anti-miR-NTC) before induction of adipogenesis. Subsequently, we analyzed adipocytes which had been differentiated according to the "brown protocol" (d16-R16). Interestingly, UCP1 mRNA levels were significantly reduced by inhibition of miR-26a, and UCP1 protein was even more decreased (Fig. 20A). Likewise, mRNA levels of the brown marker genes PGC-1 α , CPT1 β , and CIDEA were diminished (Fig. 20B). Thus, at least in hMADS cells, the establishment of a brown gene expression program by chronic PPAR γ activation appears to be controlled, at least partly, by miR-26a.

We next aimed at investigating a potential association of miR-26a with a brite/brown (thermogenic) phenotype *in vivo*. Therefore, WAT and BAT of wild type mice fed a standard diet was isolated to analyze miR-26a expression in the total tissues, as well as in the SVF and adipocyte fraction (AF). When comparing the different fractions of WAT for two biological replicates (each consisting of a pool of 15 mice), miR-26a was found to be equally expressed between SVF, AF, and total tissue, or slightly higher in the AF and total tissue compared to the SVF (Fig. 21A). In contrast, the highest levels of miR-26a in BAT could be observed in the SVF compared to the respective AF and total tissues (Fig. 21A). Importantly, for SVF and AF of both biological replicates, miR-26a abundance was higher in BAT than in WAT samples, which was furthermore observed for the total tissues of one biological replicate (Fig. 21A). Thus, miR-26a levels are higher in cells exhibiting a brown phenotype, or which are predisposed to differentiate into such cells. Beside the comparison of BAT and WAT, we

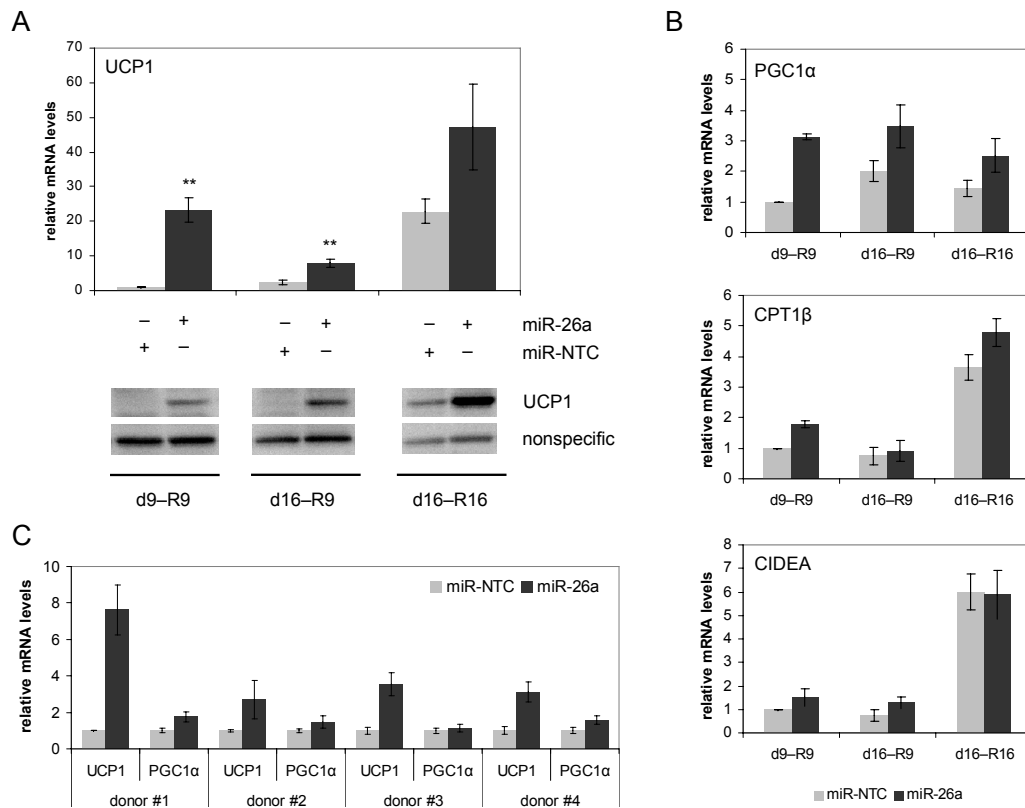


Figure 19. miR-26a promotes expression of brown adipocyte marker genes. (A) hMADS-2 cells were transfected at confluence (day -2) with 5 nM miR-26a mimic or non-targeting control mimic (miR-NTC). Adipocyte differentiation was induced 48 h later (day 0). Rosiglitazone was either withdrawn from the medium at day 9 (R9), or added throughout the entire differentiation (R16). Upper panel: UCP1 mRNA levels were analyzed by quantitative real-time RT-PCR, were normalized to TBP and are presented relative to miR-NTC-transfected cells at day 9, with error bars denoting the standard error of the mean from three independent experiments; Student's *t*-test: ** $P < 0.01$. Lower panel: Analysis of UCP1 protein by Western blot. Images from one representative of three independent experiments are shown. (B) PGC1 α , CPT1 β , and CIDEA mRNA levels were analyzed by quantitative real-time RT-PCR and are presented similar to UCP1 described above. (C) Human primary adipose-derived stromal cells (hPASCs) were isolated from WAT of four adult donors, transfected at confluence (day -2) with 5 nM miR-26a mimic or non-targeting control mimic (miR-NTC), and subjected to adipocyte differentiation two days later (d0). RNA of cells at day 16 was analyzed by quantitative real-time RT-PCR for expression of UCP1 and PGC1 α . mRNA levels were normalized to TBP and are presented relative to miR-NTC-transfected cells, with error bars denoting the standard error of the mean from quantitative real-time RT-PCR triplicates.

were also interested whether the well-described changes in WAT upon exposure to the cold, mediated by β -adrenergic signaling, might involve a regulation of miR-26a. We therefore compared total WAT of wt mice kept at ambient temperature, or at 5 °C for 10 days. As expected, cold stress significantly induced UCP1 mRNA levels in WAT, but furthermore, also miR-26a was elevated in a comparable manner (Fig. 21B). Similarly, daily injections of the β_3 -adrenergic agonist CL-316243 (CL) for 10 days resulted in upregulation of UCP1 and miR-26a, confirming the response of both genes to sympathetic stimulation (Fig. 21B).

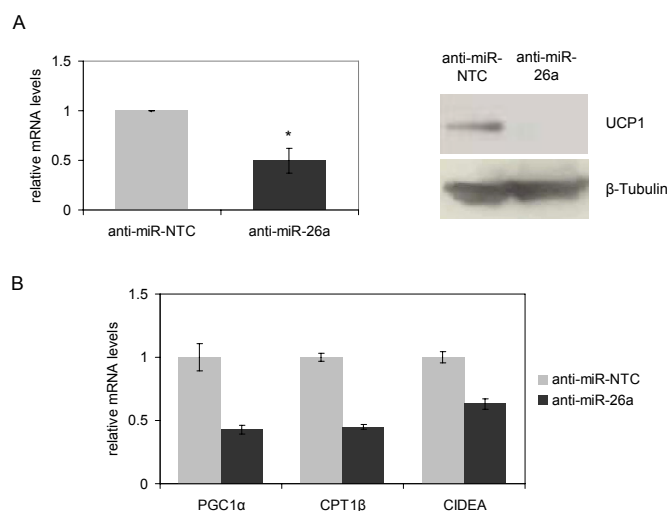


Figure 20. Establishment of a brown adipocyte gene expression program by rosiglitazone is dependent on miR-26a. hMADS-2 cells were transfected at confluence (day -2) with 25 nM anti-miR-26a antisense oligonucleotide or non-targeting control (anti-miR-NTC). Adipocyte differentiation was induced 48 h later (day 0). Rosiglitazone was added throughout the entire differentiation and cells were analyzed at day 16. (A) Left panel: UCP1 mRNA levels were analyzed in three independent experiments by quantitative real-time RT-PCR. For each experiment, UCP1 mRNA was normalized to TBP and the value for anti-miR-NTC-transfected cells was set to 1. Error bar denotes the standard error of the mean; Student's *t*-test: * $P < 0.05$. Right panel: Analysis of UCP1 protein by Western blot. Images from one of two independent experiments are shown. (B) PGC1 α , CPT1 β , and CIDEA mRNA levels were analyzed by quantitative real-time RT-PCR. Data from one of two independent and comparable experiments is shown, with mRNA levels normalized to TBP and presented relative to anti-miR-NTC-transfected adipocytes. Error bars denote the standard error of the mean from quantitative real-time RT-PCR triplicates.

Furthermore, we also investigated a potential short-term effect of β_3 -adrenergic stimulation by analysis of WAT samples that were harvested 3 h after CL injection. As described recently (Vegiopoulos et al., 2010), we found an induction of Ptg2 (COX-2), and importantly, we also observed a significant elevation of miR-26a levels (Fig. 21B). Thus, miR-26a appears to be cold-inducible in WAT of mice, which is likely mediated via β_3 -adrenergic stimulation. Altogether, our *in vitro* and *in vivo* studies suggested a direct correlation between miR-26a and UCP1. As the canonical way of miRNA action is posttranscriptional repression of protein production by interaction with the 3'UTR of mRNAs, a direct stimulation of UCP1 by miR-26a can be considered as unlikely (though not impossible). We therefore proposed that the action of miR-26a might be mediated indirectly via downregulation of at least one repressor of UCP1. By literature studies, we selected several known repressors of UCP1 or (more generally) the brown phenotype, and subsequently screened this list for putative miR-26a MREs using 10 different miRNA-target predicted algorithms. Thereby, we identified three interesting candidates: RB1, RIP140 and S6K1 (see 1.2.3). At least one MRE for miR-26a in the RB1 3'UTR was predicted by the prediction algorithms TargetScan and ElMMo. The interaction of miR-26a and RIP140 via a single MRE was predicted by TargetScan, miRanda, PITA, and ElMMo, while a binding of miR-26a to S6K1 was predicted by PITA.

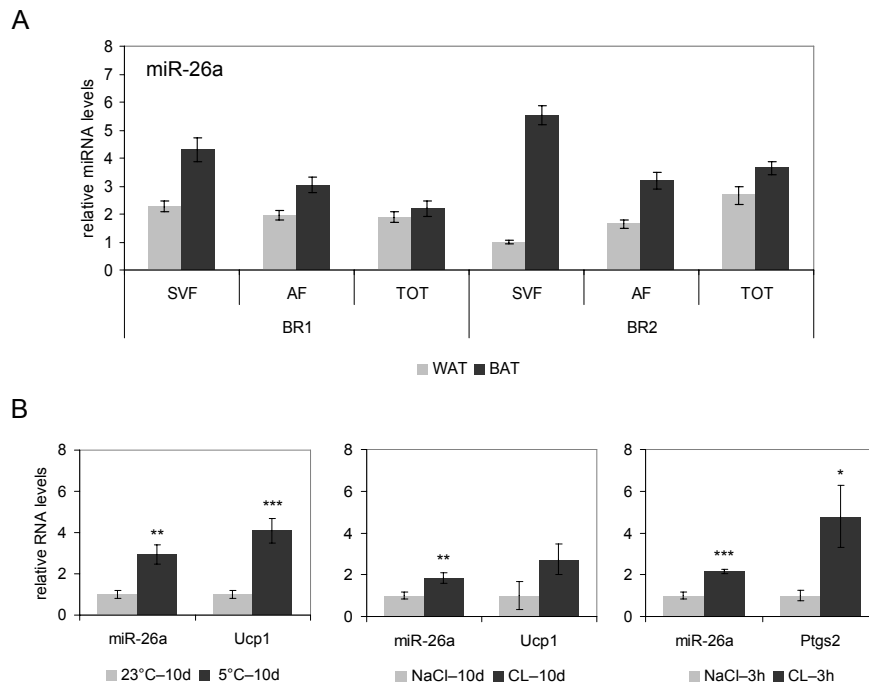


Figure 21. miR-26a is more abundant in BAT than in WAT and responsive to cold and β_3 -adrenergic stimulation. (A) WAT and BAT of wild type mice on a standard diet was harvested and RNA was isolated from the total tissues (TOT), as well as from the respective SVF and AF. Two biological replicates (BR1 and BR2), each a pool of 15 mice, were analyzed by quantitative real-time RT-PCR for the expression of miR-26a, which was normalized to RNU5G. Data is presented relative to SVF of BR2; error bars denote the standard error of the mean from quantitative real-time RT-PCR triplicates. (B) Wild type mice ($n = 4 - 7$ per group) fed a standard diet were kept at 5 °C or 23 °C for 10 days (left panel), were daily injected with CL-316243 (CL) or vehicle (NaCl) for 10 days (middle panel), or analyzed 3 h after a single CL or vehicle injection (right panel). Total RNA was isolated from perigonadal WAT to perform quantitative real-time RT-PCR for miR-26a, Ucp1 and Ptgs2. miR-26a levels were normalized to 5S rRNA; Ucp1 and Ptgs2 mRNA were normalized to Uxt. Data is presented relative to mice kept at 23 °C (left panel) or vehicle-treated mice (middle and right panel); error bars denote the standard error of the mean. Student's *t*-test: * $P < 0.05$; ** $P < 0.01$; *** $P < 0.001$.

In each case, the predicted MREs exhibited considerable evolutionary conservation (Fig. 22A). As different transcript variants of the RB1, RIP140, and S6K1 mRNAs, including different 3'UTR variants, have been annotated, we decided to validate whether those transcripts bearing the predicted MRE were expressed in hMADS cells, thereby enabling a direct interaction with miR-26a. Indeed, analysis of hMADS cells at different stages of adipocyte differentiation by RT-PCR revealed the presence of all three predicted MREs (Fig. 22 B). We next investigated whether RB1, RIP140 and S6K1 were responsive to modulation of miR-26a in hMADS cells. Therefore, we analyzed samples of confluent cells 48 – 72 h after transfection with miR-26a, anti-miR-26a, or respective control oligonucleotides. Interestingly, all three predicted direct targets showed a response on mRNA level that was inversely correlated to miR-26a modulation (Fig. 22C), thereby corroborating the *in silico* analyses that had revealed putative direct interactions. Finally, we were also interested whether a

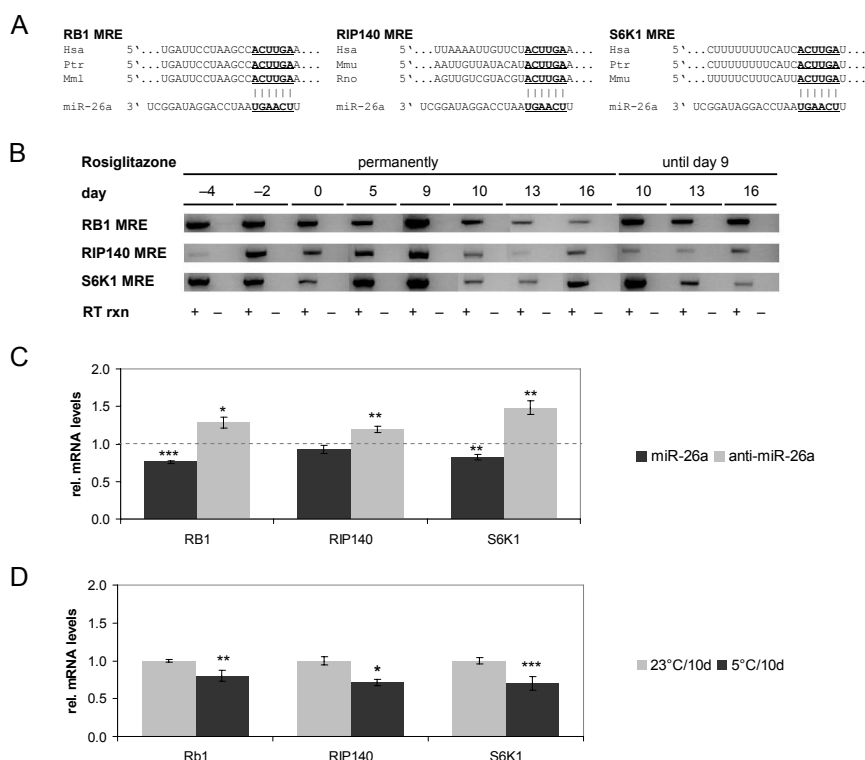


Figure 22. Predicted direct targets of miR-26a have evolutionarily conserved MREs that are expressed in hMADS cells, are responsive to miR-26a modulation, and anti-correlated to miR-26a *in vivo*. (A) Conservation of miR-26a MREs within the 3'UTRs of predicted direct targets RB1, RIP140, and S6K1 in mammals. Bold and underlined sequences denote miRNA seed and seed match. (B) Primers designed to amplify regions containing the predicted miR-26a MREs within the 3'UTRs of RB1, RIP140, and S6K1 were used to analyze hMADS-2 cells at various stages of adipocyte differentiation. RNA samples were reverse transcribed (RT) and RT-PCR was performed and analyzed on agarose gels. RNA samples that were not reverse transcribed served as controls. (C) hMADS-2 cells were transfected at confluence (day -2) with 5 nM miR-26a mimic, 25 nM anti-miR-26a antisense oligonucleotide, or the respective non-targeting control at identical concentration. RNA was harvested 48 h later and analyzed by quantitative real-time RT-PCR for expression of RB1, RIP140, and S6K1. mRNA levels were normalized to TBP. Data from three independent experiments is presented as mRNA abundance in miR-26a- or anti-miR-26a-transfected cells relative to the respective control cells (set to 1). Error bars denote the standard error of the mean. (D) Wild type mice ($n = 7$ per group) fed a standard diet were kept at 5°C or 23°C. After 10 days, total RNA was isolated from perigonadal WAT to perform quantitative real-time RT-PCR for Rb1, RIP140 and S6K1. mRNA levels were normalized to Uxt. Data is presented relative to mice kept at 23°C; error bars denote the standard error of the mean. (C, D) Student's *t*-test: * $P < 0.05$; ** $P < 0.01$, *** $P < 0.001$

similar inverse relationship between miR-26a and RB1, RIP140 and S6K1 exists *in vivo*. Indeed, WAT of cold exposed mice, which exhibited higher miR-26a abundance than WAT from mice at ambient temperature (Fig. 21B), also showed a significant downregulation of Rb1, RIP140 and S6K1 mRNA (Fig. 22D).

We thus decided to validate the direct interactions of miR-26a and the three predicted direct targets. Therefore, we amplified parts of the RB1, RIP140, and S6K1 3'UTRs to insert these sequences in reporter vectors downstream of a luciferase coding sequence (CDS). Reporter

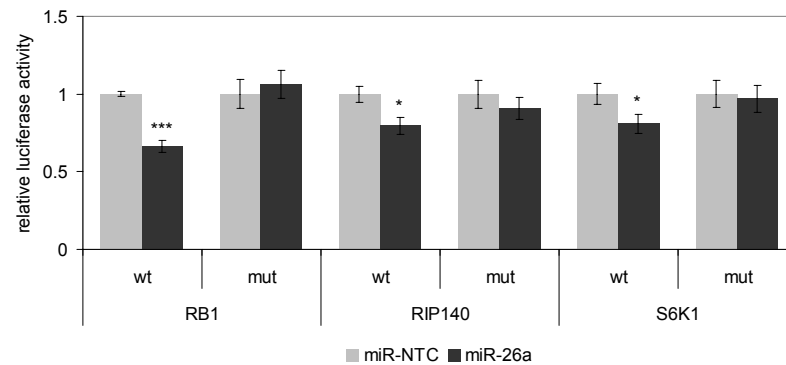


Figure 23. miR-26a directly targets human RB1, RIP140, and S6K1. Luciferase reporter vectors, containing either the wild type (wt; p2-RB1, p2-NRIP1, p2-S6K1) 3'UTR of RB1, RIP140, and S6K1, or 3'UTRs with mutated miR-26a seed matches (mut; p2-RB1-m1, p2-NRIP1-m, p2-S6K1-m1, see 3.2.2.7), were co-transfected with 50 nM miR-26a mimic or non-targeting control mimic (miR-NTC) into HEK293 cells. 48 h later, cells were harvested and luciferase reporter assays were performed. For each sample, Renilla luciferase activity was normalized to firefly luciferase. Data are presented relative to miR-NTC transfections (n=3). Student's *t*-test: * $P < 0.05$; ** $P < 0.01$ vs. corresponding co-transfection with miR-NTC.

vectors were co-transfected with miR-26a mimics or miR-NTC into HEK293 cells, and cell lysates were analyzed after 48 h by luciferase reporter assay. Indeed, all three reporters showed a significant suppression of relative luciferase activity by miR-26a (Fig. 23), confirming the direct interaction of this miRNA with the 3'UTRs of RB1, RIP140, and S6K1. In order to resolve these interactions in more detail, we introduced point mutations in the predicted miR-26a seed matches of all three reporters, generating five reporter vectors (one for RIP140, two for RB1 and S6K1, see 3.2.2.7) for a second series of luciferase reporter assays. Indeed, the single predicted miR-26a MRE within RIP140 could be validated, as miR-26a was no longer able to suppress relative luciferase activity of the mutated reporter (Fig. 23). Furthermore, for RB1 and S6K1, in each case one of the two predicted miR-26a MREs (analyzed by p2-RB1-m1 and p2-S6K1-m1 reporters, see 3.2.2.7) was found to confer the repressive action of miR-26a (Fig. 23), while mutations in the other predicted MREs (analyzed by p2-RB1-m2 and p2-S6K1-m2 reporters) did not show significant effects (data not shown). Thus, RB1, RIP140, and S6K1 are directly targeted by miR-26a, each via a single MRE located in their 3'UTR.

The hypothesis that miR-26a exerts its effect on human adipocyte differentiation via one or more of the three validated direct targets is plausible. However, it cannot be excluded that other direct miR-26a targets act as main mediators in this context. Moreover, RB1, RIP140 and S6K1 have been identified as suppressors of the brown phenotype by *in vitro* and/or *in vivo* studies performed in mouse, but to our knowledge, a possible similar effect in human *in vitro* systems has not been explored so far. We therefore decided to analyze a potential function in human adipocyte differentiation by silencing each gene via transient transfection of hMADS-2 cells with siRNAs, followed by adipocyte differentiation. In parallel, we also transfected cells with siRNA pools targeting two (double knockdown) or all (triple knock-

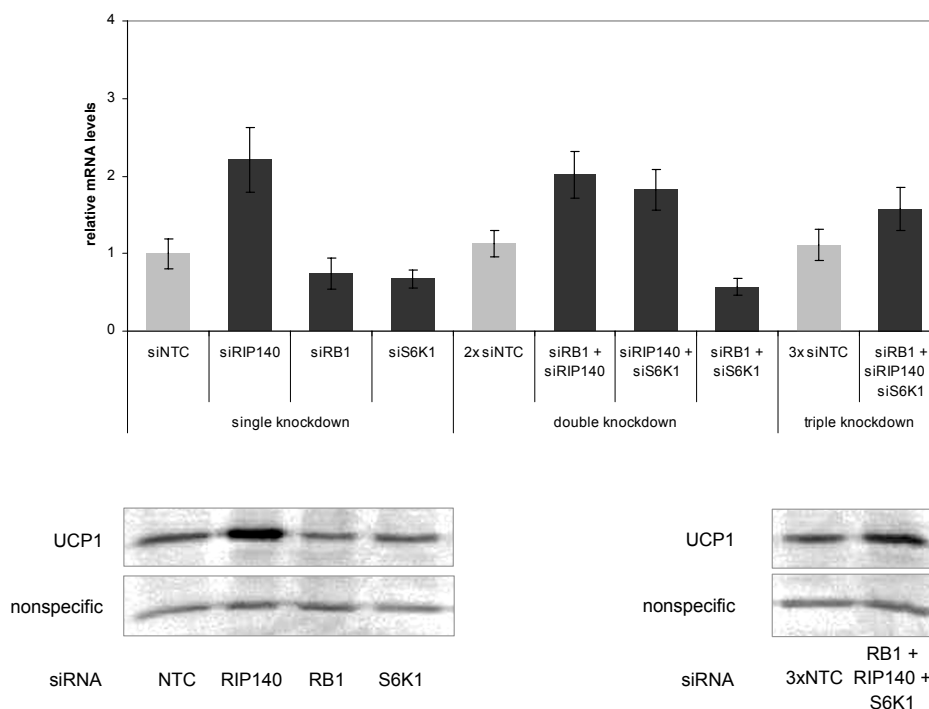


Figure 24. Knockdown of RIP140, but not RB1 and S6K1 promotes expression of UCP1 in human adipocyte differentiation. hMADS-2 cells were transfected at confluence (day -2) with siRNAs targeting RB1 (siRB1), RIP140 (siRIP140), S6K1 (siS6K1), either on their own or as pools. The final concentration of each siRNA was 5 nM; a non-targeting control siRNA (siNTC) was used at the same concentration. Adipocyte differentiation was induced 48 h after transfection (day 0) and rosiglitazone was added throughout the entire differentiation. Upper panel: UCP1 mRNA levels were analyzed by quantitative real-time RT-PCR, were normalized to TBP and are presented relative to cells transfected with 5 nM siNTC, with error bars denoting the standard error of the mean from three independent experiments. Lower panel: Analysis of UCP1 protein by Western blot.

down) of the three genes. Interestingly, while knockdown of RB1 and S6K1 on their own did not enhance (but rather dampen) rosiglitazone-induced UCP1 expression (d16-R16), knockdown of RIP140 further elevated UCP1 mRNA and protein levels compared to cells transfected with a non-targeting control siRNA (siNTC, Fig. 24). In line with these findings, simultaneous silencing of RB1 and S6K1 in combination with RIP140 was comparably effective in enhancing UCP1 expression, while the combination of RB1 and S6K1 resulted in a reduction of UCP1 mRNA levels (Fig. 24). Lastly, triple knockdown of all three direct miR-26a targets also increased UCP1 mRNA and protein, although the effect was less pronounced than the effect observed for single knockdown of RIP140 (Fig. 24). We thus suggest RIP140 to be a possible mediator of the miR-26a effect in human adipocyte differentiation. The promotion of a brown gene expression signature in human adipocytes by miR-26a raised the question whether these changes might also be reflected at the level of brown adipocyte function, which (at least primarily) is thermogenesis caused by high metabolic activity. Therefore, we transfected hMADS-2 cells with miR-26a mimics, followed by adipocyte differ-

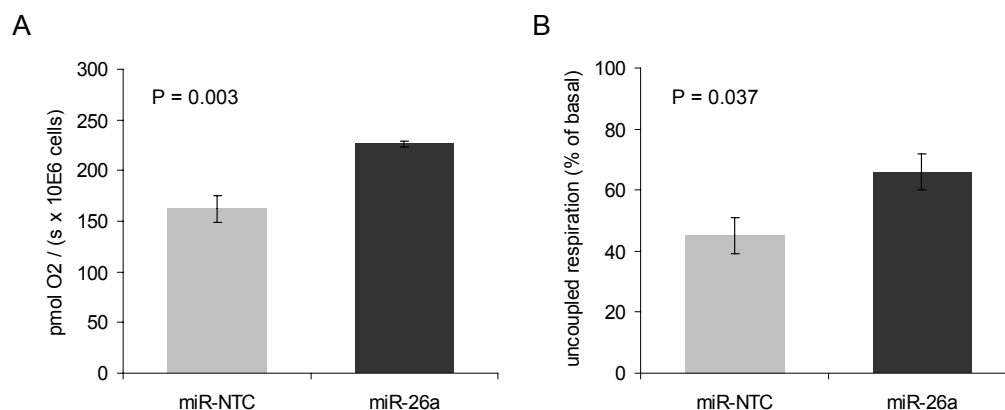


Figure 25. miR-26a enhances basal and uncoupled respiration of brown/brite hMADS adipocytes. hMADS-2 cells were transfected at confluence (day -2) with 5 nM miR-26a mimic or non-targeting control mimic (miR-NTC). Adipocyte differentiation was induced 48 h later (day 0). Rosiglitazone was added throughout the entire differentiation. All experiments were analyzed at day 16 by performing three consecutive measurements per condition as technical replicates. (A) Basal (=antimycin A-sensitive) respiration rate from four independent experiments is shown. Error bars denote the standard error of the mean. (B) Uncoupled respiration rates from five independent experiments are presented relative to basal respiration rates which were recorded in the same experiments. Error bars denote the standard error of the mean. Significance was determined using Student's *t*-test.

entiation according to the "brown protocol", and measured basal respiration in comparison to control transfected cells. Interestingly, miR-26a elevated basal respiration by approximately 40% (Fig. 25A), suggesting that miR-26a is able to enhance the metabolic rate of brown/brite adipocytes, probably via upregulation of UCP1. To test this hypothesis, we measured respiration after addition of oligomycin, which blocks ATP synthase and hence allows to quantify oxygen consumption that is not coupled to generation of ATP. Indeed, increasing miR-26a abundance also elevated uncoupled respiration of brown/brite hMADS-2 adipocytes compared to control transfected cells (Fig. 25B). Thus, miR-26a induces a brown gene expression program which ultimately results in a promotion of brown adipocyte function.

Chapter 5

Discussion

5.1 Discussion of methods

5.1.1 Microarrays

Since the first report describing the use of a DNA microarray to monitor expression of a large set of genes in 1995 (Schena et al., 1995), this technique has become the classical method for large-scale analysis of gene expression. Today, various platforms are commercially available, offering either single- or dual-color arrays which can also be customized according to specific research interests. The large amount of data available today, as well as the considerable experience gathered for the technique during the last 15 years, have even paved the way for clinical applications (Coppée, 2008), although thorough quality standards with respect to sample preparation, hybridization procedures and data analysis have been necessitated (MAQC Consortium et al., 2006; Shi et al., 2008).

The first miRNA studies were focused on particular transcripts and hence used Northern blots for their detection. However, as it became clear that the number of distinct miRNAs is in the range of at least several hundreds, efforts for microarray-based "global" miRNA expression analysis were launched (Barad et al., 2004). Yet the well-established technical strategies used for mRNA expression profiling were challenged at least for two reasons. First, the short sequence length of mature miRNAs offers only limited possibility for appending detection molecules, and virtually excludes the possibility to design conventional DNA probes with similar melting temperature (T_m) for all miRNAs to be detected. Second, the discrimination of miRNA family members which often differ by as little as a single nucleotide requires a stringency that is not demanded in the case of mRNA arrays. One strategy that addresses both issues is the design of detection probes as a mixture of DNA and modified, "locked" nucleic acid (LNA, an RNA analog where the 2'O and 4'C of the ribose sugar are linked via an additional bridge). Incorporation of a single LNA increases the T_m of an oligonucleotide by 2–7°C (compared to normal DNA) (Shi et al., 2008) and therefore offers the possibility to design probes with similar T_m by adjusting the locked nucleic acid (LNA) content of individual oligonucleotides. Indeed, an LNA-based platform for miRNA detection was in-

troduced in 2006 and could not only discriminate between miRNA family members, but also increase the detection sensitivity compared to a conventional DNA-based system (Castoldi et al., 2006). Thus, LNA-based microarray technologies appear as particularly suitable for miRNA research, and hence have been used in this study.

Although microarrays are widely used and well-established, other approaches for simultaneous detection of a large set of transcripts constitute alternatives to this technology. First, qRT-PCR has been used to screen for differentially expressed mRNAs (Gupta et al., 2010), but also miRNAs (see 5.1.2). Although a global mRNA expression profiling by qRT-PCR is still unfeasible, quantification of several hundreds of miRNAs (i.e. a large fraction of the total set of an organism's "miRNome") is possible and also surpasses microarrays in terms of sensitivity (Castoldi et al., 2008). Second, mass spectrometry (often coupled with upstream chromatography) is a powerful method to quantify thousands of genes at the protein level with a single experiment, but again, the magnitude of screens is still lower than for microarrays (i.e. still not genome-wide). Furthermore the technique is usually far more elaborate and cost-intensive. With respect to miRNA research, proteomics have appeared as valuable strategy to quantify the global effect of single miRNAs on the protein level of their targets (Selbach et al., 2008; Baek et al., 2008). Third, several platforms applying novel techniques of massive parallel ("next generation") sequencing have entered the market a few years ago. These techniques allow the simultaneous detection of millions of sequences in a single run (Ansorge, 2009), which is orders of magnitude higher than for classical Sanger sequencing. Hence, any biological sample can be assessed, within a few days, for its complete transcriptome, or for selected parts if the RNA is either size-fractionated (Rederstorff and Hüttenhofer, 2011), or if the RNA associated to distinct proteins is isolated by upstream immunoprecipitation (Leung et al., 2011). Probably the most important advantage of next generation sequencing over microarrays is their unbiasedness, meaning that novel, previously unidentified transcripts can be discovered, while a microarray can only detect transcripts corresponding to spotted sequences. This fact is of special interest for the young field of ncRNA research, which at the moment involves the rapid detection of novel transcripts. However, the accumulation of sequencing data in the range of several gigabytes per experiment presents considerable bioinformatic challenges in terms of data storage and analysis. In line with these challenges, and also with the young age of the technique, there are currently no standards for evaluation of deep sequencing data, which is in contrast to the thorough experience that exists for analysis of microarray experiments. Moreover, microarrays are still cheaper and less elaborate. However, if next generation sequencing techniques continue to improve in terms of costs, work time and data analysis, it seems plausible that microarrays might decline, at least in several areas of life science research (Ledford, 2008).

5.1.2 Quantitative real-time RT PCR

Measurement of PCR-based DNA amplification in "real-time" has been introduced in the 1990s (Higuchi et al., 1993; Heid et al., 1996) and quickly became a standard laboratory

method for quantification of gene expression. Indeed, qRT-PCR is more convenient for investigation of a single or several genes of interest compared to other, more elaborate methods like RT-PCR (followed by gel electrophoresis) or Western blots. Thus, the expression of certain marker genes indicative of a particular biological process is nowadays routinely assessed by qRT-PCR. Furthermore, qRT-PCR is the standard method for validation of differentially expressed transcripts that emerge from high-throughput screens (microarray or sequencing studies) (VanGuilder et al., 2008). With regard to miRNA research, the technique had to be modified compared to mRNA detection owing to the short length of mature miRNAs (Raymond et al., 2005), their heterogenous GC content (Benes and Castoldi, 2010), as well as the fact that the mature miRNA sequence is also present in the primary transcript and the pre-miRNA (Duncan et al., 2006). To address these issues, miRNA qRT-PCR systems involve a special reverse transcription step that generates cDNA fragments longer than the 21nt-mature miRNA, and under conditions that favour reverse transcription of mature miRNA species over longer pri- and pre-miRNAs (Benes and Castoldi, 2010). Moreover, the selective detection and amplification of specific miRNA family members has been addressed by strategies involving TaqMan detection probes, or LNA-modified primers. Conventional qRT-PCR is also useful to check for responsiveness of predicted direct target mRNAs to miRNA modulation, as many miRNA targets are decreased at mRNA level (Lim et al., 2005; Guo et al., 2010). However, one cannot definitely rule out "false negatives", i.e. miRNA-target interactions with translational repression only. In this respect, proteomic methods appear better suited (Baek et al., 2008; Selbach et al., 2008), but as already mentioned, these techniques are more complicated and more expensive.

Choice of an appropriate internal reference RNA to correct for sample-to-sample variation is a critical issue for qRT-PCR. Importantly, many such "housekeeping genes" which are widely used within the community, e.g. glyceraldehyde-3-phosphate dehydrogenase (GAPDH) or β -actin, have been shown to vary considerably under different experimental conditions (Schmittgen and Zakrajsek, 2000). Thus, for every new condition, reference RNA candidates need to be carefully evaluated with respect to potential variation, a procedure that is not necessary for microarray experiments, for which different normalization strategies based on the large number of detected genes have proven as valid and easy approaches which are routinely implemented in data analysis (Hackl et al., 2004). Similar to conventional qRT-PCR, no general reference miRNA has been identified as calibrator for miRNA qRT-PCR to date (Benes and Castoldi, 2010). Instead, different platforms usually offer a panel of other ncRNAs (e.g. ribosomal RNAs or small nucleolar RNAs) as references. As an alternative, preliminary microarray experiments can be conducted to identify stably expressed miRNAs for particular experimental settings which can subsequently be used as housekeepers for qRT-PCR. Recently, also the use of the mean expression value of all miRNAs assessed by a qRT-PCR experiment has been introduced as an appropriate normalization factor (Mestdagh et al., 2009), however, this method is only valid if a relatively large panel of distinct miRNAs is assayed.

Consideration of amplification efficiencies is another critical issue for proper evaluation of

qRT-PCR experiments, especially if subtle changes in gene expression should be reliably detected. Experimental determination of efficiency via a dilution series of the cDNA to be amplified is a possible method to account for gene-specific (i.e. primer-specific) amplification differences (Pfaffl, 2001). However, this strategy does not account for sample/reaction-specific variance, and hence, algorithms that calculate efficiencies for individual reactions based on the raw fluorescence data (i.e. the amplification curve) have been proposed (Zhao and Fernald, 2005), have been implemented in an in-house generated application for storage and evaluation of qRT-PCR data (Pabinger et al., 2009), and were used in this study.

Finally, it should be pointed out that, beside its inexpensiveness and convenience, qRT-PCR is also highly sensitive, surpassing microarrays, gel-based RT-PCR (VanGuilder et al., 2008), and classical library sequencing techniques. However, one has to be cautious as this high sensitivity can also be misleading. For instance, particular mRNAs might be robustly detected by qRT-PCR, but still be very low in abundance such that detection of the corresponding protein might not be possible, raising questions whether these "background" levels are of physiological relevance (or might be even just a contamination). Moreover, mRNA and protein levels do not necessarily correlate well, as post-transcriptional phenomena like mRNA degradation or regulation of translation (e.g. by miRNAs) can influence the actual levels of protein. Therefore, at least for key experiments and genes, direct assessment of proteins via Western blot or enzyme-linked immunosorbent assay (ELISA) should be performed.

5.1.3 Luciferase reporter assays

Luciferase is a prominent gene utilized for reporter assays in molecular biology, others being green fluorescent protein (GFP), β -galactosidase, or chloramphenicol acetyltransferase (CAT) (Bronstein et al., 1994; Kain and Ganguly, 2001). Such genetic reporters are used to investigate a wide variety of biological phenomena, e.g. protein-protein interactions, receptor or promoter activity, signal transduction, or mRNA processing.

As for miRNA research, the vast majority of studies rely on luciferase as reporter to investigate particular miRNA-mRNA interactions (Huang et al., 2010b). Indeed, luciferase (or, more generally, reporter gene) assays are the only available method to validate direct miRNA-mRNA actions, and to delineate these interactions to particular MREs. Moreover, the assay is highly sensitive, and as companies already offer reporter vectors containing the 3'UTR of interest, a relatively large panel of candidates can be assayed in parallel. However, there are also technical and biological pitfalls. First, the reporter luciferase signal has to be normalized to account for varying transfection efficiencies. This can be done by co-transfection of a second vector encoding another luciferase gene which is not responsive to the miRNA. An even better solution is the use of a single reporter vector containing both the reporter and normalization luciferase genes. Second, the function of particular MREs might depend on additional upstream or downstream sequences, influencing e.g. accessibility of the MRE for the RISC (Bartel, 2009). Thus, the full-length 3'UTRs of genes of interest should be used for luciferase assays, which can be difficult as some genes possess 3'UTRs in

the range of several kb. Third, many studies rely on easy-to-transfect cell lines like HEK293 cells or HeLa cells to perform luciferase assays, thereby placing the predicted miRNA-MRE interaction in an "artificial" environment. Such an environment might miss additional factors that are provided in the context of the original cell types. Moreover, co-transfection of miRNA mimics might result in supraphysiological intracellular miRNA concentrations, especially for easy-to-transfect cells, and thereby create a situation where the particular miRNA and MRE interact, although this is not normally the case (Kuhn et al., 2008). It would thus be best to use, if possible, the original cells of interest also for luciferase assays, and to perform not only miRNA overexpression, but also experiments in which endogenously expressed miRNA is inhibited (Tavazoie et al., 2008). Instead, a possible positive result (i.e. a validated direct interaction) can also be further supported by other types of experiments performed in the actual cells of interests. For instance, anti-correlated expression profiles of a miRNA-target pair in distinct conditions, or during the time course of a biological process, support a predicted direct interaction. Co-expression of the miRNA-target pair in the same cells is also a critical issue and should be assayed e.g. by *in situ* hybridization experiments, especially for tissue samples comprising several different cell types (Kuhn et al., 2008). In many instances, a distinct protein-coding gene can give rise to a whole set of different mRNA transcripts, and particularly the 3'UTR length has been shown to vary upon different environmental stimuli (Sandberg et al., 2008). Thus, it is also advisable to examine the presence of the predicted MREs in the cells or tissues of interest. Finally, investigating the responsiveness of the predicted target to miRNA modulation is of central importance. If such a response can be shown in the cells of interest, ideally at both mRNA and protein level, these results are supportive of a direct interaction validated by luciferase assays.

In summary, the Luciferase assay is an invaluable tool in miRNA research, which, if complemented by additional experiments, can indeed identify miRNA-mRNA pairs with critical importance in the investigated biological phenomenon.

5.1.4 Oxygen consumption measurements

The central function of brown adipocytes is cold-inducible heat production. This heat is generated as activation of UCP1 leads to disruption of the potential at the inner mitochondrial membrane, enabling substrate oxidation to run at maximum. Although measuring the produced heat would be the most direct assessment of brown adipocyte function, this method has been rarely performed (Nedergaard et al., 1977; Ricquier et al., 1979), presumably due to technical reasons (Cannon and Nedergaard, 2008). However, it is reasonable to consider respiration rates as a direct reflection of heat production, and indeed, studies suggested that measurements of respiration correlate well with microcalorimetric data (Nedergaard et al., 1977; Ricquier et al., 1979). Thus, virtually all studies on brown or brite adipocytes rely on oxygen consumption to quantify metabolic activity.

From a methodological viewpoint, *in vivo* experiments are relatively straightforward as animals (usually mice) can be placed in airtight metabolic chambers that are equipped with

oxygen sensors. *In vitro* experiments are generally more complicated, as a careful evaluation of the most optimal measurement conditions is crucial to obtain plausible results (Cannon and Nedergaard, 2008). Measurements of tissue pieces, cells, or isolated mitochondria have been described, all usually performed in continuously stirred suspensions (to ensure homogeneous changes in oxygen concentration) with a Clark type oxygen probe. Although physiologically meaningful results can be obtained with this setup, there is certainly room for improvements. Most importantly, the preparation for a measurement in suspension, as well as the measurement itself (e.g., shear stress due to constant stirring), impose considerable stress on adherent cells. This is especially true for adipocytes, which are relatively large and fragile cells, and can potentially augment the divergence of measurement conditions from the physiological situation. For instance, repeated pipetting is necessary for the procedure but inevitably leads to cell death of a certain fraction of adipocytes, resulting in release of intracellular debris, most importantly triglycerides and FAs derived thereof. As a consequence, it is likely that UCP1⁺ brown/brite adipocytes are uncoupled even without additional β -adrenergic stimulation. Buffering the concentration of free FAs by supplementation of the medium with BSA can help, although the optimal concentration needs to be determined (Shabalina et al., 2010). The measurement of adherent adipocytes could circumvent the current, stressful procedure. However, such measurements would have to be conducted in relatively small volumes of medium in order to obtain oxygen decrease rates that are comparable to the current system and thereby would result in a similar duration of measurements. In addition, these small volumes could avoid the need of continuous stirring. Indeed, a system for respiration measurements on adherent cells is already commercially available and has also been used for the study of mammalian cells, including adipocytes (Fang et al., 2011; Lidell et al., 2011; Lee et al., 2011).

Beside the classical Clark type electrode, another system based on optical rather than amperometric measurements has recently been described for measurement of oxygen concentration in biological samples (Kellner et al., 2002). The principle of this optical system is quenching of the fluorescence of a metal-organic dye by oxygen (Weigl et al., 1994). Compared to the Clark type electrode, there are at least three advantages. First, the optical sensor performs better in small measurement volumes, as no oxygen is consumed by the probe itself. Second, the optical sensor can be manufactured in a size as small as the fiber optic cable which is used to transmit the light pulse to the detector ($< 50 \mu\text{m}$). Third, the sensor does not have to be in direct contact with the sample (e.g. the cell suspension), but can also be spatially separated, provided that a translucent connection (e.g. the glass wall of a cell culture plate) exists. Although in this study, the optical sensor was used in combination with the classical setup that measures cells in suspension, the development of a non-invasive assay for cellular respiration measurements on adherent cells, based on the optical sensor technology, appears highly interesting and should be pursued in the future.

5.1.5 *In vitro* approaches to identify genes with physiological relevance

The results of this thesis have been mainly acquired by *in vitro* experiments, raising the question whether the newly identified regulators of adipocyte differentiation or function are also of relevance *in vivo*. It is fair to say that a definite answer to this issue cannot be given at the moment. However, it shall be pointed out that similar approaches have proven as powerful in identifying key regulators of physiological and pathophysiological processes. Indeed, it can be considered as a standard chronology to first identify potentially interesting genes through a comparison of various *in vitro* (and probably *in vivo*) conditions, followed by a functional analysis that is first conducted *in vitro*, and ultimately also *in vivo*. As two of many examples in adipose tissue research, the crucial roles of both C/EBP α (Birkenmeier et al., 1989; Christy et al., 1989; Lin and Lane, 1992; Freytag et al., 1994; Linhart et al., 2001) and PPAR γ 2 (Graves et al., 1992; Tontonoz et al., 1994b; Tontonoz et al., 1994c; Rosen et al., 1999; Zhang et al., 2004) genes were discovered by such a series of studies. However, the choice of appropriate *in vitro* models is a crucial issue. As for adipogenesis, the aptness of polyploid, transformed cell lines like 3T3-L1 for physiological studies is often debated (Keller et al., 2011). In this respect, adipocytes derived from hMADS cells appear as a more appropriate *in vitro* model, not only because of their human origin, but also due to the thorough studies on these cells revealing that they possess key adipocyte features (Rodriguez et al., 2004a). Furthermore, primary culture of cells isolated from the SVF of adipose tissue samples represents a model which is even closer to the *in vivo* situation, as such experiments are usually conducted only hours to days after isolation of cells (Hauner et al., 1989; Entenmann and Hauner, 1996). Thus, attempts to reproduce the most important findings obtained from experiments with cell lines by studies with such primary cells are highly recommended, as positive results increase the probability for a relevance *in vivo*.

In summary, it is proposed that the *in vitro* studies presented in this thesis, which are also partly complemented by analysis of various *in vivo* samples, lay the foundation for a potential further functional investigation *in vivo*. Such studies could include injection of substances, transplantation of genetically manipulated cells, and also the generation of transgenic and/or knockout mouse models. For each miRNA investigated in this study, questions which could be addressed by particular *in vivo* experiments, as well as potential technical challenges, will be discussed in the next section.

5.2 Discussion of results

5.2.1 miR-27b in adipogenesis, lipid metabolism and beyond

In the study summarized in 4.2 and published in 2009 (Karbiener et al., 2009), miR-27b was identified as the first miRNA to function as negative regulator of adipogenesis in human. First, we found a decreasing expression of miR-27b during adipogenesis of hMADS cells (Fig. 6A), a unique cell model for human adipogenesis (Rodriguez et al., 2004a; Scheideler et al.,

2008). Second, overexpression of miR-27b resulted in impaired triglyceride accumulation and repression of several adipogenic marker genes at terminal differentiation (Fig. 6B-D). These findings are in agreement with studies in mouse 3T3-L1 and OP9 cells in which adipogenesis likewise decreased upon miR-27a and miR-27b overexpression (Lin et al., 2009; Kim et al., 2010b). Interestingly, another recent study showed that inhibition of miR-27a and miR-27b restored cytoplasmic lipid droplets in rat hepatic stellate cells (Ji et al., 2009b). Thus, the miR-27 family might be a general regulator of triglyceride accumulation in different cell types and tissues.

To delineate at which point miR-27b is interfering with the adipogenic transcription factor cascade, and because miRNA targets, if repressed at mRNA level, are also repressed at translational level (Baek et al., 2008), we monitored the transcriptional changes of KLF4, CHOP10, C/EBP β , C/EBP δ , PPAR γ , and C/EBP α at early stages of adipogenesis (day 1, 3, and 5). Upon miR-27b overexpression, we detected no changes in mRNA level for KLF4, CHOP10, C/EBP β , and C/EBP δ (Fig. 7), whereas the core layer of the transcriptional cascade with PPAR γ and C/EBP α showed impaired induction at day 3 and 5 of differentiation (Fig. 7). Interestingly, several target prediction algorithms jointly identify a single miR-27b binding site in the 3'UTR of PPAR γ (Fig. 8A), but not in the 3'UTR of C/EBP α . Furthermore, the miR-27b MRE in the PPAR γ 3'UTR is highly conserved among mammals (Fig. 8B), and the expression of miR-27b and PPAR γ changed reciprocally during adipogenesis of hMADS cells (Fig. 8C). We thus concluded that PPAR γ might be a direct target of miR-27b, thereby challenging the rationale of the 3T3-L1 study that PPAR γ is not a direct target of miR-27b (Lin et al., 2009). To cover our hypothesis, we, unlike Lin et al., performed luciferase reporter assays, the standard validation of miRNA-mRNA interactions, with luciferase reporter vectors containing the PPAR γ 3'UTR either with the perfect or mutated predicted miR-27b MRE. Indeed, our results clearly demonstrate the first evidence that human PPAR γ is a direct target of miR-27b and that the predicted miR-27b MRE is functional (Fig. 9). The observation that C/EBP α induction was also blunted by miR-27b overexpression is concordant with this, because PPAR γ is known to induce the expression of C/EBP α to promote adipocyte differentiation (Wu et al., 1999b). Nevertheless, this does not rule out that other genes involved in adipogenesis are also direct miR-27b targets as indicated by the finding that RXR α , at least in rat hepatic stellate cells, is a direct target of miR-27 (Ji et al., 2009b).

The mature sequences of miR-27a and miR-27b are perfectly conserved between mouse and human, and highly or entirely similar mature miRNAs also exist in vertebrates of larger evolutionary distance, e.g. in zebrafish. Furthermore, miR-27a and miR-27b sequences differ only at a single nucleotide at position 19, both in human and mouse. Thus, the two family members likely target a very similar set of mRNAs and hence might regulate the same biological processes. With respect to their genomic location, it is remarkable that, for both human and mouse, miR-27a occurs in a cluster with miR-23a and miR-24-2, while miR-27b appears clustered with miR-23b and miR-24-1. It is thus proposed that the two

miR-27 family members (as well as the other miRNAs of the two clusters) occurred via a gene duplication event. In line with their clustered occurrence, we identified not only miR-27a and miR-27b, but also miR-23a, miR-23b, and miR-24 to decrease during adipocyte differentiation of hMADS cells (Fig. 5). However, another study found diverging expression profiles for miR-27b, miR-23b, and miR-24 during BMP2-induced adipogenesis of mouse C3H10T1/2 cells: miR-24 increased with differentiation, while miR-23b decreased and miR-27b was unchanged (Sun et al., 2009a). Thus, the dynamics of miRNA expression during adipogenesis depend on the cellular model, and even clustered miRNAs do not necessarily exhibit the same kinetics. Furthermore, miR-24 promoted BMP2-induced adipogenesis of C3H10T1/2 cells (Sun et al., 2009a). It can thus be assumed that miRNAs located within the same cluster (e.g. miR-27a/b and miR-24) might have opposite influences on the same biological process.

While current genome annotations depict the miR-23a~27a~24-2 cluster as intergenic in mouse and human, the miR-23b~27b~24-1 cluster is intronic to the C9orf3 gene (NM_032823), coding for the aminopeptidase AP-O, an enzyme which has been shown to convert angiotensin III to angiotensin IV (Díaz-Perales et al., 2005). Interestingly, C/EBP α was demonstrated to induce C9orf3 transcription in HeLa cells as well as murine myeloid progenitor cells, presumably via direct binding to the C9orf3 promoter (Feng et al., 2009). As C/EBP α is well known to increase during adipogenesis, this contrasts with the observed downregulation of miR-27b during adipocyte differentiation (Fig. 5, Fig. 6A). Hence, probably other mechanisms beside transcription are involved in the decrease of mature miR-27b, e.g. attenuated miRNA processing or increased miRNA degradation. Notably, a study on C2C12 myotubes demonstrated reduced miR-27a and miR-27b levels upon treatment with Dex (Allen and Loh, 2011). As natural and synthetic glucocorticoids (Dex) are an important component of the adipogenic medium, promoting differentiation of mouse preadipocytes (Schiwek and Löffler, 1987) and human primary adipocyte precursor cells (Hauner et al., 1989), it is tempting to speculate that, during adipocyte differentiation, signalling pathways downstream of Dex are involved in the decrease of miR-27 family members. It will be interesting to investigate this potential mechanism in the future, e.g. by analyzing the influence of Dex on mature miR-27a and miR-27b, but also on the pre-miRNAs and primary transcripts, as well as on the C9orf3 gene, during the first days of adipocyte differentiation.

The involvement of the miR-27 family in differentiation is not exclusive to adipogenesis. A study on human MSC revealed miR-27a to impair osteogenic differentiation, which might be mediated by the direct target grancalcin (Schoolmeesters et al., 2009). However, another study using a human fetal osteoblastic cell line showed that miR-27 overexpression increased osteogenesis, probably by direct targeting of adenomatous polyposis coli (APC), which is an inhibitor of the pro-osteogenic Wnt signaling pathway (Wang and Xu, 2010). Thus, while the miR-27 family has been consistently identified as negative regulator of adipogenesis in mouse and human (Lin et al., 2009; Karbiener et al., 2009; Kim et al., 2010b), its role in os-

teogenesis is still controversial. With respect to myogenesis, miR-27b was shown to possess a stimulatory effect on differentiation, most likely via targeting of paired box gene 3 (Pax3), a transcription factor that is expressed in SM progenitor cells and has to be downregulated to allow their differentiation (Crist et al., 2009). In the hematopoietic lineage, miR-27 has been shown to increase during differentiation of myeloblasts into granulocytes, and to directly target Runx1, a known inhibitor of this developmental process (Feng et al., 2009). Due to its negative influence on triglyceride accumulation, at least partly mediated via direct targeting of PPAR γ and RXR α , inhibition of miR-27 could have beneficial metabolic effects. Indeed, PPAR γ activation by rosiglitazone enhances the fat storing capacity of adipose tissue and hence leads to decreased release of free FAs into the circulation (Tan et al., 2005), which partly explains the insulin-sensitizing effects of TZDs and their use for treatment of type 2 diabetes (Lebovitz and Banerji, 2001). Interestingly, miR-27a was found to be upregulated in WAT of hyperglycaemic rats compared to normoglycaemic animals, and high glucose concentrations were also found to elevate miR-27a levels in 3T3-L1 adipocytes (Herrera et al., 2010). Thus, the miR-27 family is a potential mediator of pathophysiological processes leading to type 2 diabetes, which might be partially mediated via targeting of PPAR γ . Conversely, a synergistic therapeutical effect of miR-27 inhibition, resulting in higher levels of PPAR γ , and rosiglitazone, promoting PPAR γ activity, can be envisioned. However, attempts to decrease miR-27 activity *in vivo* have not been performed to date. Recently, though, systemic inhibition of particular miRNA families has been described using 8-mer antisense oligonucleotides that were fully LNA-modified: These "tiny LNAs" were synthesized with perfect complementarity to the seed region of the miRNA family to be addressed, and effective inhibition of the let-7 and miR-221/222 families was demonstrated (Obad et al., 2011). A similar approach for antagonism of the miR-27 family in WAT appears interesting, although it is not known how efficiently such tiny LNAs can enter adipose tissue if administered intravenously, as described in the pioneering study by Obad et al. (Obad et al., 2011). Thus, alternative ways of administration, e.g. direct injection into fat pads, would have to be considered. Apart from efficient delivery of the "tiny LNA" to WAT, the selectivity is probably an even more challenging task. Indeed, the miR-27 family is expressed in multiple tissues (Lagos-Quintana et al., 2002), and therefore, if other organs beside WAT also take up anti-miR-27 oligonucleotides, the risk of detrimental effects in these organs is evident.

To further investigate the physiological role of miR-27, the generation of miR-27-deficient mice would be of high interest. Indeed, knockout mice lacking individual miRNAs have been described since 2007 (Thai et al., 2007; Rodriguez et al., 2007; van Rooij et al., 2007; Zhao et al., 2007). However, the technical challenges are very high in the case of miR-27. First, mature miR-27a and miR-27b are nearly identical. Although a study deleting only one of two copies of the miR-1 gene observed strong effects (Zhao et al., 2007), it is also conceivable that loss of one family member might be compensated by the other. Hence, the separate generation of two knockout mouse models, each deficient for one miR-27 family member,

followed by crossbreeding, might be necessary at worst. Second, both miR-27a and miR-27b are clustered with other miRNAs. Although a vector for homologous recombination could be designed to disrupt only the miR-27a/miR-27b sequences, such mutations could induce potential secondary effects, e.g. altering the processing of neighbouring miRNAs. Third, as the miR-23b~27b~24-1 cluster resides in an intron of the C9orf3 gene, the DNA sequence changes necessary to invalidate miR-27b could also have potential effects on processing of the host gene.

An alternative to targeted deletion of miR-27 would be the use of a "miRNA sponge" technology. MiRNA sponges are artificial transcripts expressed from strong promoters and designed to harbour multiple copies of MREs for the miRNA of interest (Ebert and Sharp, 2010). Indeed, expression of miRNA sponges in mammalian cells could efficiently derepress endogenous miRNA targets and also demonstrate the simultaneous inhibition of miRNA family members (Ebert et al., 2007). Moreover, stable expression of miRNA sponges *in vivo* has already been shown for plants (Franco-Zorrilla et al., 2007) and drosophila (Loya et al., 2009). Similar approaches in mouse can thus be envisioned, and combination with the Cre recombinase technology could also facilitate a tissue-specific miRNA sponge expression (Ebert and Sharp, 2010).

5.2.2 miR-30c, a pro-adipogenic coordinator of distinct regulatory networks

In the study summarized in 4.3 and accepted for publication in 2011 (Karbiener et al., 2011), we first identified miR-30c to be upregulated during early adipocyte differentiation of murine and human cells (Fig. 5, Fig. 10). Subsequent functional analysis with hMADS cells demonstrated that miR-30c promotes adipocyte differentiation, as evidenced by accelerated upregulation of the adipogenic key transcription factors PPAR γ and C/EBP α , ultimately resulting in increased expression of adipocyte marker genes and enhanced triglyceride accumulation (Fig. 12A-C).

miR-30c belongs to the miR-30 family, which comprises five distinct members (a to e) that are perfectly conserved between mouse and human, and is expressed in a variety of different tissues. In line with this, studies have either proposed or validated functions of the miR-30 family in numerous types of cancer (Budhu et al., 2008; Sorrentino et al., 2008; Wang et al., 2010; Busacca et al., 2010; Braun et al., 2010; Zhong et al., 2010; Yu et al., 2010), but also in several other biological contexts such as myocardial matrix remodelling (Duisters et al., 2009), apoptosis (Li et al., 2010), and kidney development (Agrawal et al., 2009). A possible involvement of the miR-30 family in adipocyte function was first conceivable after a global miRNA expression analysis during adipogenesis of human preadipocytes showed a potent upregulation of miR-30c expression (Esau et al., 2004). This finding was subsequently confirmed for adipogenesis of mouse 3T3-L1 cells (Kajimoto et al., 2006). In line with both studies, we identified miR-30c in a miRNA screening during adipogenesis of hMADS cells as one of the miRNAs with the most dramatic upregulation. Moreover, we demonstrate for

the first time a function for this member of the miR-30 family in adipocyte differentiation (Fig. 12).

Mature miR-30c can be generated from two distinct pre-miRNAs, both residing in intronic regions of distinct host genes. While hsa-miR-30c-1 is located within the open reading frame of the NFYC gene (NM_014223) at chromosome 1, hsa-miR-30c-2 is intronic to C6orf155 (NR_026807), a processed transcript with no known protein product, at chromosome 6. We found both host genes to be expressed during adipocyte differentiation of hMADS cells (Fig. 10). Thus, it is reasonable to propose that both loci contribute to miR-30c expression during human adipogenesis. However, the expression profiles are not congruent with miR-30c, as NFYC was only modestly upregulated at late stages (day 9 and day 16), while C6orf155 expression showed a peak at day 5, followed by a decrease (Fig. 10). This could be explained by different half-lives of mRNA and miRNA. Alternatively, miR-30c could be transcribed from transcription start sites other than the host gene promoter, i.e. independently of its host genes, as recently shown for several intronic miRNAs (Monteys et al., 2010). Future studies addressing mechanisms that regulate miR-30c transcription will be of interest and will also enable the integration of this miRNA in the cascade of regulatory events that promote adipogenesis.

As genome-wide studies revealed that a single miRNA can directly regulate hundreds of target mRNAs (Lim et al., 2005; Baek et al., 2008; Selbach et al., 2008), for any biological process investigated it is therefore obvious that (i) identification of those targets that mediate (at least predominantly) the miRNA effect is challenging; and that (ii) the miRNA likely mediates its effect via more than a single target. In order to decrease the false-positive rate for predicted direct miR-30c target candidates to be further analyzed, we combined several prediction algorithms and in-house generated gene expression data of hMADS cells during adipogenesis. As a result, among the most interesting candidates we identified PAI-1 and ALK2, being not only predicted by at least four distinct algorithms, but also showing inverse expression profiles compared to miR-30c expression, i.e. downregulation during adipocyte differentiation (Fig. 13B). Furthermore, both genes were responsive to miR-30c overexpression (Fig. 13C). Lastly, luciferase assays indeed confirmed the direct interaction of miR-30c with PAI-1 and ALK2 via single miRNA binding sites in their 3'UTRs (Fig. 15). Notably, our finding of a direct PAI-1 regulation by miR-30c was recently confirmed in a different context, as PAI-1 induction in human pulmonary microvascular endothelial cells by placenta growth factor (PlGF) is presumably mediated via downregulation of miR-30c (Patel et al., 2011).

It has been demonstrated that several miRNAs are differentially expressed upon genetically induced obesity in mice (Xie et al., 2009). In line with this, we demonstrate decreased miR-30c levels in WAT upon genetically as well as diet-induced weight gain (Fig. 14). This suggests that miR-30c could be involved in the detrimental effects of obesity. Furthermore, we were interested whether miR-30c and its identified direct targets PAI-1 and ALK2 are also reciprocally expressed in this context. While ALK2 was unaltered, weight gain indeed

evoked reciprocal changes in PAI-1 and miR-30c expression. Among possibilities to explain such difference, distinct expression of the two genes between adipocytes and the cells of the stromal vascular fraction cannot be ruled out. Future experiments should shed some light on that issue.

The function of PAI-1 in adipogenesis and adipose tissue biology still remains controversial. Liang et al. showed that PAI-1 overexpression in 3T3-L1 cells inhibits adipocyte differentiation, while preadipocytes from PAI-1^{-/-} mice showed stronger differentiation (Liang et al., 2006). However, a different study showed no effects of a PAI-1 neutralizing antibody or PAI-1 overexpression on adipogenesis of 3T3-F442A preadipocytes, and also comparable adipogenesis of PAI-1^{-/-} and wt MEFs (Scroyen et al., 2007). Investigations of mouse models appear controversial as well: Morange et al. described faster weight gain of PAI1^{-/-} compared to wt mice on a high-fat diet (Morange et al., 2000), and a study of transgenic mice overexpressing PAI-1 under control of the adipocyte promoter aP2 showed reduced body and fat mass compared to wt mice (Lijnen et al., 2003). In contrast, another study showed that PAI-1 deficiency protected mice against diet-induced obesity (Ma et al., 2004). This apparent divergence of results might be explained by different mouse strains used, by different effects of local or systemic PAI-1 overexpression or knockout, due to a postulated dose-dependent effect of PAI-1 on adipogenesis (Scroyen et al., 2009), and lastly also due to different ALK2 levels. With respect to human adipogenesis, in this study we present evidence that cell-autonomous modulation (via siRNA silencing) of the newly identified miR-30c target PAI-1 in adipocyte precursors has – on its own – negligible effects on adipocyte differentiation (Fig. 16A&B), which is in line with previously published data using murine adipogenesis models (Scroyen et al., 2007).

ALK2 is a receptor tyrosine kinase belonging to the class of BMP type I receptors and has been shown to mediate BMP7 (Macías-Silva et al., 1998) and BMP9 signalling (Luo et al., 2010). Reports describing a stimulatory role of constitutively active ALK2 on osteogenic and chondrogenic differentiation (van Dinther et al., 2010; Shen et al., 2009) are in line with the identification of ALK2 mutations as the cause of fibrodysplasia ossificans progressiva (FOP), a rare autosomal disease characterized by ectopic osteogenesis and chondrogenesis in soft tissues (Shore et al., 2006). Concerning adipogenesis, there have been no indications for a direct ALK2 involvement so far. BMP7, though, has been implied in directing mesenchymal stem cell differentiation from white to brown adipogenesis (Tseng et al., 2008), however, BMP7 can also signal via type I receptors other than ALK2. Similar to PAI-1, our study showed no effects of single ALK2 silencing on adipogenesis of hMADS cells (Fig. 16A&B). Interestingly, combined silencing of both miR-30c targets, PAI-1 and ALK2, enforced adipogenesis (Fig. 16C&D), thereby recapitulating the miR-30c effect, at least partly. We thus present, for the first time in adipogenesis, a miRNA that might regulate differentiation via direct targeting of (at least) two genes which operate in distinct signalling pathways. In addition, we have revealed a cooperative, anti-adipogenic action of PAI-1 and ALK2, two proteins that were not known before to be interconnected. This opens up the question how the two corresponding gene regulatory networks might be related. PAI-1 is known to bind

to the extracellular matrix components vitronectin (VN) and urokinase-type plasminogen activator (u-PA), thereby altering binding of VN and u-PA to integrins and the urokinase plasminogen activator receptor (u-PAR) (also designated CD87) (Lijnen, 2005). Based on our observations, we could envision that subsequent downstream signalling of PAI-1 via VN/u-PA and integrins/u-PAR, as well as BMP-elicited, ALK2-mediated signalling might relay two redundant inhibitory signals, each retarding the progression of adipogenesis. Consequently, downregulation of both pathways, which might be mediated by miR-30c via PAI-1 and ALK2 targeting, removes the inhibitory signals, thereby promoting adipocyte differentiation. It will be interesting to explore this cross-talk of PAI-1 and BMP signalling in more detail in the future.

Collectively, our study depicts miR-30c as a promoter of adipocyte differentiation and – via direct targeting of PAI-1 and ALK2 – as a possible link between two distinct, so far not interrelated pathways. Thus, our findings support the idea that miRNAs might connect and co-ordinate regulatory networks larger than previously anticipated. Moreover, the identification of direct miRNA targets, combined with the analysis of their cooperative effect on a biological process, can provide novel insights into those larger regulatory networks.

Both the sequence of mature miR-30c, as well as the miRNA copy number (2 loci), are perfectly conserved between mouse and human. Thus, to further investigate the physiological role of miR-30c in adipogenesis and fat metabolism, studies on mice with fat-specific miR-30c deficiency would be of high interest. However, similar to miR-27b (see 5.2.1), the generation of such mice is a challenging task. Again, an intronic miRNA gene (i.e. miR-30c-2) would have to be disrupted without influencing the expression of its host gene (i.e. *Nfyc*). Furthermore, the disruption of both miRNA genes (i.e. miR-30c-1 and miR-30c-2) might be necessary to evoke a phenotype, as has been shown for miR-133a-1 and miR-133a-2, where only the knockout of both genes resulted in severe cardiac defects (Liu et al., 2008). Even the invalidation of both miR-30c genes might not be sufficient, as four other family members – miR-30a, miR-30b, miR-30d, miR-30e – with highly similar sequences might compensate for miR-30c loss. However, generation of a knockout mouse lacking the entire miR-30 family appears highly elaborate, although it might be advantageous that the family is partitioned in "only" three loci (miR-30a clustered with miR-30c-2, miR-30b clustered with miR-30d, miR-30c-1 clustered with miR-30e). Hence, the design of three (instead of six) vectors for homologous recombination would be sufficient to generate three mouse models, each lacking two miR-30 gene copies. Indeed, a similar approach has already been described for the miR-17~92 cluster and its two paralogous clusters, miR-106b~25 and miR-106a~363, including crossbreeding experiments to reveal compensatory effects (Ventura et al., 2008). As for miR-27b, an alternative, less tedious procedure would be the generation of transgenic mice that express a "sponge" transcript (Ebert et al., 2007; Ebert and Sharp, 2010) for the miR-30 family. At best, such transgenic mice could provide similar insights into the physiological role of this miRNA family.

5.2.3 miR-26a, a potential mediator of cold acclimation

In the study summarized in 4.4, we investigated the role of miR-26a in the balance between white and brown/brite adipocyte differentiation. Initial miRNA expression profiling performed by us (Fig. 5) and others (Oskowitz et al., 2008) revealed miR-26a to be upregulated during human adipocyte differentiation, which let us hypothesize a function in this biological process. Interestingly, hMADS cells have recently been shown to differentiate into white adipocytes, or into adipocytes exhibiting key properties of brown adipocytes (Elabd et al., 2009). We were therefore interested whether the difference between white and brite/brown culture conditions, i.e. the duration of exposure to the PPAR γ ligand rosiglitazone, might result in different expression levels of miR-26a. However, miR-26a levels were not significantly different between adipocytes subjected to the white (no rosiglitazone from day 9 on) or brown (continuous rosiglitazone exposure) protocol (Fig. 17). This implies that, at least in differentiated adipocytes, miR-26a is not under the control of PPAR γ .

As we could still reproduce our preliminary results by showing a modest upregulation of miR-26a during the first days of adipogenesis (Fig. 17), we decided to analyze a potential function of this miRNA in adipocyte differentiation. Therefore, we transfected hMADS cells with miRNA mimics to elevate intracellular miR-26a levels, a frequently used approach for *in vitro* studies on human cells (Esau et al., 2004; Luzi et al., 2008; Kim et al., 2009a; Kim et al., 2009b; Huang et al., 2010a). Indeed, miR-26a overexpression resulted in higher levels of triglycerides and FABP4 mRNA at day 9 (Fig. 18). However, no difference between miR-26a and control transfected cells was evident at day 16, the stage of terminal differentiation, for both adipocytes differentiated according to the white and brown/brite protocol (Fig. 18). As the timeframe between transient (!) transfection (day -2) and the second time point of analysis (day 16) is rather extensive, the apparent loss of the miR-26a effect could be due to technical reasons, i.e. the inevitable decrease of miRNA mimic levels within the cells over time. Alternatively, elevation of miR-26a levels during early differentiation could provide pro-adipogenic stimuli which are likewise, but later, provided by substances of the differentiation cocktail. Collectively, we propose that miR-26a accelerates human adipocyte differentiation *in vitro*, although we cannot exclude that this miRNA also augments the absolute capacity of adipocytes for triglyceride storage.

When screening a larger panel of genes related to distinct aspects of adipose tissue biology, we observed a pronounced induction of UCP1 mRNA for miR-26a-treated hMADS-3 cells (Fig. 18B). This effect could be reproduced in hMADS-2 cells, established from another donor (Rodriguez et al., 2005): Both at day 9 and in white adipocytes at day 16, miR-26a promoted high UCP1 mRNA levels, and while UCP1 protein is normally below detection limit in these conditions, it was robustly detected upon miR-26a overexpression (Fig. 19A). Furthermore, the described induction of UCP1 mRNA and protein by continuous treatment of hMADS cells with rosiglitazone (Elabd et al., 2009) was substantially elevated by miR-26a (Fig. 19A). We therefore propose that miR-26a promotes brown adipocyte characteristics during adipocyte differentiation of hMADS cells, which is further supported by elevated

expression of PGC-1 α , CPT1 β , and CIDEA (Fig. 19B).

As hMADS cells have been isolated from WAT of children and infants, it could be hypothesized that, due to the young age of donors, these cells might be exceptionally susceptible for stimuli towards the brown lineage. Indeed, it was recently shown that human fetal mesenchymal stem cells, isolated from BM of first-trimester fetuses, are capable of UCP1 expression during adipocyte differentiation *in vitro* (Morganstein et al., 2010). We thus asked whether the ability of miR-26a to induce brown adipocyte traits is restricted to progenitor cells obtained from young individuals. Therefore, we obtained subcutaneous WAT samples from adult humans aged between 30 and 53 years to isolate the SVF, which contains adipocyte progenitor cells (termed hPASC). Indeed, overexpression of miR-26a in hPASC promoted UCP1 and PGC1 α expression (Fig. 19C), recapitulating the results acquired with hMADS cells and implying a more general function of miR-26a in brown adipogenesis that is not restricted to cells from young individuals.

Fat-specific invalidation of Dicer, the indispensable enzyme for processing of pre-miRNAs to their mature form, results in a severely diminished expression of genes involved in BAT thermogenesis in mouse (Mudhasani et al., 2011). Thus, the necessity of particular miRNAs for establishment of functional brown adipocytes can be anticipated; however, no miRNA has been identified to play such a role until now. Having observed the stimulatory effect of miR-26a on expression of UCP1 and other brown markers, we next asked whether brown adipocyte differentiation of hMADS cells is dependent on this miRNA. Therefore, we inhibited miR-26a during differentiation of hMADS-2 cells according to the brown protocol. Strikingly, UCP1 mRNA was significantly reduced, UCP1 protein was even undetectable (Fig. 20A), and also the expression levels of PGC1 α , CPT1 β , and CIDEA were diminished (Fig. 20B). Thus, establishment of a brown adipocyte gene expression program due to chronic PPAR γ activation is dependent on miR-26a.

A potential physiological relevance of miR-26a could be further inferred from analysis of various murine adipose tissue samples. First, miR-26a was expressed at higher levels in the SVF and AF of BAT compared to WAT (Fig. 21A). Second, miR-26a was induced in the WAT of mice exposed to prolonged cold stress, and this is likely mediated via β -adrenergic stimulation (Fig. 21B). Thus, miR-26a is associated with a thermogenic phenotype and might be a potential mediator of cold acclimation *in vivo*. It should be highlighted that the 3-fold induction of miR-26a in WAT upon cold stress might underestimate the responsiveness of this miRNA to cold, as the control mice had been kept at ambient temperature (23 °C). It has been shown that such environmental conditions impose a chronic cold stress on the animals, reflected by a 50–60% increase in metabolism above basal (Golozoubova et al., 2004). Hence, such "control" mice might have already elevated miR-26a levels compared to thermoneutrality (=a situation where no cold stress exists), which for mice is at 30 °C (Feldmann et al., 2009). Moreover, perigonadal WAT samples have been used in this study to measure transcriptional responses to cold stress and β -adrenergic stimulation. However, abdominal WAT depots like the perigonadal are less susceptible for cold-induced "browning" than subcutaneous WAT depots (Cousin et al., 1992; Guerra et al., 1998; Cousin et al.,

1993). Thus, future cold exposure experiments with control mice kept at thermoneutrality, and using WAT from different anatomical locations, will be interesting, as such studies could reveal an even more dynamic regulation of miR-26a.

The human miR-26 family consists of two members, miR-26a and miR-26b. While miR-26b is intronic to the CTD (carboxy-terminal domain, RNA polymerase II, polypeptide A) small phosphatase 1 (CTDSP1) gene, miR-26a can be derived from either the miR-26a-1 or the miR-26a-2 gene, both residing in introns of the paralog CTDSPL and CTDSP2 genes. The same miRNA copy number, intronic location, and identical miRNA sequences can be found in mouse. Thus, the whole family is supposed to have occurred via two gene duplication events. In line with this, the sequences of miR-26a and miR-26b differ by only three nucleotides, two of them at the 3'end. Hence, a considerable functional redundancy is to be expected. Indeed, we cannot rule out that also miR-26b regulates rosiglitazone-induced brown adipogenesis of hMADS cells, as (i) CTDSP1 is expressed in hMADS cells (data not shown), and as (ii) the LNA-based antisense oligonucleotides used for inhibition of miR-26a likely also hybridize to (and hence antagonize) miR-26b.

CTDSP1, CTDSP2, and CTDSPL are a family of small C-terminal domain phosphatases implied in control of the RNA polymerase II transcription machinery (Yeo et al., 2003). Furthermore, mutations leading to inactivation or lower expression of these genes have been identified in several cancer types, including small cell and non-small cell lung carcinomas (Kashuba et al., 2009), cervical carcinomas (Mitra et al., 2010), and breast cancer (Sinha et al., 2008). It has also been shown that CTDSPL dephosphorylates RB1 protein (Kashuba et al., 2004), which may partly explain its role as tumor suppressor. The latter finding is of particular interest, as results presented herein identify RB1 as a direct target of miR-26a. Hence, it is conceivable that RB1 activity is regulated by CTDSPL and miR-26a in a negative feedback loop. An involvement of CTDSP family members in adipocyte differentiation has not been described to date, but would be interesting to investigate. Indeed, regulation of the same biological biological process by a miRNA and its host gene has already been discovered, e.g. for miR-33, which regulates cholesterol efflux and is intronic to the sterol-regulatory element binding factor-2 (SREBF-2), which itself is a transcriptional regulator of genes involved in cholesterol synthesis (Rayner et al., 2010; Najafi-Shoushtari et al., 2010). In addition to miR-26a and miR-26b, an intergenic miRNA with identical seed sequence, miR-1297, has recently been identified in human ESC (Morin et al., 2008), and has subsequently been found in non-human primates. So far, a mouse homolog has not been detected. At present, we cannot rule out that miR-1297 is also expressed and active during adipocyte differentiation of hMADS cells. Custom-designed primers for miRNA qRT-PCR should be able to check for the presence of this primate-specific miRNA without running into danger of amplifying miR-26a or miR-26b.

Expression of miR-26a and miR-26b has been detected in various tissues (Lagos-Quintana et al., 2002; Coutinho et al., 2007; Xie et al., 2011). Thus, the involvement in many biological processes, apart from white and brown adipogenesis, can be anticipated. Indeed, a link

for miR-26a and certain types of cancer has been firmly established; however, the miRNA action, i.e. as tumor suppressor or "oncomiR", depends on the cell/tissue type. For instance, the miR-26a-2 gene is frequently amplified in glioma, and overexpression of miR-26a promotes *de novo* tumor formation, probably via direct targeting of the tumor suppressor phosphatase and tensin homolog (PTEN) (Huse et al., 2009). Similar results have been obtained for glioblastoma (Kim et al., 2010a). Furthermore, increased miR-26a expression was found associated with poor outcome in acute myeloid leukemia (AML) patients (Wang et al., 2010). On the other hand, a role for miR-26a as tumor suppressor in lymphomas has been established by several studies: miR-26a was shown to be decreased in mantle cell lymphoma (Di Lisio et al., 2010) and avian lymphomas (Xu et al., 2010), to be downregulated by MYC oncogene, and to target the enhancer of zeste homolog 2 (EZH2) oncogene (Sander et al., 2009; Sander et al., 2008), which might be a crucial interaction in this context. Further roles for miR-26a as tumor suppressor have been identified in breast cancer (Maillot et al., 2009; Zhang et al., 2011) and HCC, where patients with low miR-26a levels in tumor tissue had a shorter overall survival (Ji et al., 2009a). Importantly, overexpression of miR-26a in liver (using an adeno-associated virus) inhibited tumor growth in a murine HCC model, highlighting the therapeutic potential of miRNA overexpression (Kota et al., 2009).

In addition to the herein presented role of miR-26a in adipogenesis, this miRNA has also been found to regulate differentiation towards the myogenic lineage. Kang et al. measured a pronounced upregulation of miR-26a during myogenic differentiation of C2C12 cells (Kang et al., 2011), and Wong and Tellam demonstrated that miR-26a overexpression promoted myogenesis *in vitro* (Wong and Tellam, 2008). Again, EZH2 was identified as a meaningful direct miR-26a target in the particular context, due to its already established negative influence on myogenesis (Caretti et al., 2004). The pro-myogenic effect of miR-26a is also interesting with respect to our results, as a close developmental relationship between muscle and BAT has been described in mouse (Seale et al., 2008; Kajimura et al., 2009). Indeed, muscle marker genes, e.g. myogenin or miR-206, have recently been proposed as markers of "genuine" brown adipocytes, but to be absent in brite adipocytes (Petrovic et al., 2010). Thus, it will be of interest to analyze whether miR-26a induces these genes during adipogenesis of hMADS cells in order to categorize the derived adipocytes as brown or brite.

Mechanistically, the question for transcription factors that influence miR-26a expression constitutes an important issue that has not been addressed in this study. The immediate induction of miR-26a in mouse WAT by β_3 -adrenergic stimulation (Fig. 21B) suggests a mechanism involving CREB; however, neither complementing *in vitro* experiments with hMADS cells, nor a bioinformatic analysis to identify putative CREs in vicinity to the miR-26a genes have not been performed to date. With respect to key regulators of adipogenesis, an induction by PPAR γ appears unlikely (Fig. 17); however, a recent study on human airway smooth muscle cells found that C/EBP α activates miR-26a by binding to the promoter of the miR-26a-1 host gene CTDSPL (Mohamed et al., 2010). A similar mechanism during adipogenesis is thus conceivable.

We also wanted to identify molecular mechanisms by which miR-26a regulates the brown gene expression program. The most obvious way of action would be the targeting of one or more suppressors of brown adipogenesis. A considerable number of such repressors has been identified by various studies on rodents (Hansen and Kristiansen, 2006). We therefore analyzed the 3'UTRs of these genes for predicted miR-26a MREs, using a total of ten target prediction algorithms that utilize distinct aspects of miRNA targeting (e.g. thermodynamic stability of duplex, evolutionary conservation of target site, site context) (Bartel, 2009) to suggest potential direct interactions. Indeed, three interesting putative miR-26a targets were identified: RB1, RIP140, and S6K1 (cf. 1.2.3). For each of these genes, global or fat-specific deletion resulted in an induction of UCP1 and the emergence of multilocular adipocytes in WAT, in line with reduced body weight and body fat content (Leonardsson et al., 2004; Um et al., 2004; Dali-Youcef et al., 2007). Mechanistically, the negative impact on brown adipocyte characteristics has been directly established at least for RB1 and RIP140. RB1 was shown to bind to the PGC1 α promoter and repress transcription (Scimè et al., 2005). PGC1 α , in turn, is a crucial co-activator of PPAR γ at the PPRE located in the UCP1 enhancer region (Puigserver et al., 1998; Cannon and Nedergaard, 2004), and furthermore a promoter of mitochondrial biogenesis and oxidative metabolism (Lin et al., 2005). For RIP140, repression of UCP1 transcription via binding to the UCP1 enhancer and promoter regions was demonstrated (Christian et al., 2005), which might also involve direct interaction with PGC1 α (Hallberg et al., 2008). For S6K1, however, the mechanisms leading to upregulation of UCP1 and other brown markers are less clear. S6K1 is a protein kinase which is activated by mammalian target of rapamycin (mTOR), and as such part of a network that mediates cellular responses to changes in energy state (Soliman, 2005). Among other stimuli like glucose, amino acids, or AMP, mTOR is activated by insulin signaling. This leads to activation (phosphorylation) of S6K1, which then phosphorylates insulin receptor substrate 1 (IRS1) at certain serine residues, ultimately leading to IRS1 degradation (Um et al., 2006). Thus, S6K1 acts as a negative feedback loop in insulin signaling, and in line with this, S6K1^{-/-} mice display enhanced insulin sensitivity (Um et al., 2004). Interestingly, brown preadipocytes obtained from IRS1^{-/-} mice exhibited impaired adipocyte differentiation and attenuated UCP1 expression *in vitro* (Fasshauer et al., 2001), implying a crucial role of IRS1 for establishment of brown adipocyte characteristics. Thus, the effects of S6K1 may be explained, at least partly, because of its action on IRS1.

Collectively, to the best of our knowledge, the function of RB1, RIP140, and S6K1 in adipogenesis has been investigated only in rodent studies. However, as orthologs exist in human, and as evolutionarily conserved miR-26a MREs were predicted by multiple algorithms (Fig. 22A), we decided to investigate these genes as potential mediators of the miR-26a effect. First, we demonstrated for all three genes that transcript variants containing the predicted MREs are expressed during adipocyte differentiation of hMADS cells (Fig. 22B). This is a necessary prerequisite for a potential direct miRNA-target interaction (Kuhn et al., 2008). Second, we found decreased mRNA levels of RB1, RIP140, and S6K1 upon miR-26a overexpression (Fig. 22B). Likewise, mRNA levels were significantly increased upon inhibition

of miR-26a (Fig. 22B). Third, we also observed inverse expression of miR-26a and the three predicted direct targets *in vivo*, as prolonged cold exposure of mice resulted in decreased mRNA levels of RB1, RIP140, and S6K1 in WAT (Fig. 22C). It could thus be concluded that miR-26a has a negative effect on the three genes, although the mechanism could still be either direct or indirect. We therefore performed luciferase reporter assays and could finally validate that miR-26a directly interacts with the 3'UTRs of RB1, NRIP1, and S6K1, in each case via a single evolutionarily conserved MRE (Fig. 23).

To further investigate whether the action of miR-26a might be mediated by any of the newly identified direct targets, we decided to silence RB1, RIP140, and S6K1 during adipocyte differentiation of hMADS cells. Indeed, knockdown of RIP140 recapitulated the miR-26a-induced upregulation of UCP1 mRNA and protein (Fig. 24). However, knockdown of RB1 and S6K1 resulted in slightly diminished UCP1 levels (Fig. 24). This finding is of particular interest with respect to RB1, as MEFs derived from *Rb1*^{-/-} mice acquired a brown gene expression signature during adipocyte differentiation (Hansen et al., 2004). Hence, it can be hypothesized that this mechanism is specific to mouse and not existent in human. Alternatively, diminished yet not abolished RB1 expression (via transfection of siRNAs) might evoke other cellular responses than the complete absence of the gene (via gene targeting). The crucial negative influence of RIP140 on UCP1 expression was further revealed by double knockdown studies: Either simultaneous silencing of RIP140 and RB1, or simultaneous silencing of RIP140 and S6K1, resulted in upregulation of UCP1 mRNA (Fig. 24). Finally, simultaneous silencing of all three validated miR-26a targets also resulted in upregulation of UCP1 mRNA and protein (Fig. 24). However, neither a certain double knockdown, nor the triple knockdown was more efficient in promoting UCP1 expression than the single knockdown of RIP140. It is thus proposed that miR-26a operates via RIP140 to increase UCP1. However, it is fair to say that this way of action is likely complemented by other mechanisms which have remained undiscovered so far. The further analysis of predicted direct miR-26a targets is therefore in demand. In addition, unconventional ways of action are conceivable as well, e.g. a stimulatory action of miR-26a on promoters with partially complementary DNA sequences (as described for miR-373 and E-cadherin (Place et al., 2008)), or a positive stimulation of miR-26a on mRNA translation, as described for miR-369-3 and TNF α (Vasudevan et al., 2007). A thorough bioinformatic screening of mRNA, but also genomic sequences with partial complementarity to miR-26a could therefore serve as starting point for future experiments by which the mechanism of miR-26a in adipocyte differentiation can be further dissected.

UCP1 is the indispensable gene for adaptive, non-shivering thermogenesis in brown adipocytes (Nedergaard et al., 2001), endowing these cells with an exceptionally high metabolic capacity that is of therapeutic interest as a means to fight obesity and its associated comorbidities (Nedergaard and Cannon, 2010). As such, the ability of miR-26a to promote UCP1 expression during human adipocyte differentiation is a necessary, but not sufficient criterion for an elevated thermogenic capability. We therefore decided to directly assess the

effect of miR-26a overexpression on metabolic activity of adipocytes by measurements of cellular oxygen consumption. Strikingly, miR-26a evoked a 40% increase of basal respiration (Fig. 25A), and analysis of uncoupled respiration confirmed that this increase is at least partially due to increased UCP1 levels (Fig. 25B). Thus, we propose that miR-26a promotes a brown adipocyte gene expression program during human adipogenesis, which ultimately results in an elevated oxidative capacity.

Collectively, our study on miR-26a suggests a potential utilization of this miRNA to promote weight loss *in vivo*, although this necessitates further experimental proof. Beside the induction of brown adipocyte characteristics by miR-26a during differentiation, preliminary experiments suggested that transfection of terminally differentiated white adipocytes with miR-26a can at least modestly induce UCP1 (data not shown). Indeed, direct conversion of pre-existing white adipocytes into energy-dissipating, UCP1⁺ adipocytes is of outstanding therapeutic interest. In this respect, direct injection of (pre-)miR-26a, complexed e.g. in liposomes to prevent degradation and facilitate cellular uptake (Mufamadi et al., 2011), into white fat pads of mice constitutes an interesting experimental setup. Alternatively, the generation of a transgenic mouse overexpressing miR-26a selectively in adipose tissue could be helpful for evaluating the potential of this miRNA as a "fat burner". However, although miR-26a is perfectly conserved between mouse and human, the appropriateness of such mouse experiments as models for the human situation is not self-evident. First, promotion of a brown gene expression program by miR-26a during adipocyte differentiation of mouse *in vitro* systems has not been shown to date. Therefore, trying to recapitulate results obtained with hMADS cells and hPASC in mouse, using e.g. primary preadipocytes from mouse WAT and BAT, would be important experiments to assess the comparability between these two organisms. Second, a recent study compared WAT and BAT samples from human and mouse and found only two genes that were congruently upregulated in BAT for both organisms, one of them being the "positiv control gene" UCP1 (Svensson et al., 2011). Thus, probably the molecular mechanisms that favour the development of a brown over a white phenotype are considerably different within mammalian species. If so, the aptness of preclinical animal studies (including transgenic mice) may be questionable. To test whether miR-26a is also necessary for establishment of functional BAT *in vivo*, the generation of mice with fat-specific miR-26a deficiency is in demand. However, as described above for miR-27b and miR-30c (cf. 5.2.1 and 5.2.2), considerable technical challenges exist due to the intronic location, the miRNA copy number, and potential compensatory action by other family members. Again, fat-specific expression of a miRNA sponge constitutes a more convenient method that could also provide insights into the physiological function of miR-26a.

Abbreviations

AA	arachidonic acid
AC	adenylyl cyclase
AF	adipocyte fraction
ADP	adenosine diphosphate
ATG	angiotensinogen
Ago	Argonaute
ALK2	activin A receptor, type I
AML	acute myeloid leukemia
APC	adenomatous polyposis coli
ASO	antisense oligonucleotide
ATGL	adipose triglyceride lipase
ATP	adenosine triphosphate
BAT	brown adipose tissue
BM	bone marrow
BMI	body mass index
BMP	bone morphogenetic protein
BSA	bovine serum albumin
CAT	chloramphenicol acetyltransferase
C/EBP	CCAAT-enhancer binding protein
cAMP	cyclic adenosine monophosphate
CDS	coding sequence

Cel	Caenorhabditis elegans
CHOP10	C/EBP-homologous protein 10
CIDEA	cell death-inducing DFFA-like effector a
CL	CL-316243
CLL	chronic lymphocytic leukemia
CNS	central nervous system
COL6A2	collagen, type VI, α 2
COX	cyclooxygenase
CREB	cAMP response element binding protein
CPT1 β	carnitine palmitoyl transferase 1 β
CTDSP1	CTD (carboxy-terminal domain, RNA polymerase II, polypeptide A) small phosphatase 1
CTDSP2	CTD (carboxy-terminal domain, RNA polymerase II, polypeptide A) small phosphatase 2
CTDSPL	CTD (carboxy-terminal domain, RNA polymerase II, polypeptide A) small phosphatase-like
DEPC	Diethylpyrocarbonate
Dex	Dexamethasone
DGCR8	DiGeorge syndrome critical region gene 8
Dme	Drosophila melanogaster
DMEM	Dulbecco's Modified Eagle Medium
DMSO	dimethylsulfoxide
dsRNA	double-stranded RNA
ECL	enhanced chemiluminescence
ELISA	enzyme-linked immunosorbent assay
En1	Engrailed 1
EOD	European Obesity Day
ERK	extracellular signal-regulated kinase
ESC	embryonic stem cells

ETC	electron transport chain
EZH2	enhancer of zeste homolog 2
FA	fatty acids
FADH2	Flavine adenine dinucleotide
FABP4	fatty acid binding protein 4
FASN	fatty acid synthase
FBS	fetal bovine serum
FCS	fetal calf serum
FDA	Food and Drug Administration
FL	firefly luciferase
FOP	fibrodysplasia ossificans progressiva
GAPDH	glyceraldehyde-3-phosphate dehydrogenase
GFP	green fluorescent protein
GH	growth hormone
GLP-1	glucagon-like peptide-1
GLUT4	glucose transporter 4
GPDH	glycerol-3-phosphate dehydrogenase
HCC	hepatocellular carcinoma
HEK293 cells	human embryonic kidney 293 cells
HFD	high fat diet
hFGF2	human Fibroblast Growth Factor 2
hMADS cells	human multipotent adipose-derived stem cells
hPASC	human primary adipose-derived stromal cells
HCV	Hepatitis C virus
HDL	high density lipoprotein
HSL	hormone sensitive lipase
HSC	hematopoietic stem cell
IBMX	1-methyl-3-isobutylxanthine

ICD-10	International Statistical Classification of Diseases and Related Health Problems 10th revision
IGF-1	insulin-like growth factor 1
IP-R	prostacyclin receptor
IRS1	insulin receptor substrate 1
KLF4	Kruppel-like factor 4
LA	linoleic acid
LB	Luria-Bertani
LCD	low-calorie diet
LEP	Leptin
LIF	leukemia inhibitory factor
LNA	locked nucleic acid
LPL	lipoprotein lipase
MAPK	Mitogen-activated protein kinase
MEF	mouse embryonic fibroblast
MetS	Metabolic Syndrome
miRISC	miRNA-induced silencing complex
miRNAs	microRNAs
MC4R	Melanocortin receptor 4
MCS	multiple cloning site
MRE	miRNA recognition element
MSC	mesenchymal stem cells
mTOR	mammalian target of rapamycin
Myf5	Myogenic factor 5
NADH	Nicotinamide adenine dinucleotide
ncRNA	non-coding RNA
NE	norepinephrine
NFYC	nuclear transcription factor Y, γ

NTC	non-targeting control
ORFs	open reading frames
PAGE	Polyacrylamid Gel Electrophoresis
PAI-1	Plasminogen activator inhibitor-1
Pax3	paired box gene 3
PBS	phosphate buffered saline
PCR	polymerase chain reaction
PEB	protein extraction buffer
PET/CT	positron-emission tomography and computer tomography
PGC-1 α	PPAR γ coactivator 1 α
PGF _{2α}	prostaglandin F _{2α}
PGH ₂	prostaglandin H ₂
PGL ₂	prostacyclin
PKA	protein kinase A
PIGF	placenta growth factor
POMC	Proopiomelanocortin
PPAR γ	peroxisome proliferator-activated receptor γ
PPRE	PPAR response element
PRDM16	PR domain containing 16
pre-miRNA	precursor miRNA
pri-miRNAs	primary miRNAs
PTEN	phosphatase and tensin homolog
PTGS	post-transcriptional gene silencing
RAAS	renin-angiotensin-aldosterone system
RB1	retinoblastoma
RIP140	Nuclear receptor interacting protein 1
RISC	RNA-induced silencing complex
RL	renilla luciferase

RMR	resting metabolic rate
RNAi	RNA interference
ROS	reactive oxygen species
RQ	respiratory quotient
RXR α	retinoid X receptor α
S6K1	ribosomal protein S6 kinase
SDS	sodium dodecyl sulfate
SEM	standard error of the mean
siRNAs	small interfering RNAs
SM	skeletal muscle
SMAD1	SMAD family member 1
SNS	sympathetic nervous system
Sox10	Sex determining region Y-box 10
SREBF-2	sterol-regulatory element-binding factor-2
SREBP1c	sterol regulatory element binding transcription factor 1
SSC	saline sodium citrate
SVF	stromal vascular fraction
T3	triiodothyronine
TG	triglycerides
T _m	melting temperature
TNF α	Tumor necrosis factor- α
TRBP	TAR (HIV) RNA-binding protein 2
TSS	transcription start site
TZD	thiazolidinedione
UCP1	Uncoupling protein 1
u-PA	urokinase-type plasminogen activator
u-PAR	urokinase plasminogen activator receptor
3'UTR	3'-untranslated region

VLCD	very low calorie diet
VN	vitronectin
WAT	white adipose tissue
WHR	waist-to-hip ratio
WHO	World Health Organization
wt	wild type

Bibliography

- Agrawal, R., Tran, U. and Wessely, O. (2009). The miR-30 miRNA family regulates *Xenopus* pronephros development and targets the transcription factor *Xlim1/Lhx1*. *Development* *136*, 3927–3936.
- Agurs-Collins, T. and Bouchard, C. (2008). Gene-nutrition and gene-physical activity interactions in the etiology of obesity. Introduction. *Obesity (Silver Spring)* *16 Suppl 3*, 2–4.
- Ahima, R. S. and Flier, J. S. (2000). Adipose tissue as an endocrine organ. *Trends Endocrinol Metab* *11*, 327–332.
- Ahn, J., Lee, H., Kim, S. and Ha, T. (2007). Resveratrol inhibits TNF-alpha-induced changes of adipokines in 3T3-L1 adipocytes. *Biochem Biophys Res Commun* *364*, 972–977.
- Ailhaud, G., Dani, C., Amri, E. Z., Djian, P., Vannier, C., Doglio, A., Forest, C., Gaillard, D., Négre, R. and Grimaldi, P. (1989). Coupling growth arrest and adipocyte differentiation. *Environ Health Perspect* *80*, 17–23.
- Ailhaud, G., Grimaldi, P. and Negrel, R. (1992). Cellular and molecular aspects of adipose tissue development. *Annu Rev Nutr* *12*, 207–233.
- Ailhaud, G. and Guesnet, P. (2004). Fatty acid composition of fats is an early determinant of childhood obesity: a short review and an opinion. *Obes Rev* *5*, 21–26.
- Alberts, B., Johnson, A., Lewis, J., Raff, M., Roberts, K. and Walter, P. (2002a). *Molecular Biology of the Cell* chapter 14. 29 West 35th Street, New York, NY 10001-2299: Garland Science, 4th edition.
- Alberts, B., Johnson, A., Lewis, J., Raff, M., Roberts, K. and Walter, P. (2002b). *Molecular Biology of the Cell*, chapter 1. 29 West 35th Street, New York, NY 10001-2299: Garland Science, 4th edition.
- Alessi, M. and Juhan-Vague, I. (2006). PAI-1 and the metabolic syndrome: links, causes, and consequences. *Arteriosclerosis, Thrombosis, and Vascular Biology* , *26*, 2200–2207.
- Alessi, M. C., Bastelica, D., Morange, P., Berthet, B., Leduc, I., Verdier, M., Geel, O. and Juhan-Vague, I. (2000). Plasminogen activator inhibitor 1, transforming growth factor-beta1, and BMI are closely associated in human adipose tissue during morbid obesity. *Diabetes* , *49*, 1374–1380.
- Allen, D. L. and Loh, A. S. (2011). Posttranscriptional mechanisms involving microRNA-27a and b contribute to fast-specific and glucocorticoid-mediated myostatin expression in skeletal muscle. *Am J Physiol Cell Physiol* , *300*, 124–137.
- Amri, E. Z., Ailhaud, G. and Grimaldi, P. A. (1994). Fatty acids as signal transducing molecules: involvement in the differentiation of preadipose to adipose cells. *J Lipid Res* , *35*, 930–937.
- Amri, E. Z., Dani, C., Doglio, A., Etienne, J., Grimaldi, P. and Ailhaud, G. (1986). Adipose cell differentiation: evidence for a two-step process in the polyamine-dependent Ob1754 clonal line. *Biochem J* , *238*, 115–122.
- Ansorge, W. J. (2009). Next-generation DNA sequencing techniques. *N Biotechnol* , *25*, 195–203.
- Arita, Y., Kihara, S., Ouchi, N., Takahashi, M., Maeda, K., Miyagawa, J., Hotta, K., Shimomura, I., Nakamura, T., Miyaoaka, K., Kuriyama, H., Nishida, M., Yamashita, S., Okubo, K., Matsubara, K., Muraguchi, M., Ohmoto, Y., Funahashi, T. and Matsuzawa, Y. (1999). Paradoxical decrease of an adipose-specific protein, adiponectin, in obesity. *Biochem Biophys Res Commun* , *257*, 79–83.
- Armani, A., Mammi, C., Marzolla, V., Calanchini, M., Antelmi, A., Rosano, G. M., Fabbri, A. and Caprio, M. (2010). Cellular models for understanding adipogenesis, adipose dysfunction, and obesity. *J Cell Biochem* , *110*, 564–572.

- Atit, R., Sgaier, S. K., Mohamed, O. A., Taketo, M. M., Dufort, D., Joyner, A. L., Niswander, L. and Conlon, R. A. (2006). Beta-catenin activation is necessary and sufficient to specify the dorsal dermal fate in the mouse. *Dev Biol* , 296, 164–176.
- Atkinson, R. L., Dietz, W. H., P, F. J., J, G. N., Hill, J. O., J, H., Pi-Sunyer, F. X., L, W. R. and R, W. (1993). Very low-calorie diets. National Task Force on the Prevention and Treatment of Obesity, National Institutes of Health. *JAMA* , 270, 967–974.
- Aubert, J., Dessolin, S., Belmonte, N., Li, M., McKenzie, F. R., Staccini, L., Villageois, P., Barhanin, B., Vernallis, A., Smith, A. G., Ailhaud, G. and Dani, C. (1999). Leukemia inhibitory factor and its receptor promote adipocyte differentiation via the mitogen-activated protein kinase cascade. *J Biol Chem* , 274, 24965–24972.
- Baek, D., Villén, J., Shin, C., Camargo, F. D., Gygi, S. P. and Bartel, D. P. (2008). The impact of microRNAs on protein output. *Nature* , 455, 64–71.
- Barad, O., Meiri, E., Avniel, A., Aharonov, R., Barzilai, A., Bentwich, I., Einav, U., Gilad, S., Hurban, P., Karov, Y., Lobenhofer, E. K., Sharon, E., Shibolet, Y. M., Shtutman, M., Bentwich, Z. and Einat, P. (2004). MicroRNA expression detected by oligonucleotide microarrays: system establishment and expression profiling in human tissues. *Genome Res* , 14, 2486–2494.
- Barak, Y., Nelson, M. C., Ong, E. S., Jones, Y. Z., Ruiz-Lozano, P., Chien, K. R., Koder, A. and Evans, R. M. (1999). PPAR gamma is required for placental, cardiac, and adipose tissue development. *Mol Cell* , 4, 585–595.
- Barbatelli, G., Murano, I., Madsen, L., Hao, Q., Jimenez, M., Kristiansen, K., Giacobino, J. P., De Matteis, R. and Cinti, S. (2010). The emergence of cold-induced brown adipocytes in mouse white fat depots is determined predominantly by white to brown adipocyte transdifferentiation. *Am J Physiol Endocrinol Metab* , 298, 1244–1253.
- Barbera, M. J., Schluter, A., Pedraza, N., Iglesias, R., Villarroya, F. and Giralt, M. (2001). Peroxisome proliferator-activated receptor alpha activates transcription of the brown fat uncoupling protein-1 gene. A link between regulation of the thermogenic and lipid oxidation pathways in the brown fat cell. *J Biol Chem* , 276, 1486–1493.
- Barnett, A. H. (2009). New treatments in type 2 diabetes: a focus on the incretin-based therapies. *Clin Endocrinol (Oxf)* , 70, 343–353.
- Bartel, D. P. (2009). MicroRNAs: target recognition and regulatory functions. *Cell* , 136, 215–233.
- Bastelica, D., Morange, P., Berthet, B., Borghi, H., Lacroix, O., Grino, M., Juhan-Vague, I. and Alessi, M. C. (2002). Stromal cells are the main plasminogen activator inhibitor-1-producing cells in human fat: evidence of differences between visceral and subcutaneous deposits. *Arterioscler Thromb Vasc Biol* , 22, 173–178.
- Belmonte, N., Phillips, B. W., Massiera, F., Villageois, P., Wdziekonski, B., Saint-Marc, P., Nichols, J., Aubert, J., Saeki, K., Yuo, A., Narumiya, S., Ailhaud, G. and Dani, C. (2001). Activation of extracellular signal-regulated kinases and CREB/ATF-1 mediate the expression of CCAAT/enhancer binding proteins beta and -delta in preadipocytes. *Mol Endocrinol* , 15, 2037–2049.
- Benes, V. and Castoldi, M. (2010). Expression profiling of microRNA using real-time quantitative PCR, how to use it and what is available. *Methods* , 50, 244–249.
- Berg, J. M., Tymoczko, J. L. and Stryer, L. (2002). *Biochemistry*, chapter 30. New York: W H Freeman, 5th edition.
- Bernlohr, D. A., Bolanowski, M. A., Kelly, T. J. and Lane, M. D. (1985). Evidence for an increase in transcription of specific mRNAs during differentiation of 3T3-L1 preadipocytes. *J Biol Chem* , 260, 5563–5567.
- Berster, J. M. and Göke, B. (2008). Type 2 diabetes mellitus as risk factor for colorectal cancer. *Arch Physiol Biochem* , 114, 84–98.
- Betel, D., Wilson, M., Gabow, A., Marks, D. S. and Sander, C. (2008). The microRNA.org resource: targets and expression. *Nucleic Acids Research* , 36, D149–153.
- Bezaire, V., Mairal, A., Ribet, C., Lefort, C., Grousse, A., Jocken, J., Laurencikiene, J., Anesia, R., Rodriguez, A. M., Ryden, M., Stenson, B. M., Dani, C., Ailhaud, G., Arner, P. and Langin, D. (2009). Contribution of adipose triglyceride lipase and hormone-sensitive lipase to lipolysis in hMADS adipocytes. *J Biol Chem* , 284, 18282–18291.
- Billon, N., Iannarelli, P., Monteiro, M. C., Glavieux-Pardanaud, C., Richardson, W. D., Kessar, N., Dani, C. and Dupin, E. (2007). The generation of adipocytes by the neural crest. *Development* , 134, 2283–2292.

- Birkenmeier, E. H., Gwynn, B., Howard, S., Jerry, J., Gordon, J. I., Landschulz, W. H. and McKnight, S. L. (1989). Tissue-specific expression, developmental regulation, and genetic mapping of the gene encoding CCAAT/enhancer binding protein. *Genes Dev* , 3, 1146–1156.
- Bonnet, F. and Rocour-Brumioul, D. (1981). Fat cells in leanness, growth retardation, and adipose tissue dystrophic syndromes. In: *Adipose Tissue in Childhood*, pp. 155–63. Boca Raton, FL: CRC Press.
- Borchert, G. M., Lanier, W. and Davidson, B. L. (2006). RNA polymerase III transcribes human microRNAs. *Nat Struct Mol Biol* , 13, 1097–1101.
- Bostjancic, E., Zidar, N., Stajer, D. and Glavac, D. (2010). MicroRNAs miR-1, miR-133a, miR-133b and miR-208 are dysregulated in human myocardial infarction. *Cardiology* , 115, 163–169.
- Bouchard, C., Tremblay, A., Després, J. P., Nadeau, A., Lupien, P. J., Thériault, G., Dussault, J., Moorjani, S., Pinault, S. and Fournier, G. (1990). The response to long-term overfeeding in identical twins. *N Engl J Med* , 322, 1477–1482.
- Braun, J., Hoang-Vu, C., Dralle, H. and Hüttelmaier, S. (2010). Downregulation of microRNAs directs the EMT and invasive potential of anaplastic thyroid carcinomas. *Oncogene* , 29, 4237–4244.
- Bronnikov, G., Houstěk, J. and Nedergaard, J. (1992). Beta-adrenergic, cAMP-mediated stimulation of proliferation of brown fat cells in primary culture. Mediation via beta 1 but not via beta 3 adrenoceptors. *J Biol Chem* , 267, 2006–2013.
- Bronstein, I., Fortin, J., Stanley, P. E., Stewart, G. S. and Kricka, L. J. (1994). Chemiluminescent and bioluminescent reporter gene assays. *Anal Biochem* , 219, 169–181.
- Brown, K. A., McInnes, K. J., Hunger, N. I., Oakhill, J. S., Steinberg, G. R. and Simpson, E. R. (2009). Subcellular localization of cyclic AMP-responsive element binding protein-regulated transcription coactivator 2 provides a link between obesity and breast cancer in postmenopausal women. *Cancer Res* , 69, 5392–5399.
- Brug, J. (2007). The European charter for counteracting obesity: a late but important step towards action. Observations on the WHO-Europe ministerial conference, Istanbul, November 15-17, 2006. *Int J Behav Nutr Phys Act* , 4, 11–11.
- Buchwald, H., Avidor, Y., Braunwald, E., Jensen, M. D., Pories, W., Fahrbach, K. and Schoelles, K. (2004). Bariatric surgery: a systematic review and meta-analysis. *JAMA* , 292, 1724–1737.
- Buchwald, H., Estok, R., Fahrbach, K., Banel, D., Jensen, M. D., Pories, W. J., Bantle, J. P. and Sledge, I. (2009). Weight and type 2 diabetes after bariatric surgery: systematic review and meta-analysis. *Am J Med* , 122, 248–256.
- Budhu, A., Jia, H. L., Forgues, M., Liu, C. G., Goldstein, D., Lam, A., Zanetti, K. A., Ye, Q. H., Qin, L. X., Croce, C. M., Tang, Z. Y. and Wang, X. W. (2008). Identification of metastasis-related microRNAs in hepatocellular carcinoma. *Hepatology* , 47, 897–907.
- Bult, M. J., van Dalen, T. and Muller, A. F. (2008). Surgical treatment of obesity. *Eur J Endocrinol* , 158, 135–145.
- Busacca, S., Germano, S., De Cecco, L., Rinaldi, M., Comoglio, F., Favero, F., Murer, B., Mutti, L., Pierotti, M. and Gaudino, G. (2010). MicroRNA signature of malignant mesothelioma with potential diagnostic and prognostic implications. *Am J Respir Cell Mol Biol* , 42, 312–319.
- Cai, X., Hagedorn, C. H. and Cullen, B. R. (2004). Human microRNAs are processed from capped, polyadenylated transcripts that can also function as mRNAs. *RNA* , 10, 1957–1966.
- Cali, J. J., Niles, A., Valley, M. P., O'Brien, M. A., Riss, T. L. and Shultz, J. (2008). Bioluminescent assays for ADMET. *Expert Opin Drug Metab Toxicol* , 4, 103–120.
- Calin, G. A., Dumitru, C. D., Shimizu, M., Bichi, R., Zupo, S., Noch, E., Aldler, H., Rattan, S., Keating, M., Rai, K., Rassenti, L., Kipps, T., Negrini, M., Bullrich, F. and Croce, C. M. (2002). Frequent deletions and down-regulation of micro- RNA genes miR15 and miR16 at 13q14 in chronic lymphocytic leukemia. *Proc Natl Acad Sci U S A* , 99, 15524–15529.
- Calin, G. A., Ferracin, M., Cimmino, A., Di Leva, G., Shimizu, M., Wojcik, S. E., Iorio, M. V., Visone, R., Sever, N. I., Fabbri, M., Iuliano, R., Palumbo, T., Pichiorri, F., Roldo, C., Garzon, R., Sevignani, C., Rassenti, L., Alder, H., Volinia, S., Liu, C. G., Kipps, T. J., Negrini, M. and Croce, C. M. (2005). A MicroRNA signature associated with prognosis and progression in chronic lymphocytic leukemia. *N Engl J Med* , 353, 1793–1801.

- Calle, E. E., Rodriguez, C., Walker-Thurmond, K. and Thun, M. J. (2003). Overweight, obesity, and mortality from cancer in a prospectively studied cohort of U.S. adults. *N Engl J Med* , *348*, 1625–1638.
- Cancello, R., Zingaretti, M. C., Sarzani, R., Ricquier, D. and Cinti, S. (1998). Leptin and UCP1 genes are reciprocally regulated in brown adipose tissue. *Endocrinology* , *139*, 4747–4750.
- Cannon, B. and Nedergaard, J. (2004). Brown adipose tissue: function and physiological significance. *Physiological Reviews* , *84*, 277–359.
- Cannon, B. and Nedergaard, J. (2008). Studies of thermogenesis and mitochondrial function in adipose tissues. *Methods Mol Biol* , *456*, 109–121.
- Cannon, B. and Nedergaard, J. (2010). Metabolic consequences of the presence or absence of the thermogenic capacity of brown adipose tissue in mice (and probably in humans). *Int J Obes (Lond)* , *34 Suppl 1*, 7–16.
- Cao, Z., Umek, R. M. and McKnight, S. L. (1991). Regulated expression of three C/EBP isoforms during adipose conversion of 3T3-L1 cells. *Genes Dev* , *5*, 1538–1552.
- Carè, A., Catalucci, D., Felicetti, F., Bonci, D., Addario, A., Gallo, P., Bang, M. L., Segnalini, P., Gu, Y., Dalton, N. D., Elia, L., Latronico, M. V., Hoydal, M., Autore, C., Russo, M. A., Dorn, G. W., Ellingsen, O., Ruiz-Lozano, P., Peterson, K. L., Croce, C. M., Peschle, C. and Condorelli, G. (2007). MicroRNA-133 controls cardiac hypertrophy. *Nat Med* , *13*, 613–618.
- Caretti, G., Di Padova, M., Micales, B., Lyons, G. E. and Sartorelli, V. (2004). The Polycomb Ezh2 methyltransferase regulates muscle gene expression and skeletal muscle differentiation. *Genes Dev* , *18*, 2627–2638.
- Carmona, M. C., Louche, K., Lefebvre, B., Pilon, A., Hennuyer, N., Audinot-Bouchez, V., Fievet, C., Torpier, G., Formstecher, P., Renard, P., Lefebvre, P., Dacquet, C., Staels, B., Casteilla, L., Pénicaud, L. and Consortium of the French Ministry of Research and Technology (2007). S 26948: a new specific peroxisome proliferator activated receptor gamma modulator with potent antidiabetes and antiatherogenic effects. *Diabetes* , *56*, 2797–2808.
- Casimir, D. A., Miller, C. W. and Ntambi, J. M. (1996). Preadipocyte differentiation blocked by prostaglandin stimulation of prostanoid FP2 receptor in murine 3T3-L1 cells. *Differentiation* , *60*, 203–210.
- Casteilla, L., Nougès, J., Reyne, Y. and Ricquier, D. (1991). Differentiation of ovine brown adipocyte precursor cells in a chemically defined serum-free medium. Importance of glucocorticoids and age of animals. *Eur J Biochem* , *198*, 195–199.
- Castoldi, M., Schmidt, S., Benes, V., Hentze, M. W. and Muckenthaler, M. U. (2008). miChip: an array-based method for microRNA expression profiling using locked nucleic acid capture probes. *Nat Protoc* , *3*, 321–329.
- Castoldi, M., Schmidt, S., Benes, V., Noerholm, M., Kulozik, A. E., Hentze, M. W. and Muckenthaler, M. U. (2006). A sensitive array for microRNA expression profiling (miChip) based on locked nucleic acids (LNA). *RNA* , *12*, 913–920.
- Caulfield, M., Lavender, P., Newell-Price, J., Kamdar, S., Farrall, M. and Clark, A. J. (1996). Angiotensinogen in human essential hypertension. *Hypertension* , *28*, 1123–1125.
- Cawthorn, W. P. and Sethi, J. K. (2008). TNF-alpha and adipocyte biology. *FEBS Lett* , *582*, 117–131.
- Cederberg, A., Gronning, L. M., Ahrén, B., Taskén, K., Carlsson, P. and Enerbäck, S. (2001). FOXC2 is a winged helix gene that counteracts obesity, hypertriglyceridemia, and diet-induced insulin resistance. *Cell* , *106*, 563–573.
- Champigny, O., Holloway, B. R. and Ricquier, D. (1992). Regulation of UCP gene expression in brown adipocytes differentiated in primary culture. Effects of a new beta-adrenoceptor agonist. *Mol Cell Endocrinol* , *86*, 73–82.
- Chandran, M., Phillips, S. A., Ciaraldi, T. and Henry, R. R. (2003). Adiponectin: more than just another fat cell hormone? *Diabetes Care* , *26*, 2442–2450.
- Chen, H., Charlat, O., Tartaglia, L. A., Woolf, E. A., Weng, X., Ellis, S. J., Lakey, N. D., Culpepper, J., Moore, K. J., Breitbart, R. E., Duyk, G. M., Tepper, R. I. and Morgenstern, J. P. (1996a). Evidence that the diabetes gene encodes the leptin receptor: identification of a mutation in the leptin receptor gene in db/db mice. *Cell* , *84*, 491–495.
- Chen, P. L., Riley, D. J., Chen, Y. and Lee, W. H. (1996b). Retinoblastoma protein positively regulates terminal adipocyte differentiation through direct interaction with C/EBPs. *Genes Dev* , *10*, 2794–2804.

- Chen, X., Ba, Y., Ma, L., Cai, X., Yin, Y., Wang, K., Guo, J., Zhang, Y., Chen, J., Guo, X., Li, Q., Li, X., Wang, W., Zhang, Y., Wang, J., Jiang, X., Xiang, Y., Xu, C., Zheng, P., Zhang, J., Li, R., Zhang, H., Shang, X., Gong, T., Ning, G., Wang, J., Zen, K., Zhang, J. and Zhang, C. Y. (2008). Characterization of microRNAs in serum: a novel class of biomarkers for diagnosis of cancer and other diseases. *Cell Res* , 18, 997–1006.
- Chen, Y. F., Wu, C. Y., Kao, C. H. and Tsai, T. F. (2010). Longevity and lifespan control in mammals: lessons from the mouse. *Ageing Res Rev* , 9 Suppl 1, 28–35.
- Chiellini, C., Cochet, O., Negroni, L., Samson, M., Poggi, M., Ailhaud, G., Alessi, M., Dani, C. and Amri, E. (2008). Characterization of human mesenchymal stem cell secretome at early steps of adipocyte and osteoblast differentiation. *BMC Molecular Biology* , 9, 26.
- Choi, W. Y., Giraldez, A. J. and Schier, A. F. (2007). Target protectors reveal dampening and balancing of Nodal agonist and antagonist by miR-430. *Science* , 318, 271–274.
- Christian, M., Kiskinis, E., Debevec, D., Leonardsson, G., White, R. and Parker, M. G. (2005). RIP140-targeted repression of gene expression in adipocytes. *Mol Cell Biol* , 25, 9383–9391.
- Christy, R. J., Kaestner, K. H., Geiman, D. E. and Lane, M. D. (1991). CCAAT/enhancer binding protein gene promoter: binding of nuclear factors during differentiation of 3T3-L1 preadipocytes. *Proc Natl Acad Sci U S A* , 88, 2593–2597.
- Christy, R. J., Yang, V. W., Ntambi, J. M., Geiman, D. E., Landschulz, W. H., Friedman, A. D., Nakabeppu, Y., Kelly, T. J. and Lane, M. D. (1989). Differentiation-induced gene expression in 3T3-L1 preadipocytes: CCAAT/enhancer binding protein interacts with and activates the promoters of two adipocyte-specific genes. *Genes Dev* , 3, 1323–1335.
- Cimmino, A., Calin, G. A., Fabbri, M., Iorio, M. V., Ferracin, M., Shimizu, M., Wojcik, S. E., Aqeilan, R. I., Zupo, S., Dono, M., Rassenti, L., Alder, H., Volinia, S., Liu, C. G., Kipps, T. J., Negrini, M. and Croce, C. M. (2005). miR-15 and miR-16 induce apoptosis by targeting BCL2. *Proc Natl Acad Sci U S A* , 102, 13944–13949.
- Cinti, S. (1999). *The Adipose Organ*. Editrice Kurtis, Milan, Italy.
- Cinti, S. (2001). The adipose organ: morphological perspectives of adipose tissues. *Proc Nutr Soc* 60, 319–328.
- Cinti, S. (2005). The adipose organ. *Prostaglandins Leukot Essent Fatty Acids* 73, 9–15.
- Clarke, S. L., Robinson, C. E. and Gimble, J. M. (1997). CAAT/enhancer binding proteins directly modulate transcription from the peroxisome proliferator-activated receptor gamma 2 promoter. *Biochem Biophys Res Commun* 240, 99–103.
- Cleland, W. H., Mendelson, C. R. and Simpson, E. R. (1985). Effects of aging and obesity on aromatase activity of human adipose cells. *J Clin Endocrinol Metab* 60, 174–177.
- Clément, K., Vaisse, C., Lahlou, N., Cabrol, S., Pelloux, V., Cassuto, D., Gormelen, M., Dina, C., Chambaz, J., Lacorte, J. M., Basdevant, A., Bougnères, P., Lebouc, Y., Froguel, P. and Guy-Grand, B. (1998). A mutation in the human leptin receptor gene causes obesity and pituitary dysfunction. *Nature* 392, 398–401.
- Colditz, G. A., Willett, W. C., Rotnitzky, A. and Manson, J. E. (1995). Weight gain as a risk factor for clinical diabetes mellitus in women. *Ann Intern Med* 122, 481–486.
- Coll, A. P., Yeo, G. S., Farooqi, I. S. and O’Rahilly, S. (2008). SnapShot: the hormonal control of food intake. *Cell* 135, 1–2.
- Colman, R. J., Anderson, R. M., Johnson, S. C., Kastman, E. K., Kosmatka, K. J., Beasley, T. M., Allison, D. B., Cruzen, C., Simmons, H. A., Kemnitz, J. W. and Weindruch, R. (2009). Caloric restriction delays disease onset and mortality in rhesus monkeys. *Science* 325, 201–204.
- Combs, T. P., Pajvani, U. B., Berg, A. H., Lin, Y., Jelicks, L. A., Laplante, M., Nawrocki, A. R., Rajala, M. W., Parlow, A. F., Cheeseboro, L., Ding, Y. Y., Russell, R. G., Lindemann, D., Hartley, A., Baker, G. R., Obici, S., Deshaies, Y., Ludgate, M., Rossetti, L. and Scherer, P. E. (2004). A transgenic mouse with a deletion in the collagenous domain of adiponectin displays elevated circulating adiponectin and improved insulin sensitivity. *Endocrinology* 145, 367–383.
- Cook, J. R. and Kozak, L. P. (1982). Sn-glycerol-3-phosphate dehydrogenase gene expression during mouse adipocyte development in vivo. *Dev Biol* 92, 440–448.

- Coppée, J. Y. (2008). Do DNA microarrays have their future behind them? *Microbes Infect* 10, 1067–1071.
- Cousin, B., Casteilla, L., Dani, C., Muzzin, P., Revelli, J. P. and Penicaud, L. (1993). Adipose tissues from various anatomical sites are characterized by different patterns of gene expression and regulation. *Biochem J* 292 (Pt 3), 873–876.
- Cousin, B., Cinti, S., Morroni, M., Raimbault, S., Ricquier, D., Pénicaud, L. and Casteilla, L. (1992). Occurrence of brown adipocytes in rat white adipose tissue: molecular and morphological characterization. *J Cell Sci* 103 (Pt 4), 931–942.
- Coutinho, L. L., Matukumalli, L. K., Sonstegard, T. S., Van Tassell, C. P., Gasbarre, L. C., Capuco, A. V. and Smith, T. P. (2007). Discovery and profiling of bovine microRNAs from immune-related and embryonic tissues. *Physiol Genomics* 29, 35–43.
- Crison, M., Casteilla, L., Lehr, L., Carmona, M., Paoloni-Giacobino, A., Yap, S., Sun, B., Léger, B., Logar, A., Pénicaud, L., Schrauwen, P., Cameron-Smith, D., Russell, A. P., Péault, B. and Giacobino, J. P. (2008a). A reservoir of brown adipocyte progenitors in human skeletal muscle. *Stem Cells* 26, 2425–2433.
- Crison, M., Yap, S., Casteilla, L., Chen, C. W., Corselli, M., Park, T. S., Andriolo, G., Sun, B., Zheng, B., Zhang, L., Norotte, C., Teng, P. N., Traas, J., Schugar, R., Deasy, B. M., Badylak, S., Buhning, H. J., Giacobino, J. P., Lazzari, L., Huard, J. and Péault, B. (2008b). A perivascular origin for mesenchymal stem cells in multiple human organs. *Cell Stem Cell* 3, 301–313.
- Crist, C. G., Montarras, D., Pallafacchina, G., Rocancourt, D., Cumano, A., Conway, S. J. and Buckingham, M. (2009). Muscle stem cell behavior is modified by microRNA-27 regulation of Pax3 expression. *Proc Natl Acad Sci U S A* 106, 13383–13387.
- Crossno, J. T., Majka, S. M., Grazia, T., Gill, R. G. and Klemm, D. J. (2006). Rosiglitazone promotes development of a novel adipocyte population from bone marrow-derived circulating progenitor cells. *J Clin Invest* 116, 3220–3228.
- Cullen, B. R. (2006). Is RNA interference involved in intrinsic antiviral immunity in mammals? *Nat Immunol* 7, 563–567.
- Daimon, M., Oizumi, T., Saitoh, T., Kameda, W., Hirata, A., Yamaguchi, H., Ohnuma, H., Igarashi, M., Tominaga, M., Kato, T. and Funagata study (2003). Decreased serum levels of adiponectin are a risk factor for the progression to type 2 diabetes in the Japanese Population: the Funagata study. *Diabetes Care* 26, 2015–2020.
- Dali-Youcef, N., Matak, C., Coste, A., Messaddeq, N., Giroud, S., Blanc, S., Koehl, C., Champy, M. F., Chambon, P., Fajas, L., Metzger, D., Schoonjans, K. and Auwerx, J. (2007). Adipose tissue-specific inactivation of the retinoblastoma protein protects against diabetes because of increased energy expenditure. *Proc Natl Acad Sci U S A* 104, 10703–10708.
- Dandona, P., Weinstock, R., Thusu, K., Abdel-Rahman, E., Aljada, A. and Wadden, T. (1998). Tumor necrosis factor- α in sera of obese patients: fall with weight loss. *J Clin Endocrinol Metab* 83, 2907–2910.
- Dansinger, M. L., Gleason, J. A., Griffith, J. L., Selker, H. P. and Schaefer, E. J. (2005). Comparison of the Atkins, Ornish, Weight Watchers, and Zone diets for weight loss and heart disease risk reduction: a randomized trial. *JAMA* 293, 43–53.
- Deslex, S., Negrel, R. and Ailhaud, G. (1987). Development of a chemically defined serum-free medium for differentiation of rat adipose precursor cells. *Exp Cell Res* 168, 15–30.
- Di Lisio, L., Gómez-López, G., Sánchez-Beato, M., Gómez-Abad, C., Rodríguez, M. E., Villuendas, R., Ferreira, B. I., Carro, A., Rico, D., Mollejo, M., Martínez, M. A., Menárguez, J., Díaz-Alderete, A., Gil, J., Cigudosa, J. C., Pisano, D. G., Piris, M. A. and Martínez, N. (2010). Mantle cell lymphoma: transcriptional regulation by microRNAs. *Leukemia* 24, 1335–1342.
- Díaz-Perales, A., Quesada, V., Sánchez, L. M., Ugalde, A. P., Suárez, M. F., Fueyo, A. and López-Otín, C. (2005). Identification of human aminopeptidase O, a novel metalloprotease with structural similarity to aminopeptidase B and leukotriene A4 hydrolase. *J Biol Chem* 280, 14310–14317.
- Djian, P., Grimaldi, P., Négre, R. and Ailhaud, G. (1982). Adipose conversion of OB17 preadipocytes. Relationships between cell division and fat cell cluster formation. *Exp Cell Res* 142, 273–281.

- Doench, J. G. and Sharp, P. A. (2004). Specificity of microRNA target selection in translational repression. *Genes Dev* 18, 504–511.
- Doglio, A., Dani, C., Fredrikson, G., Grimaldi, P. and Ailhaud, G. (1987). Acute regulation of insulin-like growth factor-I gene expression by growth hormone during adipose cell differentiation. *EMBO J* 6, 4011–4016.
- Drew, B. S., Dixon, A. F. and Dixon, J. B. (2007). Obesity management: update on orlistat. *Vasc Health Risk Manag* 3, 817–821.
- Duisters, R. F., Tijssen, A. J., Schroen, B., Leenders, J. J., Lentink, V., van der Made, I., Herias, V., van Leeuwen, R. E., Schellings, M. W., Barenbrug, P., Maessen, J. G., Heymans, S., Pinto, Y. M. and Creemers, E. E. (2009). miR-133 and miR-30 regulate connective tissue growth factor: implications for a role of microRNAs in myocardial matrix remodeling. *Circ Res* 104, 170–178.
- Duncan, D. D., Eshoo, M., Esau, C., Freier, S. M. and Lollo, B. A. (2006). Absolute quantitation of microRNAs with a PCR-based assay. *Anal Biochem* 359, 268–270.
- Ebert, M. S., Neilson, J. R. and Sharp, P. A. (2007). MicroRNA sponges: competitive inhibitors of small RNAs in mammalian cells. *Nat Methods* 4, 721–726.
- Ebert, M. S. and Sharp, P. A. (2010). MicroRNA sponges: progress and possibilities. *RNA* 16, 2043–2050.
- Eisen, J. A., Coyne, R. S., Wu, M., Wu, D., Thiagarajan, M., Wortman, J. R., Badger, J. H., Ren, Q., Amedeo, P., Jones, K. M., Tallon, L. J., Delcher, A. L., Salzberg, S. L., Silva, J. C., Haas, B. J., Majoros, W. H., Farzad, M., Carlton, J. M., Smith, R. K. and Garg, J. et al. (2006). Macronuclear genome sequence of the ciliate *Tetrahymena thermophila*, a model eukaryote. *PLoS Biol* 4.
- Elabd, C., Chiellini, C., Carmona, M., Galitzky, J., Cochet, O., Petersen, R., Pénicaud, L., Kristiansen, K., Bouloumié, A., Casteilla, L., Dani, C., Ailhaud, G. and Amri, E. (2009). Human multipotent adipose-derived stem cells differentiate into functional brown adipocytes. *Stem Cells (Dayton, Ohio)* 27, 2753–2760.
- Elabd, C., Chiellini, C., Massoudi, A., Cochet, O., Zaragosi, L., Trojani, C., Michiels, J., Weiss, P., Carle, G., Rochet, N., Dechesne, C. A., Ailhaud, G., Dani, C. and Amri, E. (2007). Human adipose tissue-derived multipotent stem cells differentiate in vitro and in vivo into osteocyte-like cells. *Biochemical and Biophysical Research Communications* 361, 342–348.
- Elbashir, S. M., Harborth, J., Lendeckel, W., Yalcin, A., Weber, K. and Tuschl, T. (2001a). Duplexes of 21-nucleotide RNAs mediate RNA interference in cultured mammalian cells. *Nature* 411, 494–498.
- Elbashir, S. M., Lendeckel, W. and Tuschl, T. (2001b). RNA interference is mediated by 21- and 22-nucleotide RNAs. *Genes Dev* 15, 188–200.
- Elmén, J., Lindow, M., Schütz, S., Lawrence, M., Petri, A., Obad, S., Lindholm, M., Hedtjärn, M., Hansen, H. F., Berger, U., Gullans, S., Kearney, P., Sarnow, P., Straarup, E. M. and Kauppinen, S. (2008). LNA-mediated microRNA silencing in non-human primates. *Nature* 452, 896–899.
- ENCODE Project Consortium, Birney, E., Stamatoyannopoulos, J. A., Dutta, A., Guigó, R., Gingeras, T. R., Margulies, E. H., Weng, Z., Snyder, M., Dermitzakis, E. T., Thurman, R. E., Kuehn, M. S., Taylor, C. M., Neph, S., Koch, C. M., Asthana, S., Malhotra, A., Adzhubei, I., Greenbaum, J. A., Andrews, R. M., Flicek, P., Boyle, P. J. and Cao, H. et al. (2007). Identification and analysis of functional elements in 1 genome by the ENCODE pilot project. *Nature* 447, 799–816.
- Enerback, S. (2010). Human brown adipose tissue. *Cell Metab* 11, 248–252.
- Enerbäck, S., Jacobsson, A., Simpson, E. M., Guerra, C., Yamashita, H., Harper, M. E. and Kozak, L. P. (1997). Mice lacking mitochondrial uncoupling protein are cold-sensitive but not obese. *Nature* 387, 90–94.
- Entenmann, G. and Hauner, H. (1996). Relationship between replication and differentiation in cultured human adipocyte precursor cells. *Am J Physiol* 270, 1011–1016.
- Esau, C., Davis, S., Murray, S. F., Yu, X. X., Pandey, S. K., Pear, M., Watts, L., Booten, S. L., Graham, M., McKay, R., Subramaniam, A., Propp, S., Lollo, B. A., Freier, S., Bennett, C. F., Bhanot, S. and Monia, B. P. (2006). miR-122 regulation of lipid metabolism revealed by in vivo antisense targeting. *Cell Metab* 3, 87–98.
- Esau, C., Kang, X., Peralta, E., Hanson, E., Marcusson, E. G., Ravichandran, L. V., Sun, Y., Koo, S., Perera, R. J., Jain, R., Dean, N. M., Freier, S. M., Bennett, C. F., Lollo, B. and Griffey, R. (2004). MicroRNA-143 regulates adipocyte differentiation. *The Journal of Biological Chemistry* 279, 52361–52365.

- Fain, J. N., Bahouth, S. W. and Madan, A. K. (2004a). TNF α release by the nonfat cells of human adipose tissue. *Int J Obes Relat Metab Disord* *28*, 616–622.
- Fain, J. N., Madan, A. K., Hiler, M. L., Cheema, P. and Bahouth, S. W. (2004b). Comparison of the release of adipokines by adipose tissue, adipose tissue matrix, and adipocytes from visceral and subcutaneous abdominal adipose tissues of obese humans. *Endocrinology* *145*, 2273–2282.
- Fajas, L., Auboeuf, D., Raspé, E., Schoonjans, K., Lefebvre, A. M., Saladin, R., Najib, J., Laville, M., Fruchart, J. C., Deeb, S., Vidal-Puig, A., Flier, J., Briggs, M. R., Staels, B., Vidal, H. and Auwerx, J. (1997). The organization, promoter analysis, and expression of the human PPAR γ gene. *J Biol Chem* *272*, 18779–18789.
- Fang, S., Suh, J. M., Atkins, A. R., Hong, S. H., Leblanc, M., Nofsinger, R. R., Yu, R. T., Downes, M. and Evans, R. M. (2011). Corepressor SMRT promotes oxidative phosphorylation in adipose tissue and protects against diet-induced obesity and insulin resistance. *Proc Natl Acad Sci U S A* *108*, 3412–3417.
- Farmer, S. R. (2006). Transcriptional control of adipocyte formation. *Cell Metabolism* *4*, 263–273.
- Fasshauer, M., Klein, J., Kriauciunas, K. M., Ueki, K., Benito, M. and Kahn, C. R. (2001). Essential role of insulin receptor substrate 1 in differentiation of brown adipocytes. *Mol Cell Biol* *21*, 319–329.
- Fasshauer, M., Klein, J., Neumann, S., Eszlinger, M. and Paschke, R. (2002). Hormonal regulation of adiponectin gene expression in 3T3-L1 adipocytes. *Biochem Biophys Res Commun* *290*, 1084–1089.
- Feldmann, H. M., Golozoubova, V., Cannon, B. and Nedergaard, J. (2009). UCP1 ablation induces obesity and abolishes diet-induced thermogenesis in mice exempt from thermal stress by living at thermoneutrality. *Cell Metabolism* *9*, 203–209.
- Feng, J., Iwama, A., Satake, M. and Kohu, K. (2009). MicroRNA-27 enhances differentiation of myeloblasts into granulocytes by post-transcriptionally downregulating Runx1. *Br J Haematol* *145*, 412–423.
- Festa, A., Williams, K., Tracy, R. P., Wagenknecht, L. E. and Haffner, S. M. (2006). Progression of plasminogen activator inhibitor-1 and fibrinogen levels in relation to incident type 2 diabetes. *Circulation* *113*, 1753–1759.
- Filipowicz, W., Bhattacharyya, S. N. and Sonenberg, N. (2008). Mechanisms of post-transcriptional regulation by microRNAs: are the answers in sight? *Nat Rev Genet* *9*, 102–114.
- Fire, A., Albertson, D., Harrison, S. W. and Moerman, D. G. (1991). Production of antisense RNA leads to effective and specific inhibition of gene expression in *C. elegans* muscle. *Development* *113*, 503–514.
- Fire, A., Xu, S., Montgomery, M. K., Kostas, S. A., Driver, S. E. and Mello, C. C. (1998). Potent and specific genetic interference by double-stranded RNA in *Caenorhabditis elegans*. *Nature* *391*, 806–811.
- Foster, G. D., Wyatt, H. R., Hill, J. O., McGuckin, B. G., Brill, C., Mohammed, B. S., Szapary, P. O., Rader, D. J., Edman, J. S. and Klein, S. (2003). A randomized trial of a low-carbohydrate diet for obesity. *N Engl J Med* *348*, 2082–2090.
- Franco-Zorrilla, J. M., Valli, A., Todesco, M., Mateos, I., Puga, M. I., Rubio-Somoza, I., Leyva, A., Weigel, D., García, J. A. and Paz-Ares, J. (2007). Target mimicry provides a new mechanism for regulation of microRNA activity. *Nat Genet* *39*, 1033–1037.
- Freytag, S. O., Paielli, D. L. and Gilbert, J. D. (1994). Ectopic expression of the CCAAT/enhancer-binding protein alpha promotes the adipogenic program in a variety of mouse fibroblastic cells. *Genes Dev* *8*, 1654–1663.
- Friedenstein, A. J., Petrakova, K. V., Kurolesova, A. I. and Frolova, G. P. (1968). Heterotopic of bone marrow. Analysis of precursor cells for osteogenic and hematopoietic tissues. *Transplantation* *6*, 230–247.
- Friedenstein, A. J., Piatetzky-Shapiro, I. I. and Petrakova, K. V. (1966). Osteogenesis in transplants of bone marrow cells. *J Embryol Exp Morphol* *16*, 381–390.
- Friedman, J. M. (2000). Obesity in the new millennium. *Nature* *404*, 632–634.
- Friedman, R. C., Farh, K. K., Burge, C. B. and Bartel, D. P. (2009). Most mammalian mRNAs are conserved targets of microRNAs. *Genome Res* *19*, 92–105.
- Frühbeck, G. (2010). Is Europe really battling obesity? *Obes Facts* *3*, 219–221.

- Gaidatzis, D., van Nimwegen, E., Hausser, J. and Zavolan, M. (2007). Inference of miRNA targets using evolutionary conservation and pathway analysis. *BMC Bioinformatics* 8, 69.
- Gaillard, D., Négrel, R., Lagarde, M. and Ailhaud, G. (1989). Requirement and role of arachidonic acid in the differentiation of pre-adipose cells. *Biochem J* 257, 389–397.
- Garzon, R., Calin, G. A. and Croce, C. M. (2009). MicroRNAs in Cancer. *Annu Rev Med* 60, 167–179.
- Gehrke, S., Imai, Y., Sokol, N. and Lu, B. (2010). Pathogenic LRRK2 negatively regulates microRNA-mediated translational repression. *Nature* 466, 637–641.
- Géloën, A., Collet, A. J., Guay, G. and Bukowiecki, L. J. (1989). Insulin stimulates in vivo cell proliferation in white adipose tissue. *Am J Physiol* 256, 190–196.
- Gerin, I., Bommer, G. T., McCoin, C. S., Sousa, K. M., Krishnan, V. and MacDougald, O. A. (2010). Roles for miRNA-378/378* in adipocyte gene expression and lipogenesis. *American Journal of Physiology. Endocrinology and Metabolism* 299, E198–206.
- Gesta, S., Tseng, Y. H. and Kahn, C. R. (2007). Developmental origin of fat: tracking obesity to its source. *Cell* 131, 242–256.
- Ghildiyal, M. and Zamore, P. D. (2009). Small silencing RNAs: an expanding universe. *Nat Rev Genet* 10, 94–108.
- Glandt, M. and Raz, I. (2011). Present and future: pharmacologic treatment of obesity. *J Obes* 2011, 636181–636181.
- Golozoubova, V., Gullberg, H., Matthias, A., Cannon, B., Vennström, B. and Nedergaard, J. (2004). Depressed thermogenesis but competent brown adipose tissue recruitment in mice devoid of all hormone-binding thyroid hormone receptors. *Mol Endocrinol* 18, 384–401.
- Golozoubova, V., Hohtola, E., Matthias, A., Jacobsson, A., Cannon, B. and Nedergaard, J. (2001). Only UCP1 can mediate adaptive nonshivering thermogenesis in the cold. *FASEB J* 15, 2048–2050.
- Goodstadt, L. and Ponting, C. P. (2006). Phylogenetic reconstruction of orthology, paralogy, and conserved synteny for dog and human. *PLoS Comput Biol* 2.
- Graves, R. A., Tontonoz, P. and Spiegelman, B. M. (1992). Analysis of a tissue-specific enhancer: ARF6 regulates adipogenic gene expression. *Mol Cell Biol* 12, 1202–1208.
- Green, H. and Kehinde, O. (1974). Sublines of Mouse 3T3 Lines That Accumulate Lipid. *Cell* 1, 113–116.
- Green, H. and Kehinde, O. (1976). Spontaneous heritable changes leading to increased adipose conversion in 3T3 cells. *Cell* 7, 105–113.
- Gregoire, F. M., Smas, C. M. and Sul, H. S. (1998). Understanding adipocyte differentiation. *Physiol Rev* 78, 783–809.
- Gregor, M. F. and Hotamisligil, G. S. (2011). Inflammatory mechanisms in obesity. *Annu Rev Immunol* 29, 415–445.
- Grishok, A., Pasquinelli, A. E., Conte, D., Li, N., Parrish, S., Ha, I., Baillie, D. L., Fire, A., Ruvkun, G. and Mello, C. C. (2001). Genes and mechanisms related to RNA interference regulate expression of the small temporal RNAs that control *C. elegans* developmental timing. *Cell* 106, 23–34.
- Guerra, C., Koza, R. A., Yamashita, H., Walsh, K. and Kozak, L. P. (1998). Emergence of brown adipocytes in white fat in mice is under genetic control. Effects on body weight and adiposity. *J Clin Invest* 102, 412–420.
- Guo, H., Ingolia, N. T., Weissman, J. S. and Bartel, D. P. (2010). Mammalian microRNAs predominantly act to decrease target mRNA levels. *Nature* 466, 835–840.
- Gupta, A. and Gupta, V. (2010). Metabolic syndrome: what are the risks for humans? *Biosci Trends* 4, 204–212.
- Gupta, R. K., Arany, Z., Seale, P., Mepani, R. J., Ye, L., Conroe, H. M., Roby, Y. A., Kulaga, H., Reed, R. R. and Spiegelman, B. M. (2010). Transcriptional control of preadipocyte determination by Zfp423. *Nature* 464, 619–623.
- Hackl, H., Sanchez Cabo, F., Sturn, A., Wolkenhauer, O. and Trajanoski, Z. (2004). Analysis of DNA microarray data. *Curr Top Med Chem* 4, 1357–1370.

- Halaas, J. L., Gajiwala, K. S., Maffei, M., Cohen, S. L., Chait, B. T., Rabinowitz, D., Lallone, R. L., Burley, S. K. and Friedman, J. M. (1995). Weight-reducing effects of the plasma protein encoded by the obese gene. *Science* *269*, 543–546.
- Hallberg, M., Morganstein, D. L., Kiskinis, E., Shah, K., Kralli, A., Dilworth, S. M., White, R., Parker, M. G. and Christian, M. (2008). A functional interaction between RIP140 and PGC-1alpha regulates the expression of the lipid droplet protein CIDEA. *Mol Cell Biol* *28*, 6785–6795.
- Hammond, S. M., Bernstein, E., Beach, D. and Hannon, G. J. (2000). An RNA-directed nuclease mediates post-transcriptional gene silencing in *Drosophila* cells. *Nature* *404*, 293–296.
- Han, J., Lee, Y., Yeom, K. H., Nam, J. W., Heo, I., Rhee, J. K., Sohn, S. Y., Cho, Y., Zhang, B. T. and Kim, V. N. (2006). Molecular basis for the recognition of primary microRNAs by the Drosha-DGCR8 complex. *Cell* *125*, 887–901.
- Hansen, J. B., Jorgensen, C., Petersen, R. K., Hallenborg, P., De Matteis, R., Boye, H. A., Petrovic, N., Enerbäck, S., Nedergaard, J., Cinti, S., te Riele, H. and Kristiansen, K. (2004). Retinoblastoma protein functions as a molecular switch determining white versus brown adipocyte differentiation. *Proc Natl Acad Sci U S A* *101*, 4112–4117.
- Hansen, J. B. and Kristiansen, K. (2006). Regulatory circuits controlling white versus brown adipocyte differentiation. *Biochem J* *398*, 153–168.
- Harris, R. B. and Leibel, R. L. (2008). Location, location, location.. *Cell Metab* *7*, 359–361.
- Haslam, D. W. and James, W. P. (2005). Obesity. *Lancet* *366*, 1197–1209.
- Hauner, H., Bender, M., Haastert, B. and Hube, F. (1998). Plasma concentrations of soluble TNF-alpha receptors in obese subjects. *Int J Obes Relat Metab Disord* *22*, 1239–1243.
- Hauner, H., Entenmann, G., Wabitsch, M., Gaillard, D., Ailhaud, G., Negrel, R. and Pfeiffer, E. F. (1989). Promoting effect of glucocorticoids on the differentiation of human adipocyte precursor cells cultured in a chemically defined medium. *J Clin Invest* *84*, 1663–1670.
- Hauner, H., Schmid, P. and Pfeiffer, E. F. (1987). Glucocorticoids and insulin promote the differentiation of human adipocyte precursor cells into fat cells. *J Clin Endocrinol Metab* *64*, 832–835.
- Haynes, W. G., Morgan, D. A., Walsh, S. A., Mark, A. L. and Sivitz, W. I. (1997). Receptor-mediated regional sympathetic nerve activation by leptin. *J Clin Invest* *100*, 270–278.
- He, H., Jazdzewski, K., Li, W., Liyanarachchi, S., Nagy, R., Volinia, S., Calin, G. A., Liu, C. G., Franssila, K., Suster, S., Kloos, R. T., Croce, C. M. and de la Chapelle, A. (2005). The role of microRNA genes in papillary thyroid carcinoma. *Proc Natl Acad Sci U S A* *102*, 19075–19080.
- Heid, C. A., Stevens, J., Livak, K. J. and Williams, P. M. (1996). Real time quantitative PCR. *Genome Res* *6*, 986–994.
- Herold, G. (2006). *Innere Medizin*. Gerd Herold, Kandel, Germany.
- Herrera, B. M., Lockstone, H. E., Taylor, J. M., Ria, M., Barrett, A., Collins, S., Kaisaki, P., Argoud, K., Fernandez, C., Travers, M. E., Grew, J. P., Randall, J. C., Gloyn, A. L., Gauguier, D., McCarthy, M. I. and Lindgren, C. M. (2010). Global microRNA expression profiles in insulin target tissues in a spontaneous rat model of type 2 diabetes. *Diabetologia* *53*, 1099–1109.
- Heymsfield, S. B., Greenberg, A. S., Fujioka, K., Dixon, R. M., Kushner, R., Hunt, T., Lubina, J. A., Patane, J., Self, B., Hunt, P. and McCamish, M. (1999). Recombinant leptin for weight loss in obese and lean adults: a randomized, controlled, dose-escalation trial. *JAMA* *282*, 1568–1575.
- Higuchi, R., Fockler, C., Dollinger, G. and Watson, R. (1993). Kinetic PCR analysis: real-time monitoring of DNA amplification reactions. *Biotechnology (N Y)* *11*, 1026–1030.
- Himms-Hagen, J., Melnyk, A., Zingaretti, M. C., Ceresi, E., Barbatelli, G. and Cinti, S. (2000). Multilocular fat cells in WAT of CL-316243-treated rats derive directly from white adipocytes. *Am J Physiol Cell Physiol* *279*, 670–681.
- Himms-Hagen, J., Triandafillou, J. and Gwilliam, C. (1981). Brown adipose tissue of cafeteria-fed rats. *Am J Physiol* *241*, 116–120.

- Horie, T., Ono, K., Horiguchi, M., Nishi, H., Nakamura, T., Nagao, K., Kinoshita, M., Kuwabara, Y., Marusawa, H., Iwanaga, Y., Hasegawa, K., Yokode, M., Kimura, T. and Kita, T. (2010). MicroRNA-33 encoded by an intron of sterol regulatory element-binding protein 2 (Srebp2) regulates HDL in vivo. *Proc Natl Acad Sci U S A* 107, 17321–17326.
- Hossain, P., Kowar, B. and El Nahas, M. (2007). Obesity and diabetes in the developing world—a growing challenge. *N Engl J Med* 356, 213–215.
- Hotamisligil, G. S., Arner, P., Caro, J. F., Atkinson, R. L. and Spiegelman, B. M. (1995). Increased adipose tissue expression of tumor necrosis factor- α in human obesity and insulin resistance. *J Clin Invest* 95, 2409–2415.
- Hotamisligil, G. S., Budavari, A., Murray, D. and Spiegelman, B. M. (1994). Reduced tyrosine kinase activity of the insulin receptor in obesity-diabetes. Central role of tumor necrosis factor- α . *J Clin Invest* 94, 1543–1549.
- Hotamisligil, G. S., Shargill, N. S. and Spiegelman, B. M. (1993). Adipose expression of tumor necrosis factor- α : direct role in obesity-linked insulin resistance. *Science* 259, 87–91.
- Hotta, K., Funahashi, T., Arita, Y., Takahashi, M., Matsuda, M., Okamoto, Y., Iwahashi, H., Kuriyama, H., Ouchi, N., Maeda, K., Nishida, M., Kihara, S., Sakai, N., Nakajima, T., Hasegawa, K., Muraguchi, M., Ohmoto, Y., Nakamura, T., Yamashita, S., Hanafusa, T. and Matsuzawa, Y. (2000). Plasma concentrations of a novel, adipose-specific protein, adiponectin, in type 2 diabetic patients. *Arterioscler Thromb Vasc Biol* 20, 1595–1599.
- Hou, B., Eren, M., Painter, C. A., Covington, J. W., Dixon, J. D., Schoenhard, J. A. and Vaughan, D. E. (2004). Tumor necrosis factor α activates the human plasminogen activator inhibitor-1 gene through a distal nuclear factor kappaB site. *J Biol Chem* 279, 18127–18136.
- Huang, J., Zhao, L., Xing, L. and Chen, D. (2010a). MicroRNA-204 regulates Runx2 protein expression and mesenchymal progenitor cell differentiation. *Stem Cells* 28, 357–364.
- Huang, Y., Zou, Q., Song, H., Song, F., Wang, L., Zhang, G. and Shen, X. (2010b). A study of miRNAs targets prediction and experimental validation. *Protein Cell* 1, 979–986.
- Huse, J. T., Brennan, C., Hambardzumyan, D., Wee, B., Pena, J., Rouhanifard, S. H., Sohn-Lee, C., le Sage, C., Agami, R., Tuschl, T. and Holland, E. C. (2009). The PTEN-regulating microRNA miR-26a is amplified in high-grade glioma and facilitates gliomagenesis in vivo. *Genes Dev* 23, 1327–1337.
- Hyde, R. (2008). Europe battles with obesity. *Lancet* 371, 2160–2161.
- Iorio, M. V., Ferracin, M., Liu, C. G., Veronese, A., Spizzo, R., Sabbioni, S., Magri, E., Pedriali, M., Fabbri, M., Campiglio, M., Ménard, S., Palazzo, J. P., Rosenberg, A., Musiani, P., Volinia, S., Nenci, I., Calin, G. A., Querzoli, P., Negrini, M. and Croce, C. M. (2005). MicroRNA gene expression deregulation in human breast cancer. *Cancer Res* 65, 7065–7070.
- Irie, Y., Asano, A., Cañas, X., Nikami, H., Aizawa, S. and Saito, M. (1999). Immortal brown adipocytes from p53-knockout mice: differentiation and expression of uncoupling proteins. *Biochem Biophys Res Commun* 255, 221–225.
- Ji, J., Shi, J., Budhu, A., Yu, Z., Forgues, M., Roessler, S., Ambs, S., Chen, Y., Meltzer, P. S., Croce, C. M., Qin, L. X., Man, K., Lo, C. M., Lee, J., Ng, I. O., Fan, J., Tang, Z. Y., Sun, H. C. and Wang, X. W. (2009a). MicroRNA expression, survival, and response to interferon in liver cancer. *N Engl J Med* 361, 1437–1447.
- Ji, J., Zhang, J., Huang, G., Qian, J., Wang, X. and Mei, S. (2009b). Over-expressed microRNA-27a and 27b influence fat accumulation and cell proliferation during rat hepatic stellate cell activation. *FEBS Lett* 583, 759–766.
- Jin, W., Takagi, T., Kaneshashi, S. N., Kurahashi, T., Nomura, T., Harada, J. and Ishii, S. (2006). Schnurri-2 controls BMP-dependent adipogenesis via interaction with Smad proteins. *Dev Cell* 10, 461–471.
- Jinek, M. and Doudna, J. A. (2009). A three-dimensional view of the molecular machinery of RNA interference. *Nature* 457, 405–412.
- Johnson, J. M., Edwards, S., Shoemaker, D. and Schadt, E. E. (2005). Dark matter in the genome: evidence of widespread transcription detected by microarray tiling experiments. *Trends Genet* 21, 93–102.
- Jopling, C. L., Yi, M., Lancaster, A. M., Lemon, S. M. and Sarnow, P. (2005). Modulation of hepatitis C virus RNA abundance by a liver-specific MicroRNA. *Science* 309, 1577–1581.

- Kahn, S. E., Prigeon, R. L., McCulloch, D. K., Boyko, E. J., Bergman, R. N., Schwartz, M. W., Neifing, J. L., Ward, W. K., Beard, J. C. and Palmer, J. P. (1993). Quantification of the relationship between insulin sensitivity and beta-cell function in human subjects. Evidence for a hyperbolic function. *Diabetes* *42*, 1663–1672.
- Kaila, B. and Raman, M. (2008). Obesity: a review of pathogenesis and management strategies. *Can J Gastroenterol* *22*, 61–68.
- Kain, S. R. and Ganguly, S. (2001). Overview of genetic reporter systems. *Curr Protoc Mol Biol* *Chapter 9*.
- Kajimoto, K., Naraba, H. and Iwai, N. (2006). MicroRNA and 3T3-L1 pre-adipocyte differentiation. *RNA* (New York, N.Y.) *12*, 1626–1632.
- Kajimura, S., Seale, P., Kubota, K., Lunsford, E., Frangioni, J. V., Gygi, S. P. and Spiegelman, B. M. (2009). Initiation of myoblast to brown fat switch by a PRDM16-C/EBP-beta transcriptional complex. *Nature* *460*, 1154–1158.
- Kajimura, S., Seale, P., Tomaru, T., Erdjument-Bromage, H., Cooper, M. P., Ruas, J. L., Chin, S., Tempst, P., Lazar, M. A. and Spiegelman, B. M. (2008). Regulation of the brown and white fat gene programs through a PRDM16/CtBP transcriptional complex. *Genes & Development* *22*, 1397–1409.
- Kamon, J., Naitoh, T., Kitahara, M. and Tsuruzoe, N. (2001). Prostaglandin F(2)alpha enhances glucose consumption through neither adipocyte differentiation nor GLUT1 expression in 3T3-L1 cells. *Cell Signal* *13*, 105–109.
- Kang, W. J., Cho, Y. L., Chae, J. R., Lee, J. D., Choi, K. J. and Kim, S. (2011). Molecular beacon-based bioimaging of multiple microRNAs during myogenesis. *Biomaterials* *32*, 1915–1922.
- Kannel, W. B., Garrison, R. J. and Dannenberg, A. L. (1993). Secular blood pressure trends in normotensive persons: the Framingham Study. *Am Heart J* *125*, 1154–1158.
- Karbiener, M., Fischer, C., Nowitsch, S., Opriessnig, P., Papak, C., Ailhaud, G., Dani, C., Amri, E. and Scheideler, M. (2009). microRNA miR-27b impairs human adipocyte differentiation and targets PPARgamma. *Biochemical and Biophysical Research Communications* *390*, 247–251.
- Karbiener, M., Neuhold, C., Opriessnig, P., Prokesch, A., Strauss, J. G. and Scheideler, M. (2011). MicroRNA-30c promotes human adipocyte differentiation and co-represses PAI-1 and ALK2. *RNA Biology* *8* (*in press*).
- Karelis, A. D., St-Pierre, D. H., Conus, F., Rabasa-Lhoret, R. and Poehlman, E. T. (2004). Metabolic and body composition factors in subgroups of obesity: what do we know? *J Clin Endocrinol Metab* *89*, 2569–2575.
- Karlsson, C., Lindell, K., Ottosson, M., Sjöström, L., Carlsson, B. and Carlsson, L. M. (1998). Human adipose tissue expresses angiotensinogen and enzymes required for its conversion to angiotensin II. *J Clin Endocrinol Metab* *83*, 3925–3929.
- Kashuba, V. I., Li, J., Wang, F., Senchenko, V. N., Protopopov, A., Malyukova, A., Kutsenko, A. S., Kadyrova, E., Zabarovska, V. I., Muravenko, O. V., Zelenin, A. V., Kisselev, L. L., Kuzmin, I., Minna, J. D., Winberg, G., Ernberg, I., Braga, E., Lerman, M. I., Klein, G. and Zabarovsky, E. R. (2004). RBSP3 (HYA22) is a tumor suppressor gene implicated in major epithelial malignancies. *Proc Natl Acad Sci U S A* *101*, 4906–4911.
- Kashuba, V. I., Pavlova, T. V., Grigorieva, E. V., Kutsenko, A., Yenamandra, S. P., Li, J., Wang, F., Protopopov, A. I., Zabarovska, V. I., Senchenko, V., Haraldson, K., Eshchenko, T., Kobliakova, J., Vorontsova, O., Kuzmin, I., Braga, E., Blinov, V. M., Kisselev, L. L., Zeng, Y. X., Ernberg, I., Lerman, M. I., Klein, G. and Zabarovsky, E. R. (2009). High mutability of the tumor suppressor genes RASSF1 and RBSP3 (CTDSPL) in cancer. *PLoS One* *4*.
- Kaye, S. A., Folsom, A. R., Sprafka, J. M., Prineas, R. J. and Wallace, R. B. (1991). Increased incidence of diabetes mellitus in relation to abdominal adiposity in older women. *J Clin Epidemiol* *44*, 329–334.
- Keller, P., Gburcik, V., Petrovic, N., Gallagher, I. J., Nedergaard, J., Cannon, B. and Timmons, J. A. (2011). Gene-chip studies of adipogenesis-regulated microRNAs in mouse primary adipocytes and human obesity. *BMC Endocr Disord* *11*, 7–7.
- Kellner, K., Liebsch, G., Klimant, I., Wolfbeis, O. S., Blunk, T., Schulz, M. B. and Göpferich, A. (2002). Determination of oxygen gradients in engineered tissue using a fluorescent sensor. *Biotechnol Bioeng* *80*, 73–83.
- Kenchaiah, S., Evans, J. C., Levy, D., Wilson, P. W., Benjamin, E. J., Larson, M. G., Kannel, W. B. and Vasan, R. S. (2002). Obesity and the risk of heart failure. *N Engl J Med* *347*, 305–313.

- Kennell, J. A., Gerin, I., MacDougald, O. A. and Cadigan, K. M. (2008). The microRNA miR-8 is a conserved negative regulator of Wnt signaling. *Proceedings of the National Academy of Sciences of the United States of America* *105*, 15417–15422.
- Kershaw, E. E. and Flier, J. S. (2004). Adipose tissue as an endocrine organ. *J Clin Endocrinol Metab* *89*, 2548–2556.
- Khraiwesh, B., Arif, M. A., Seumel, G. I., Ossowski, S., Weigel, D., Reski, R. and Frank, W. (2010). Transcriptional control of gene expression by microRNAs. *Cell* *140*, 111–122.
- Khurana, J. S. and Theurkauf, W. (2010). piRNAs, transposon silencing, and *Drosophila* germline development. *J Cell Biol* *191*, 905–913.
- Kim, H., Huang, W., Jiang, X., Pennicooke, B., Park, P. J. and Johnson, M. D. (2010a). Integrative genome analysis reveals an oncomir/oncogene cluster regulating glioblastoma survivorship. *Proc Natl Acad Sci U S A* *107*, 2183–2188.
- Kim, S. Y., Kim, A. Y., Lee, H. W., Son, Y. H., Lee, G. Y., Lee, J., Lee, Y. S. and Kim, J. B. (2010b). miR-27a is a negative regulator of adipocyte differentiation via suppressing PPARgamma expression. *Biochemical and Biophysical Research Communications* *392*, 323–328.
- Kim, Y. J., Bae, S. W., Yu, S. S., Bae, Y. C. and Jung, J. S. (2009a). miR-196a regulates proliferation and osteogenic differentiation in mesenchymal stem cells derived from human adipose tissue. *J Bone Miner Res* *24*, 816–825.
- Kim, Y. J., Hwang, S. J., Bae, Y. C. and Jung, J. S. (2009b). MiR-21 regulates adipogenic differentiation through the modulation of TGF-beta signaling in mesenchymal stem cells derived from human adipose tissue. *Stem Cells* *27*, 3093–3102.
- Kinoshita, M., Ono, K., Horie, T., Nagao, K., Nishi, H., Kuwabara, Y., Takanabe-Mori, R., Hasegawa, K., Kita, T. and Kimura, T. (2010). Regulation of adipocyte differentiation by activation of serotonin (5-HT) receptors 5-HT2AR and 5-HT2CR and involvement of microRNA-448-mediated repression of KLF5. *Mol Endocrinol* *24*, 1978–1987.
- Kiriakidou, M., Tan, G. S., Lamprinak, S., De Planell-Saguer, M., Nelson, P. T. and Mourelatos, Z. (2007). An mRNA m7G cap binding-like motif within human Ago2 represses translation. *Cell* *129*, 1141–1151.
- Kissebah, A. H. and Krakower, G. R. (1994). Regional adiposity and morbidity. *Physiol Rev* *74*, 761–811.
- Klaus, S., Cassard-Doulcier, A. M. and Ricquier, D. (1991). Development of *Phodopus sungorus* brown preadipocytes in primary cell culture: effect of an atypical beta-adrenergic agonist, insulin, and triiodothyronine on differentiation, mitochondrial development, and expression of the uncoupling protein UCP. *J Cell Biol* *115*, 1783–1790.
- Klaus, S., Choy, L., Champigny, O., Cassard-Doulcier, A. M., Ross, S., Spiegelman, B. and Ricquier, D. (1994). Characterization of the novel brown adipocyte cell line HIB 1B. Adrenergic pathways involved in regulation of uncoupling protein gene expression. *J Cell Sci* *107 (Pt 1)*, 313–319.
- Klaus, S., Ely, M., Encke, D. and Heldmaier, G. (1995). Functional assessment of white and brown adipocyte development and energy metabolism in cell culture. Dissociation of terminal differentiation and thermogenesis in brown adipocytes. *J Cell Sci* *108 (Pt 10)*, 3171–3180.
- Klötting, N., Berthold, S., Kovacs, P., Schön, M. R., Fasshauer, M., Ruschke, K., Stumvoll, M. and Blüher, M. (2009). MicroRNA expression in human omental and subcutaneous adipose tissue. *PLoS One* *4*.
- Knittle, J. L., Timmers, K., Ginsberg-Fellner, F., Brown, R. E. and Katz, D. P. (1979). The growth of adipose tissue in children and adolescents. Cross-sectional and longitudinal studies of adipose cell number and size. *J Clin Invest* *63*, 239–246.
- Kohler, H. P. and Grant, P. J. (2000). Plasminogen-activator inhibitor type 1 and coronary artery disease. *The New England Journal of Medicine* *342*, 1792–1801.
- Kota, J., Chivukula, R. R., O'Donnell, K. A., Wentzel, E. A., Montgomery, C. L., Hwang, H. W., Chang, T. C., Vivekanandan, P., Torbenson, M., Clark, K. R., Mendell, J. R. and Mendell, J. T. (2009). Therapeutic microRNA delivery suppresses tumorigenesis in a murine liver cancer model. *Cell* *137*, 1005–1017.

- Kozak, L. P. (2010). Brown fat and the myth of diet-induced thermogenesis. *Cell Metab* *11*, 263–267.
- Krek, A., Grün, D., Poy, M. N., Wolf, R., Rosenberg, L., Epstein, E. J., MacMenamin, P., da Piedade, I., Gunsalus, K. C., Stoffel, M. and Rajewsky, N. (2005). Combinatorial microRNA target predictions. *Nat Genet* *37*, 495–500.
- Krichevsky, A. M. and Gabriely, G. (2009). miR-21: a small multi-faceted RNA. *J Cell Mol Med* *13*, 39–53.
- Krol, J., Loedige, I. and Filipowicz, W. (2010). The widespread regulation of microRNA biogenesis, function and decay. *Nat Rev Genet* *11*, 597–610.
- Krude, H., Biebermann, H., Luck, W., Horn, R., Brabant, G. and Grüters, A. (1998). Severe early-onset obesity, adrenal insufficiency and red hair pigmentation caused by POMC mutations in humans. *Nat Genet* *19*, 155–157.
- Krützfeldt, J., Rajewsky, N., Braich, R., Rajeev, K. G., Tuschl, T., Manoharan, M. and Stoffel, M. (2005). Silencing of microRNAs in vivo with 'antagomirs'. *Nature* *438*, 685–689.
- Kubota, N., Terauchi, Y., Miki, H., Tamemoto, H., Yamauchi, T., Komeda, K., Satoh, S., Nakano, R., Ishii, C., Sugiyama, T., Eto, K., Tsubamoto, Y., Okuno, A., Murakami, K., Sekihara, H., Hasegawa, G., Naito, M., Toyoshima, Y., Tanaka, S., Shiota, K., Kitamura, T., Fujita, T., Ezaki, O., Aizawa, S. and Kadowaki, T. (1999). PPAR gamma mediates high-fat diet-induced adipocyte hypertrophy and insulin resistance. *Mol Cell* *4*, 597–609.
- Kubota, N., Terauchi, Y., Yamauchi, T., Kubota, T., Moroi, M., Matsui, J., Eto, K., Yamashita, T., Kamon, J., Satoh, H., Yano, W., Froguel, P., Nagai, R., Kimura, S., Kadowaki, T. and Noda, T. (2002). Disruption of adiponectin causes insulin resistance and neointimal formation. *J Biol Chem* *277*, 25863–25866.
- Kuhn, D. E., Martin, M. M., Feldman, D. S., Terry, A. V., Nuovo, G. J. and Elton, T. S. (2008). Experimental validation of miRNA targets. *Methods* *44*, 47–54.
- Kurth, T., Gaziano, J. M., Berger, K., Kase, C. S., Rexrode, K. M., Cook, N. R., Buring, J. E. and Manson, J. E. (2002). Body mass index and the risk of stroke in men. *Arch Intern Med* *162*, 2557–2562.
- Lagos-Quintana, M., Rauhut, R., Lendeckel, W. and Tuschl, T. (2001). Identification of novel genes coding for small expressed RNAs. *Science* *294*, 853–858.
- Lagos-Quintana, M., Rauhut, R., Yalcin, A., Meyer, J., Lendeckel, W. and Tuschl, T. (2002). Identification of tissue-specific microRNAs from mouse. *Curr Biol* *12*, 735–739.
- Laharrague, P. and Casteilla, L. (2010). The emergence of adipocytes. *Endocr Dev* *19*, 21–30.
- Lall, S., Grün, D., Krek, A., Chen, K., Wang, Y. L., Dewey, C. N., Sood, P., Colombo, T., Bray, N., Macmenamin, P., Kao, H. L., Gunsalus, K. C., Pachter, L., Piano, F. and Rajewsky, N. (2006). A genome-wide map of conserved microRNA targets in *C. elegans*. *Curr Biol* *16*, 460–471.
- Lanford, R. E., Hildebrandt-Eriksen, E. S., Petri, A., Persson, R., Lindow, M., Munk, M. E., Kauppinen, S. and Ørum, H. (2010). Therapeutic silencing of microRNA-122 in primates with chronic hepatitis C virus infection. *Science* *327*, 198–201.
- Lang, C. H., Dobrescu, C. and Bagby, G. J. (1992). Tumor necrosis factor impairs insulin action on peripheral glucose disposal and hepatic glucose output. *Endocrinology* *130*, 43–52.
- Laplante, M., Sell, H., MacNaul, K. L., Richard, D., Berger, J. P. and Deshaies, Y. (2003). PPAR-gamma activation mediates adipose depot-specific effects on gene expression and lipoprotein lipase activity: mechanisms for modulation of postprandial lipemia and differential adipose accretion. *Diabetes* *52*, 291–299.
- Lau, N. C., Lim, L. P., Weinstein, E. G. and Bartel, D. P. (2001). An abundant class of tiny RNAs with probable regulatory roles in *Caenorhabditis elegans*. *Science* *294*, 858–862.
- Lean, M. E. and James, W. P. (1986). Brown adipose tissue in man. pp. 339–365. London: Edward Arnold.
- Lebovitz, H. E. and Banerji, M. A. (2001). Insulin resistance and its treatment by thiazolidinediones. *Recent Prog Horm Res* , *56*, 265–294.
- Ledford, H. (2008). The death of microarrays? *Nature* , *455*, 847–847.
- Lee, E. K., Lee, M. J., Abdelmohsen, K., Kim, W., Kim, M. M., Srikantan, S., Martindale, J. L., Hutchinson, E. R., Kim, H. H., Marasa, B. S., Selimyan, R., Egan, J. M., Smith, S. R., Fried, S. K. and Gorospe, M. (2010). miR-130 suppresses adipogenesis by inhibiting PPARgamma expression. *Molecular and Cellular Biology* , *31*, 626–638.

- Lee, G. H., Proenca, R., Montez, J. M., Carroll, K. M., Darvishzadeh, J. G., Lee, J. I. and Friedman, J. M. (1996). Abnormal splicing of the leptin receptor in diabetic mice. *Nature* , *379*, 632–635.
- Lee, I., Ajay, S. S., Yook, J. I., Kim, H. S., Hong, S. H., Kim, N. H., Dhanasekaran, S. M., Chinnaiyan, A. M. and Athey, B. D. (2009). New class of microRNA targets containing simultaneous 5'-UTR and 3'-UTR interaction sites. *Genome Res* , *19*, 1175–1183.
- Lee, J. Y., Hashizaki, H., Goto, T., Sakamoto, T., Takahashi, N. and Kawada, T. (2011). Activation of peroxisome proliferator-activated receptor- α enhances fatty acid oxidation in human adipocytes. *Biochem Biophys Res Commun* , *407*, 818–822.
- Lee, K., Villena, J. A., Moon, Y. S., Kim, K. H., Lee, S., Kang, C. and Sul, H. S. (2003). Inhibition of adipogenesis and development of glucose intolerance by soluble preadipocyte factor-1 (Pref-1). *J Clin Invest* , *111*, 453–461.
- Lee, R. C. and Ambros, V. (2001). An extensive class of small RNAs in *Caenorhabditis elegans*. *Science* , *294*, 862–864.
- Lee, R. C., Feinbaum, R. L. and Ambros, V. (1993). The *C. elegans* heterochronic gene *lin-4* encodes small RNAs with antisense complementarity to *lin-14*. *Cell* , *75*, 843–854.
- Lee, Y. S. and Dutta, A. (2009). MicroRNAs in cancer. *Annu Rev Pathol* , *4*, 199–227.
- Lefterova, M. I., Zhang, Y., Steger, D. J., Schupp, M., Schug, J., Cristancho, A., Feng, D., Zhuo, D., Stoeckert, C. J., Liu, X. S. and Lazar, M. A. (2008). PPAR γ and C/EBP factors orchestrate adipocyte biology via adjacent binding on a genome-wide scale. *Genes Dev* , *22*, 2941–2952.
- Leonardsson, G., Steel, J. H., Christian, M., Pocock, V., Milligan, S., Bell, J., So, P. W., Medina-Gomez, G., Vidal-Puig, A., White, R. and Parker, M. G. (2004). Nuclear receptor corepressor RIP140 regulates fat accumulation. *Proc Natl Acad Sci U S A* , *101*, 8437–8442.
- Leung, A. K., Young, A. G., Bhutkar, A., Zheng, G. X., Bosson, A. D., Nielsen, C. B. and Sharp, P. A. (2011). Genome-wide identification of Ago2 binding sites from mouse embryonic stem cells with and without mature microRNAs. *Nat Struct Mol Biol* , *18*, 237–244.
- Lewis, B. P., Shih, I. H., Jones-Rhoades, M. W., Bartel, D. P. and Burge, C. B. (2003). Prediction of mammalian microRNA targets. *Cell* , *115*, 787–798.
- Li, J., Donath, S., Li, Y., Qin, D., Prabhakar, B. S. and Li, P. (2010). miR-30 regulates mitochondrial fission through targeting p53 and the dynamin-related protein-1 pathway. *PLoS Genet* , *6*.
- Liang, X., Kanjanabuch, T., Mao, S., Hao, C., Tang, Y., Declerck, P. J., Hastly, A. H., Wasserman, D. H., Fogo, A. B. and Ma, L. (2006). Plasminogen activator inhibitor-1 modulates adipocyte differentiation. *American Journal of Physiology. Endocrinology and Metabolism* , *290*, E103–E113.
- Lidell, M. E., Seifert, E. L., Westergren, R., Heglind, M., Gowing, A., Sukonina, V., Arani, Z., Itkonen, P., Wallin, S., Westberg, F., Fernandez-Rodriguez, J., Laakso, M., Nilsson, T., Peng, X. R., Harper, M. E. and Enerbäck, S. (2011). The adipocyte-expressed forkhead transcription factor *Foxc2* regulates metabolism through altered mitochondrial function. *Diabetes* , *60*, 427–435.
- Lijnen, H. R. (2005). Pleiotropic functions of plasminogen activator inhibitor-1. *Journal of Thrombosis and Haemostasis: JTH* , *3*, 35–45.
- Lijnen, H. R., Maquoi, E., Morange, P., Voros, G., Van Hoef, B., Kopp, F., Collen, D., Juhan-Vague, I. and Alessi, M. C. (2003). Nutritionally induced obesity is attenuated in transgenic mice overexpressing plasminogen activator inhibitor-1. *Arterioscler Thromb Vasc Biol* , *23*, 78–84.
- Lim, L. P., Lau, N. C., Garrett-Engle, P., Grimson, A., Schelter, J. M., Castle, J., Bartel, D. P., Linsley, P. S. and Johnson, J. M. (2005). Microarray analysis shows that some microRNAs downregulate large numbers of target mRNAs. *Nature* , *433*, 769–773.
- Lin, F. T. and Lane, M. D. (1992). Antisense CCAAT/enhancer-binding protein RNA suppresses coordinate gene expression and triglyceride accumulation during differentiation of 3T3-L1 preadipocytes. *Genes Dev* , *6*, 533–544.
- Lin, J., Handschin, C. and Spiegelman, B. M. (2005). Metabolic control through the PGC-1 family of transcription coactivators. *Cell Metab* , *1*, 361–370.

- Lin, J., Wu, P. H., Tarr, P. T., Lindenberg, K. S., St-Pierre, J., Zhang, C. Y., Mootha, V. K., Jäger, S., Vianna, C. R., Reznick, R. M., Cui, L., Manieri, M., Donovan, M. X., Wu, Z., Cooper, M. P., Fan, M. C., Rohas, L. M., Zavacki, A. M., Cinti, S., Shulman, G. I., Lowell, B. B., Krainc, D. and Spiegelman, B. M. (2004). Defects in adaptive energy metabolism with CNS-linked hyperactivity in PGC-1alpha null mice. *Cell* , *119*, 121–135.
- Lin, Q., Gao, Z., Alarcon, R. M., Ye, J. and Yun, Z. (2009). A role of miR-27 in the regulation of adipogenesis. *The FEBS Journal* , *276*, 2348–2358.
- Ling, H. Y., Wen, G. B., Feng, S. D., Tuo, Q. H., Ou, H. S., Yao, C. H., Zhu, B. Y., Gao, Z. P., Zhang, L. and Liao, D. F. (2011). MicroRNA-375 promotes 3T3-L1 adipocyte differentiation through modulation of extracellular signal-regulated kinase signalling. *Clin Exp Pharmacol Physiol* , *38*, 239–246.
- Linhart, H. G., Ishimura-Oka, K., DeMayo, F., Kibe, T., Repka, D., Poindexter, B., Bick, R. J. and Darlington, G. J. (2001). C/EBPalpha is required for differentiation of white, but not brown, adipose tissue. *Proc Natl Acad Sci U S A* , *98*, 12532–12537.
- Liu, N., Bezprozvannaya, S., Williams, A. H., Qi, X., Richardson, J. A., Bassel-Duby, R. and Olson, E. N. (2008). microRNA-133a regulates cardiomyocyte proliferation and suppresses smooth muscle gene expression in the heart. *Genes Dev* , *22*, 3242–3254.
- Liu, X., Rossmeisl, M., McClaine, J., Riachi, M., Harper, M. E. and Kozak, L. P. (2003). Paradoxical resistance to diet-induced obesity in UCP1-deficient mice. *J Clin Invest* , *111*, 399–407.
- Longo, K. A., Wright, W. S., Kang, S., Gerin, I., Chiang, S. H., Lucas, P. C., Opp, M. R. and MacDougald, O. A. (2004). Wnt10b inhibits development of white and brown adipose tissues. *J Biol Chem* , *279*, 35503–35509.
- López-Alemán, R., Redondo, J. M., Nagamine, Y. and Muñoz-Cánoves, P. (2003). Plasminogen activator inhibitor type-1 inhibits insulin signaling by competing with alphavbeta3 integrin for vitronectin binding. *Eur J Biochem* , *270*, 814–821.
- Loya, C. M., Lu, C. S., Van Vactor, D. and Fulga, T. A. (2009). Transgenic microRNA inhibition with spatiotemporal specificity in intact organisms. *Nat Methods* , *6*, 897–903.
- Lu, J., Getz, G., Miska, E. A., Alvarez-Saavedra, E., Lamb, J., Peck, D., Sweet-Cordero, A., Ebert, B. L., Mak, R. H., Ferrando, A. A., Downing, J. R., Jacks, T., Horvitz, H. R. and Golub, T. R. (2005). MicroRNA expression profiles classify human cancers. *Nature* , *435*, 834–838.
- Lunca, S., Perțea, M., Bouras, G., Dumitru, L. and Hatjissalatas, S. G. (2005). Morbid obesity: a surgical perspective. *Rom J Gastroenterol* , *14*, 151–158.
- Lund, E., Güttinger, S., Calado, A., Dahlberg, J. E. and Kutay, U. (2004). Nuclear export of microRNA precursors. *Science* , *303*, 95–98.
- Luo, J., Tang, M., Huang, J., He, B., Gao, J., Chen, L., Zuo, G., Zhang, W., Luo, Q., Shi, Q., Zhang, B., Bi, Y., Luo, X., Jiang, W., Su, Y., Shen, J., Kim, S. H., Huang, E., Gao, Y., Zhou, J., Yang, K., Luu, H. H., Pan, X., Haydon, R. C., Deng, Z. and He, T. (2010). TGFbeta/BMP type I receptors ALK1 and ALK2 are essential for BMP9-induced osteogenic signaling in mesenchymal stem cells. *The Journal of Biological Chemistry* , *285*, 29588–29598.
- Luque, C. A. and Rey, J. A. (1999). Sibutramine: a serotonin-norepinephrine reuptake-inhibitor for the treatment of obesity. *Ann Pharmacother* , *33*, 968–978.
- Luzi, E., Marini, F., Sala, S. C., Tognarini, I., Galli, G. and Brandi, M. L. (2008). Osteogenic differentiation of human adipose tissue-derived stem cells is modulated by the miR-26a targeting of the SMAD1 transcription factor. *J Bone Miner Res* , *23*, 287–295.
- Ma, L., Mao, S., Taylor, K. L., Kanjanabuch, T., Guan, Y., Zhang, Y., Brown, N. J., Swift, L. L., McGuinness, O. P., Wasserman, D. H., Vaughan, D. E. and Fogo, A. B. (2004). Prevention of obesity and insulin resistance in mice lacking plasminogen activator inhibitor 1. *Diabetes* , *53*, 336–346.
- Macías-Silva, M., Hoodless, P. A., Tang, S. J., Buchwald, M. and Wrana, J. L. (1998). Specific activation of Smad1 signaling pathways by the BMP7 type I receptor, ALK2. *The Journal of Biological Chemistry* , *273*, 25628–25636.
- Madsen, L., Pedersen, L. M., Lillefosse, H. H., Fjaere, E., Bronstad, I., Hao, Q., Petersen, R. K., Hallenborg, P., Ma, T., De Matteis, R., Araujo, P., Mercader, J., Bonet, M. L., Hansen, J. B., Cannon, B., Nedergaard, J., Wang, J., Cinti, S., Voshol, P., Dorskeland, S. O. and Kristiansen, K. (2010). UCP1 induction during recruitment of brown adipocytes in white adipose tissue is dependent on cyclooxygenase activity. *PLoS One* , *5*.

- Madsen, L., Petersen, R. K., Sørensen, M. B., Jørgensen, C., Hallenborg, P., Pridal, L., Fleckner, J., Amri, E., Krieg, P., Furstenberger, G., Berge, R. K. and Kristiansen, K. (2003). Adipocyte differentiation of 3T3-L1 preadipocytes is dependent on lipoxygenase activity during the initial stages of the differentiation process. *The Biochemical Journal* , *375*, 539–549.
- Maeda, K., Okubo, K., Shimomura, I., Funahashi, T., Matsuzawa, Y. and Matsubara, K. (1996). cDNA cloning and expression of a novel adipose specific collagen-like factor, apM1 (AdiPose Most abundant Gene transcript 1). *Biochem Biophys Res Commun* , *221*, 286–289.
- Maeda, N., Shimomura, I., Kishida, K., Nishizawa, H., Matsuda, M., Nagaretani, H., Furuyama, N., Kondo, H., Takahashi, M., Arita, Y., Komuro, R., Ouchi, N., Kihara, S., Tochino, Y., Okutomi, K., Horie, M., Takeda, S., Aoyama, T., Funahashi, T. and Matsuzawa, Y. (2002). Diet-induced insulin resistance in mice lacking adiponectin/ACRP30. *Nat Med* , *8*, 731–737.
- Maeda, N., Takahashi, M., Funahashi, T., Kihara, S., Nishizawa, H., Kishida, K., Nagaretani, H., Matsuda, M., Komuro, R., Ouchi, N., Kuriyama, H., Hotta, K., Nakamura, T., Shimomura, I. and Matsuzawa, Y. (2001). PPARgamma ligands increase expression and plasma concentrations of adiponectin, an adipose-derived protein. *Diabetes* , *50*, 2094–2099.
- Maffei, M., Halaas, J., Ravussin, E., Pratley, R. E., Lee, G. H., Zhang, Y., Fei, H., Kim, S., Lallone, R. and Ranganathan, S. (1995). Leptin levels in human and rodent: measurement of plasma leptin and ob RNA in obese and weight-reduced subjects. *Nat Med* , *1*, 1155–1161.
- Maillot, G., Lacroix-Triki, M., Pierredon, S., Grataudou, L., Schmidt, S., Bénès, V., Roché, H., Dalenc, F., Auboeuf, D., Millevoi, S. and Vagner, S. (2009). Widespread estrogen-dependent repression of microRNAs involved in breast tumor cell growth. *Cancer Res* , *69*, 8332–8340.
- Mair, W. and Dillin, A. (2008). Aging and survival: the genetics of life span extension by dietary restriction. *Annu Rev Biochem* , *77*, 727–754.
- Majid, S., Dar, A. A., Saini, S., Yamamura, S., Hirata, H., Tanaka, Y., Deng, G. and Dahiya, R. (2010). MicroRNA-205-directed transcriptional activation of tumor suppressor genes in prostate cancer. *Cancer* , *116*, 5637–5649.
- Majka, S. M., Fox, K. E., Psilas, J. C., Helm, K. M., Childs, C. R., Acosta, A. S., Janssen, R. C., Friedman, J. E., Woessner, B. T., Shade, T. R., Varella-Garcia, M. and Klemm, D. J. (2010). De novo generation of white adipocytes from the myeloid lineage via mesenchymal intermediates is age, adipose depot, and gender specific. *Proc Natl Acad Sci U S A* , *107*, 14781–14786.
- MAQC Consortium, Shi, L., Reid, L. H., Jones, W. D., Shippy, R., Warrington, J. A., Baker, S. C., Collins, P. J., de Longueville, F., Kawasaki, E. S., Lee, K. Y., Luo, Y., Sun, Y. A., Willey, J. C., Setterquist, R. A., Fischer, G. M., Tong, W., Dragan, Y. P., Dix, D. J., Frueh, F. W. and Goodsaid, F M et al. (2006). The MicroArray Quality Control (MAQC) project shows inter- and intraplatform reproducibility of gene expression measurements. *Nat Biotechnol* , *24*, 1151–1161.
- Maroney, P. A., Yu, Y., Fisher, J. and Nilsen, T. W. (2006). Evidence that microRNAs are associated with translating messenger RNAs in human cells. *Nat Struct Mol Biol* , *13*, 1102–1107.
- Martinelli, R., Nardelli, C., Pilone, V., Buonomo, T., Liguori, R., Castanò, I., Buono, P., Masone, S., Persico, G., Forestieri, P., Pastore, L. and Sacchetti, L. (2010). miR-519d overexpression is associated with human obesity. *Obesity (Silver Spring)* , *18*, 2170–2176.
- Massiera, F., Barbry, P., Guesnet, P., Joly, A., Luquet, S., Moreilhon-Brest, C., Mohsen-Kanson, T., Amri, E. Z. and Ailhaud, G. (2010). A Western-like fat diet is sufficient to induce a gradual enhancement in fat mass over generations. *J Lipid Res* , *51*, 2352–2361.
- Massiera, F., Bloch-Faure, M., Ceiler, D., Murakami, K., Fukamizu, A., Gasc, J. M., Quignard-Boulange, A., Negrel, R., Ailhaud, G., Seydoux, J., Meneton, P. and Teboul, M. (2001). Adipose angiotensinogen is involved in adipose tissue growth and blood pressure regulation. *FASEB J* , *15*, 2727–2729.
- Massiera, F., Saint-Marc, P., Seydoux, J., Murata, T., Kobayashi, T., Narumiya, S., Guesnet, P., Amri, E. Z., Negrel, R. and Ailhaud, G. (2003). Arachidonic acid and prostacyclin signaling promote adipose tissue development: a human health concern? *J Lipid Res* , *44*, 271–279.
- Mathew, B., Francis, L., Kayalar, A. and Cone, J. (2008). Obesity: effects on cardiovascular disease and its diagnosis. *J Am Board Fam Med* , *21*, 562–568.

- Mattick, J. S. (2001). Non-coding RNAs: the architects of eukaryotic complexity. *EMBO Rep* , 2, 986–991.
- Maumus, M., Peyrafitte, J. A., D'Angelo, R., Fournier-Wirth, C., Bouloumie, A., Casteilla, L., Sengenès, C. and Bourin, P. (2011). Native human adipose stromal cells: localization, morphology and phenotype. *Int J Obes (Lond)* , *Epub ahead of print*.
- McCarthy, J. J. (2008). MicroRNA-206: the skeletal muscle-specific myomiR. *Biochim Biophys Acta* , 1779, 682–691.
- Mello, C. C. and Conte, D. (2004). Revealing the world of RNA interference. *Nature* , 431, 338–342.
- Mestdagh, P., Van Vlierberghe, P., De Weer, A., Muth, D., Westermann, F., Speleman, F. and Vandesompele, J. (2009). A novel and universal method for microRNA RT-qPCR data normalization. *Genome Biol* , 10.
- Miller, C. W., Casimir, D. A. and Ntambi, J. M. (1996). The mechanism of inhibition of 3T3-L1 preadipocyte differentiation by prostaglandin F2alpha. *Endocrinology* , 137, 5641–5650.
- Miranda, K. C., Huynh, T., Tay, Y., Ang, Y. S., Tam, W. L., Thomson, A. M., Lim, B. and Rigoutsos, I. (2006). A pattern-based method for the identification of MicroRNA binding sites and their corresponding heteroduplexes. *Cell* , 126, 1203–1217.
- Mitchell, P. S., Parkin, R. K., Kroh, E. M., Fritz, B. R., Wyman, S. K., Pogosova-Agadjanian, E. L., Peterson, A., Noteboom, J., O'Briant, K. C., Allen, A., Lin, D. W., Urban, N., Drescher, C. W., Knudsen, B. S., Stirewalt, D. L., Gentleman, R., Vessella, R. L., Nelson, P. S., Martin, D. B. and Tewari, M. (2008). Circulating microRNAs as stable blood-based markers for cancer detection. *Proc Natl Acad Sci U S A* , 105, 10513–10518.
- Mitra, S., Mazumder Indra, D., Bhattacharya, N., Singh, R. K., Basu, P. S., Mondal, R. K., Roy, A., Zabarovsky, E. R., Roychoudhury, S. and Panda, C. K. (2010). RBSP3 is frequently altered in premalignant cervical lesions: clinical and prognostic significance. *Genes Chromosomes Cancer* , 49, 155–170.
- Miyazono, K. (2000). TGF-beta signaling by Smad proteins. *Cytokine Growth Factor Rev* , 11, 15–22.
- Mohamed, J. S., Lopez, M. A. and Boriek, A. M. (2010). Mechanical stretch up-regulates microRNA-26a and induces human airway smooth muscle hypertrophy by suppressing glycogen synthase kinase-3b. *J Biol Chem* , 285, 29336–29347.
- Mokdad, A. H., Ford, E. S., Bowman, B. A., Dietz, W. H., Vinicor, F., Bales, V. S. and Marks, J. S. (2003). Prevalence of obesity, diabetes, and obesity-related health risk factors, 2001. *JAMA* , 289, 76–79.
- Monteys, A. M., Spengler, R. M., Wan, J., Tecedor, L., Lennox, K. A., Xing, Y. and Davidson, B. L. (2010). Structure and activity of putative intronic miRNA promoters. *RNA* , 16, 495–505.
- Moon, Y. S., Smas, C. M., Lee, K., Villena, J. A., Kim, K. H., Yun, E. J. and Sul, H. S. (2002). Mice lacking paternally expressed Pref-1/Dlk1 display growth retardation and accelerated adiposity. *Mol Cell Biol* , 22, 5585–5592.
- Morange, P. E., Alessi, M. C., Verdier, M., Casanova, D., Magalon, G. and Juhan-Vague, I. (1999). PAI-1 produced ex vivo by human adipose tissue is relevant to PAI-1 blood level. *Arteriosclerosis, Thrombosis, and Vascular Biology* , 19, 1361–1365.
- Morange, P. E., Lijnen, H. R., Alessi, M. C., Kopp, F., Collen, D. and Juhan-Vague, I. (2000). Influence of PAI-1 on adipose tissue growth and metabolic parameters in a murine model of diet-induced obesity. *Arteriosclerosis, Thrombosis, and Vascular Biology* , 20, 1150–1154.
- Morganstein, D. L., Wu, P., Mane, M. R., Fisk, N. M., White, R. and Parker, M. G. (2010). Human fetal mesenchymal stem cells differentiate into brown and white adipocytes: a role for ERRalpha in human UCP1 expression. *Cell Res* , 20, 434–444.
- Morikawa, M., Nixon, T. and Green, H. (1982). Growth hormone and the adipose conversion of 3T3 cells. *Cell* , 29, 783–789.
- Morin, R. D., O'Connor, M. D., Griffith, M., Kuchenbauer, F., Delaney, A., Prabhu, A. L., Zhao, Y., McDonald, H., Zeng, T., Hirst, M., Eaves, C. J. and Marra, M. A. (2008). Application of massively parallel sequencing to microRNA profiling and discovery in human embryonic stem cells. *Genome Res* , 18, 610–621.
- Mudhasani, R., Imbalzano, A. N. and Jones, S. N. (2010). An essential role for Dicer in adipocyte differentiation. *J Cell Biochem* , 110, 812–816.

- Mudhasani, R., Puri, V., Hoover, K., Czech, M. P., Imbalzano, A. N. and Jones, S. N. (2011). Dicer is required for the formation of white but not brown adipose tissue. *J Cell Physiol* , *226*, 1399–1406.
- Mueller, E., Drori, S., Aiyer, A., Yie, J., Sarraf, P., Chen, H., Hauser, S., Rosen, E. D., Ge, K., Roeder, R. G. and Spiegelman, B. M. (2002). Genetic analysis of adipogenesis through peroxisome proliferator-activated receptor gamma isoforms. *J Biol Chem* , *277*, 41925–41930.
- Mufamadi, M. S., Pillay, V., Choonara, Y. E., Du Toit, L. C., Modi, G., Naidoo, D. and Ndesendo, V. M. (2011). A review on composite liposomal technologies for specialized drug delivery. *J Drug Deliv* , *2011*, 939851–939851.
- Najafi-Shoushtari, S. H., Kristo, F., Li, Y., Shioda, T., Cohen, D. E., Gerszten, R. E. and Näär, A. M. (2010). MicroRNA-33 and the SREBP host genes cooperate to control cholesterol homeostasis. *Science* , *328*, 1566–1569.
- Nakano, Y., Tobe, T., Choi-Miura, N. H., Mazda, T. and Tomita, M. (1996). Isolation and characterization of GBP28, a novel gelatin-binding protein purified from human plasma. *J Biochem* , *120*, 803–812.
- Nedergaard, J., Bengtsson, T. and Cannon, B. (2007). Unexpected evidence for active brown adipose tissue in adult humans. *American Journal of Physiology. Endocrinology and Metabolism* , *293*, E444–452.
- Nedergaard, J. and Cannon, B. (2010). The changed metabolic world with human brown adipose tissue: therapeutic visions. *Cell Metab* , *11*, 268–272.
- Nedergaard, J., Cannon, B. and Lindberg, O. (1977). Microcalorimetry of isolated mammalian cells. *Nature* , *267*, 518–520.
- Nedergaard, J., Golozoubova, V., Matthias, A., Asadi, A., Jacobsson, A. and Cannon, B. (2001). UCP1: the only protein able to mediate adaptive non-shivering thermogenesis and metabolic inefficiency. *Biochimica Et Biophysica Acta* , *1504*, 82–106.
- Nedergaard, J. and Lindberg, O. (1979). Norepinephrine-stimulated fatty-acid release and oxygen consumption in isolated hamster brown-fat cells. Influence of buffers, albumin, insulin and mitochondrial inhibitors. *Eur J Biochem* , *95*, 139–145.
- Négrel, R., Gaillard, D. and Ailhaud, G. (1989). Prostacyclin as a potent effector of adipose-cell differentiation. *Biochem J* , *257*, 399–405.
- Négrel, R., Grimaldi, P. and Ailhaud, G. (1978). Establishment of preadipocyte clonal line from epididymal fat pad of ob/ob mouse that responds to insulin and to lipolytic hormones. *Proc Natl Acad Sci U S A* , *75*, 6054–6058.
- Newell, F. S., Su, H., Tornqvist, H., Whitehead, J. P., Prins, J. B. and Hutley, L. J. (2006). Characterization of the transcriptional and functional effects of fibroblast growth factor-1 on human preadipocyte differentiation. *FASEB J* , *20*, 2615–2617.
- Ng, E. K., Chong, W. W., Jin, H., Lam, E. K., Shin, V. Y., Yu, J., Poon, T. C., Ng, S. S. and Sung, J. J. (2009). Differential expression of microRNAs in plasma of patients with colorectal cancer: a potential marker for colorectal cancer screening. *Gut* , *58*, 1375–1381.
- Nicholls, D. G. (1976). Hamster brown-adipose-tissue mitochondria. Purine nucleotide control of the ion conductance of the inner membrane, the nature of the nucleotide binding site. *Eur J Biochem* , *62*, 223–228.
- Nicholls, D. G. (2006). The physiological regulation of uncoupling proteins. *Biochim Biophys Acta* , *1757*, 459–466.
- Nicolas, F. E., Pais, H., Schwach, F., Lindow, M., Kauppinen, S., Moulton, V. and Dalmay, T. (2008). Experimental identification of microRNA-140 targets by silencing and overexpressing miR-140. *RNA* , *14*, 2513–2520.
- Nixon, T. and Green, H. (1984). Contribution of growth hormone to the adipogenic activity of serum. *Endocrinology* , *114*, 527–532.
- Nussey, S. and Whitehead, S. (2001). *Endocrinology: An Integrated Approach.*, chapter 2. The endocrine pancreas. Oxford OX4 1RE, UK: Oxford: BIOS Scientific Publishers.
- Obad, S., dos Santos, C. O., Petri, A., Heidenblad, M., Broom, O., Ruse, C., Fu, C., Lindow, M., Stenvang, J., Straarup, E. M., Hansen, H. F., Koch, T., Pappin, D., Hannon, G. J. and Kauppinen, S. (2011). Silencing of microRNA families by seed-targeting tiny LNAs. *Nat Genet* , *43*, 371–378.
- Obernosterer, G., Tafer, H. and Martinez, J. (2008). Target site effects in the RNA interference and microRNA pathways. *Biochem Soc Trans* , *36*, 1216–1219.

- Ogden, C. L., Carroll, M. D., Curtin, L. R., McDowell, M. A., Tabak, C. J. and Flegal, K. M. (2006). Prevalence of overweight and obesity in the United States, 1999-2004. *JAMA* , *295*, 1549-1555.
- Ohlson, L. O., Larsson, B., Svärdsudd, K., Welin, L., Eriksson, H., Wilhelmsen, L., Björntorp, P. and Tibblin, G. (1985). The influence of body fat distribution on the incidence of diabetes mellitus. 13.5 years of follow-up of the participants in the study of men born in 1913. *Diabetes* , *34*, 1055-1058.
- Okamoto, Y., Kihara, S., Ouchi, N., Nishida, M., Arita, Y., Kumada, M., Ohashi, K., Sakai, N., Shimomura, I., Kobayashi, H., Terasaka, N., Inaba, T., Funahashi, T. and Matsuzawa, Y. (2002). Adiponectin reduces atherosclerosis in apolipoprotein E-deficient mice. *Circulation* , *106*, 2767-2770.
- Oskowitz, A. Z., Lu, J., Penfornis, P., Ylostalo, J., McBride, J., Flemington, E. K., Prockop, D. J. and Pochampally, R. (2008). Human multipotent stromal cells from bone marrow and microRNA: regulation of differentiation and leukemia inhibitory factor expression. *Proc Natl Acad Sci U S A* , *105*, 18372-18377.
- Oswal, A. and Yeo, G. (2010). Leptin and the control of body weight: a review of its diverse central targets, signaling mechanisms, and role in the pathogenesis of obesity. *Obesity (Silver Spring)* , *18*, 221-229.
- Otto, T. C. and Lane, M. D. (2005). Adipose development: from stem cell to adipocyte. *Crit Rev Biochem Mol Biol* , *40*, 229-242.
- Ouchi, N., Kihara, S., Arita, Y., Maeda, K., Kuriyama, H., Okamoto, Y., Hotta, K., Nishida, M., Takahashi, M., Nakamura, T., Yamashita, S., Funahashi, T. and Matsuzawa, Y. (1999). Novel modulator for endothelial adhesion molecules: adipocyte-derived plasma protein adiponectin. *Circulation* , *100*, 2473-2476.
- Ouchi, N., Kihara, S., Arita, Y., Okamoto, Y., Maeda, K., Kuriyama, H., Hotta, K., Nishida, M., Takahashi, M., Muraguchi, M., Ohmoto, Y., Nakamura, T., Yamashita, S., Funahashi, T. and Matsuzawa, Y. (2000). Adiponectin, an adipocyte-derived plasma protein, inhibits endothelial NF-kappaB signaling through a cAMP-dependent pathway. *Circulation* , *102*, 1296-1301.
- Ozsolak, F., Poling, L. L., Wang, Z., Liu, H., Liu, X. S., Roeder, R. G., Zhang, X., Song, J. S. and Fisher, D. E. (2008). Chromatin structure analyses identify miRNA promoters. *Genes Dev* , *22*, 3172-3183.
- Pabinger, S., Thallinger, G. G., Snajder, R., Eichhorn, H., Rader, R. and Trajanoski, Z. (2009). QPCR: Application for real-time PCR data management and analysis. *BMC Bioinformatics* , *10*, 268.
- Padwal, R., Li, S. K. and Lau, D. C. (2003). Long-term pharmacotherapy for obesity and overweight. *Cochrane Database Syst Rev* , *4*.
- Pairault, J. and Green, H. (1979). A study of the adipose conversion of suspended 3T3 cells by using glycerophosphate dehydrogenase as differentiation marker. *Proc Natl Acad Sci U S A* , *76*, 5138-5142.
- Pan, D., Fujimoto, M., Lopes, A. and Wang, Y. X. (2009). Twist-1 is a PPARdelta-inducible, negative-feedback regulator of PGC-1alpha in brown fat metabolism. *Cell* , *137*, 73-86.
- Pannacciulli, N., Mitrio, V. D., Marino, R., Giorgino, R. and Pergola, G. D. (2002). Effect of glucose tolerance status on PAI-1 plasma levels in overweight and obese subjects. *Obesity Research* , *10*, 717-725.
- Pasquinelli, A. E., Reinhart, B. J., Slack, F., Martindale, M. Q., Kuroda, M. I., Maller, B., Hayward, D. C., Ball, E. E., Degnan, B., Müller, P., Spring, J., Srinivasan, A., Fishman, M., Finnerty, J., Corbo, J., Levine, M., Leahy, P., Davidson, E. and Ruvkun, G. (2000). Conservation of the sequence and temporal expression of let-7 heterochronic regulatory RNA. *Nature* , *408*, 86-89.
- Patel, N., Tahara, S. M., Malik, P. and Kalra, V. K. (2011). Involvement of miR-30c and miR-301a in immediate induction of plasminogen activator inhibitor-1 by placental growth factor in human pulmonary endothelial cells. *Biochem J* , *434*, 473-482.
- Patton, J. S., Shepard, H. M., Wilking, H., Lewis, G., Aggarwal, B. B., Eessalu, T. E., Gavin, L. A. and Grunfeld, C. (1986). Interferons and tumor necrosis factors have similar catabolic effects on 3T3 L1 cells. *Proc Natl Acad Sci U S A* , *83*, 8313-8317.
- Petersen, R. K., Jorgensen, C., Rustan, A. C., Froyland, L., Muller-Decker, K., Furstenberger, G., Berge, R. K., Kristiansen, K. and Madsen, L. (2003). Arachidonic acid-dependent inhibition of adipocyte differentiation requires PKA activity and is associated with sustained expression of cyclooxygenases. *J Lipid Res* , *44*, 2320-2330.

- Petrovic, N., Walden, T. B., Shabalina, I. G., Timmons, J. A., Cannon, B. and Nedergaard, J. (2010). Chronic peroxisome proliferator-activated receptor gamma (PPARgamma) activation of epididymally derived white adipocyte cultures reveals a population of thermogenically competent, UCP1-containing adipocytes molecularly distinct from classic brown adipocytes. *J Biol Chem* , *285*, 7153–7164.
- Pfaffl, M. W. (2001). A new mathematical model for relative quantification in real-time RT-PCR. *Nucleic Acids Res* , *29*.
- Pi-Sunyer, F. X. (2002). The obesity epidemic: pathophysiology and consequences of obesity. *Obes Res* , *10 Suppl 2*, –104.
- Pieler, R., Sanchez-Cabo, F., Hackl, H., Thallinger, G. G. and Trajanoski, Z. (2004). ArrayNorm: comprehensive normalization and analysis of microarray data. *Bioinformatics (Oxford, England)* , *20*, 1971–1973.
- Pilgrim, C. (1971). DNA synthesis and differentiation in developing white adipose tissue. *Dev Biol* , *26*, 69–76.
- Pillai, R. S., Bhattacharyya, S. N., Artus, C. G., Zoller, T., Cougot, N., Basyuk, E., Bertrand, E. and Filipowicz, W. (2005). Inhibition of translational initiation by Let-7 MicroRNA in human cells. *Science* , *309*, 1573–1576.
- Pittenger, M. F., Mackay, A. M., Beck, S. C., Jaiswal, R. K., Douglas, R., Mosca, J. D., Moorman, M. A., Simonetti, D. W., Craig, S. and Marshak, D. R. (1999). Multilineage potential of adult human mesenchymal stem cells. *Science* , *284*, 143–147.
- Place, R. F., Li, L. C., Pookot, D., Noonan, E. J. and Dahiya, R. (2008). MicroRNA-373 induces expression of genes with complementary promoter sequences. *Proc Natl Acad Sci U S A* , *105*, 1608–1613.
- Plagemann, A., Harder, T., Brunn, M., Harder, A., Roepke, K., Wittrock-Staar, M., Ziska, T., Schellong, K., Rodekamp, E., Melchior, K. and Dudenhausen, J. W. (2009). Hypothalamic proopiomelanocortin promoter methylation becomes altered by early overfeeding: an epigenetic model of obesity and the metabolic syndrome. *J Physiol* , *587*, 4963–4976.
- Plum, L., Rother, E., Münzberg, H., Wunderlich, F. T., Morgan, D. A., Hampel, B., Shanabrough, M., Janoschek, R., Könnner, A. C., Alber, J., Suzuki, A., Krone, W., Horvath, T. L., Rahmouni, K. and Brüning, J. C. (2007). Enhanced leptin-stimulated Pi3k activation in the CNS promotes white adipose tissue transdifferentiation. *Cell Metab* , *6*, 431–445.
- Poulos, S. P., Hausman, D. B. and Hausman, G. J. (2010). The development and endocrine functions of adipose tissue. *Mol Cell Endocrinol* , *323*, 20–34.
- Powell, T. M. and Khera, A. (2010). Therapeutic approaches to obesity. *Curr Treat Options Cardiovasc Med* , *12*, 381–395.
- Poy, M. N., Eliasson, L., Krutzfeldt, J., Kuwajima, S., Ma, X., Macdonald, P. E., Pfeffer, S., Tuschl, T., Rajewsky, N., Rorsman, P. and Stoffel, M. (2004). A pancreatic islet-specific microRNA regulates insulin secretion. *Nature* , *432*, 226–230.
- Poy, M. N., Hausser, J., Trajkovski, M., Braun, M., Collins, S., Rorsman, P., Zavolan, M. and Stoffel, M. (2009). miR-375 maintains normal pancreatic alpha- and beta-cell mass. *Proc Natl Acad Sci U S A* , *106*, 5813–5818.
- Prestwich, T. C. and MacDougald, O. A. (2007). Wnt/beta-catenin signaling in adipogenesis and metabolism. *Curr Opin Cell Biol* , *19*, 612–617.
- Prokesch, A., Bogner-Strauss, J. G., Hackl, H., Rieder, D., Neuhold, C., Walenta, E., Krogsdam, A., Scheideler, M., Papak, C., Wong, W. C., Vinson, C., Eisenhaber, F. and Trajanoski, Z. (2011). Arxes: retrotransposed genes required for adipogenesis. *Nucleic Acids Res* , *39*, 3224–3239.
- Puigserver, P., Wu, Z., Park, C. W., Graves, R., Wright, M. and Spiegelman, B. M. (1998). A cold-inducible coactivator of nuclear receptors linked to adaptive thermogenesis. *Cell* , *92*, 829–839.
- Qiu, Z., Wei, Y., Chen, N., Jiang, M., Wu, J. and Liao, K. (2001). DNA synthesis and mitotic clonal expansion is not a required step for 3T3-L1 preadipocyte differentiation into adipocytes. *J Biol Chem* , *276*, 11988–11995.
- Rankinen, T., Zuberi, A., Chagnon, Y. C., Weisnagel, S. J., Argyropoulos, G., Walts, B., Pérusse, L. and Bouchard, C. (2006). The human obesity gene map: the 2005 update. *Obesity (Silver Spring, Md.)* , *14*, 529–644.
- Ratcliff, F. G., MacFarlane, S. A. and Baulcombe, D. C. (1999). Gene silencing without DNA. rna-mediated cross-protection between viruses. *Plant Cell* , *11*, 1207–1216.

- Ravussin, E., Lillioja, S., Knowler, W. C., Christin, L., Freymond, D., Abbott, W. G., Boyce, V., Howard, B. V. and Bogardus, C. (1988). Reduced rate of energy expenditure as a risk factor for body-weight gain. *N Engl J Med* , *318*, 467–472.
- Raymond, C. K., Roberts, B. S., Garrett-Engle, P., Lim, L. P. and Johnson, J. M. (2005). Simple, quantitative primer-extension PCR assay for direct monitoring of microRNAs and short-interfering RNAs. *RNA* , *11*, 1737–1744.
- Rayner, K. J., Suárez, Y., Dávalos, A., Parathath, S., Fitzgerald, M. L., Tamehiro, N., Fisher, E. A., Moore, K. J. and Fernández-Hernando, C. (2010). MiR-33 contributes to the regulation of cholesterol homeostasis. *Science* , *328*, 1570–1573.
- Rebuffé-Scrive, M., Krotkiewski, M., Elfverson, J. and Björntorp, P. (1988). Muscle and adipose tissue morphology and metabolism in Cushing's syndrome. *J Clin Endocrinol Metab* , *67*, 1122–1128.
- Rederstorff, M. and Hüttenhofer, A. (2011). cDNA library generation from ribonucleoprotein particles. *Nat Protoc* , *6*, 166–174.
- Regulus Therapeutics (2010). Regulus Therapeutics Secures Additional Patents on microRNA Therapeutics for the Treatment of Hepatitis C Virus (HCV) Infection. Retrieved from <http://www.businesswire.com/news/home/20100923005479/en/Regulus-Therapeutics-Secures-Additional-Patents-microRNA-Therapeutics>. accessed: 2011-05-25.
- Rehmark, S., Kopecky, J., Jacobsson, A., Néchad, M., Herron, D., Nelson, B. D., Obregon, M. J., Nedergaard, J. and Cannon, B. (1989). Brown adipocytes differentiated in vitro can express the gene for the uncoupling protein thermogenin: effects of hypothyroidism and norepinephrine. *Exp Cell Res* , *182*, 75–83.
- Reinhart, B. J., Slack, F. J., Basson, M., Pasquinelli, A. E., Bettinger, J. C., Rougvie, A. E., Horvitz, H. R. and Ruvkun, G. (2000). The 21-nucleotide let-7 RNA regulates developmental timing in *Caenorhabditis elegans*. *Nature* , *403*, 901–906.
- Ricquier, D., Gaillard, J. L. and Turc, J. M. (1979). Microcalorimetry of isolated mitochondria from brown adipose tissue. Effect of guanosine-di-phosphate. *FEBS Lett* , *99*, 203–206.
- Ricquier, D. and Kader, J. C. (1976). Mitochondrial protein alteration in active brown fat: a sodium dodecyl sulfate-polyacrylamide gel electrophoretic study. *Biochem Biophys Res Commun* , *73*, 577–583.
- Robinson, M. K. (2009). Surgical treatment of obesity—weighing the facts. *N Engl J Med* , *361*, 520–521.
- Rodriguez, A., Elabd, C., Delteil, F., Astier, J., Vernochet, C., Saint-Marc, P., Guesnet, J., Guezennec, A., Amri, E., Dani, C. and Ailhaud, G. (2004a). Adipocyte differentiation of multipotent cells established from human adipose tissue. *Biochemical and Biophysical Research Communications* , *315*, 255–263.
- Rodriguez, A., Griffiths-Jones, S., Ashurst, J. L. and Bradley, A. (2004b). Identification of mammalian microRNA host genes and transcription units. *Genome Res* , *14*, 1902–1910.
- Rodriguez, A., Pisani, D., Dechesne, C. A., Turc-Carel, C., Kurzenne, J., Wdziekonski, B., Villageois, A., Bagnis, C., Breitmayer, J., Groux, H., Ailhaud, G. and Dani, C. (2005). Transplantation of a multipotent cell population from human adipose tissue induces dystrophin expression in the immunocompetent mdx mouse. *The Journal of Experimental Medicine* , *201*, 1397–1405.
- Rodriguez, A., Vigorito, E., Clare, S., Warren, M. V., Couttet, P., Soond, D. R., van Dongen, S., Grocock, R. J., Das, P. P., Miska, E. A., Vetrie, D., Okkenhaug, K., Enright, A. J., Dougan, G., Turner, M. and Bradley, A. (2007). Requirement of bic/microRNA-155 for normal immune function. *Science* , *316*, 608–611.
- Rohlf, E. M., Daniel, K. W., Premont, R. T., Kozak, L. P. and Collins, S. (1995). Regulation of the uncoupling protein gene (Ucp) by beta 1, beta 2, and beta 3-adrenergic receptor subtypes in immortalized brown adipose cell lines. *J Biol Chem* , *270*, 10723–10732.
- Ron, D., Brasier, A. R., McGehee, R. E. and Habener, J. F. (1992). Tumor necrosis factor-induced reversal of adipocytic phenotype of 3T3-L1 cells is preceded by a loss of nuclear CCAAT/enhancer binding protein (C/EBP). *J Clin Invest* , *89*, 223–233.
- Rosen, E. D. and MacDougald, O. A. (2006). Adipocyte differentiation from the inside out. *Nature Reviews Molecular Cell Biology* , *7*, 885–896.

- Rosen, E. D., Sarraf, P., Troy, A. E., Bradwin, G., Moore, K., Milstone, D. S., Spiegelman, B. M. and Mortensen, R. M. (1999). PPAR gamma is required for the differentiation of adipose tissue in vivo and in vitro. *Mol Cell* , *4*, 611–617.
- Rosen, E. D. and Spiegelman, B. M. (2000). Molecular regulation of adipogenesis. *Annu Rev Cell Dev Biol* , *16*, 145–171.
- Ross, A. S., Tsang, R., Shewmake, K. and McGehee, R. E. (2008). Expression of p107 and p130 during human adipose-derived stem cell adipogenesis. *Biochem Biophys Res Commun* , *366*, 927–931.
- Ross, S. E., Hemati, N., Longo, K. A., Bennett, C. N., Lucas, P. C., Erickson, R. L. and MacDougald, O. A. (2000). Inhibition of adipogenesis by Wnt signaling. *Science* , *289*, 950–953.
- Rothwell, N. J. and Stock, M. J. (1979). A role for brown adipose tissue in diet-induced thermogenesis. *Nature* , *281*, 31–35.
- Rothwell, N. J. and Stock, M. J. (1981). Influence of noradrenaline on blood flow to brown adipose tissue in rats exhibiting diet-induced thermogenesis. *Pflugers Arch* , *389*, 237–242.
- Rothwell, N. J. and Stock, M. J. (1983). Luxuskonsumtion, diet-induced thermogenesis and brown fat: the case in favour. *Clin Sci (Lond)* , *64*, 19–23.
- Sacks, F. M., Bray, G. A., Carey, V. J., Smith, S. R., Ryan, D. H., Anton, S. D., McManus, K., Champagne, C. M., Bishop, L. M., Laranjo, N., Leboff, M. S., Rood, J. C., de Jonge, L., Greenway, F. L., Loria, C. M., Obarzanek, E. and Williamson, D. A. (2009). Comparison of weight-loss diets with different compositions of fat, protein, and carbohydrates. *N Engl J Med* , *360*, 859–873.
- Saini, H. K., Griffiths-Jones, S. and Enright, A. J. (2007). Genomic analysis of human microRNA transcripts. *Proc Natl Acad Sci U S A* , *104*, 17719–17724.
- Saint-Marc, P., Kozak, L. P., Ailhaud, G., Darimont, C. and Negrel, R. (2001). Angiotensin II as a trophic factor of white adipose tissue: stimulation of adipose cell formation. *Endocrinology* , *142*, 487–492.
- Saito, M., Okamatsu-Ogura, Y., Matsushita, M., Watanabe, K., Yoneshiro, T., Nio-Kobayashi, J., Iwanaga, T., Miyagawa, M., Kameya, T., Nakada, K., Kawai, Y. and Tsujisaki, M. (2009). High incidence of metabolically active brown adipose tissue in healthy adult humans: effects of cold exposure and adiposity. *Diabetes* , *58*, 1526–1531.
- Salem, H. K. and Thiernemann, C. (2010). Mesenchymal stromal cells: current understanding and clinical status. *Stem Cells* , *28*, 585–596.
- Samad, F. and Loskutoff, D. J. (1996). Tissue distribution and regulation of plasminogen activator inhibitor-1 in obese mice. *Mol Med* , *2*, 568–582.
- Sandberg, R., Neilson, J. R., Sarma, A., Sharp, P. A. and Burge, C. B. (2008). Proliferating cells express mRNAs with shortened 3' untranslated regions and fewer microRNA target sites. *Science* , *320*, 1643–1647.
- Sander, S., Bullinger, L., Klapproth, K., Fiedler, K., Kestler, H. A., Barth, T. F., Möller, P., Stilgenbauer, S., Pollack, J. R. and Wirth, T. (2008). MYC stimulates EZH2 expression by repression of its negative regulator miR-26a. *Blood* , *112*, 4202–4212.
- Sander, S., Bullinger, L. and Wirth, T. (2009). Repressing the repressor: a new mode of MYC action in lymphomagenesis. *Cell Cycle* , *8*, 556–559.
- Santaris Pharma (2010). Miravirsin for the treatment of Hepatitis C. Retrieved from <http://www.santaris.com/patients/clinical-trials-resources>. Accessed: 2011-04-01.
- Sassen, S., Miska, E. A. and Caldas, C. (2008). MicroRNA: implications for cancer. *Virchows Arch* , *452*, 1–10.
- Sawdey, M. S. and Loskutoff, D. J. (1991). Regulation of murine type 1 plasminogen activator inhibitor gene expression in vivo. Tissue specificity and induction by lipopolysaccharide, tumor necrosis factor-alpha, and transforming growth factor-beta. *J Clin Invest* , *88*, 1346–1353.
- Scheidler, M., Elabd, C., Zaragosi, L., Chiellini, C., Hackl, H., Sanchez-Cabo, F., Yadav, S., Duszka, K., Friedl, G., Papak, C., Prokesch, A., Windhager, R., Ailhaud, G., Dani, C., Amri, E. and Trajanoski, Z. (2008). Comparative transcriptomics of human multipotent stem cells during adipogenesis and osteoblastogenesis. *BMC Genomics* , *9*, 340.

- Schena, M., Shalon, D., Davis, R. W. and Brown, P. O. (1995). Quantitative monitoring of gene expression patterns with a complementary DNA microarray. *Science* , 270, 467–470.
- Scherer, P. E., Williams, S., Fogliano, M., Baldini, G. and Lodish, H. F. (1995). A novel serum protein similar to C1q, produced exclusively in adipocytes. *J Biol Chem* , 270, 26746–26749.
- Schetter, A. J., Leung, S. Y., Sohn, J. J., Zanetti, K. A., Bowman, E. D., Yanaihara, N., Yuen, S. T., Chan, T. L., Kwong, D. L., Au, G. K., Liu, C. G., Calin, G. A., Croce, C. M. and Harris, C. C. (2008). MicroRNA expression profiles associated with prognosis and therapeutic outcome in colon adenocarcinoma. *JAMA* , 299, 425–436.
- Schiwek, D. R. and Löffler, G. (1987). Glucocorticoid hormones contribute to the adipogenic activity of human serum. *Endocrinology* , 120, 469–474.
- Schling, P., Mallow, H., Trindl, A. and Löffler, G. (1999). Evidence for a local renin angiotensin system in primary cultured human preadipocytes. *Int J Obes Relat Metab Disord* , 23, 336–341.
- Schmidt, W., Pöll-Jordan, G. and Löffler, G. (1990). Adipose conversion of 3T3-L1 cells in a serum-free culture system depends on epidermal growth factor, insulin-like growth factor I, corticosterone, and cyclic AMP. *J Biol Chem* , 265, 15489–15495.
- Schmittgen, T. D. and Zakrajsek, B. A. (2000). Effect of experimental treatment on housekeeping gene expression: validation by real-time, quantitative RT-PCR. *J Biochem Biophys Methods* , 46, 69–81.
- Schoolmeesters, A., Eklund, T., Leake, D., Vermeulen, A., Smith, Q., Force Aldred, S. and Fedorov, Y. (2009). Functional profiling reveals critical role for miRNA in differentiation of human mesenchymal stem cells. *PLoS One* , 4.
- Scimè, A., Grenier, G., Huh, M. S., Gillespie, M. A., Bevilacqua, L., Harper, M. E. and Rudnicki, M. A. (2005). Rb and p107 regulate preadipocyte differentiation into white versus brown fat through repression of PGC-1alpha. *Cell Metab* , 2, 283–295.
- Scroyen, I., Christiaens, V. and Lijnen, H. R. (2007). No functional role of plasminogen activator inhibitor-1 in murine adipogenesis or adipocyte differentiation. *Journal of Thrombosis and Haemostasis: JTH* , 5, 139–145.
- Scroyen, I., Jacobs, F., Cosemans, L., Geest, B. D. and Lijnen, H. R. (2009). Effect of plasminogen activator inhibitor-1 on adipogenesis in vivo. *Thrombosis and Haemostasis* , 101, 388–393.
- Seale, P., Bjork, B., Yang, W., Kajimura, S., Chin, S., Kuang, S., Scimè, A., Devarakonda, S., Conroe, H. M., Erdjument-Bromage, H., Tempst, P., Rudnicki, M. A., Beier, D. R. and Spiegelman, B. M. (2008). PRDM16 controls a brown fat/skeletal muscle switch. *Nature* , 454, 961–967.
- Seale, P., Conroe, H. M., Estall, J., Kajimura, S., Frontini, A., Ishibashi, J., Cohen, P., Cinti, S. and Spiegelman, B. M. (2011). Prdm16 determines the thermogenic program of subcutaneous white adipose tissue in mice. *J Clin Invest* , 121, 96–105.
- Seale, P., Kajimura, S., Yang, W., Chin, S., Rohas, L. M., Uldry, M., Tavernier, G., Langin, D. and Spiegelman, B. M. (2007). Transcriptional control of brown fat determination by PRDM16. *Cell Metabolism* , 6, 38–54.
- Sears, I. B., MacGinnitie, M. A., Kovacs, L. G. and Graves, R. A. (1996). Differentiation-dependent expression of the brown adipocyte uncoupling protein gene: regulation by peroxisome proliferator-activated receptor gamma. *Mol Cell Biol* , 16, 3410–3419.
- Selbach, M., Schwanhäusser, B., Thierfelder, N., Fang, Z., Khanin, R. and Rajewsky, N. (2008). Widespread changes in protein synthesis induced by microRNAs. *Nature* , 455, 58–63.
- Sera, Y., LaRue, A. C., Moussa, O., Mehrotra, M., Duncan, J. D., Williams, C. R., Nishimoto, E., Schulte, B. A., Watson, P. M., Watson, D. K. and Ogawa, M. (2009). Hematopoietic stem cell origin of adipocytes. *Exp Hematol* , 37, 1108–1120.
- Serrero, G., Lepak, N. M. and Goodrich, S. P. (1992). Prostaglandin F2 alpha inhibits the differentiation of adipocyte precursors in primary culture. *Biochem Biophys Res Commun* , 183, 438–442.
- Shabalina, I. G., Ost, M., Petrovic, N., Vrbacky, M., Nedergaard, J. and Cannon, B. (2010). Uncoupling protein-1 is not leaky. *Biochim Biophys Acta* , 1797, 773–784.
- Sharma, G. and Goalstone, M. L. (2005). Dominant negative FTase (DNFTalpha) inhibits ERK5, MEF2C and CREB activation in adipogenesis. *Mol Cell Endocrinol* , 245, 93–104.

- Shen, Q., Little, S. C., Xu, M., Haupt, J., Ast, C., Katagiri, T., Mundlos, S., Seemann, P., Kaplan, F. S., Mullins, M. C. and Shore, E. M. (2009). The fibrodysplasia ossificans progressiva R206H ACVR1 mutation activates BMP-independent chondrogenesis and zebrafish embryo ventralization. *The Journal of Clinical Investigation* , *119*, 3462–3472.
- Shenouda, S. K. and Alahari, S. K. (2009). MicroRNA function in cancer: oncogene or a tumor suppressor? *Cancer Metastasis Rev* , *28*, 369–378.
- Shi, L., Perkins, R. G., Fang, H. and Tong, W. (2008). Reproducible and reliable microarray results through quality control: good laboratory proficiency and appropriate data analysis practices are essential. *Curr Opin Biotechnol* , *19*, 10–18.
- Shore, E. M., Xu, M., Feldman, G. J., Fenstermacher, D. A., Cho, T., Choi, I. H., Connor, J. M., Delai, P., Glaser, D. L., LeMerrer, M., Morhart, R., Rogers, J. G., Smith, R., Triffitt, J. T., Urtizberea, J. A., Zasloff, M., Brown, M. A. and Kaplan, F. S. (2006). A recurrent mutation in the BMP type I receptor ACVR1 causes inherited and sporadic fibrodysplasia ossificans progressiva. *Nature Genetics* , *38*, 525–527.
- Sims, E. A., Danforth, E., Horton, E. S., Bray, G. A., Glennon, J. A. and Salans, L. B. (1973). Endocrine and metabolic effects of experimental obesity in man. *Recent Prog Horm Res* , *29*, 457–496.
- Sinha, S., Singh, R. K., Alam, N., Roy, A., Roychoudhury, S. and Panda, C. K. (2008). Frequent alterations of hMLH1 and RBP3/HYA22 at chromosomal 3p22.3 region in early and late-onset breast carcinoma: clinical and prognostic significance. *Cancer Sci* , *99*, 1984–1991.
- Small, E. M., Frost, R. J. and Olson, E. N. (2010). MicroRNAs add a new dimension to cardiovascular disease. *Circulation* , *121*, 1022–1032.
- Smas, C. M. and Sul, H. S. (1993). Pref-1, a protein containing EGF-like repeats, inhibits adipocyte differentiation. *Cell* , *73*, 725–734.
- Smith, P. J., Wise, L. S., Berkowitz, R., Wan, C. and Rubin, C. S. (1988). Insulin-like growth factor-I is an essential regulator of the differentiation of 3T3-L1 adipocytes. *J Biol Chem* , *263*, 9402–9408.
- Soliman, G. A. (2005). The mammalian target of rapamycin signaling network and gene regulation. *Curr Opin Lipidol* , *16*, 317–323.
- Sorrentino, A., Liu, C. G., Addario, A., Peschle, C., Scambia, G. and Ferlini, C. (2008). Role of microRNAs in drug-resistant ovarian cancer cells. *Gynecol Oncol* , *111*, 478–486.
- Spalding, K. L., Arner, E., Westermark, P. O., Bernard, S., Buchholz, B. A., Bergmann, O., Blomqvist, L., Hoffstedt, J., Näslund, E., Britton, T., Concha, H., Hassan, M., Rydén, M., Frisén, J. and Arner, P. (2008). Dynamics of fat cell turnover in humans. *Nature* , *453*, 783–787.
- Stevens, J., Couper, D., Pankow, J., Folsom, A. R., Duncan, B. B., Nieto, F. J., Jones, D. and Tyroler, H. A. (2001). Sensitivity and specificity of anthropometrics for the prediction of diabetes in a biracial cohort. *Obes Res* , *9*, 696–705.
- Stunkard, A. J., Sorensen, T. I., Hanis, C., Teasdale, T. W., Chakraborty, R., Schull, W. J. and Schulsinger, F. (1986). An adoption study of human obesity. *N Engl J Med* , *314*, 193–198.
- Sturn, A., Quackenbush, J. and Trajanoski, Z. (2002). Genesis: cluster analysis of microarray data. *Bioinformatics (Oxford, England)* , *18*, 207–208.
- Sugihara, H., Yonemitsu, N., Miyabara, S. and Toda, S. (1987). Proliferation of unilocular fat cells in the primary culture. *J Lipid Res* , *28*, 1038–1045.
- Sul, H. S. (2009). Minireview: Pref-1: role in adipogenesis and mesenchymal cell fate. *Mol Endocrinol* , *23*, 1717–1725.
- Sun, F., Wang, J., Pan, Q., Yu, Y., Zhang, Y., Wan, Y., Wang, J., Li, X. and Hong, A. (2009a). Characterization of function and regulation of miR-24-1 and miR-31. *Biochemical and Biophysical Research Communications* , *380*, 660–665.
- Sun, T., Fu, M., Bookout, A. L., Kliewer, S. A. and Mangelsdorf, D. J. (2009b). MicroRNA let-7 regulates 3T3-L1 adipogenesis. *Molecular Endocrinology (Baltimore, Md.)* , *23*, 925–931.

- Svensson, P. A., Jernäs, M., Sjöholm, K., Hoffmann, J. M., Nilsson, B. E., Hansson, M. and Carlsson, L. M. (2011). Gene expression in human brown adipose tissue. *Int J Mol Med* , 27, 227–232.
- Taft, R. J., Kaplan, C. D., Simons, C. and Mattick, J. S. (2009). Evolution, biogenesis and function of promoter-associated RNAs. *Cell Cycle* , 8, 2332–2338.
- Taft, R. J., Pheasant, M. and Mattick, J. S. (2007). The relationship between non-protein-coding DNA and eukaryotic complexity. *Bioessays* , 29, 288–299.
- Tainter, M. L., Cutting, W. C. and Stockton, A. B. (1934). Use of Dinitrophenol in Nutritional Disorders : A Critical Survey of Clinical Results. *Am J Public Health Nations Health* , 24, 1045–1053.
- Tan, G. D., Fielding, B. A., Currie, J. M., Humphreys, S. M., Désage, M., Frayn, K. N., Laville, M., Vidal, H. and Karpe, F. (2005). The effects of rosiglitazone on fatty acid and triglyceride metabolism in type 2 diabetes. *Diabetologia* , 48, 83–95.
- Tanaka, T., Akira, S., Yoshida, K., Umemoto, M., Yoneda, Y., Shirafuji, N., Fujiwara, H., Suematsu, S., Yoshida, N. and Kishimoto, T. (1995). Targeted disruption of the NF-IL6 gene discloses its essential role in bacteria killing and tumor cytotoxicity by macrophages. *Cell* , 80, 353–361.
- Tanaka, T., Yoshida, N., Kishimoto, T. and Akira, S. (1997). Defective adipocyte differentiation in mice lacking the C/EBPbeta and/or C/EBPdelta gene. *EMBO J* , 16, 7432–7443.
- Tang, W., Zeve, D., Suh, J. M., Bosnakovski, D., Kyba, M., Hammer, R. E., Tallquist, M. D. and Graff, J. M. (2008). White fat progenitor cells reside in the adipose vasculature. *Science* , 322, 583–586.
- Tavazoie, S. F., Alarcón, C., Oskarsson, T., Padua, D., Wang, Q., Bos, P. D., Gerald, W. L. and Massagué, J. (2008). Endogenous human microRNAs that suppress breast cancer metastasis. *Nature* , 451, 147–152.
- Tay, Y., Zhang, J., Thomson, A. M., Lim, B. and Rigoutsos, I. (2008). MicroRNAs to Nanog, Oct4 and Sox2 coding regions modulate embryonic stem cell differentiation. *Nature* , 455, 1124–1128.
- Taylor, S. M. and Jones, P. A. (1979). Multiple new phenotypes induced in 10T1/2 and 3T3 cells treated with 5-azacytidine. *Cell* , 17, 771–779.
- Thai, T. H., Calado, D. P., Casola, S., Ansel, K. M., Xiao, C., Xue, Y., Murphy, A., Frenthewey, D., Valenzuela, D., Kutok, J. L., Schmidt-Supprian, M., Rajewsky, N., Yancopoulos, G., Rao, A. and Rajewsky, K. (2007). Regulation of the germinal center response by microRNA-155. *Science* , 316, 604–608.
- Timmons, J. A., Wennmalm, K., Larsson, O., Walden, T. B., Lassmann, T., Petrovic, N., Hamilton, D. L., Gimeno, R. E., Wahlestedt, C., Baar, K., Nedergaard, J. and Cannon, B. (2007). Myogenic gene expression signature establishes that brown and white adipocytes originate from distinct cell lineages. *Proc Natl Acad Sci U S A* , 104, 4401–4406.
- Todaro, G. J. and Green, H. (1963). Quantitative studies of the growth of mouse embryo cells in culture and their development into established lines. *J Cell Biol* , 17, 299–313.
- Tomé, M., López-Romero, P., Albo, C., Sepúlveda, J. C., Fernández-Gutiérrez, B., Dopazo, A., Bernad, A. and González, M. A. (2010). miR-335 orchestrates cell proliferation, migration and differentiation in human mesenchymal stem cells. *Cell Death Differ* , 18, 985–995.
- Tong, Q., Dalgin, G., Xu, H., Ting, C. N., Leiden, J. M. and Hotamisligil, G. S. (2000). Function of GATA transcription factors in preadipocyte-adipocyte transition. *Science* , 290, 134–138.
- Tontonoz, P., Graves, R. A., Budavari, A. I., Erdjument-Bromage, H., Lui, M., Hu, E., Tempst, P. and Spiegelman, B. M. (1994a). Adipocyte-specific transcription factor ARF6 is a heterodimeric complex of two nuclear hormone receptors, PPAR gamma and RXR alpha. *Nucleic Acids Res* , 22, 5628–5634.
- Tontonoz, P., Hu, E., Graves, R. A., Budavari, A. I. and Spiegelman, B. M. (1994b). mPPAR gamma 2: tissue-specific regulator of an adipocyte enhancer. *Genes Dev* , 8, 1224–1234.
- Tontonoz, P., Hu, E. and Spiegelman, B. M. (1994c). Stimulation of adipogenesis in fibroblasts by PPAR gamma 2, a lipid-activated transcription factor. *Cell* , 79, 1147–1156.
- Tritschler, F., Huntzinger, E. and Izaurralde, E. (2010). Role of GW182 proteins and PABPC1 in the miRNA pathway: a sense of déjà vu. *Nat Rev Mol Cell Biol* , 11, 379–384.

- Tseng, Y., Kokkotou, E., Schulz, T. J., Huang, T. L., Winnay, J. N., Taniguchi, C. M., Tran, T. T., Suzuki, R., Espinoza, D. O., Yamamoto, Y., Ahrens, M. J., Dudley, A. T., Norris, A. W., Kulkarni, R. N. and Kahn, C. R. (2008). New role of bone morphogenetic protein 7 in brown adipogenesis and energy expenditure. *Nature* , *454*, 1000–1004.
- Tsuchida, A., Yamauchi, T., Takekawa, S., Hada, Y., Ito, Y., Maki, T. and Kadowaki, T. (2005). Peroxisome proliferator-activated receptor (PPAR)alpha activation increases adiponectin receptors and reduces obesity-related inflammation in adipose tissue: comparison of activation of PPARalpha, PPARgamma, and their combination. *Diabetes* , *54*, 3358–3370.
- Tsukiyama-Kohara, K., Poulin, F., Kohara, M., DeMaria, C. T., Cheng, A., Wu, Z., Gingras, A. C., Katsume, A., Elchebly, M., Spiegelman, B. M., Harper, M. E., Tremblay, M. L. and Sonenberg, N. (2001). Adipose tissue reduction in mice lacking the translational inhibitor 4E-BP1. *Nat Med* , *7*, 1128–1132.
- Turner-McGrievy, G. M., Barnard, N. D. and Scialli, A. R. (2007). A two-year randomized weight loss trial comparing a vegan diet to a more moderate low-fat diet. *Obesity (Silver Spring)* , *15*, 2276–2281.
- Uldry, M., Yang, W., St-Pierre, J., Lin, J., Seale, P. and Spiegelman, B. M. (2006). Complementary action of the PGC-1 coactivators in mitochondrial biogenesis and brown fat differentiation. *Cell Metab* , *3*, 333–341.
- Um, S. H., D'Alessio, D. and Thomas, G. (2006). Nutrient overload, insulin resistance, and ribosomal protein S6 kinase 1, S6K1. *Cell Metab* , *3*, 393–402.
- Um, S. H., Frigerio, F., Watanabe, M., Picard, F., Joaquin, M., Sticker, M., Fumagalli, S., Allegrini, P. R., Kozma, S. C., Auwerx, J. and Thomas, G. (2004). Absence of S6K1 protects against age- and diet-induced obesity while enhancing insulin sensitivity. *Nature* , *431*, 200–205.
- Van, R. L., Bayliss, C. E. and Roncari, D. A. (1976). Cytological and enzymological characterization of adult human adipocyte precursors in culture. *J Clin Invest* , *58*, 699–704.
- van Dinther, M., Visser, N., de Gorter, D. J. J., Doorn, J., Goumans, M., de Boer, J. and ten Dijke, P. (2010). ALK2 R206H mutation linked to fibrodysplasia ossificans progressiva confers constitutive activity to the BMP type I receptor and sensitizes mesenchymal cells to BMP-induced osteoblast differentiation and bone formation. *Journal of Bone and Mineral Research: The Official Journal of the American Society for Bone and Mineral Research* , *25*, 1208–1215.
- Van Harmelen, V., Ariapart, P., Hoffstedt, J., Lundkvist, I., Bringman, S. and Arner, P. (2000). Increased adipose angiotensinogen gene expression in human obesity. *Obes Res* , *8*, 337–341.
- van Marken Lichtenbelt, W. D., Vanhommerig, J. W., Smulders, N. M., Drossaerts, J. M., Kemerink, G. J., Bouvy, N. D., Schrauwen, P. and Teule, G. J. (2009a). Cold-activated brown adipose tissue in healthy men. *N Engl J Med* , *360*, 1500–1508.
- van Marken Lichtenbelt, W. D., Vanhommerig, J. W., Smulders, N. M., Drossaerts, J. M. A. F. L., Kemerink, G. J., Bouvy, N. D., Schrauwen, P. and Teule, G. J. J. (2009b). Cold-activated brown adipose tissue in healthy men. *The New England Journal of Medicine* , *360*, 1500–1508.
- van Mourik, J. A., Lawrence, D. A. and Loskutoff, D. J. (1984). Purification of an inhibitor of plasminogen activator (antiactivator) synthesized by endothelial cells. *J Biol Chem* , *259*, 14914–14921.
- van Rooij, E., Sutherland, L. B., Qi, X., Richardson, J. A., Hill, J. and Olson, E. N. (2007). Control of stress-dependent cardiac growth and gene expression by a microRNA. *Science* , *316*, 575–579.
- VanGuilder, H. D., Vrana, K. E. and Freeman, W. M. (2008). Twenty-five years of quantitative PCR for gene expression analysis. *Biotechniques* , *44*, 619–626.
- Vassaux, G., Gaillard, D., Ailhaud, G. and Nègre, R. (1992). Prostacyclin is a specific effector of adipose cell differentiation. Its dual role as a cAMP- and Ca(2+)-elevating agent. *J Biol Chem* , *267*, 11092–11097.
- Vasudevan, S., Tong, Y. and Steitz, J. A. (2007). Switching from repression to activation: microRNAs can up-regulate translation. *Science* , *318*, 1931–1934.
- Vegiopoulos, A., Müller-Decker, K., Strzoda, D., Schmitt, I., Chichelnitskiy, E., Ostertag, A., Berriel Diaz, M., Rozman, J., Hrabe de Angelis, M., Nüsing, R. M., Meyer, C. W., Wahli, W., Klingenspor, M. and Herzig, S. (2010). Cyclooxygenase-2 controls energy homeostasis in mice by de novo recruitment of brown adipocytes. *Science* , *328*, 1158–1161.

- Vella, M. C., Choi, E. Y., Lin, S. Y., Reinert, K. and Slack, F. J. (2004). The *C. elegans* microRNA let-7 binds to imperfect let-7 complementary sites from the lin-41 3'UTR. *Genes Dev* , *18*, 132–137.
- Ventura, A., Young, A. G., Winslow, M. M., Lintault, L., Meissner, A., Erkeland, S. J., Newman, J., Bronson, R. T., Crowley, D., Stone, J. R., Jaenisch, R., Sharp, P. A. and Jacks, T. (2008). Targeted deletion reveals essential and overlapping functions of the miR-17 through 92 family of miRNA clusters. *Cell* , *132*, 875–886.
- Virtanen, K. A., Lidell, M. E., Orava, J., Heglind, M., Westergren, R., Niemi, T., Taittonen, M., Laine, J., Savisto, N. J., Enerbäck, S. and Nuutila, P. (2009). Functional brown adipose tissue in healthy adults. *N Engl J Med* , *360*, 1518–1525.
- Visone, R. and Croce, C. M. (2009). MiRNAs and cancer. *Am J Pathol* , *174*, 1131–1138.
- Vodyanik, M. A., Yu, J., Zhang, X., Tian, S., Stewart, R., Thomson, J. A. and Slukvin, I. I. (2010). A mesoderm-derived precursor for mesenchymal stem and endothelial cells. *Cell Stem Cell* , *7*, 718–729.
- Vohl, M. C., Sladek, R., Robitaille, J., Gurd, S., Marceau, P., Richard, D., Hudson, T. J. and Tchernof, A. (2004). A survey of genes differentially expressed in subcutaneous and visceral adipose tissue in men. *Obes Res* , *12*, 1217–1222.
- Waki, H., Yamauchi, T., Kamon, J., Ito, Y., Uchida, S., Kita, S., Hara, K., Hada, Y., Vasseur, F., Froguel, P., Kimura, S., Nagai, R. and Kadowaki, T. (2003). Impaired multimerization of human adiponectin mutants associated with diabetes. Molecular structure and multimer formation of adiponectin. *J Biol Chem* , *278*, 40352–40363.
- Walden, T. B., Timmons, J. A., Keller, P., Nedergaard, J. and Cannon, B. (2009). Distinct expression of muscle-specific microRNAs (myomirs) in brown adipocytes. *Journal of Cellular Physiology* , *218*, 444–449.
- Wang, G., Zhang, H., He, H., Tong, W., Wang, B., Liao, G., Chen, Z. and Du, C. (2010). Up-regulation of microRNA in bladder tumor tissue is not common. *Int Urol Nephrol* , *42*, 95–102.
- Wang, Q., Li, Y. C., Wang, J., Kong, J., Qi, Y., Quigg, R. J. and Li, X. (2008). miR-17-92 cluster accelerates adipocyte differentiation by negatively regulating tumor-suppressor Rb2/p130. *Proc Natl Acad Sci U S A* , *105*, 2889–2894.
- Wang, T. and Xu, Z. (2010). miR-27 promotes osteoblast differentiation by modulating Wnt signaling. *Biochem Biophys Res Commun* , *402*, 186–189.
- Wang, Y., Li, Z., He, C., Wang, D., Yuan, X., Chen, J. and Jin, J. (2010). MicroRNAs expression signatures are associated with lineage and survival in acute leukemias. *Blood Cells Mol Dis* , *44*, 191–197.
- Wang, Y. X. (2010). PPARs: diverse regulators in energy metabolism and metabolic diseases. *Cell Res* , *20*, 124–137.
- Weigl, B. H., Holobar, A., Trettnak, W., Klimant, I., Kraus, H., O'Leary, P. and Wolfbeis, O. S. (1994). Optical triple sensor for measuring pH, oxygen and carbon dioxide. *J Biotechnol* , *32*, 127–138.
- Weisberg, S. P., McCann, D., Desai, M., Rosenbaum, M., Leibel, R. L. and Ferrante, A. W. (2003). Obesity is associated with macrophage accumulation in adipose tissue. *J Clin Invest* , *112*, 1796–1808.
- WHO (2010). Fact Files: Ten facts on obesity. Retrieved from <http://www.who.int/features/factfiles/obesity/en/index.html>. Accessed: 2011-02-23.
- Wilson-Fritch, L., Nicoloso, S., Chouinard, M., Lazar, M. A., Chui, P. C., Leszyk, J., Straubhaar, J., Czech, M. P. and Corvera, S. (2004). Mitochondrial remodeling in adipose tissue associated with obesity and treatment with rosiglitazone. *J Clin Invest* , *114*, 1281–1289.
- Wilusz, J. E., Sunwoo, H. and Spector, D. L. (2009). Long noncoding RNAs: functional surprises from the RNA world. *Genes Dev* , *23*, 1494–1504.
- Wolbank, S., Stadler, G., Peterbauer, A., Gillich, A., Karbiener, M., Streubel, B., Wieser, M., Katinger, H., van Griensven, M., Redl, H., Gabriel, C., Grillari, J. and Grillari-Voglauer, R. (2009). Telomerase immortalized human amnion- and adipose-derived mesenchymal stem cells: maintenance of differentiation and immunomodulatory characteristics. *Tissue Engineering. Part A* , *15*, 1843–1854.
- Wolf, H. K., Tuomilehto, J., Kuulasmaa, K., Domarkiene, S., Cepaitis, Z., Molarius, A., Sans, S., Dobson, A., Keil, U. and Rywik, S. (1997). Blood pressure levels in the 41 populations of the WHO MONICA Project. *J Hum Hypertens* , *11*, 733–742.

- Wong, C. F. and Tellam, R. L. (2008). MicroRNA-26a targets the histone methyltransferase Enhancer of Zeste homolog 2 during myogenesis. *J Biol Chem* , 283, 9836–9843.
- Wu, L., Fan, J. and Belasco, J. G. (2006). MicroRNAs direct rapid deadenylation of mRNA. *Proc Natl Acad Sci U S A* , 103, 4034–4039.
- Wu, Q. and Suzuki, M. (2006). Parental obesity and overweight affect the body-fat accumulation in the offspring: the possible effect of a high-fat diet through epigenetic inheritance. *Obes Rev* , 7, 201–208.
- Wu, Z., Bucher, N. L. and Farmer, S. R. (1996). Induction of peroxisome proliferator-activated receptor gamma during the conversion of 3T3 fibroblasts into adipocytes is mediated by C/EBPbeta, C/EBPdelta, and glucocorticoids. *Mol Cell Biol* , 16, 4128–4136.
- Wu, Z., Puigserver, P., Andersson, U., Zhang, C., Adelmant, G., Mootha, V., Troy, A., Cinti, S., Lowell, B., Scarpulla, R. C. and Spiegelman, B. M. (1999a). Mechanisms controlling mitochondrial biogenesis and respiration through the thermogenic coactivator PGC-1. *Cell* , 98, 115–124.
- Wu, Z., Rosen, E. D., Brun, R., Hauser, S., Adelmant, G., Troy, A. E., McKeon, C., Darlington, G. J. and Spiegelman, B. M. (1999b). Cross-regulation of C/EBP alpha and PPAR gamma controls the transcriptional pathway of adipogenesis and insulin sensitivity. *Mol Cell* , 3, 151–158.
- Xie, H., Lim, B. and Lodish, H. F. (2009). MicroRNAs induced during adipogenesis that accelerate fat cell development are downregulated in obesity. *Diabetes* , 58, 1050–1057.
- Xie, S. S., Li, X. Y., Liu, T., Cao, J. H., Zhong, Q. and Zhao, S. H. (2011). Discovery of porcine microRNAs in multiple tissues by a Solexa deep sequencing approach. *PLoS One* , 6.
- Xu, H., Barnes, G. T., Yang, Q., Tan, G., Yang, D., Chou, C. J., Sole, J., Nichols, A., Ross, J. S., Tartaglia, L. A. and Chen, H. (2003). Chronic inflammation in fat plays a crucial role in the development of obesity-related insulin resistance. *J Clin Invest* , 112, 1821–1830.
- Xu, H., Sethi, J. K. and Hotamisligil, G. S. (1999). Transmembrane tumor necrosis factor (TNF)-alpha inhibits adipocyte differentiation by selectively activating TNF receptor 1. *J Biol Chem* , 274, 26287–26295.
- Xu, H., Yao, Y., Smith, L. P. and Nair, V. (2010). MicroRNA-26a-mediated regulation of interleukin-2 expression in transformed avian lymphocyte lines. *Cancer Cell Int* , 10, 15–15.
- Xu, P., Vernooy, S. Y., Guo, M. and Hay, B. A. (2003). The Drosophila microRNA Mir-14 suppresses cell death and is required for normal fat metabolism. *Curr Biol* , 13, 790–795.
- Xue, Y., Cao, R., Nilsson, D., Chen, S., Westergren, R., Hedlund, E. M., Martijn, C., Rondahl, L., Krauli, P., Walum, E., Enerbäck, S. and Cao, Y. (2008). FOXC2 controls Ang-2 expression and modulates angiogenesis, vascular patterning, remodeling, and functions in adipose tissue. *Proc Natl Acad Sci U S A* , 105, 10167–10172.
- Xue, Y., Petrovic, N., Cao, R., Larsson, O., Lim, S., Chen, S., Feldmann, H. M., Liang, Z., Zhu, Z., Nedergaard, J., Cannon, B. and Cao, Y. (2009). Hypoxia-independent angiogenesis in adipose tissues during cold acclimation. *Cell Metab* , 9, 99–109.
- Yamauchi, T., Kamon, J., Minokoshi, Y., Ito, Y., Waki, H., Uchida, S., Yamashita, S., Noda, M., Kita, S., Ueki, K., Eto, K., Akanuma, Y., Froguel, P., Foufelle, F., Ferre, P., Carling, D., Kimura, S., Nagai, R., Kahn, B. B. and Kadowaki, T. (2002). Adiponectin stimulates glucose utilization and fatty-acid oxidation by activating AMP-activated protein kinase. *Nat Med* , 8, 1288–1295.
- Yamauchi, T., Kamon, J., Waki, H., Terauchi, Y., Kubota, N., Hara, K., Mori, Y., Ide, T., Murakami, K., Tsuboyama-Kasaoka, N., Ezaki, O., Akanuma, Y., Gavrilova, O., Vinson, C., Reitman, M. L., Kagechika, H., Shudo, K., Yoda, M., Nakano, Y., Tobe, K., Nagai, R., Kimura, S., Tomita, M., Froguel, P. and Kadowaki, T. (2001). The fat-derived hormone adiponectin reverses insulin resistance associated with both lipodystrophy and obesity. *Nat Med* , 7, 941–946.
- Yan, L. X., Wu, Q. N., Zhang, Y., Li, Y. Y., Liao, D. Z., Hou, J. H., Fu, J., Zeng, M. S., Yun, J. P., Wu, Q. L., Zeng, Y. X. and Shao, J. Y. (2011). Knockdown of miR-21 in human breast cancer cell lines inhibits proliferation, in vitro migration and in vivo tumor growth. *Breast Cancer Res* , 13.
- Yanaihara, N., Caplen, N., Bowman, E., Seike, M., Kumamoto, K., Yi, M., Stephens, R. M., Okamoto, A., Yokota, J., Tanaka, T., Calin, G. A., Liu, C. G., Croce, C. M. and Harris, C. C. (2006). Unique microRNA molecular profiles in lung cancer diagnosis and prognosis. *Cancer Cell* , 9, 189–198.

- Yeo, G. S., Farooqi, I. S., Aminian, S., Halsall, D. J., Stanhope, R. G. and O'Rahilly, S. (1998). A frameshift mutation in MC4R associated with dominantly inherited human obesity. *Nat Genet* , *20*, 111–112.
- Yeo, M., Lin, P. S., Dahmus, M. E. and Gill, G. N. (2003). A novel RNA polymerase II C-terminal domain phosphatase that preferentially dephosphorylates serine 5. *J Biol Chem* , *278*, 26078–26085.
- Yu, F., Deng, H., Yao, H., Liu, Q., Su, F. and Song, E. (2010). Mir-30 reduction maintains self-renewal and inhibits apoptosis in breast tumor-initiating cells. *Oncogene* , *29*, 4194–4204.
- Yu, F., Yao, H., Zhu, P., Zhang, X., Pan, Q., Gong, C., Huang, Y., Hu, X., Su, F., Lieberman, J. and Song, E. (2007). let-7 regulates self renewal and tumorigenicity of breast cancer cells. *Cell* , *131*, 1109–1123.
- Zahorska-Markiewicz, B., Janowska, J., Olszanecka-Glinianowicz, M. and Zurakowski, A. (2000). Serum concentrations of TNF-alpha and soluble TNF-alpha receptors in obesity. *Int J Obes Relat Metab Disord* , *24*, 1392–1395.
- Zampetaki, A., Kiechl, S., Drozdov, I., Willeit, P., Mayr, U., Prokopi, M., Mayr, A., Weger, S., Oberhollenzer, F., Bonora, E., Shah, A., Willeit, J. and Mayr, M. (2010). Plasma microRNA profiling reveals loss of endothelial miR-126 and other microRNAs in type 2 diabetes. *Circ Res* , *107*, 810–817.
- Zechner, R., Strauss, J. G., Haemmerle, G., Lass, A. and Zimmermann, R. (2005). Lipolysis: pathway under construction. *Curr Opin Lipidol* , *16*, 333–340.
- Zezulak, K. M. and Green, H. (1986). The generation of insulin-like growth factor-1-sensitive cells by growth hormone action. *Science* , *233*, 551–553.
- Zhang, B., Liu, X. X., He, J. R., Zhou, C. X., Guo, M., He, M., Li, M. F., Chen, G. Q. and Zhao, Q. (2011). Pathologically decreased miR-26a antagonizes apoptosis and facilitates carcinogenesis by targeting MTDH and EZH2 in breast cancer. *Carcinogenesis* , *32*, 2–9.
- Zhang, J., Fu, M., Cui, T., Xiong, C., Xu, K., Zhong, W., Xiao, Y., Floyd, D., Liang, J., Li, E., Song, Q. and Chen, Y. E. (2004). Selective disruption of PPARgamma 2 impairs the development of adipose tissue and insulin sensitivity. *Proc Natl Acad Sci U S A* , *101*, 10703–10708.
- Zhang, Y., Proenca, R., Maffei, M., Barone, M., Leopold, L. and Friedman, J. M. (1994). Positional cloning of the mouse obese gene and its human homologue. *Nature* , *372*, 425–432.
- Zhao, S. and Fernald, R. D. (2005). Comprehensive algorithm for quantitative real-time polymerase chain reaction. *J Comput Biol* , *12*, 1047–1064.
- Zhao, Y., Ransom, J. F., Li, A., Vedantham, V., von Drehle, M., Muth, A. N., Tsuchihashi, T., McManus, M. T., Schwartz, R. J. and Srivastava, D. (2007). Dysregulation of cardiogenesis, cardiac conduction, and cell cycle in mice lacking miRNA-1-2. *Cell* , *129*, 303–317.
- Zhong, X., Li, N., Liang, S., Huang, Q., Coukos, G. and Zhang, L. (2010). Identification of microRNAs regulating reprogramming factor LIN28 in embryonic stem cells and cancer cells. *J Biol Chem* , *285*, 41961–41971.
- Zhou, Z., Yon Toh, S., Chen, Z., Guo, K., Ng, C. P., Ponniah, S., Lin, S. C., Hong, W. and Li, P. (2003). Cidea-deficient mice have lean phenotype and are resistant to obesity. *Nat Genet* , *35*, 49–56.
- Zimmermann, R., Lass, A., Haemmerle, G. and Zechner, R. (2009). Fate of fat: the role of adipose triglyceride lipase in lipolysis. *Biochim Biophys Acta* , *1791*, 494–500.
- Zingaretti, M. C., Crosta, F., Vitali, A., Guerrieri, M., Frontini, A., Cannon, B., Nedergaard, J. and Cinti, S. (2009). The presence of UCP1 demonstrates that metabolically active adipose tissue in the neck of adult humans truly represents brown adipose tissue. *The FASEB Journal: Official Publication of the Federation of American Societies for Experimental Biology* , *23*, 3113–3120.
- Zuk, P. A., Zhu, M., Ashjian, P., De Ugarte, D. A., Huang, J. I., Mizuno, H., Alfonso, Z. C., Fraser, J. K., Benhaim, P. and Hedrick, M. H. (2002). Human adipose tissue is a source of multipotent stem cells. *Mol Biol Cell* , *13*, 4279–4295.
- Zuk, P. A., Zhu, M., Mizuno, H., Huang, J., Futrell, J. W., Katz, A. J., Benhaim, P., Lorenz, H. P. and Hedrick, M. H. (2001). Multilineage cells from human adipose tissue: implications for cell-based therapies. *Tissue Eng* , *7*, 211–228.
- Zurlo, F., Lillioja, S., Esposito-Del Puente, A., Nyomba, B. L., Raz, I., Saad, M. F., Swinburn, B. A., Knowler, W. C., Bogardus, C. and Ravussin, E. (1990). Low ratio of fat to carbohydrate oxidation as predictor of weight gain: study of 24-h RQ. *Am J Physiol* , *259*, 650–657.